UNIVERSITY OF SOUTHAMPTON

FACULTY OF MEDICINE

Clinical and Experimental Sciences

Volume 1 of 1

The role of the gene *SERPING1* as a pharmacogenetic biomarker for choroidal neovascularization (CNV) response to anti vascular endothelial growth factor (VEGF) treatment in clinical practice

by

Charles Pierce

Thesis for the degree of Doctor of Medicine

April_2015

UNIVERSITY OF SOUTHAMPTON

ABSTRACT

FACULTY OF MEDICINE

Medicine

Thesis for the degree of Doctor of Medicine

THE ROLE OF THE GENE *SERPING1* AS A PHARMACOGENETIC BIOMARKER FOR CHOROIDAL NEOVASCULARIZATION (CNV) RESPONSE TO ANTI VASCULAR ENDOTHELIAL GROWTH FACTOR (VEGF) TREATMENT IN CLINICAL PRACTICE

Charles Pierce

Age related macular degeneration is the commonest cause of blindness in the western world and current treatment regimens represent a significant output for national health services. The disease process is multifactorial in origin and has a variable progression and response to current methods of treatment. A targeted approach with individualized therapy based on recognized biomarkers to predict disease outcome would be the ideal treatment modality.

We plan to investigate the role of genes known to influence the progression of early AMD to the advanced stage (wet AMD) with emphasis on genes involved in complement regulation (*SERPING1, CFB, CFI, CFH, C2* and *C3).* The investigation will also encompass other genotypes involved in AMD pathogenesis.

Polymorphic variations in the gene *SERPING1,* which codes for complement 1 inhibitor (C1Inh), have been previously implicated in AMD pathogenesis. Many clinical trials involving complement antagonists are currently proceeding at various stages of development. We plan to investigate the role of C1Inh in AMD development and explore its potential as a therapeutic agent, utilising $Ccl2^{-/-}$ /$Cx3cr1^{-/-}$ (in the presence of an *rd8* mutation in the *Crb1* gene) and wild type C57BL/6 mice.

In the neurodegenerative condition Alzheimer's disease, acute or chronic and chronic systemic inflammation have been associated with progression of symptoms. Both chronic and acute inflammation have been implicated in choroidal angiogenesis and subsequent AMD development. We hypothesised that systemic inflammation may alter the response of AMD to the anti-vascular endothelial growth factor (VEGF) agent ranibizumab. Inflammatory markers may therefore offer an objective indicator of future treatment response. These experiments will provide a comprehensive analysis of prognostic indicators for AMD and investigate a potentially new therapeutic agent.

Table of Contents

List of figures

List of tables

DECLARATION OF AUTHORSHIP

I, Charles Pierce declare that the thesis entitled:
The role of the gene *SERPING1* as a pharmacogenetic biomarker for choroidal neovascularization (CNV) response to anti vascular endothelial growth factor (VEGF) treatment in clinical practice

and the work presented in the thesis are both my own, and have been generated by me as the result of my own original research. I confirm that:

- this work was done wholly or mainly while in candidature for a research degree at this University;
- where any part of this thesis has previously been submitted for a degree or any other qualification at this University or any other institution, this has been clearly stated;
- where I have consulted the published work of others, this is always clearly attributed;
- where I have quoted from the work of others, the source is always given. With the exception of such quotations, this thesis is entirely my own work;
- I have acknowledged all main sources of help;
- where the thesis is based on work done by myself jointly with others, I have made clear exactly what was done by others and what I have contributed myself;
- none of this work has been published before submission, or [delete as appropriate] parts of this work have been published as: [please list references]

Signed: ……

Date:……

Acknowledgements

I would like to thank my supervisors Prof Andrew Lotery, Ms. Angela Cree and Dr. Heather Thomson for their mentorship during the course of this degree.

Marie Nelson and her dedicated research nurses (Catrin, Georgiana and Jane) have been a source of support throughout this project. Their help has made the research possible and I am sincerely grateful.

I would also like to thank Dr Roxana Carare, Sam, Xiaoli, Jenny, Helen, Maureen and Srini for their daily advice and encouragement.

Finally, I would like to thank my family who offer their support over the many miles and months of separation. They provide a constant reminder of purpose and relationship to a wider community.

Definitions and abbreviations

ABCA4 ATP-binding cassette sub-family, member 4

AD Alzheimer's disease

AMD Age related macular degeneration

ANCHOR trial Ranibizumab versus Verteporfin for Neovascular Age-Related Macular Degeneration

ApoE Apolipoprotein E

AREDS Age related eye disease study

ARMS2 Age-related maculopathy susceptibility 2

ATE Atherothrombotic event

A□ Amyloid □

BCVA Best corrected visual acuity

BlamD Basal laminar deposits

BlinD Basal linear deposits

BMI Body mass index

BRF Biomedical research facility

CATT Comparison of Age-Related Macular Degeneration Treatment Trials

CEP Carboxyethyl pyrrole

CFH Complement factor H

CI Chief Investigator

CMT Change CMT change from baseline to Visit 7

CNV Choroidal neovascularization

CRP C reactive protein

DAF Decay accelerating factor

DNA Deoxyribonucleic acid

EDTA EthyleneDiamineTetraacetic acid

ELB Erythrocyte lysis buffer

ELM External limiting membrane

ETDRS Early treatment diabetic retinopathy study

FFA Fundus fluorescein angiogram

FPH Frimley Park Hospital

GA Geographic atrophy

H & E Haematoxylin and eosin

HAO Hereditary angioedema

HTRA-1 High temperature required heat-shock protein 1

ICF Informed Consent Form

Il Interleukin
ILM Internal limiting membrane
INL Inner nuclear layer
IPL Inner plexiform layer
IRAS Integrated Research Application System
IV Intravitreal
IVAN Ranibizumab vs. bevacizumab to treat neovascular age related macular degeneration
LDL Low density lipoprotein
LogMAR Logarithmic minimal angle of resolution
MAC Membrane attack complex
MARINA trial Ranibizumab for neovascular age-related macular degeneration
NFT Neurofibrillary tangles
NICE National Institute for Health and Clinical Excellence
OCT Optical coherence tomography
ONL Outer nuclear layer
OPL Outer plexiform layer
PAMP Pathogen-associated molecular patterns
PBS Phosphate buffered saline
PED Pigment epithelium detachment
PFA Paraformaldehyde
PI Principal Investigator
PIER Trial Phase IIIb, multi-centre, randomized, double-masked, sham injection-controlled study of efficacy and safety of Ranibizumab in subjects with subfoveal CNV with or without classic CNV secondary to AMD
PIL Patient information leaflet
PRN Pro re nata
PrONTO Prospective Optical Coherence Tomography Imaging of Patients with Neovascular AMD Treated with intra-Ocular Ranibizumab
PRR Pathogen recognition receptor
R&D Research and development
RAP Retinal angiomatous polyposis
REC Research Ethics Committee
ROS Reactive oxygen species
RPE Retinal pigment epithelium
SGH Southampton General Hospital
SIE Systemic inflammatory events
SNP Single nucleotide polymorphism

SRNVM Subretinal neovascular membrane

TNF Tumour necrosis factor

UHS University Hospitals of Southampton

VA Visual acuity

VAS Change VA change from baseline to Visit 7

VEGF Vascular endothelial growth factor

1. Introduction

This chapter presents an overview of the current and projected burden of AMD to healthcare resources and explores the association between AMD and other neurodegenerative diseases such as Alzheimer's disease. This relationship offers the possibility of defining specific factors which influence disease progression and alter prognosis. I also hope to explore a novel therapeutic target for AMD treatment utilising a murine model of AMD.

1.1 Epidemiology of AMD

AMD represents a huge burden to national healthcare planners. It is the leading cause of blindness in the developed world and the third most common cause of severe visual impairment worldwide[1]. This trend of increasing prevalence of AMD is set to rise with a progressively ageing population[2]. There are currently 26 000 new cases of AMD in the United Kingdom (UK) per year[3]. The two main forms of advanced AMD are responsible for two-thirds of severe sight impairment registrations in the UK with 250 000 adults being affected[4, 5]. The estimated prevalence in the UK population for late AMD is 4.8% (95% CI 3.4% to 6.6%) of those over 65 years of age and 12.2% (95% CI 8.8% to 16.3%) of those aged 80 years or more in the UK[6]. The current estimate of patients affected with AMD is 50 million worldwide of which 14 million are blind or partially sighted[7].

The current cost of a single ranibizumab (Lucentis®) (Genentech, South San Francisco, California, USA) injection for the treatment of AMD is £761. This is equivalent to £6398 per year per person with AMD for treatment in the UK[8]. At the time of the study, ranibizumab was the only licensed drug available for treatment of neovascular AMD. Aflibercept (Eylea) (Bayer Cambridge, UK) has since been approved by the National Institute for Health and Care Excellence (NICE) for treatment of neovascular AMD.

1.2 Anatomy of the posterior pole

The section below details the macroscopic and microscopic histology of the human eye with an emphasis on the retina and macula (Figure 1).

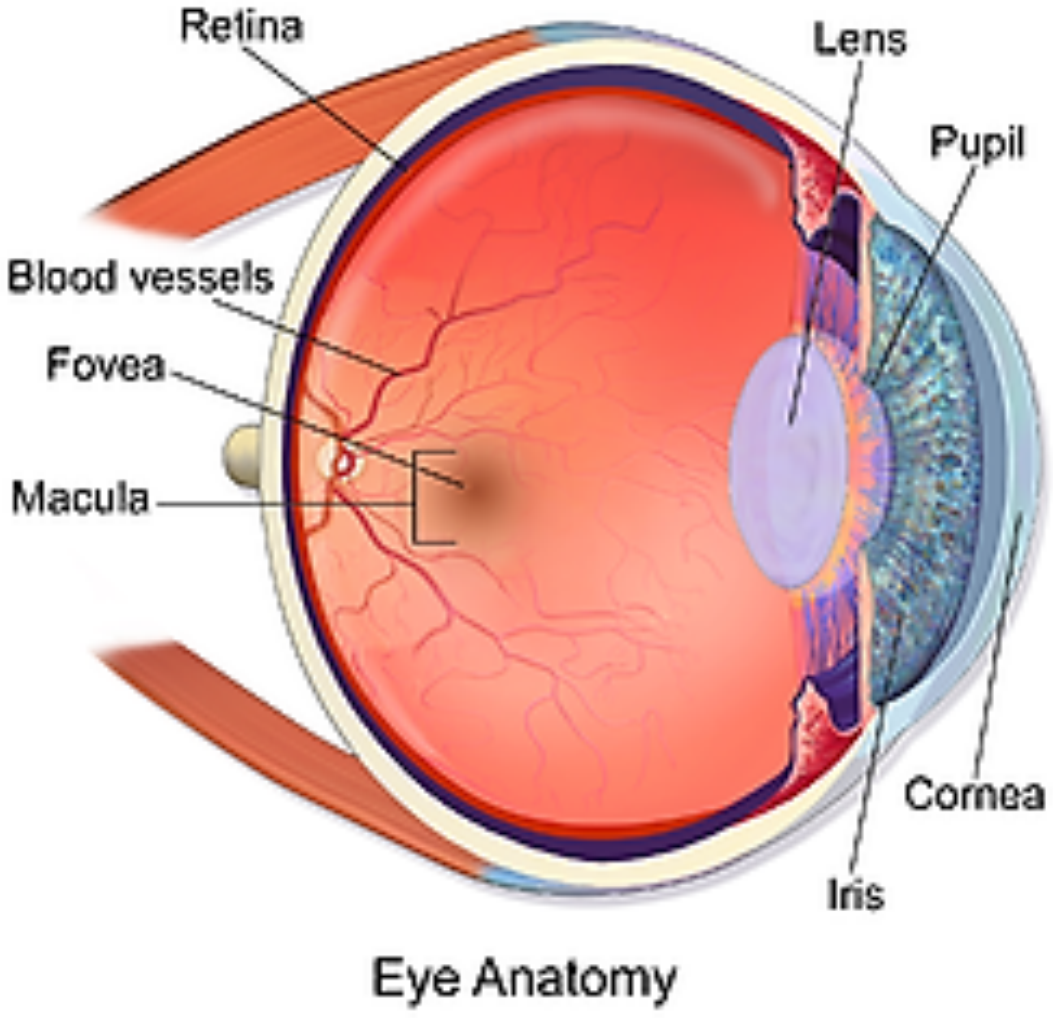

Figure 1 Diagram of the human eye. Diagram representing the gross anatomical components of the human globe. The composite diagram illustrates the anatomic location of the main structues of the human eye. Adapted from Blausen.com staff. "Blausen gallery 2014". Wikiversity Journal of Medicine. DOI:10.15347/wjm/2014.010. ISSN 20018762.

1.2.1 The retina

The eye has often been compared to a camera with the retina and more specifically, the macula being described as the film (pre-digitalization). This simplistic representation should be expanded.

The retina consists of two layers of tissue that line the posterior segment of the globe. There is a transparent neurosensory layer and pigmented retinal pigment epithelium (RPE) layer that extend from the optic disc posteriorly to the ora serrata anteriorly where the two layers become continuous with the bilayered ciliary body.
The retina is approximately 266mm^2 in surface area and at its thickest surrounding the optic disc. The thinnest portion is located at the ora serrata.

The macula is located at the posterior pole of the globe and consists of an area of specialized retinal tissue devoid of blood vessels approximately 5-6mm in diameter (Figure 2). At the centre, lies the fovea with a central depressed area represented by the foveola and is approximately 1.5mm in diameter. The fovea is essential for spatial discrimination, colour vision and fine visual acuity as it has the highest density of cones in the macula[9]. Anatomical features such as lack of vascularity, absence of rod cells and peripheral displacement of overlying inner retinal tissue also assist in this dedicated role[10].

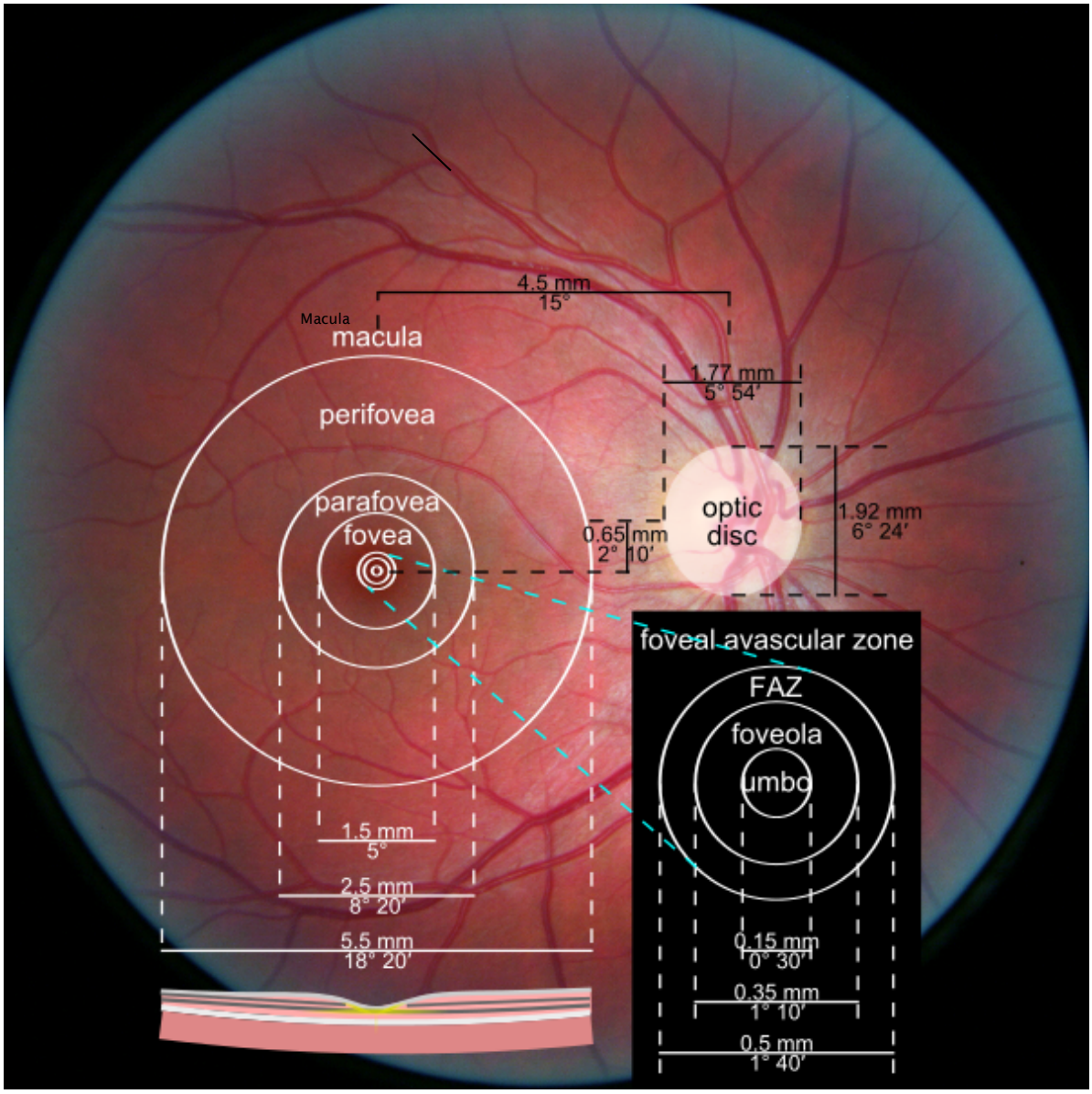

Figure 2 Human retina. Fundus photograph of the human retina illustrating the macula region and central fovea. This highlighted region is primarily responsible for the majority of visual processing and is the main focus of AMD pathology. The macula is surrounded by arcades of blood vessels that radiate from the optic nerve supplying the innermost layers of the retina. The illustration above demonstrates the relative size of the areas described. Photograph courtesy of Danny Hope (Brighton and Hove, UK) and licensed under the Creative Commons Attribution 2.0 Generic license

Retinal microstructure consists of 10 layers of cells or membrane constructs (Figure 3). From inner to outermost, these consist of an internal limiting membrane (ILM), nerve fibre layer, ganglion cell layer, photoreceptor layer and retinal pigment epithelium (RPE)[11].

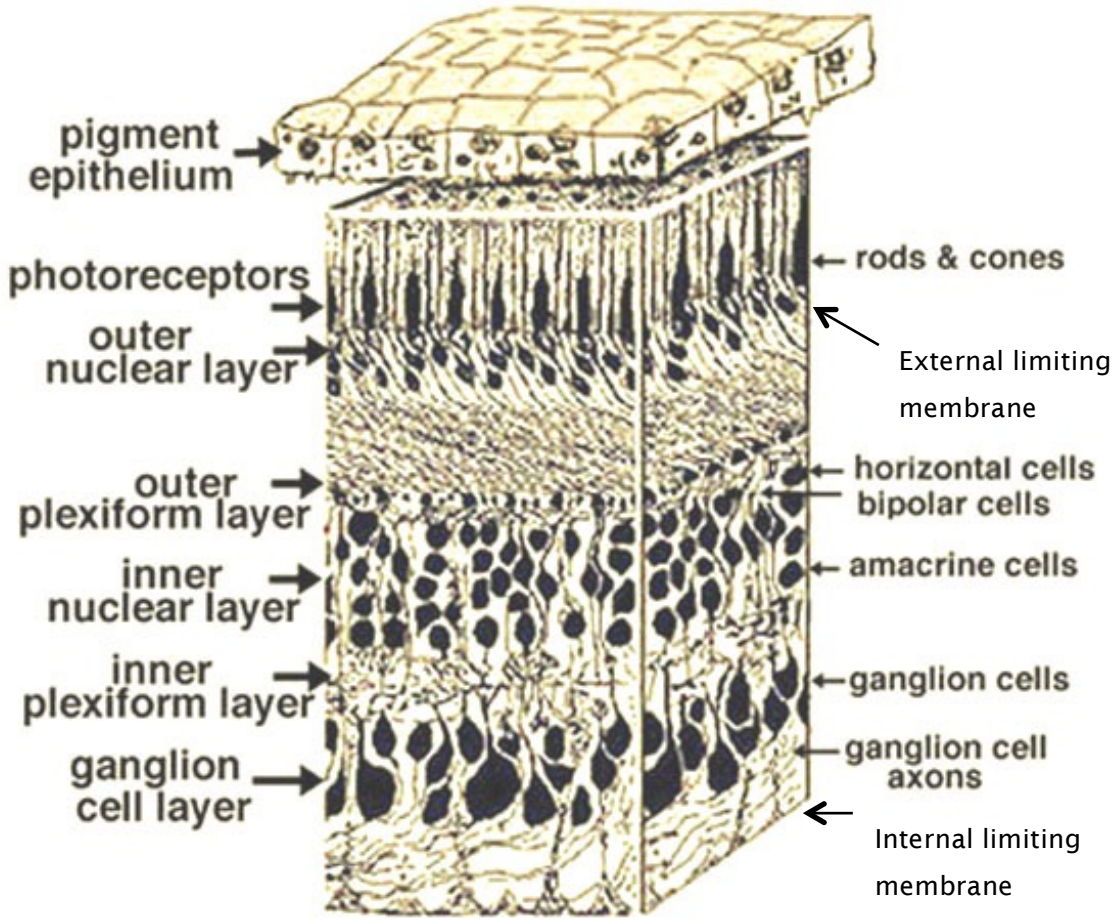

Figure 3 Cross section of human retina. The laminar structure of the transected retina consists of three layers of neuronal cell bodies and two layers of axonal synapses. The outer nuclear layer contains the neuronal cell bodies of the photoreceptors. The inner nuclear layer contains the neuronal cell bodies of bipolar, horizontal and amacrine cells. Ganglion cell bodies are located in the ganglion cell layer. The outer plexiform layer represents axonal connections between photoreceptors, horizontal and bipolar cells. The inner plexiform layer contains dendritic arborizations between bipolar and ganglion cells with horizontal interactions from amacrine cells. Adapted from Webvision, http://webvision.med.utah.edu/

Ganglion cells are responsible for the collating of visual-spatial information received from intermediary horizontal and amacrine cells and relaying it via long axons along the optic nerve, chiasm and tracts to the vision processing centres of the brain. There are also photosensitive ganglion cells responsible for maintaining the circadian rhythm[12].

Bipolar cells communicate information between photoreceptor cells and ganglion cells (via amacrine cells). Each cell specifically forms synapses with either rods (rod bipolar) or

cones (cone bipolar) with 10 different forms of cone bipolar cells but only 1 rod bipolar[13].

Amacrine cells, located within the IPL are responsible for local processing of signals between the photoreceptors and ganglion cells. Horizontal cells act as interneuronal connections between photoreceptors (with contributions from bipolar cells). They therefore, play a role in modulating photoreceptor signal output.

Muller cell bodies are located within the inner nuclear layer of the retina with dendritic extensions across the retina from the outer to inner limiting membrane. Their roles within the retina are extensive:

1. Maintain aerobic metabolism in the nerve cells by supplying end products of anaerobic metabolism.
2. Removal of neural waste products such as carbon dioxide and ammonia and recycle spent amino acid transmitters.
3. Protect neurons from exposure to excess neurotransmitters such as glutamate
4. Phagocytosis of neuronal debris and release of neuroactive substances such as GABA, taurine and dopamine.
5. Synthesis of retinoic acid from retinol
6. Maintain homeostasis and protect neurons from excess extracellular potassium ions.
7. They contribute to the generation of the electroretinogram (ERG) b-wave

The RPE is a pigmented monolayer of cells responsible for active transport of nutrients from the choroid to the photosensitive cells, metabolizes end segments of cone cells, creates a basement (Bruch's) membrane which forms part of the blood retinal barrier and reduces light scattering[14]. The main functions of the RPE layer are outlined in Table 1 below.

Function of the retinal pigment epithelium (RPE)	
Forms part of the blood/retinal barrier through the apical tight-junctions	
Absorbs light energy	Forms a dark pigmented cover that reduces light scatter and improves image quality
Transports ions, water, metabolic end products from the subretinal space to the choroidal blood vessels	The high metabolic turnover of the neurones and photoreceptors leads to a large amount of water and ion production. Water also moves from the vitreous body into the retina
Delivers nutrients from the choroidal blood vessels to photoreceptors	Transports glucose and nutrients from the blood to the photoreceptors
Reisomerizes all-trans-retinal into 11-cis-retinal to allow the visual cycle to continue in photoreceptors	
Phagocytosis of shed photoreceptor outer segments with recycling of retinal to the photoreceptors	The intense exposure of photoreceptors to light leads to the accumulation of photo-damaged proteins and lipids. The photoreceptor outer segments undergo a constant renewal with the tips of the segments being shed and phagocytosed by RPE cells and recycling of molecules essential to phototransduction.
Secretes growth and immunosuppressive factors	These include fibroblast growth factors (FGF-1, FGF-2, and FGF-5), transforming growth factor-□ (TGF-□), insulin-like growth factor-I (IGF-I), ciliary neurotrophic factor (CNTF), platelet-derived growth factor (PDGF), VEGF, lens epithelium-derived growth factor (LEDGF), members of the interleukin and pigment epithelium-derived factor (PEDF)

Table 1 Summary of functions of the RPE. The main functions of the RPE layer as outlined above relate to the ability of the monolayer to improve image quality by

reducing light scatter. This is achieved through the melanosome content of the RPE Table 1 cont'd. cells. RPE cells form part of the blood/retinal barrier through their apical tight-junctions. The monolayer is responsible transporting metabolic end products from photoreceptors to the choroidal blood vessels and nutrients from the choroid to the outer retina. The RPE is integral to phototransduction through catalysing the reisomerization of all-trans-retinal to 11-cis-retinal and the recycling of shed rod photoreceptor outer segments.

The photoreceptor layer consists of 110 to 125 million rod cells and 6.3 to 6.8 million cone cells. The highest density of cone cells is in the fovea with decreasing density to the periphery[15]. The role of photoreceptors will be discussed in greater detail later in the chapter.

The ELM (External Limiting Membrane) is not a true membrane but rather consists of the terminal end plate junctions of the photoreceptors and Muller cells. The ONL (Outer Nuclear Layer) contains the cell bodies of the photoreceptors and is thickest at the macula. The OPL (Outer Plexiform Layer) represents a zone of synapsing dendrites formed between the photoreceptors and second order interneurons e.g. Muller cells. Cell bodies of Amacrine, Muller and Horizontal cells form the INL (Inner Nuclear Layer). It consists of two layers with the horizontal cells forming the external and the remaining cells occupying the internal space. The IPL (Inner Plexiform Layer) contains the dendritic processes from the cells in the INL and ganglion cells. The ganglion cell layer contains the cell bodies of the third order interneurons (ganglion cells). The dendritic processes from these cells arborize in the nerve fibre layer. The ILM is the most internal layer of the retina and is composed of the end foot processes from the Muller cells.

1.2.2 The Choroid

The choroid lies between the retina and sclera. It is a highly vascularized spongiform uveal tissue which extends from the optic disc to the ora serrata where it becomes continuous with the ciliary body[16]. There are four layers within the choroid:

1. Suprachoroid: Lies between the sclera and stroma. It mainly contains collagen fibres which connect the choroid to the sclera.
2. Stroma: Consists mainly of large venous channels as well as unfenestrated arteries of varying sizes within a fibrous meshwork.
3. Choriocapillaris: A layer comprising of an extensive network of fenestrated capillaries.
4. Bruch's membrane: A pentalaminar structure containing the basement membrane of the RPE, the inner collagenous zone, elastic layer, outer collagenous zone and the basement membrane of the choriocapillaris.

1.3 Visual processing

The retina is an embryological extension of the brain and shares similarities in its architectural organization and method of neurotransmission. However, the main function of the retina is phototransduction i.e. the conversion of phototic energy into electrochemical impulses[9].

The rod and cone cells have distinctive physiological adaptations that allow light energy to hydrolyse pigments located on the outer segments of the photoreceptor cells. The inner segment of the cells is responsible for synthesis of new pigment molecules and other metabolically active substances.

Each photoreceptor is the first part of a three chained network with photoreceptors forming the first order. Amacrine, horizontal, bipolar and Muller cells are second order interneurons that are responsible for signal modification prior to synapsing with ganglion cells. Axons from these cells form the optic nerve[9].

The visual cycle (or phototransduction cascade) (Figure 4) is an active process that involves phototic energy converting 11-cis retinal into an isomer of higher energy, rhodopsin. The path then follows an active process of biochemical recycling involving both the outer segments of the photoreceptors and the RPE cells[17].

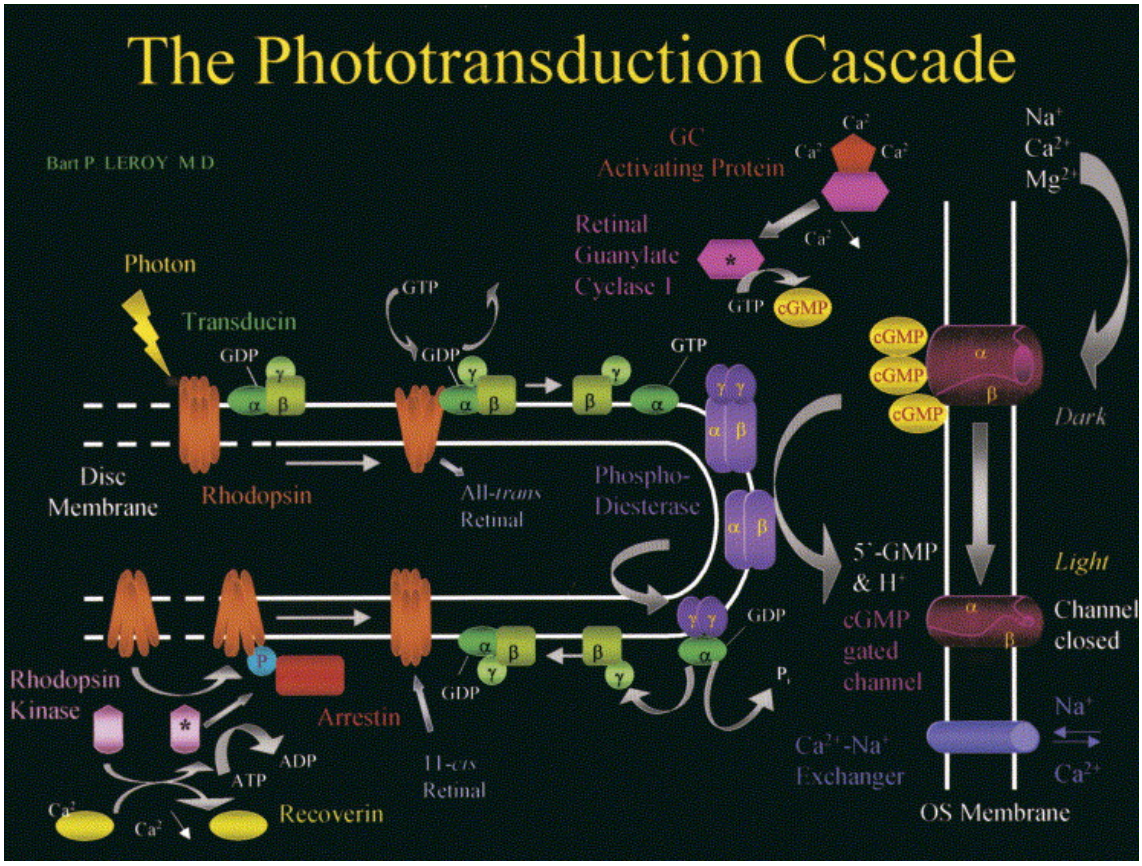

Figure 4 Phototransduction cascade. This diagram represents the main process of phototransduction, a G protein dependent system for amplification of phototic energy signals via secondary chemical messengers. The cascade is initiated by photon absorption by the rhodopsin molecule. The activated rhodopsin molecule catalyses the activation of transducin. Transducin then activates phosphodiesterase via a conformational change of all-trans retinal. Phosphodiesterase hydrolyses cGMP leading to a reduction in cytoplasmic concentration. This leads to a closure of cGMP gated ion channels and subsequent reduced ion flow across outer segment membranes. All-trans retinal is converted to 11-cis retinol in the RPE then to 11-cis retinal via a conformational change. 11-cis retinal is transported to photoreceptors where it is recycled to rhodopsin. Adapted from Koenekoop RK. An overview of Leber congenital amaurosis: a model to understand human retinal development. Surv Ophthalmol 2004;49(4):379-398.

1.4 Classification of AMD

Clinically, most forms of AMD are classified into dry or wet. This has therapeutic implications as no treatment is currently widely available for the dry type of AMD. A more precise classification would be early and advanced divisions with geographic atrophy (GA) and CNV forming subgroups of the advanced form.

Proposed AMD Clinical Classification

Classification of AMD	Definition (lesions assessed within 2 disc diameters of fovea in either eye)
No apparent aging changes	No drusen and No AMD pigmentary abnormalities*
Normal aging changes	Only drupelets (small drusen ≤63 µm) and No AMD pigmentary abnormalities*
Early AMD	Medium drusen >63 µm and ≤125 µm and No AMD pigmentary abnormalities*
Intermediate AMD	Large drusen > 125 µm and/or Any AMD pigmentary abnormalities*
Late AMD	Neovascular AMD and/or Any geographic atrophy

Figure 5 Proposed clinical classification of AMD from the expert panel of the Arnold and Mabel Beckman Initiative for Macular research. The above table outlines the proposed classification for AMD-ranging from no AMD to late AMD. Modified from Ferris FL, III, Wilkinson CP, Bird A et al. Clinical classification of age-related macular degeneration. Ophthalmology 2013;120(4):844-851.

1.4.1 Early AMD

Early phenotypic changes of AMD are characterised by drusen within the macular region with or without focal RPE hyperpigmentation[18] (Figure 6). The earliest detectable histopathological changes occur in the RPE with focal basal laminar (BlamD) and basal linear (BlinD) deposits. BlamD is a membranogranular accumulation on the basement membrane of the RPE. BlinD is a vesicular deposit within the inner collagenous zone of Bruch's membrane and its presence correlates strongly with AMD progression[18-20].

Drusen are formed from deposits of a variety of waste lipid and glycoprotein extracellular material from photoreceptor metabolism that lie between the basal lamina of the RPE basement membrane and the inner collagenous layer of Bruch's membrane[21-23].

Clinically drusen are defined as either hard or soft (≥ 63µm) depending on their ophthalmoscopic and characteristic fundus fluorescein angiography (FFA) appearance. Large numbers of drusen, especially soft confluent drusen within the macular region

represent a significant risk factor for the development of advanced AMD[24]. This proportion of people found to transform from early to advanced AMD 12.9% for confluent macular drusen and 17.8% for RPE pigmentary changes[25].

Protein isolated from drusen

Clusterin	Novel leucine-rich protein
TIMP3	Vimentin
Serum albumin	Crystallin, beta B1
Vitronectin	Lactoglobulin, beta A chain
Complement component 9	Clusterin
Actin, beta	Complement component 9
Annexin II	Crystallin, alpha B
Histone H2B C	Crystallin, beta A3
Lactoglobulin, beta A chain	Vitronectin
Apolipoprotein E	Crystallin, beta A4
Complement component 3	Crystallin, beta B2
Complement component 8	Crystallin, beta S
Histone H2Ao	Haemoglobin beta 2
Serum amyloid P	Histone H2A2
AMBP protein	Serum albumin
Histone H2A2	TIMP3

Table 2 Common proteins isolated from drusen by mass spectrophotometry. The table above identifies the most common proteins isolated by mass spectrometry in drusen. Modified from Crabb JW, Miyagi M, Gu X et al. Drusen proteome analysis: an approach to the etiology of age-related macular degeneration. Proc Natl Acad Sci U S A 2002;99(23):14682-14687.

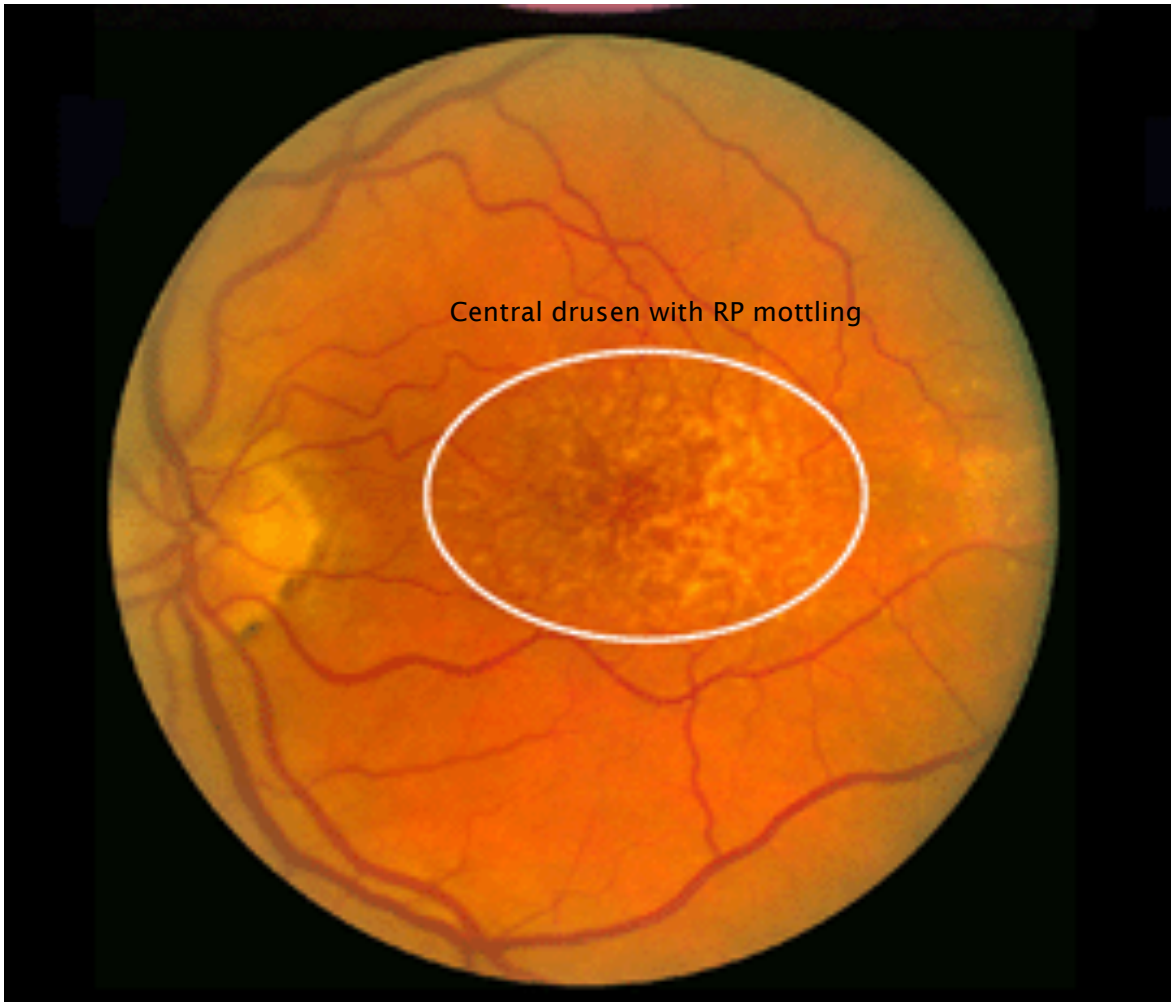

Figure 6 Colour fundus photo of early AMD changes with highlighted drusen and RP mottling at the macula. Modified from Webvision, http://webvision.med.utah.edu/

1.4.2 Advanced AMD

Advanced AMD is subclassified into geographic atrophy (GA) and choroidal neovascularization (CNV) or wet AMD. These conditions are discussed in the following sections.

1.4.2.1 Geographic atrophy (GA)

GA refers to areas within the macular region with RPE cell death and overlying neuroretinal atrophy[26, 27] (Figure 7). It is a demarcated area within the macular region representing loss of underlying RPE. The disease process tends to be slow with the foveal region often spared until late stages of the disease[18, 28, 29, 30]. The two advanced forms of AMD can develop concurrently[31].

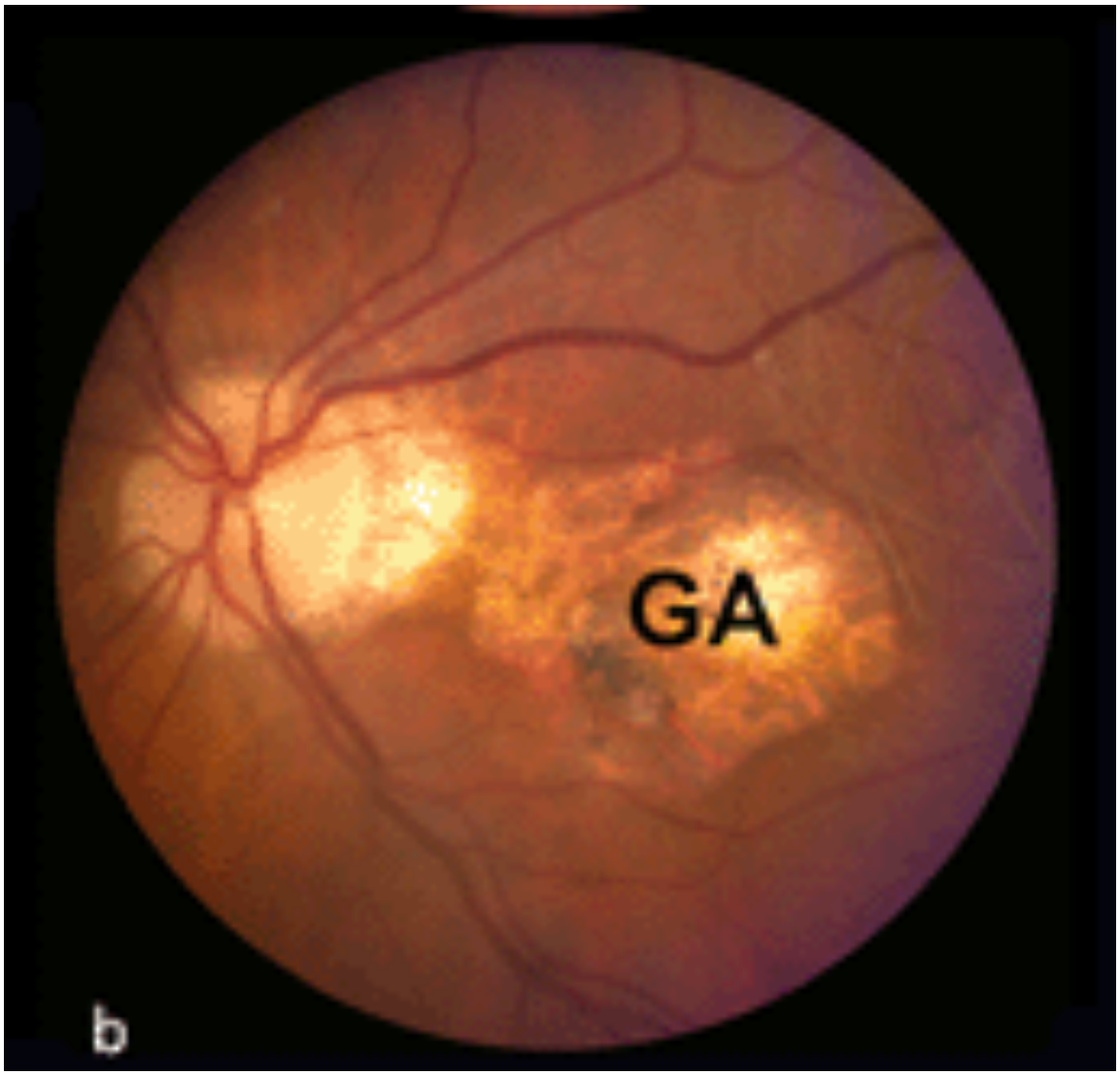

Figure 7 Colour fundus photo of geographic atrophy (GA) located at the macula highlighting overlying neuroretinal degeneration and scleral reflectance and visible choroidal vessels on fundoscopy. Adapted from Webvision, http://webvision.med.utah.edu/

1.4.2.2 Choroidal neovascularization (CNV)

CNV is the abnormal growth of blood vessels from the choroid through Bruch's membrane[32]. They may either subsequently penetrate the RPE or remain subretinal. These vessels are highly permeable and allow exudate and often whole blood to extravasate into the subretinal space. This creates a characteristic appearance on FFA which allows for diagnosis and classification of the process[33].

Retinal angiomatous polyposis (RAP) is a relatively rare form of CNV and occurs when abnormal blood vessels grow from the neurosensory retina into the choroidal space[34, 35]. This creates a picture of punctate haemorrhages on fundoscopy and can lead to a disciform scar formation in advanced disease.

Retinal pigment epithelium detachments (PED) are formed from large areas of confluent drusen that subsequently develop a serous detachment of the RPE. A high proportion of these patients subsequently develop CNV[36, 37].

The end stage of these neovascular processes is fibrosis and scar formation (Figure 8) often associated with a subretinal haemorrhage (Figure 10).

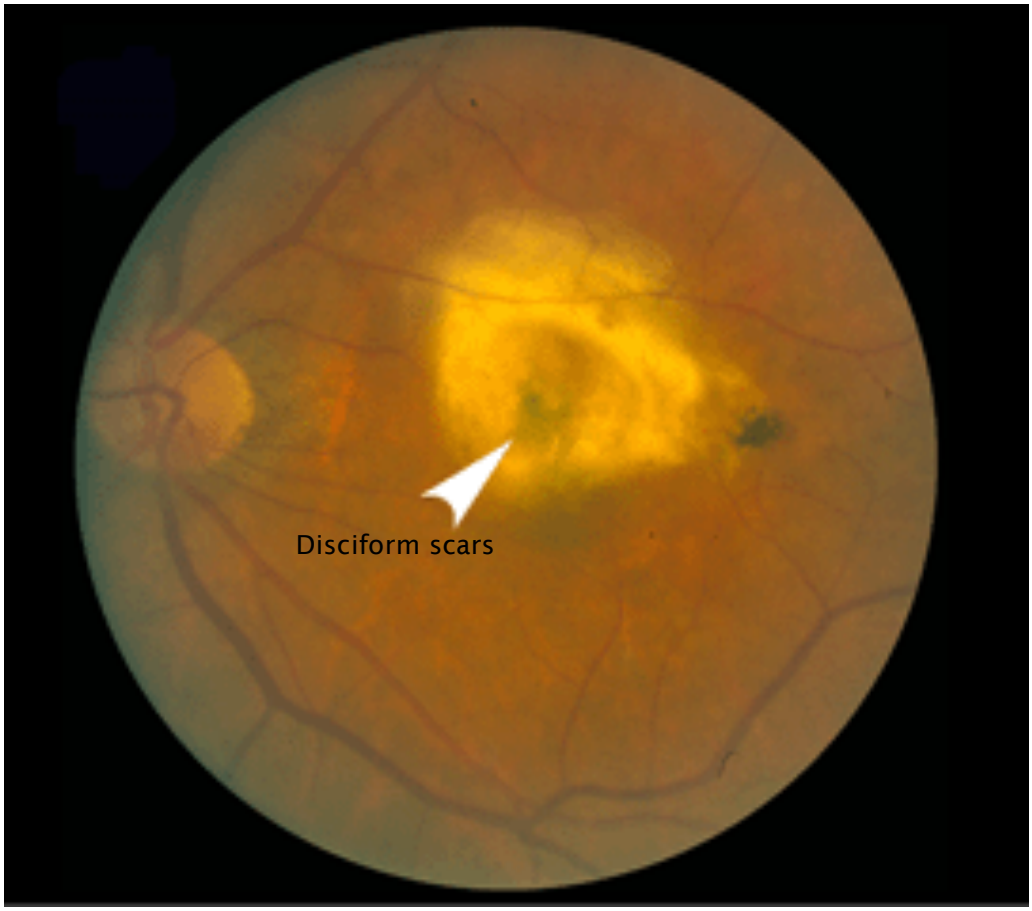

Figure 8 Disciform scar. Colour fundus photo of a disciform scar (indicated by arrow) at the macula in advanced wet AMD. Adapted from Webvision, http://webvision.med.utah.edu/

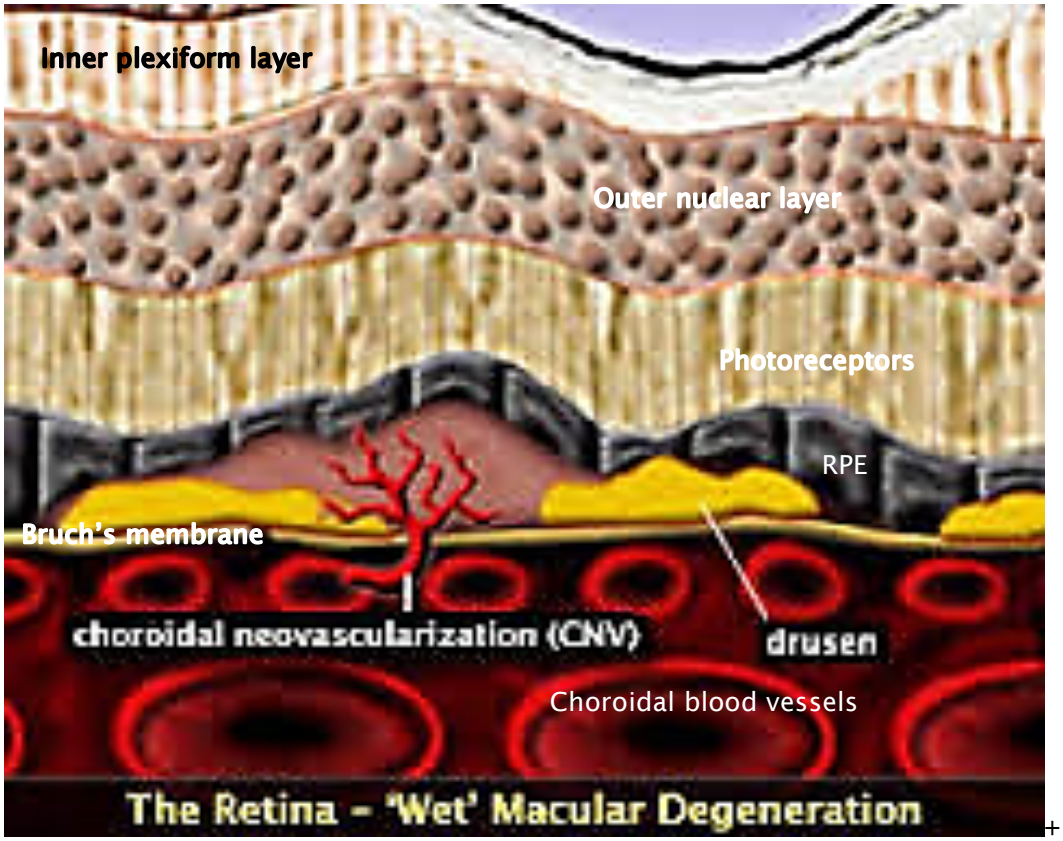

Figure 9 Diagram of choroidal neovascularization. Figure illustrating choroidal new vessels extending through breaks in Bruch's membrane into the sub RPE space. Modified from Invest Ophthalmol Vis Sci. 2009 Oct;50(10):4982-91 Relationship between RPE and Choriocapillaris in Age-Related Macular Degeneration. D. Scott McLeod, Rhonda Grebe, Imran Bhutto, Carol Merges, Takayuki Baba and Gerard A. Lutty

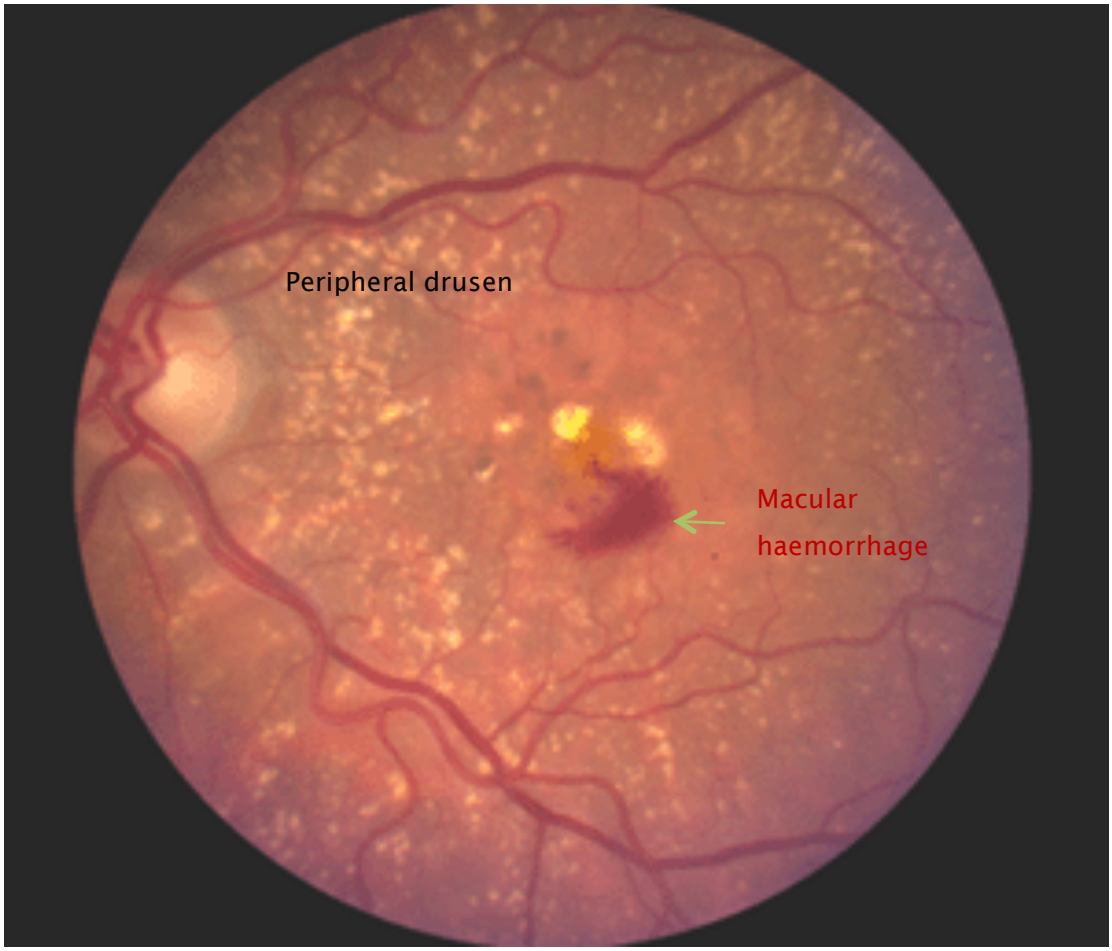

Figure 10 Macular haemorrhage. Colour fundus photo of a macular haemorrhage resulting from active CNV. Modified from Webvision, http://webvision.med.utah.edu/

Dry AMD (GA)	Wet AMD (CNV)
Slow progression of visual loss	Rapid progression
Early stage is characterized by drusen deposition and RPE migration	Early stage is characterized by drusen deposition and RPE migration
Characterized by loss of retinal photoreceptors, choriocapillaris and RPE	Characterized by loss of retinal photoreceptors, choriocapillaris and RPE
Expansion of circumscribed areas of outer retinal atrophy within the macula	Development of choroidal new vessels that advance through breaks in Bruch's membrane

Table 3 Comparison of GA and CNV. This table demonstrates the main differerences between the gross and microscopic changes between GA and CNV- The advanced stages of AMD are characterised by a slow progression of central visual loss in GA whereas wet AMD often develops a rapid progression of symptoms. Both forms of the advanced disease are characterised by drusenogenesis and RPE cell migration from the outer to inner retina. Choroidal new vessels develop under influence of VEGF and related angiogenic molecules. NLRP3 inflammasome and Il-18 suppression have been implicated GA progression.

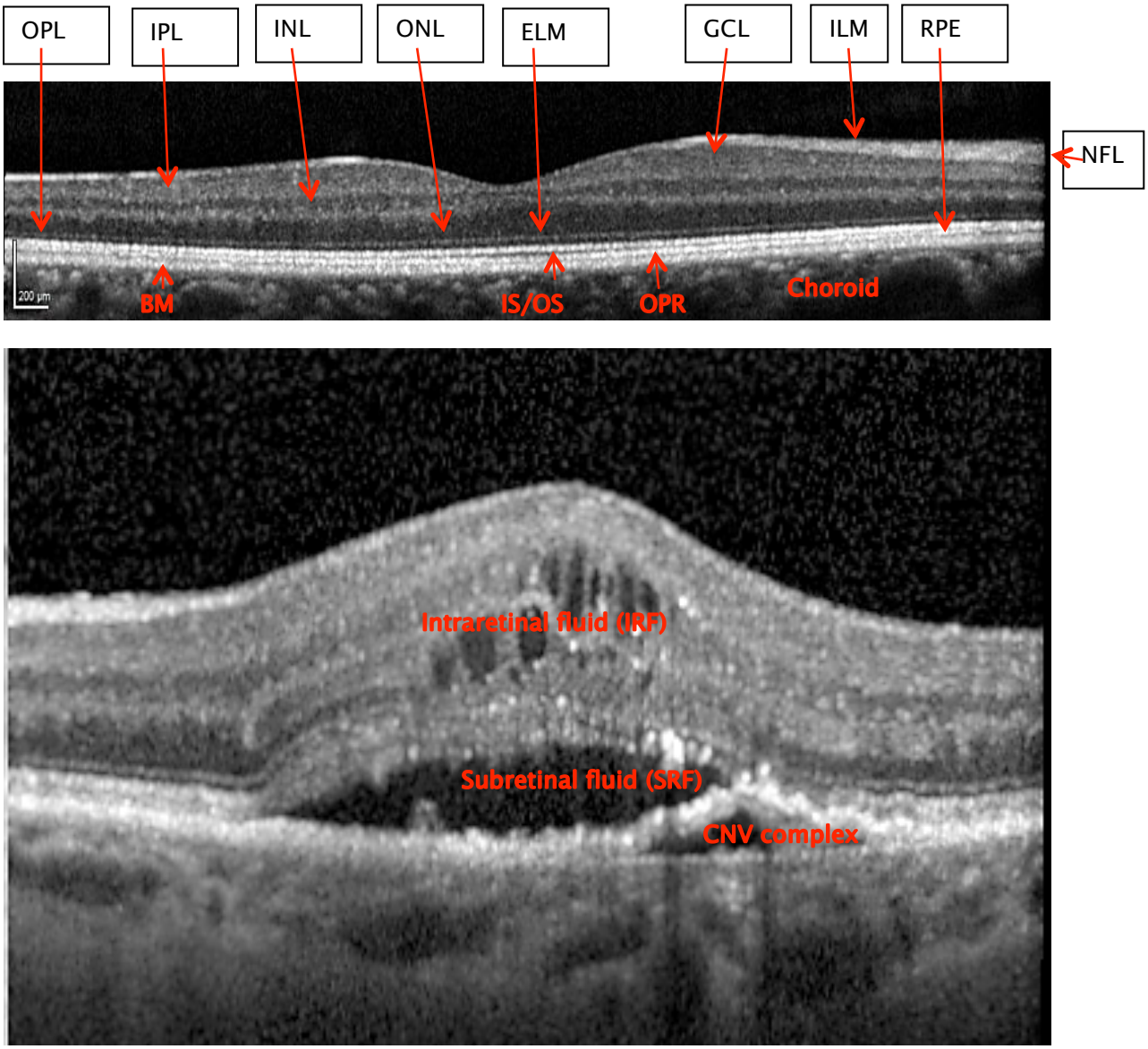

Figure 11 OCT of normal and AMD affected retina. The bands of hyper- and hyporeflective layers represent an optical cross section of the retina. (NF)- nerve fibre layer, (GCL)- ganglion cell layer, (IPL)- inner plexiform layer, (INL)- inner nuclear layer, (OPL)- outer plexiform layer, (ONL)- outer nuclear layer, (ELM)- external limiting membrane, (IS/OS)- inner segment/outer segment junction of photoreceptors, (OPR)- outer photoreceptor/RPE junction, (BM)- Bruch's membrane.

1.5 Pathogenesis of AMD

This section reviews the main risk factors in the development of AMD. I examine the local and systemic factors involved in the pathogenesis of the disease.

1.5.1 Ocular risk factors for advanced AMD development

Drusen (>125μm) are the main precursor lesions of advanced AMD in combination with RPE pigmentary changes and the presence of advanced AMD in one eye[5]. Based on this, a scoring classification was developed (Table 4):

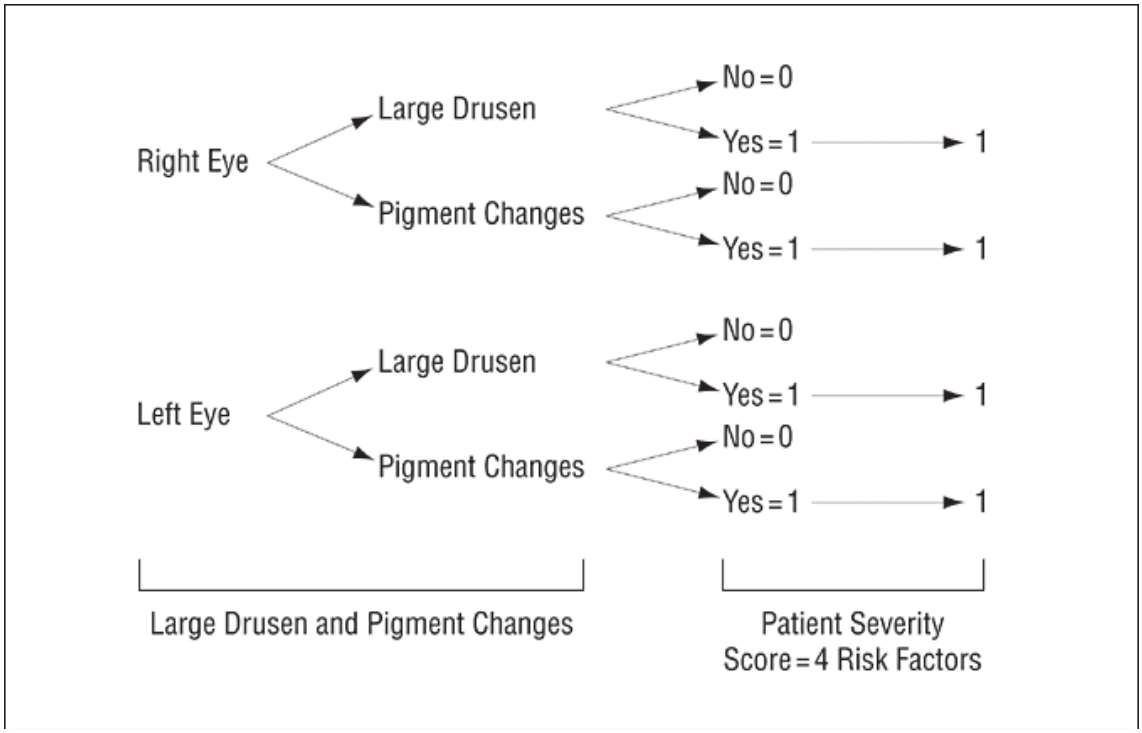

Figure 12 Flow chart demonstrating calculation of risk score. The figure provides a scoring system for the calculation of risk of CNV development based on the presence or absence of large drusen, pigmentary RP changes and advanced AMD in the fellow eye. Adapted from Ferris FL, III, Wilkinson CP, Bird A et al. Clinical classification of age-related macular degeneration. Ophthalmology 2013;120(4):844-851.

Score	Risk
0	0.5%
1	3%
2	12%
3	25%
4	50%

Table 4 Risk of developing advanced AMD based on score. This table outlines the risk of development of advanced AMD from the risk score calculation in Figure 12. The risk of development of advanced AMD ranges from 0.5% for a score of 0 to 50% for a score of 4. Adapted from Ferris FL, III, Wilkinson CP, Bird A et al. Clinical classification of age-related macular degeneration. Ophthalmology 2013;120(4):844-851.

The presence of advanced AMD in 1 eye confers a baseline risk score of 2 for progression in the fellow eye. Figure 12 above demonstrates the calculation of risk score.

1.5.2 Non ocular risk factors for advanced AMD development

AMD follows the pattern of many degenerative diseases whereby the pathological causes is multifactorial[38, 39]. There is a complex interaction between genetic and environmental factors which alters an individual's risk of developing the disease[40, 41].

Smoking confers a two to three times increased risk of developing advanced AMD. This is a dose-dependent relationship correlating to the number of packyears[42]. Smoking has long been an established risk factor in AMD progression linked to an increase in oxidative stress on RPE cells mainly through the generation of reactive oxygen species[43-45].

Dietary intake may also play an essential role. The Age Related Eye Disease Study (AREDS) demonstrated a reduced risk of progression from early to late stage AMD in patients taking zinc antioxidant supplements (adjusted odds ratio 0.68; 99% confidence intervals 0.53 to 0.87). This cohort of patients had significant risk factors for developing advanced AMD[44, 46]. In addition, several studies have also demonstrated a positive effect of diets rich in Omega fatty acids[47-49] (pooled odds ratio [OR], 0.62; 95% CI 0.48 to 0.82). Conversely, diets high in saturated fats and obesity have been linked with disease progression[50-52].

The development of atherosclerosis has been associated with a chronic local inflammation leading to endothelial cell dysfunction and accumulation of extracellular deposits of lipids and lipoproteins[53]. These are important constituents of both drusen and atherosclerotic plaques[54, 55]. Complement system dysregulation is an important factor in the generation of reactive oxygen species, a process seen also in AMD[56, 57]. This process is demonstrated histologically by the presence of complement system proteins in both drusen and atherosclerotic plaques[58]. Similar to AMD, macrophage recruitment is essential to early development of the pathological process and progression of the disease[59].

A meta-analysis of the relationship between AMD and hypertension demonstrated a statistically significant relationship (OR 1.48, 95% CI 1.22 - 1.78)[60]. The presumed mechanism relates its effect on choroidal circulation[61]. Choroidal thickness is reduced in both AMD and hypertension[62].

Local risk factors	Systemic risk factors
Phototic exposure	Smoking
High metabolic activity of retina leading to highly reactive oxygen species generation	Obesity
Failure of microglial clearance of waste products of RP metabolism	Hypertension
Failure of RPE autophagy leading to lipofuscin accumulation	Hypercholesterolaemia
	Increased age
	(Genetics)

Table 5 Summary of risk factors for AMD development. This table summarises the main local and systemic factors associated with the development of CNV. The main systemic factors highlighted are smoking measured in pack years, individual BMI, systemic hypertension, hypercholesterolaemia, advanced age and genetic predisposition. The local risk factors refer to conditions within the photoreceptor/RPE microenvironment that lead to the development of advanced AMD. High levels of ultraviolet exposure and metabolic activity lead to the generation of reactive oxygen species and a chronic inflammatory process. Failure of microglial clearance and RPE autophagy contribute to lipofuscin accumulation and a nidus for drusen development.

1.5.2.1 Genetics of AMD

A family history of AMD confers an increased risk of the disease. The population attributable risk for a positive family history is 0.34 with the highest risk being an affected parent (0.56)[44]. The genetic influence on AMD development is multifactorial in origin. However, genes associated with inflammation have been one of the main areas under investigation (Table 6).

Gene name	Variants	Odds ratio for risk of AMD	Association *P* value	Positive studies	Cases	Controls	Function of gene	References
Genes with only positive findings								
Complement factors B and C2	Haplotypes H1 (increased risk)	1.32	0.0013	1	900	400	Complement regulators	(Gold et al. 2006)
	Haplotypes H7	0.45	<0.0001					
	H10 (decreased risk)	0.36	<0.0001					
CST3	Genotype B/B	2.97	0.037	1	167	517	Cysteine protease inhibitor	(Zundel et al. 2002)
CX3CR1	I249 and M280	3.57	0.04	1	85	105	Chemokine receptor	(Tuo et al. 2004)
FBLN5	Seven missense variants	Not stated	<0.01	1	402	429	Extracellular-matrix protein	(Stone et al. 2004)
TLR4	D299G	2.65	0.025	1	667	439	Toll-like receptor	(Zareparsi et al. 2005b)
VEGF	Five SNPs	4.13	0.002	2	399	159	Vascular endothelial growth factor	(Haines et al. 2006)
	Haplotype analysis	18.24	0.0074		45	94		(Churchill et al. 2006)
LRP6	Five SNPs	1.76	0.004	1	399	159	Interacts with APOE	(Haines et al. 2006)
MMP9	Promoter ca repeat	3	<0.0005	1	107	223	Degrades extracellular matrix	(Fiotti et al. 2005)
HTRA1	rs11200638	10	10^{-11}	4	>1,000	>1,000	Serine protease	(Cameron et al. 2007; De Wan et al. 2006; Yang et al. 2006; Yoshida et al. 2007)
HLA	Cw0701	1.85	0.036	1	100	92	Regulate immune response	(Goverdhan et al. 2006)
	B 4001	0.39	0.027					
	DRB11301	0.31	0.009					
Gene name	Variants	Association *P* value	Number of studies	Cases	Controls	Function of the gene	References	
Genes with conflicting findings								
APOE	e4							
	Positive studies	*P* < 0.01	5	>1,000	>1,000	Cholesterol transport to liver	(Baird et al. 2004b; Schmidt et al. 2002; Simonelli et al. 2001; Souied et al. 1998; Zareparsi et al. 2004)	
	Negative studies	NS	6	>1,000	>1,000		(Conley et al. 2005; Gotoh et al. 2004; Pang et al. 2000; Schmidt et al. 2005; Schulte et al. 2006a; Wong et al. 2006)	
ABCA4	Multiple missense changes							
	Positive studies	*P* < 0.0001	≥2	>1,000	>1,000	Outwardly directed flippase for *N*-retinylidene-PE in photoreceptors	(Allikmets 2000; Allikmets et al. 1997a)	
	Negative studies	NS	5	>1,000	>1,000		(De La Paz et al. 1999; Guymer et al. 2001; Souied et al. 2000; Stone et al. 1998; Webster et al. 2001)	

Gene name	Variants		Association *P* value	Number of studies	Cases	Controls	Function of the gene	References
CFH	Y402H	Positive studies	$P < 10^{-11}$	>7	>1,000	>1,000	Key regulator of alternative complement pathway	(Edwards et al. 2005; Hageman et al. 2005; Haines et al. 2005; Klein et al. 2005; Lau et al. 2006; Simonelli et al. 2006; Zareparsi et al. 2005a)
		Negative studies	NS	2	213	212	Negative in 2 studies of Japanese patients	(Gotoh et al. 2006; Ulta et al. 2006)
HEMICENTIN-1	Gln6346Arg	Positive studies	Not stated	1	One large family (27 members)	174	Fibulin gene	(Schultz et al. 2003b)
		Negative studies	NS		>1,000	>1,000		
PON1	Leu-Met54	Positive study	0.009	1	72	140	Prevents low-density lipoprotein oxidation	(Abecasis et al. 2004; Conley et al. 2006; Hayashi et al. 2004; Iyengar et al. 2004; McKay et al. 2004; Setoguchi et al. 2006; Stone et al. 2004)
	Gln-Arg192	Negative study	0.0127	1	72	140		(Ikeda et al. 2001)
		Negative study	NS	1	94	95		
			NS	1	62	115		
ELOVL4	Met299Val		<0.0001	1	196	120	Mutated in Stargardt like autosomal dystrophy	(Conley et al. 2005)
ACE	Alu(+/+)	0.22	NS		245	243		(Baird et al. 2004a; Esfandiary et al. 2006)
			NS		778	551		(Zhang et al. 2001)
			0.004		173	189	Angiotensin converting enzyme	(Ayyagari et al. 2001)
			NS		338 families			(Hamdi et al. 2002)
			NS		196	120		(Conley et al. 2005)
			NS		162 families			(Haines et al. 2006)
			NS		399	159		(Haines et al. 2006)
SOD2		10.14	0.0005		102	200	Intramitochondrial free radical scavenging enzyme	(Kimura et al. 2000)
			0.71		94	95		(Esfandiary et al. 2006)

Table 6 Summary of recent genetic studies in AMD subgrouped into genetic markers with only positive findings and those with confounding findings. Adapted from Lotery

Table 6 cont'd. A, Trump D. Progress in defining the molecular biology of age related macular degeneration. Hum Genet 2007;122(3-4):219-236.

1.5.2.1.1 *SERPING1*

In 2008, Ennis *et al.* in their seminal paper published in the Lancet provided evidence that the gene *SERPING1* which codes for C1 inhibitor was associated with AMD development[63]. C1 inhibitor is important as a modulator of the classical component of the complement pathway[64]. It is a serine protease that prevents activation of complement components 2 and 4 (by inhibiting complement component C1) and ultimately resulting in several downstream effects on the complement cascade. It is also responsible for inhibiting other serine proteases such as plasmin, kallikrein and coagulation factors Xia and XIIa[65]. The most widely known clinical association is Herditary Angioedema (HAO), resulting from reduced functional levels of C1 inhibitor[66].

479 cases and equal number of controls were recruited for the study. 233 of the cases had active CNV. 93 SNPs from 33 genes were screened. The rs2511989 SNP of *SERPING1* found in intron 6 was highly associated with protection from AMD development after Bonferoni correction. This finding was replicated in a US cohort of patients[66]. However, independent studies following have shown no significant relationship between the rs2511989 SNP and AMD ($p>0.3$ in all cohorts)[67-69]. This was true for all forms of CNV subtypes. A recently reported study has shown an elevation of serum C1 inhibitor in patients with AMD (particularly advanced AMD) compared to controls[70]. This has a direct relation to my experimental model, where I will try to determine the role of C1 inhibitor in a murine model of AMD.

1.5.2.1.2 *Complement*

Many studies have demonstrated the presence of complement components in drusen and RPE cells of patients with AMD[55, 71, 72]. Complement factor H (CFH) is a negative regulator of complement activation[73]. Single nucleotide polymorphisms (SNPs) associated with CFH are known to influence AMD[74, 75]. The Y402H SNP for *CFH* is a major risk factor for AMD development[73, 76]. The protein product has a reduced binding affinity to inflammatory molecules such as CRP leading to a significantly reduced level of effectiveness[77].

There have been numerous studies to identify a relationship between the risk complement alleles and subtypes of CNV or GA[78-80]. The results have shown no conclusive evidence of an association. There has however, been an established

relationship between basal laminar drusen and the Y402H allele[81]. My study will also address this problem, with a view to determine if a relationship exists between complement risk alleles, CNV subtypes and response to current anti-VEGF therapy with ranibizumab (Lucentis®; Genentech, South San Francisco, California, USA) (see page … for details of anti-VEGF drugs).

The relationship between progression from early to late AMD has also been previously explored. The risk alleles of *CFH* and *C3* have been reported to be associated with progression. There have been retrospective studies that investigated both the response of AMD patients treated with bevacizumab and ranibizumab[82, 83]. Their data showed no relationship between visual acuity and the identified genotype. However, they did identify a higher frequency of administered ranibizumab in patients with the homozygous risk Y402H allele (CC). These studies however, were all retrospective as compared to the prospective study reported here.

Recent evidence has shown that infection with Chlamydia Pneumoniae and a CFH risk-associated SNP, results in a significantly higher risk of developing AMD. C Pneumoniae is a potent activator of complement and chronic infection may be responsible for the association with AMD[84-86].

A past history of smoking is the greatest environmental risk factor for AMD. This is additive to and independent of the increased risk conferred by established deleterious complement alleles[87-89]. SNPs encoding complement factor B (CFB), complement component 2 (C2), C3, C7 and factor I (CFI) have all been implicated in AMD pathogenesis[90-93].

1.5.2.1.3 ***Interleukin-8 (Il-8)***

Il-8 is a pro-inflammatory chemokine produced by epithelial cells and acts primarily as a neutrophil chemoattractant. It also stimulates angiogenesis[94]. Goverdhan *et al.* demonstrated a relationship between the *IL8 –251AA* genotype and AMD affected individuals in a case-controlled study[95] associated with increased risk of AMD progression. However, this significant association has not been replicated.

1.5.2.1.4 *Chemokines*

The chemokine receptor CX3CR1 is found on a variety of inflammatory cells especially those native to neural tissue (microglia)[96]. Activation of this receptor leads to stimulation of an immune response and release of further chemokines. AMD affected individuals have been found to have a higher incidence of two genetic polymorphisms for this receptor[97-100].

1.5.2.1.5 *Age-related maculopathy susceptibility 2 (ARMS2) and high temperature required heat-shock protein 1 (HTRA-1)*

Genome wide association and linkage analysis studies have demonstrated significant levels of association with advanced AMD and polymorphisms of this gene[101]. The protein product is expressed in the mitochondria of photoreceptors. The high level of oxidative stress imposed on photoreceptor cells in combination with mitochondrial dysfunction likely leads to AMD progression[102].

The gene for HTRA-1 is also located at locus 10q26 and the *ARMS2/HTRA-1* genes show significant linkage disequilibrium. The exact functional role of HTRA-1 protein in the macula has not been identified. However, several studies demonstrate significant associations with advanced AMD[103].

1.5.2.1.6 *Apolipoprotein E (ApoE)*

ApoE is an essential cell membrane component responsible for transporting low density lipoprotein (LDL) into cells. ApoE is therefore essential in the process of lipid recycling and plays an important role in the metabolically active RPE and photoreceptor cells[104, 105].

ApoE has been found in drusen as well as in higher concentrations of maculae with AMD[104, 106]. The risk conferring SNP (ApoE2 isoform) results in reduced lipid processing and increased lipid accumulation within Bruch's membrane. This leads to thickening and impaired function[107].

1.5.2.1.7 *ATP-binding cassette sub-family, member 4 (ABCA4)*

This gene is responsible for the development of Stargardt's disease which shares phenotypic similarities with AMD. A case study has demonstrated a relationship between allelic variations in this gene and AMD in a small percentage of the cohort[108].

1.5.2.1.8 *Vascular Endothelial Growth Factor (VEGF)*

The first report was in 1983 by Senger *et al.*[109] of a vascular permeability enhancing protein named vascular permeability factor (VPF). In 1989, Connolly *et al.* [110] isolated the VEGF isoforms $VEGF_{121}$, $VEGF_{165}$ and $VEGF_{189}$. Alternative exon splicing is now known to create four main VEGF isoforms ($VEGF_{206}$ was discovered subsequently) of which the 165 amino acid molecule is the most physiologically active[111, 112].

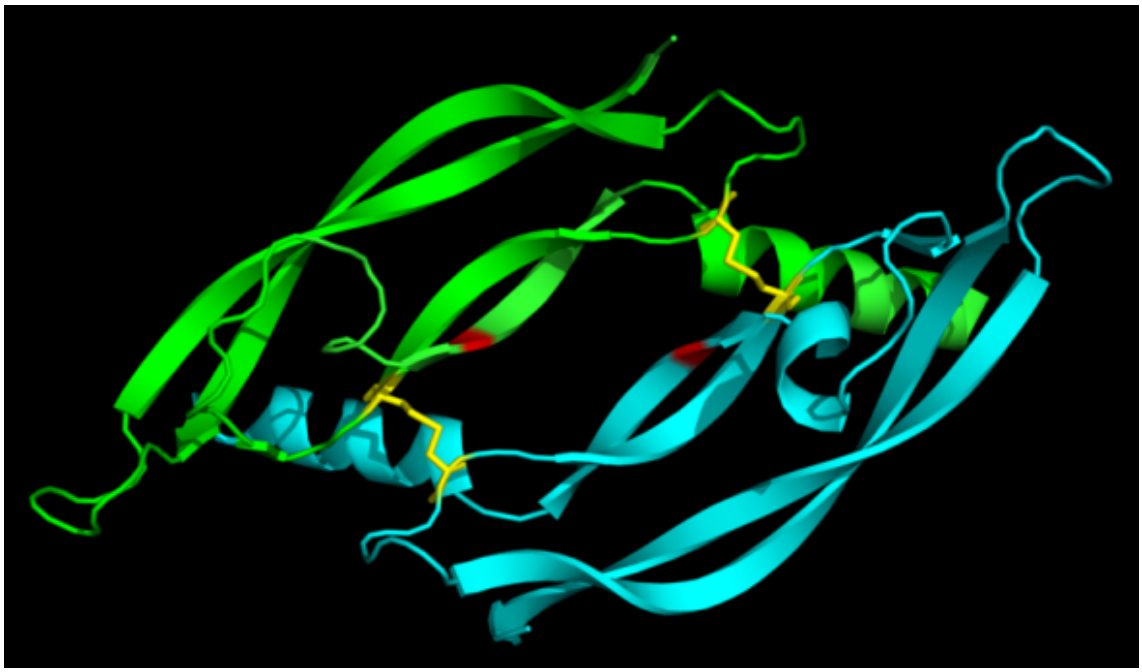

Figure 13 Vascular endothelial growth factor C molecule. A ribbon representation of the receptor-binding domain of VEGF with each monomer labelled in green and blue. Disulphide bonds are indicated by yellow links. Adapted from Pymol rendering of VEGF-C, 27 March 2015 by Michael Jeltsch.

VEGF-A (Figure 13) is a key determinant in the regulation of angiogenesis. *VEGF* belongs to a large gene family that includes *placental growth factor (PLGF), VEGFB, VEGFC, VEGFD and VEGFE*[113] (see Table 7).

The VEGF-A has a number of key properties including promoting endothelial cell growth, angiogenesis and increasing vascular permeability. It also has the effect of promoting endothelial cell survival and altering the morphological characteristics of new vessels e.g. increasing pericyte coverage[113].

There are 2 main receptors of VEGF-A. VEGFR-1 and -2 are both tyrosine kinases of which VEGFR-2 has the greater effect mediating angiogenesis and vascular permeability. VEGFR-1 is implicated in inflammatory cell chemotaxis[113].

This important role of VEGF-A in angiogenesis and more specifically tumour angiogenesis made it a key target as a potential cancer therapeutic agent. This led to the development in 1997, of bevacizumab a full-length monoclonal IgG antibody to VEGF-A[114]. It was approved in 2004 by the US FDA for metastatic colorectal cancer.

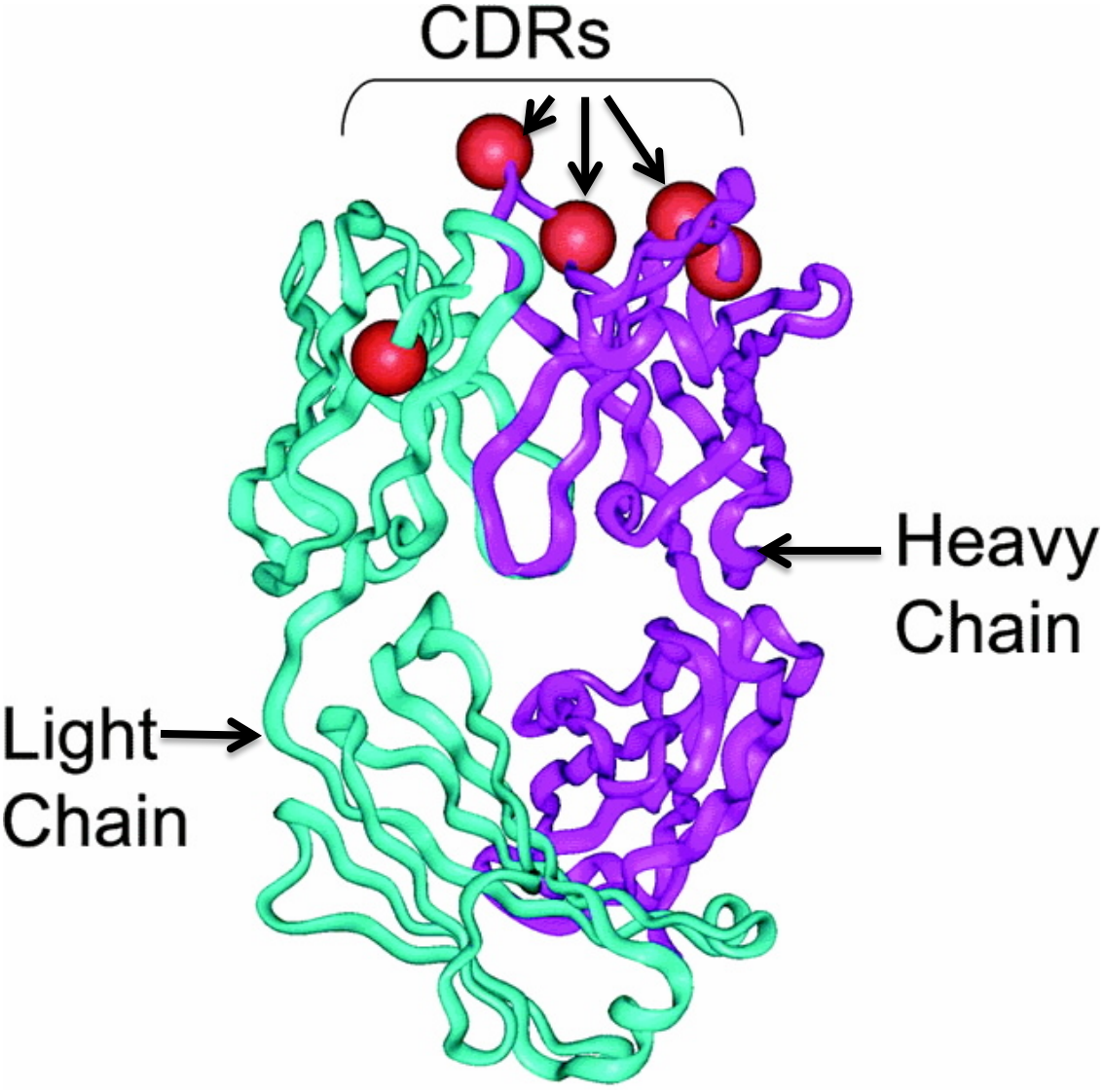

Figure 14 Ranibizumab molecule. A ribbon diagram illustrating the structure of ranibizumab with the red spheres identifying amino acid changes compared to the bevacizumab Fab. CDRs, complementarity-determining regions. Green represents light chain and purple, heavy chain.

In the context of AMD, VEGF overexpression results in angiogenesis producing immature blood vessels which are structurally more fragile due to loss of scaffolding pericytes and increased tortuosity. The vessels are therefore more likely to bleed and allow extravasation leading to photoreceptor death. The direct effect of VEGF to increase vessel permeability likely acts as a positive feedback.

Vascular endothelial growth factor (VEGF) isoform	Function
VEGF-A: The human VEGFA gene is organized as eight exons separated by seven introns. Alternative exon splicing results in four different isoforms ($VEGF_{121}$, $VEGF_{165}$, $VEGF_{189}$, $VEGF_{206}$). $VEGF_{145}$ and $VEGF_{183}$ are less frequent variants	Promotes growth and survival of endothelial cells. Interacts with lymphatics, veins and arteries. Promotes monocyte chemotaxis Increases vascular permeability Induces vasodilation through stimulating endothelial cell nitric oxide production
VEGF-B	Founds primarily in cardiac and skeletal muscle and the pancreas. Implicated in regulating endothelial cell function
VEGF-C	Promotes lymphatic growth and maturation
VEGF-D	Promotes lymphatic growth and maturation
VEGF-E	Stimulates angiogenesis
PlGF	Promotes angiogenesis and macrophage recruitment

Table 7 Function of VEGF isoforms. This table lists the known human VEGF isoforms and their functions. VEGF-A is primarily responsible for endothelial cell growth. It also stimulates monocyte chemotaxis, increases vascular premeability and vasodilation through release of endothelial cell nitric oxide. VEGF-B is produced in cardiac and skeletal muscle and pancreatic tissue. VEGF-C and -D interact with lymphatics. VEGF-E and platelet growth factor (PlGF) both stimulate angiogenesis.

1.5.2.2 Role of Complement in AMD

There has been great progress in elucidating the function of complement in AMD pathogenesis. To present an overview of the complement cascade (Figure 15); it is activated via three main pathways: the classic, lectin and alternate pathways[65].

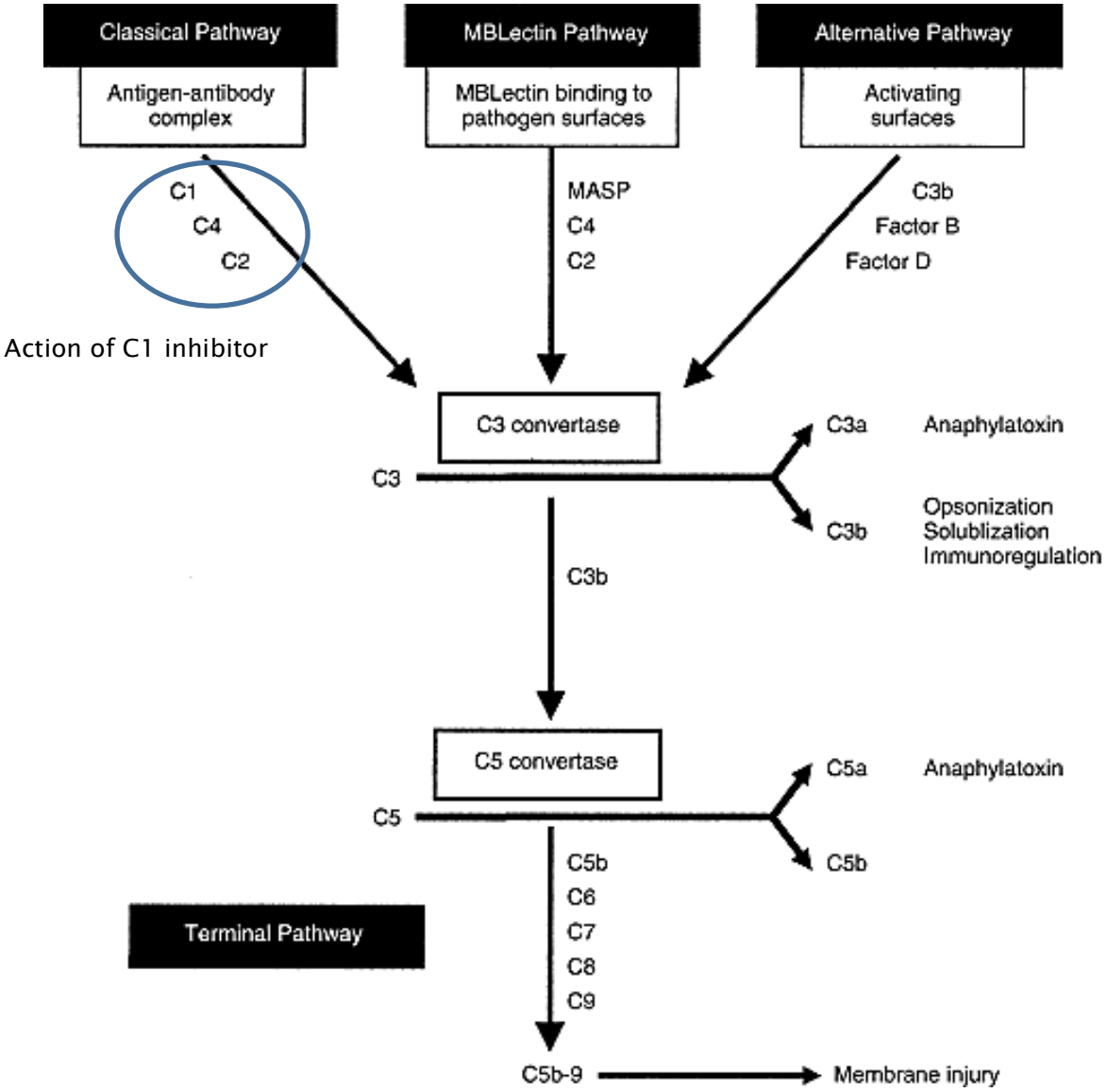

Figure 15 A diagram of the complement cascade. Mannan-binding lectin (MBLectin) in association with the serine protease MBLectin-associated serine protease (MASP) promotes hydrolysis of C4 and C2 leading to further activation of the cascade. Modified from Dunkelberger JR, Song WC. Complement and its role in innate and adaptive immune responses. Cell Res 2010;20(1):34-50.

The entire cascade acts as an amplification system with both positive and negative feedback loops to prevent self-damage. C3 is at the centre of the activation pathway. The main effector molecules are classified into the anaphylatoxins-C3a and C5a, the membrane attack complex (MAC)-C5b-9 and opsonins-C3b[57].

The alternative pathway is activated by the hydrolysis of C3 that occurs spontaneously and constantly into C3a and C3b. C3 also binds to Factor B; Factor D then catalyses the conversion of Factor B to Ba and Bb. C3bBb, also known as C3 convertase increases the conversion of C3 to C3a and C3b. To prevent uncontrolled production of C3a and C3b, regulating factors are present[57].

These factors may prevent the formation of C3 convertase e.g. Factor I, or accelerate the decay of C3 convertase e.g. decay accelerating factor (DAF), complement receptor 1 and complement factor H. There are also regulators that affect MAC production e.g. vitronectin, S protein and CD59 or anaphylatoxins e.g. carboxypeptidase N, B and R[57].

Activation of the classic pathway occurs when C1q binds to an antigen-antibody complex. The lectin pathway is stimulated by pathogen-associated molecular patterns (PAMPs) which activate pattern recognition receptors (PRRs)[57].

Proteomic analyses of donor eyes, specifically drusen components and Bruch's membrane, have provided comprehensive evidence of the role of complement in AMD pathogenesis[115]. The evidence demonstrated a marked elevation of complement and associated inflammatory molecules in AMD affected eyes compared to controls. This in combination with oxidative stress e.g. from smoking and the ageing process leading to morphological changes in Bruch's membrane and the choroid, results in elevated complement and other inflammatory components e.g. carboxyethyl pyrrole CEP[115].

Prior studies have demonstrated an elevation in systemic levels of complement proteins in AMD affected patients compared to controls[116]. This may suggest a role for systemic complement in AMD development.

The *complement factor H* gene, as previously described, contains binding sites for CRP[117]. A SNP in the short consensus repeat 7 domain results in a substitution of histidine for tyrosine at position 402. This results in a decreased affinity of CFH, in homozygous CFH_{402H} individuals, for CRP.

CRP attaches to damaged cells and binds soluble CFH forming a CRP-CFH complex on the cell surface. This complex then inhibits complement MAC formation by inhibiting C3

convertase. Patients with AMD have elevated levels of CRP in the choroid[118]. The reduced binding affinity of CRP in CFH_{402H} homozygotes in combination with cellular injury at the level of the RPE leading to increased choroidal vascular permeability to CRP, may account for the higher levels recorded. This local accumulation may be an indicator of ongoing inflammation and cellular damage in AMD patients[118].

1.5.2.3 Role of macrophages in AMD

Resident tissue macrophages (microglia) have been implicated in the development of advanced AMD[119]. Resident microglia are derived from bone marrow precursor cells that enter the retina via blood vessels during embryogenesis. They remain in an inactive state, appearing as stellate cells surrounding inner retinal blood vessels. Once activated by oxidised proteins and lipids, Advanced Glycosylation End products or cell apoptosis they change appearance to larger amoeboid cells and migrate to the site of cell damage[120].

Retinas from various animal models have demonstrated microglial activation precedes retinal degeneration and apoptosis. One hypothesis suggests that in the ageing retina, microglia migrate from their usual location in the inner retina to the subretinal space where they actively phagocytose lipofuscin in support of the RPE cells. The subretinal space, in physiological conditions is an area of immune privilege protected by the blood-retina barrier. Recent evidence suggests that in the ageing retina, microglia may become trapped in the subretinal space and act as a nidus point for further accumulation of cellular deposits, immune complexes and complement components[121]. Histological assessment of drusen has previously identified these constituents as integral intrinsic components.

Microglia in the subretinal space may actively exit via retinal vessels, the choroid or the ciliary body. The activated retinal microglia could potentially reach the spleen and act as antigen-presenting cells (APCs) and elicit systemic adaptive immune responses[122]. This is significant as elevated levels of anti-retinal antibodies have been found in the serum of AMD patients.

1.5.2.4 Failure of RPE cell heterophagy and autophagy

The RPE cell is one of the most metabolically and phagocytically active cells in the human body (function summarised in Table 8). Each cell is responsible for the removal of shed photoreceptor outer segments (POS) of 30-40 photoreceptors. This process (heterophagy) exerts a huge metabolic burden on the cells[123]. Death of nonreproducing

RPE cells with advancing age, increases the stress on neighbouring cells and leads to lipofuscin accumulation within the lysosome system[124].

Heterophagy begins at the apical side of RPE cells, which is in close apposition to photoreceptors. The shed POS are ingested as a phagosome and transported to the basal side of the cell. There it is fused to a lysosome and degraded[124].

RPE functional failure	Summary
Failure of lysosomal function	Oxidised lipid and protein end-products reduce the RPE cell's ability to degrade POS. This may be the inciting factor in the production of lipofuscin. Lipofuscin cannot be enzymatically degraded within the lysosome or transported into the extracellular space
Mitochondrial dysfunction	Oxidative stress can result in mitochondrial dysfunction and creation of ROS. These highly reactive molecules lead to protein misfolding and aggregation. Resulting compounds have been found in lipofuscin. Mitochondrial DNA is more susceptible to oxidative damage than nuclear DNA. This leads to increased mitochondrial stress and dysfunction and ROS generation
Failure of autophagy	Increased oxidative stress leads to misfolding of proteins and protein aggregation. These are usually removed by autophagy, failure of this process leads to cell death.
Inflammasome activation	Increased ROS, lipofuscin accumulation, protein aggregation and reduced autophagy leads to NLRP3 inflammasome activation and a chronic low-grade inflammation.

Table 8 RPE cell contributing factors that lead to AMD development. RPE cell dysfunction has been implicated in AMD pathogenesis via several pathways. There is a recognised failure of lysosomal function leading to lipofuscin generation. Mitochondrial dysfunction leads to ROS molecule formation, protein aggregation and further RP dysfunction and failure of autophagy. These errors in RPE performance culminate in a chronic inflammatory process.

1.6 Models of AMD

The creation of a suitable animal model to fully represent a complex disease such as AMD has as yet not been possible. However, one model which I have utilized in my experiments is the $Ccl2^{-/-}$/$Cx3cr1^{-/-}$ murine model.

Ccl2 is a chemokine responsible for attracting monocytes from capillary blood vessels to sites of inflammation. Studies have demonstrated that macrophages play a vital role in the immune modulation process in AMD[125]. Cx3cr1 is a receptor found on microglia native to the CNS, including the retina. It has a role in deactivation of the cell[125]. Double knockout murine models can demonstrate histologically, activated microglia or recruited macrophages with large lipid accumulations. This is similar to human AMD pathology[126, 127].

The $Ccl2^{-/-}$/$Cx3cr1^{-/-}$ model created by Chan *et al.* demonstrated phenotypically, characteristics consistent with drusen on fundus examination at a6 weeks[128]. Histological preparations also showed evidence of basement membrane thickening, microglial accumulation and activation, local RPE hypopigmentation and CNV in some mice[129]. Recent evidence has however cast significant doubt on the validity of this model as an ideal AMD representation. Many of these mice have a *rd8* retinal degeneration mutation which also produces characteristic phenotypic changes associated with AMD[130, 131].

A mouse model of AMD previously utilised is the APOE model of AMD. These mice had targeted knock in of a human Apolipoprotein E allele E2, E3 or E4[132]. They were then fed a diet high in fat and cholesterol. The Apo E E4 mice developed drusenoid deposits, thickened Bruch's membrane and RPE changes consistent with atrophy. A few mice progressed to CNV formation.

The superoxide dismutase (SOD) 1 knockout mouse has many features of an ideal model of AMD[133]. It develops a thickened Bruch's membrane, drusen, CNV and RPE changes. The SOD system is important for reducing oxidative damage to the retinal cells. SOD1 isoenzyme is cytosolic whereas SOD2 is mitochondrial and SOD3 is secreted into the extracellular matrix.

Experimental models such as $CFH^{-/-}$ and $ABCA4^{-/-}$ knockout mice often show characteristics on histological examination similar to AMD but lack many phenotypically defining characteristics eg. CNV formation[132, 134, 135].

Dobi *et al.*[136] first reported the use of focal spots of argon laser in the retina of rats to produce breaks in Bruch's membrane. This resulted in the onset of areas of choroidal

neovascularization, producing a reproducible model of the disease process. I plan to use a modification of this model of laser induced CNV in my future investigation into the role of *SERPING1*. Current mouse models of AMD are summarised in Table 9.

AMD model	Description	AMD features
CFH Y402H transgenic[137]	Expresses the CFH Y402H polymorphism	Drusen-like deposits
$CFH^{-/-}$[138]	Depletion of C3 and deposition of C3a in the retina	Develop loss of photoreceptors, reduced rod function, increased subretinal autofluorescence, complement deposition in the retina and disorganization of photoreceptor outer segments
C3a and C5a $receptor^{-/-}$	Lacks C3a and C5a receptors	CNV in laser-induced model, decreased levels of VEGF expression and impaired leukocyte recruitment.
Transgenic C3[138]	Elevated levels of C3	Proliferation and migration of endothelial cells within the retina, disruption of the RPE with migration of pigmented cells into the retina, complement deposition and atrophy of the photoreceptor outer segments

AMD model	Description	AMD features
Cc12□/□and Ccr2□/□knockout mice[139]	Impaired macrophage recruitment at sites of complement deposition	Subretinal drusen-like deposits, RPE loss, choroidal neovascularization, photoreceptor atrophy and increased RPE deposition of C3 and C5 from defective complement clearance resulting from macrophage chemotactic defect.
Cx3cr1□/□		Drusen-like deposits, photoreceptor degeneration and choroidal neovascularization with microglial accumulation.
Ccl2□/□Cx3cr1□/□double knockout[126]		Drusen-like deposits, thickening of the Bruch's membrane (BrM), local RPE degeneration, photoreceptor disorganization, atrophy and increased levels of A2E and choroidal neovascularization
Carboxyethylpyrrole (CEP) adducted albumin immune mouse model[140]	Oxidation of docosahexaenoic acid (DHA) fatty acids in the retina lead to formation of carboxyethylpyrrole (CEP) adducted proteins. These modified proteins are found in drusen and are prevalent in the RPE/BrM of AMD patients. Mice immunized with CEP-adducted serum albumin develop AMD like lesions.	

Table 9 Table of main mouse models of AMD. This table highlights the main models of CNV. The CFH Y402H transgenic mouse model develops drusen-like deposits without Table 9 cont'd. evidence of advanced AMD. The $CFH^{-/-}$ mouse develops outer retinal cell loss, impaired photoreceptor function and evidence of RPE dysfunction and cellular stress. Mutations affecting C3 and C5 receptors and complement component production lead to alterations in leucocyte function and drusen deposition. $Cc12^{□/□}$, $Cx3cr1^{□/□}$ and $Ccr2^{□/□}$ knockout mice have impaired microglial function leading to drusen-like deposition and secondary photoreceptor degeneration. Carboxyethylpyrrole (CEP) adducted albumin immune mouse model also develop drusen-like deposits.

1.7 Treatment strategies for AMD

This section examines the various historical and current treatment methods for AMD. The initial therapeutic strategy involved lasers and has evolved to intravitreal drug injections.

1.7.1 PDT and argon laser

The macular photocoagulation study (MPS) group conducted a series of clinical trials between 1979 and 1994 analysing the effect of argon laser on CNV located either extrafoveal, juxtafoveal or subfoveal locations[141]. This treatment modality proved not to be very effective as the majority of CNV identified on FFA were not small or well delineated enough to be treated. Membranes which were eligible and received treatment often developed further areas of leakage. Treatment with argon laser often produced large central scotomas and had a devastating visual impact from subfoveal CNV extension.

Photodynamic therapy (PDT) for AMD utilized verteporfin as a photosensitizer in the treatment of CNV. Irradiation of new blood vessels leads to the production of reactive oxygen species, damage to vessel endothelium and subsequent closure of the targeted vessel bed. PDT delayed or prevented loss of vision during at least one year of follow-up in patients with predominantly classic neovascular lesions. Within that subgroup, only 33 percent of the patients who received PDT had substantial loss of vision, as compared with 61 percent of those given a placebo photosensitizer. The treatment however only demonstrated a modest effect on a small percentage of affected patients and often left a large scotomatous field loss[142].

1.7.2 Intravitreal pharmacological strategies for AMD treatment

This section highlights the modern development of a treatment strategy for AMD revolving around intravitreal drug injection.

1.7.2.1 Pegaptanib

The United Stated Food and Drug Administration (US FDA) approved Pegaptanib sodium (Macugen; Eyetech Pharmaceuticals/Pfizer) in 2004. It was the first aptamer developed for therapeutic use in humans and is an RNA aptamer directed against the $VEGF_{165}$ isoform while sparing the $VEGF_{121}$[143]. The selective evolution of ligands by exponential enrichment (SELEX) technique was utilised in the 1990s to develop the aptamer which effectively inhibited $VEGF_{165.}$ This had applications in both neovascular AMD and diabetic retinopathy.

Pre-clinical and clinical trials at the time demonstrated safety and efficacy of the drug[144] with approval of 0.3mg intravitreal injection concentration granted by the regulatory authorities. Eventually pegaptanib was superseded by ranibizumab which demonstrated a superior efficacy.

1.7.2.2 Bevacizumab and ranibizumab

The anti-VEGF agent bevacizumab was initially developed from the murine Mab A.4.6.1 for treatment of cancer. In 1996, *in vitro* studies examined the potential role of the anti VEGF agent in AMD. This initially required the establishment of VEGFA as an important factor in ischaemic neovascularization and demonstrated bevacizumab's potential to reduce CNV activity in animal models[145].

A delivery method also needed to be established. Bevacizumab in its anti-cancer therapeutic role is delivered intravenously. However, there is considerable risk of haemorrhage and arterothrombotic events (ATEs) from systemic administration[146]. This was confirmed later by the higher rate of ATEs in patients treated for GI cancer on combination chemotherapy with bevacizumab.

The suggested mode of delivery was therefore via an intravitreal (IV) injection. This raised further hurdles such as the ability of the molecule to cross the retinal barrier and reach the choroid. To answer this question, humanized antibodies of the VEGF and the Fab portion of the antibody were tested in animal models[147]. The preponderance of studies confirmed better penetration of the Fab portion of the molecule into the choroid compared to the entire IgG antibody[147].

As part of chemotherapy, bevacizumab was administered fortnightly. However, this was not thought to be a practical solution for intravitreal administration. Ranibizumab (Figure 14) was therefore developed from a modification of a different humanized anti-VEGF Fab variant (MB1.6) than bevacizumab (Fab-12) producing a higher affinity molecule with a longer half life[110].

1.7.2.3 Aflibercept

Aflibercept (Eylea, Regeneron Pharmaceuticals) is an engineered recombinant protein designed to bind all isoforms of VEGF-A, VEGF-B and placental growth factor (PGF). It is composed of the second immunoglobulin binding domain of VEGF receptor 1 and the

third immunoglobulin binding domain of VEGF receptor 2 combined with the Fc portion of human IgG1.

Aflibercept has been demonstrated to have a stronger binding affinity to all VEGF isoforms[148]. Additionally, mathematical models have suggested a longer duration of action of the aflibercept molecule within the eye[149].

1.8 Landmark trials in the treatment of AMD

The development of ranibizumab as an effective treatment for AMD has been marked by several significant clinical trials (Table 10) that validated the anti-VEGF agent as a safe and effective therapeutic agent for treating wet AMD.

Study	Results
ANCHOR trial (Ranibizumab versus Verteporfin for Neovascular Age-Related Macular Degeneration)[150]	94.3% of patients in the 0.3mg and 96.4% in the 0.5mg treatment arms for Ranibizumab achieved the primary endpoint. This compared to only 64.3% in the PDT treatment arm (P<0.001) at 1 year. The mean change in visual acuity demonstrated an 11.3 letter gain in VA following monthly Ranibizumab injection over baseline in the 0.5mg arm and an 8.5 letter gain in the 0.3mg arm. This compared with a mean decline of 9.5 letters over the 12 months in the Verteporfin treated arm (P<0.0001)
MARINA (Ranibizumab for neovascular age-related macular degeneration)[151]	At 1 year, 94.5% and 94.6% of the 0.3mg and 0.5mg Ranibizumab treatment arms lost less than 15 letters from baseline VA. 62.2% of patients in the sham arm in comparison lost less than 15 letters from baseline (P<0.0001). The results were similarly represented at 2 years with 92.0% of the 0.5mg and 90.0% of the 0.3mg group achieving the primary endpoint. Only 52.9% of the sham injected arm lost fewer than 15 letters from baseline (P<0.0001). There was a mean increase over baseline VA of 7.2 letters in the 0.5mg treated group and 6.5 letters in the 0.3mg arm at

Study	Results
MARINA cont'd	12 months (P<0.0001). The sham-injection arm loss 10.4 letters at 1 year. This trend continued to the 2 year timepoint (P<0.001)
PIER Trial (Phase IIIb, multi-centre, randomized, double-masked, sham injection-controlled study of efficacy and safety of Ranibizumab in subjects with subfoveal CNV with or without classic CNV secondary to AMD)[152]	The results of the trial were consistent with Marina and Anchor, demonstrating that all treated patients showed an improvement during the initial 3 months of the loading phase. The 2 year results however, demonstrated a significant decline in VA. This was reported as 21.4, 2.2 and 2.3 letter decreases from baseline for the sham, 0.3mg and 0.5mg cohorts. The data also demonstrated an increase in CNV area of 1.9, 0.29 and 0.64 disc areas for the sham, 0.3mg and 0.5mg groups respectively. The results from PIER demonstrated conclusively that patients on fixed quarterly injections had worse results compared to the monthly dosing schedule in ANCHOR and MARINA.
PrONTO (Prospective Optical Coherence Tomography Imaging of Patients with Neovascular AMD Treated with intra-Ocular Ranibizumab)[153]	There was a mean VA improvement at 2 years of 11.1 letters compared to baseline and a mean reduction in CMT of 212µm. During the first year, an average of 5.6 injections was necessary and 9.9 over 2 years. There were no reported ocular or systemic adverse events. PrONTO demonstrated that similar results could be achieved with fewer injections (but not fewer clinical visits) as the MARINA and ANCHOR studies utilizing an OCT guided therapeutic regimen.

Study	Results
1.9.5 CATT (Comparison of Age-Related Macular Degeneration Treatment Trials)[154]	The mean visual acuity demonstrated the greatest level of improvement during the first 6 months of treatment, comparable to the ANCHOR and MARINA trials. The 1 year results provided substantial evidence that Avastin was noninferior to Lucentis both under the monthly and prn protocols. A longitudinal regression model over the year showed that patients in the Lucentis monthly group had a 7.2±0.7 letter gain, 7.3±0.8 letter gain in the Avastin monthly group, 6.4±0.6 in the Lucentis prn and 6.1±0.7 in the Avastin prn groups. There was a 9.8 mean letter increase in numbers read after 1 year using the MARINA inclusion criteria (10.8 based on ANCHOR) for patients receiving Lucentis. Greater than 90% of patients in all subgroups did not lose 15 or more letters. There were also similar levels of CMT reduction for all study groups with a small but not visually significant advantage for Lucentis.
IVAN (Ranibizumab vs. bevacizumab to treat neovascular age related macular degeneration)[155]	The 1 year analysis showed mean BCVA of 69.0 and 66.1 ETDRS letters for Lucentis and Avastin respectively. The results concluded that Avastin was neither inferior nor equivalent to Lucentis and that discontinuous was equivalent to continuous therapy. The trial also provided a similar finding to the CATT trial with serum VEGF being lowest in the discontinuous/prn arm of the Avastin subgroup. There were also more serious adverse events reported with Avastin than Lucentis however, this was

Study	Results
IVAN cont'd	not statistically significant. Neither trial was powered sufficiently to conclude an association. The findings also agreed with CATT relating to anatomical features of the CNV. Lucentis resulted in a reduced CMT but without a statistically significant correlation in improved VA.
Intravitreal aflibercept (VEGF trap-eye) in wet age-related macular degeneration[156]	Intravitreal aflibercept dosed monthly for an initial loading dose for 3 months followed by bimonthly injections produced similar efficacy and safety outcomes as monthly ranibizumab. This potentially reduces the number of clinical appointments for patients on a prn regime and monthly reviews with similar visual outcomes.

Table 10 Landmark clinical trials in the treatment of AMD. This table outlines the main trials in the modern strategy of anti-VEGF treatment for AMD. Ranging from the initial efficacy trials for ranibizumab in ANCHOR and MARINA, to the establishment of the comparative efficacy of prn dosing demonstrated by PrONTO utilising OCT based treatment protocol. CATT and IVAN demonstrated similar efficacy of bevacizumab and ranibizumab. Aflibercept is a protein aptamer of the VEGF receptor molecule with high binding potential for all VEGF isoforms. Therapy with aflibercept has been shown to be as effective as ranibizumab.

1.9 Symptoms of AMD

The main symptoms of AMD show significant interpersonal variation depending on severity of the pathological process and/or location of the disease. Some patients who have early disease may be asymptomatic but may demonstrate on objective testing loss of contrast sensitivity, microscotomas or mild metamorphopsia. More severe forms of AMD may describe distortion of linear images and loss of central vision.

1.10 Current management of AMD

Early AMD is usually managed conservatively with the provision of visual aids such as lights and magnifiers. Social support is also provided in specific circumstances. All patients are advised not to smoke. AREDS supplementation is also recommended in appropriate cases.

Patients suspected on clinical examination to have advanced AMD are investigated with Fundus Fluorescein Angiography (FFA) and Optical Coherence Tomography (OCT).

The current method of treatment is with intravitreal injections of ranibizumab. This is a humanized antibody to VEGF-A which stops its interaction with VEGF receptors 1 and 2.

The treatment criteria as outlined by the National Institute for Health and Clinical Excellence (NICE) are as follows:

1) the best-corrected visual acuity is between 6/12 and 6/96
2) there is no permanent structural damage to the central fovea
3) the lesion size is less than or equal to 12 disc areas in greatest linear dimension
4) there is evidence of recent presumed disease progression (blood vessel growth, as indicated by fluorescein angiography, or recent visual acuity changes)

Treatment consists of a loading dose of three injections of 0.5mg of ranibizumab monthly for three months followed by monthly review to determine CNV activity and re treatment. Bevacizumab (utilised off license) 1.24mg is also administered monthly for three months followed by a prn regime based on visual acuity and OCT characteristics. Aflibercept (0.5mg) has a license for a treat and extend protocol. All patients receive an initial loading dose of monthly intravitreal injections for 3 months followed by treatment every 2 months for 1 year. Thereafter, the interval between treatments can be extended

by 2 weekly increments (or decreased) based on clinical interpretation of OCT findings and vision response.

Intraocular Galilean telescopes[157], macular translocation surgery[158] and subretinal microchip implants[159] have also been trialled with varying results.

1.11 Related neurodegenerative diseases

This section identifies known neurodegenerative diseases with similar pathogenesis as AMD. The main diseases investigated include Alzheimer's disease and multiple sclerosis.

1.11.1 Alzheimer's disease

Alzheimer's disease (AD) shares many similarities with AMD. They are both neurodegenerative diseases with related risk factors i.e. more common in older age, cardiovascular risk factors such as hypertension, hyperlipidaemia and obesity (Figure 16). They also have a common aetiology related to oxidative stress and inflammation.

AD is characterised clinically by progressive cognitive decline and is the leading cause of dementia[160]. Histopathologicaly, AD exhibits amyloid-beta (A□) plaques, cerebral amyloid angiopathy (CAA) and intraneuronal neurofibrillary tangles (NFT)[161]. This correlates with drusen deposits in AMD. Both represent failure of glycoprotein and lipid metabolism in specialised cells.

The retina exists in an environment exposed to high levels of oxidative stress. This occurs not only from obvious ultraviolet exposure but also from the metabolically active RPE and photoreceptor cells which produce significant amount of reactive oxygen species (ROS). These ROS are mainly produced as a result of polyunsaturated fat peroxidation (from lipid membrane recycling)[162]. The presence of ROS alters protein interaction and induces conformational change. One result is the deposition of lipofuscin, an insoluble, cross linked protein that reduces lysosmal function and mitochondrial efficacy[163]. This acts as a positive feedback on the aging RPE cell leading to further degenerative changes[164]. The brains of AD patients demonstrate many features suggestive of oxidative damage[165] e.g. iron deposition in the cerebral cortex, often years before cognitive changes begin.

In both AD and AMD there is a failure of extracellular clearance of lysosomes to clear protein degradation products-A□ and lipofuscin respectively[166]. In AMD, this is mainly a result of RPE senescence leading to mitochondrial dysfunction and RPE cell death[164].

Amyloid plaques, characteristically seen on pathological section and CT imaging of patients with AD share a similar composition with drusen in AMD. They both contain A□, clusterin, vitronectin, amyloid P, apolipoprotein E, and inflammatory mediators, such as acute phase reactants and complement components[54]. These inflammatory products

form a background for our investigation into the function of C1 inhibitor in AMD pathogenesis (see chapter 2).

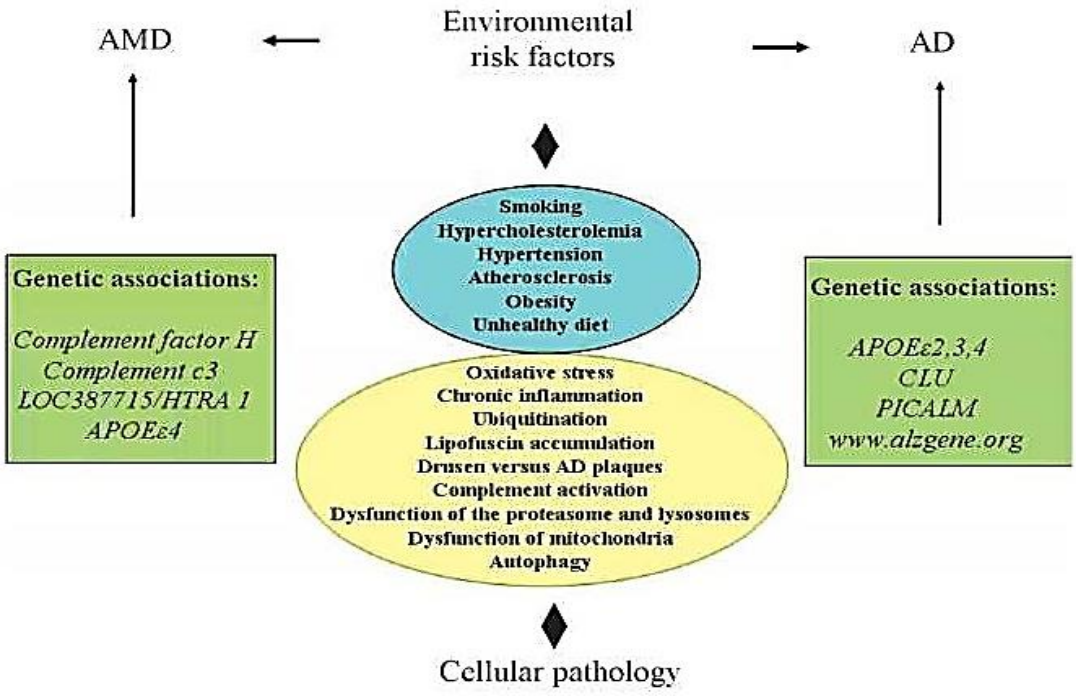

Figure 16 Comparison of risk factors associated with AMD and AD. Late-onset Alzheimer's disease has a strong association with the risk allele C of the clusterin (*CLU*) gene variant rs11136000. The phosphatidylinositol binding clathrin assembly protein (*PICALM*) gene has also shown a strong association with late-onset AD. Modified from Kaarniranta K, Salminen A, Haapasalo A, Soininen H, Hiltunen M. Age-related macular degeneration (AMD): Alzheimer's disease in the eye? J Alzheimers Dis 2011;24(4):615-631.

1.12 Known related biomarkers of disease progression

1.12.1 Alzheimer's disease and TNF-□

Holmes *et al*. in his paper in 2009 demonstrated a direct correlation between episodes of cognitive decline and acute systemic events[167]. These events lead to an increase in proinflammatory cytokines resulting in measured episodic declines in cognitive function (Figure 17). This had a cumulative effect with long term progressive deterioration resulting in dementia. His work showed a direct correlation between elevated levels of the proinflammatory cytokine tumour necrosis factor alpha (TNF-□) associated with an acute systemic event and cognitive decline.

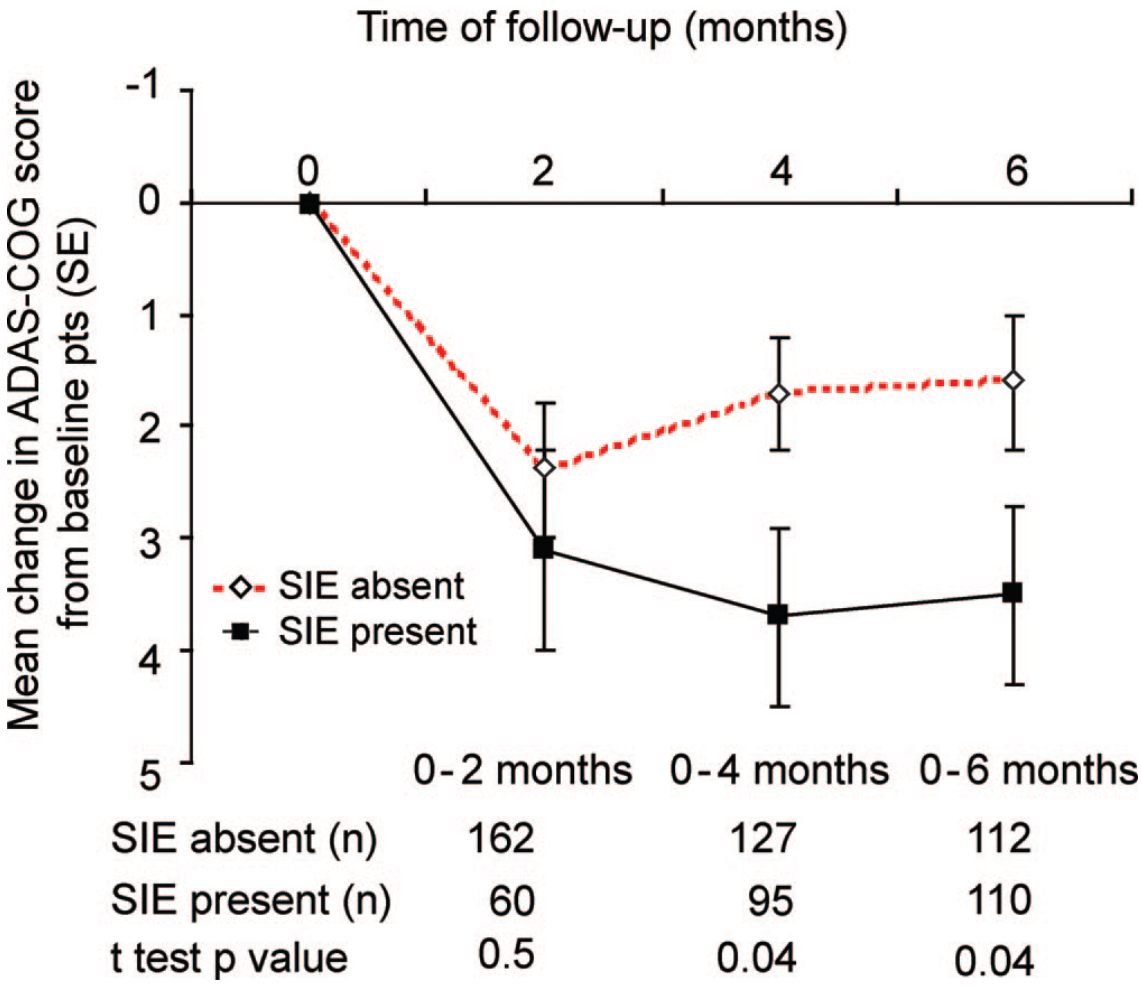

Figure 17 Graph illustrating cognitive decline associated with SIEs in AD. Mean change in cognitive levels were assessed using the Alzheimer's Disease Assessment Scale Cognitive Subscale (ADAS-COG). The graph above demonstrated a higher score in the presence of recorded systemic inflammatory events (SIEs) as compared to the absence of such inflammatory events over a 6 month period. Adapted from Holmes C, Cunningham C, Zotova E et al. Systemic inflammation and disease progression in Alzheimer disease. Neurology 2009;73(10):768-774.

In view of the similarities between AD and AMD elaborated above, I hope to determine whether acute systemic events with associated elevated serum TNF-□ produces objective changes in CNV activity.

1.12.2 Eotaxin

CCL24 is important in the recruitment of eosinophils in co-ordination with CCR3 receptors. It is secreted by a wide variety of cellular types including endothelial cells, smooth muscle cells, fibroblasts, bronchial epithelial cells, macrophages and

eosinophils[168]. CCR3 has been implicated in angiogenesis and reports suggest a higher concentration in surgically excised CNV membranes[169].

A recent paper by Sharma *et al.* discussed the role of the chemokine Eotaxin 2 (CCL24) as both a biomarker for AMD development[170]. This was a cross sectional study looking at patients recruited in the Indian subcontinent. There were 133 AMD affected and 80 age-matched controls included in the study.

A demographic survey, fundal imaging and disease characterization was performed on all recruited patients. Serum samples were analysed for Eotaxin-2 concentrations. The results demonstrated an elevation in the serum concentration of wet AMD affected patients compared to dry AMD and controls.

1.12.3 CRP and Il-6

CRP was the first acute-phase protein to be described and is an indicator of systemic levels of inflammation. It activates both the alternative (via binding to CFH) and the classical pathway, through C1q and stimulation of the MAC. Il-6 has mainly been described as a pro-inflammatory molecule, important in the acute phase response.

Seddon *et al.* in his prospective longitudinal study demonstrated a direct relationship between elevated levels of serum CRP and Il-6 and AMD progression from early to intermediate to advanced stages of the disease. However, Klein *et al.* found no such relationship between these inflammatory cytokines and progression to advanced AMD in 2 of his studies.

1.12.4 Multiple sclerosis and CFH

I previously discussed (1.5.2.1.2) the role CFH played as a risk factor for disease progression in AMD. Prof Paul Morgan and his group in Cardiff demonstrated that CFH was an effective biomarker to predict the rate of relapse of patients with multiple sclerosis[171]. Those patients with sustained elevated levels of CFH had a progressive deterioration in their disease. I plan to determine whether a similar effect applies to AMD.

1.13 Aims, objectives and hypothesis

1.13.1 Hypothesis

SERPING1 influences the pathogenesis of AMD and the clinical response of CNV to therapeutic intervention with the anti VEGF drug ranibizumab.

1.13.2 Aims

1. To determine the role of the gene *SERPING1* in AMD development
2. To identify whether systemic inflammation influences CNV activation similar to AD
3. To determine whether known genotypes and/or cytokines are biomarkers of AMD reactivation
4. To investigate the potential of C1 inhibitor as a therapeutic agent in a murine model of AMD

1.13.3 Objectives

1. The role of the gene *SERPING1* will be determined through a series of experiments utilising C1Inh, the protein product of *SERPING1*, delivered via subretinal injection to C57/BL6 and $Ccl2^{-/-}$/$Cx3cr1^{-/-}$ mice. The eyes will be photographed, harvested and immunohistochemical analysis performed to determine any significant difference between the 2 groups.
2. Serum will be collected monthly from patients known to have AMD and undergoing treatment with intravitreal Lucentis. A questionnaire will be administered at the same research visit to determine any recent episodes of systemic illnesses. The serum will subsequently be analysed for inflammatory marker levels.
3. Genotyping will be performed on all patients included in the study for genes known to be involved in progression from early to advanced AMD. This information in conjunction with inflammatory marker levels may be a biomarker of CNV reactivation.
4. C1Inh will be investigated as a potential therapeutic agent to prevent the formation of AMD in the $Ccl2^{-/-}$/$Cx3cr1^{-/-}$ murine model.

2 Methodology

My investigation into the function of *SERPING1* is based on two approaches: 1) An in vivo and histological examination of the effect of C1Inh on the retina of C57BL/6 and $Ccl2^{-/-}$ /$Cx3cr1^{-/-}$ mice and 2) a cross sectional, longitudinal observation study of patients who had received Lucentis® (Novartis, Frimley UK) for AMD.

2.1 Setup of Murine model to investigate the function of the gene *SERPING1*

2.1.1 Mouse models

Two strains of mice were used in the experiment under Home Office license. C57BL/6 (The Jackson Laboratory Maine, USA) and Ccl2/Cx3cr1-deficient mice (on the background of C57BL/6 strain) (courtesy of Dr Chi-Chao Chan, MD, Chief of Immunopathology Section, Laboratory of Immunology Head, NEI Histology Core, National Eye Institute National Institutes of Health, Building 10, Room 10N103, 10 Center Drive Bethesda, MD 20892-1857 USA) were used in the experimental model and housed in the Biomedical Research Facility (BRF) at SGH under Home Office license (Project license number 30/2843). Mice were housed in a climate controlled room at 21 ± 2°C with a 12 hour light and dark schedule. They had free access to standard rodent pellet diet and water. All animal studies were performed in accordance with the Animals (Scientific Procedures) Act 1986.

2.1.2 Subretinal injection technique

The procedure utilised graduated glass micropipettes ((Sigma-Aldrich, Dorset UK) with a drawn tip (0.5mm diameter). The animals were initially sedated with an intraperitoneal injection of ketamine-xylazine (ketamine, 100 to 125 mg/kg of body weight; xylazine, 10 to 12.5 mg/kg) (Sigma-Aldrich, Dorset UK) and subsequently dilated with Tropicamide 1% (Chauvin Pharmaceuticals Ltd., Kingston upon Thames UK). A surface lubricating gel was then applied to the cornea and a 6mm coverslip (UKGE, Suffolk UK) placed over the gel. This allowed direct visualisation of the retina under an operating microscope. The mouse was mounted on a specially designed bed that allowed for stabilisation of the head during the procedure as well as instrument manipulation. Using straight toothed microforceps (John Weiss Int., Milton Keynes UK) the superior rectus muscle was firmly held and indented at the ora serata. This created a space for the micropipette to be manoeuvred under the retina. An assistant depressed a plunger

to deliver the drug. The presence of a retinal detachment and location was confirmed and the micropipette was removed with minimal reflux of the drug.

2.1.3 Standardization of C1Inh concentration

As previously described, commercial C1Inh (CSL Behring Sussex, UK) is produced for the treatment of Hereditary Angioedema (HAO). The product is distributed in a powder form which is reconstituted by mixing with water. To determine toxicity levels associated with subretinal administration in mice, we injected 3 concentrations of 100U/ml, 50U/ml and 25U/ml into the subretinal space of the right eye of 3 groups of 3 mice. Maximum concentration was determined by the level of solubility of the powder in varying volumes of water without precipitation. The eyes were photographed and harvested at 1 week post injection. The histological sections were examined under a high power microscope to detect any gross anatomical changes following treatment. There was no obvious difference found in the 3 groups on fundal or histological examination. The highest concentration, 100U/ml, was therefore selected.

2.1.4 Design of study

49 C57BL/6 mice (in house colony) and 34 $Ccl2^{-/-}$/$Cx3cr1^{-/-}$ in house bred mice (line supplied by Dr Chi-Chan, Chief of Immunopathology Section, National Eye Institute) aged 4-6 weeks were used in the experiment. The mice were all given a 1µl injection of either C1Inh or saline. At time points 12, 24 and 52 weeks post injection, 11 C57BL/6 mice that received the C1Inh injection and 1 saline injected mouse were anaesthetised, had fundal photographs and their eyes were harvested. This was also performed for 8 transgenic mice receiving the drug therapy and 1 control at each time point.

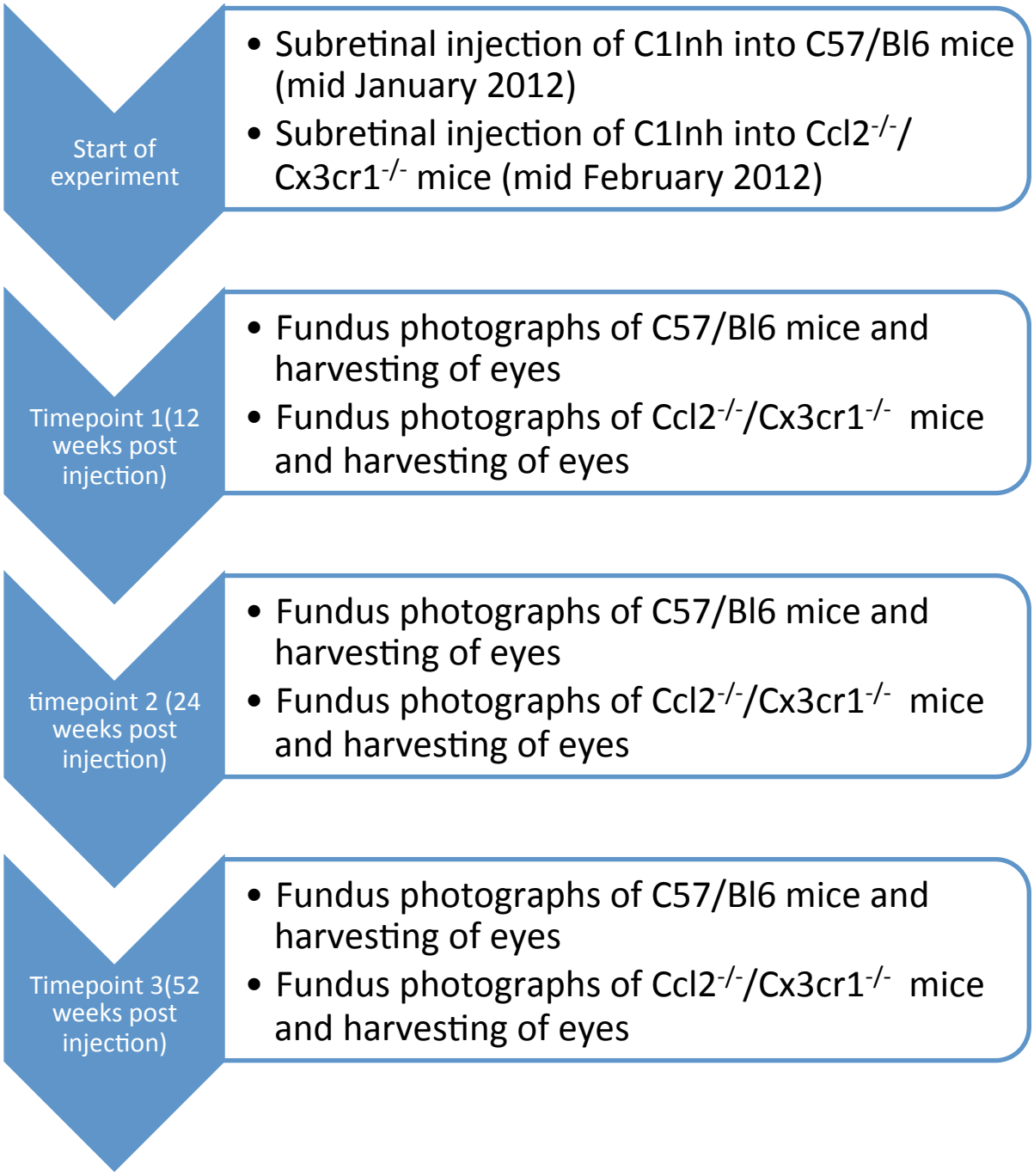

Figure 18 Figure demonstrating the study design of murine experiments to investigate the function of*SERPING1*. Subretinal injection of 1µl of C1Inh was first delivered to the C57/Bl6 mice in mid-January 2012 followed by the $Ccl2^{-/-}$/$Cx3cr1^{-/-}$ mice in mid-February 2012. Following this, fundus photos and harvesting of eyes take place at 12, 24 and 52 weeks post injection.

2.1.5 Photographing fundi

Following sedation and before harvesting, the fundi of all mice were photographed using a Phoenix Research Labs Micron III™ camera. To achieve this, each mouse was sedated with an intraperitoneal anaesthetic and dilated with Tropicamide 1% eye drops. A Viscotears lubricating gel (Centaur services Somerset, UK) was applied to the corneas and the mouse placed in a specially adapted stand. Each fundus was then photographed with the Micron III camera and the images stored on a secure database for future analysis of any phenotypic changes related to AMD.

2.1.6 Processing of harvested eyes

Eyes from sacrificed animals were extracted using curvilinear forceps (John Weiss Int., Milton Keynes UK) and placed immediately in 4% Paraformaldehyde (PFA) (Sigma-Aldrich, Dorset UK) at room temperature. The container was labelled with a unique code for the animal and whether a treated (right) or untreated eye.

The PFA was removed after 1 hour fixation and washed 3 times with phosphate buffered saline (PBS) (Fisher Scientific, Loughborough UK). 30% sucrose (Fisher Scientific, Loughborough UK) solution was then added for preservation and the eyes refrigerated at 4°C until analysis.

Prior to cryosectioning, the anterior segment of the eyes were removed under microscopy. The remaining posterior segment was embedded in OCT Embedding Matrix (Fisher Scientific, Loughborough UK). The eyes were sectioned at 16µm thickness using an OTF 5030 cryostat (Bright Instrument Company, Cambridgeshire UK) and transferred onto glass slides (Fisher Scientific, Loughborough UK). These were subsequently allowed to air dry and stored for immunohistological analysis.

2.1.7 Immunohistochemistry

Immunohistological analysis was performed on slides from all timepoints. For each antigen under investigation, 5 animals from each timepoint plus the control were selected. Two slides for each animal were utilised.

Antibodies selected were for laminin (Sigma-Aldrich pharmaceuticals, Dorset UK), Rhodopsin (Abcam, Cambridge UK), Vitronectin (Abcam, Cambridge UK), C5 (Abcam, Cambridge UK) and C5b-9 (Abcam, Cambridge UK). Prior to staining all slides were dried in an oven at 37°C for 1 hour. They were then washed with PBS. 5% donkey blocking serum (Sigma- Aldrich, Dorset UK) was then applied for 30 minutes at room temperature. Table 11 lists the primary antibodies and dilutions utilised in the study.

The blocking serum was removed and primary antibody (1:500) was applied. The slides were then incubated overnight at 4 °C in a fridge. The following day, the slides were washed with PBS and the secondary antibodies (Alexa fluor – donkey anti-rabbit or mouse 488 (green) or 555 (red)) (Invitrogen, Paisley UK) applied for 2 hours at room temperature in the dark.

The slides were washed again with PBS and 4',6-diamidino-2-phenylindole (DAPI) (Sigma-Aldrich, Dorset UK) added for 6 minutes at room temperature in the dark.
The slides were washed with PBS, mounted with Mowiol (Fisher Scientific, Loughborough UK), coverslipped (Fisher Scientific, Loughborough UK) and stored in the fridge for analysis.

Primary antibody	
Antibody	Dilution
Laminin	1:200
Rhodopsin	1:200
Complement component 5 (C5)	1:100
Complement component 5b-9 (C5b-9)	1:100
Vitronectin	1:100
Secondary antibody	Dilution
Alexa fluor – donkey anti-rabbit or mouse 488 (green) or 555 (red)	1:500

Table 11 Table of primary and secondary antibodies and dilutions. This table lists the primary and secondary antibodies utilised in the immunohistochemistry analysis of harvested C57/Bl6 and $Ccl2^{-/-}$/$Cx3cr1^{-/-}$ harvested retinal tissue.

2.1.8 Transmission Electron Microscopy (TEM) imaging

The processing and cutting for this stage of the experiment was carried out by the staff of the Biomedical Imaging Unit (BIU) at the University of Southampton. I selected the areas of interest for photography. The processing of samples followed the protocol outlined below:

2.1.8.1 Fixation:

1. 1mm blocks of isolated retinal tissue were fixed in 4% formaldehyde (Sigma-Aldrich, Dorset UK) and 1% glutaraldehyde (Sigma-Aldrich, Dorset UK) in 0.1 M PBS (pH 7.4) for 12 hours.
2. The samples were then immersed in 8% (0.2M) sucrose (Sigma-Aldrich, Dorset UK) in 0.1 M PBS 3x15minutes.
3. Post-fixation, the tissue blocks were suspended in 1% osmium tetroxide (Sigma-Aldrich, Dorset UK) in 0.1 M PB for 1 hour.

2.1.8.2 Dehydration:

The dehydration process consisted of a series of suspensions:

1. 50% ethanol 15min
2. 70% ethanol 15min
3. 95% Ethanol 15min
4. 100% Ethanol 2x15min
5. 100% Propylene oxide (Sigma-Aldrich, Dorset UK) 2x15min
6. 1:1 ratio mix of EMBed 812 (Electron Microscopy Sciences, Hatfield Philadelphia USA) and Propylene Oxide for1-2 hour.
7. The samples were then suspended in a 2:1 EMBed 812:Propylene Oxide mix overnight in a dessicator.

2.1.8.3 Embedding:

1. The dehydrated samples were embedded in beam capsules and baked at 60□ for 48 hours.

2.1.8.4 Sectioning:

1. Thick sections (1.0 µm) were cut and placed on a slide with water.
2. The sections were dried on a slide warmer and subsequently stained with Toluidine blue (Sigma-Aldrich, Dorset UK) for 2-5 minutes.
3. I selected the areas of interest under the light microscope for the location to cut ultrathin sections.
4. Ultrathin sections were created at 60-90nm thickness
5. The sections were collected onto grids and dried overnight.

2.1.8.5 Staining:

1. The grids were stained with uranyl acetate for 15 minutes and lead citrate for 5 minutes.
2. Observed and photographed under electron microscope.

2.1.9 Haematoxylin and eosin (H & E)

A slide from 5 animals, plus a control, within each timepoint were selected for H & E (Fisher Scientific, Loughborough UK) staining.

1) The slides were first transferred to Xylene (Fisher Scientific, Loughborough UK) for 5 minutes to dehydrate the sections.
2) They were then placed in 100% Absolute alcohol (Fisher Scientific, Loughborough UK) for 2 minutes.
3) Following this, they were washed in tap water for 2 minutes.
4) Placed in haematoxylin (Fisher Scientific, Loughborough UK) for 5 minutes.
5) The slides were again washed in tap water for 2 minutes and placed in 0.5% Eosin for 1 minute.
6) They were passed through successively higher concentrations of alcohol and finally dipped in Xylene.
7) Mounted with distyrene, plasticizer and xylene (DPX) (Fisher Scientific, Loughborough UK).

2.1.10 5-bromo-4-chloro-3-indolyl-phosphate in conjunction with nitro blue tetrazolium (BCIP/NBT)

BCIP/NBT (Vector labs, Dorset UK) analysis was performed using a kit supplied by Vector labs.

1) A BCIP/NBT substrate working solution was first created by preparing 5ml of 100mM Tris-HCL (Fisher Scientific, Loughborough UK), pH 9.5
2) 2 drops of Reagent 1 (from the Vector supplied kit) was added and mixed; followed by Reagent 2 and Reagent 3.
3) The sections were incubated at room temperature in darkness until suitable staining occurred (approximately 10 mins)
4) The sections were then washed in Tris-HCl buffer for 5 mins and washed in tap water
5) The slides were dehydrated and coverslipped and mounted with Permount (ABD Serotec, Kidlington UK)

2.1.11 Oil red O (OrO) staining

Oil red O (Fisher Scientific, Loughborough UK) staining was performed to determine the relative amount of lipids present. The investigation first required the sections from each timepoint to be:

1) Warmed in an oven to 37°C for 30 minutes.
2) The slides were immersed in 60% triethyl phosphate (Sigma-Aldrich pharmaceuticals, Dorset UK) and stained with 0.5% Oil Red O for 10 minutes.
3) Immediately following, the sections were rinsed in water, stained with eosin and mounted with coverslips utilising DPX.

2.1.12 Terminal deoxynucleotidyl transferase dUTP nick end labeling (TUNEL) analysis

TUNEL analysis was performed using a kit purchased from Promega (catalogue number, G3250), to compare the level of apoptosis between timepoints and also between wild-type and knockout mice. The steps in the analysis were as follows:

1) The slides were first warmed in a convection oven at 37°C for 30 minutes
2) They were washed twice with PBS for 5 minutes each time
3) The sections were permeabilized by covering the slides with 0.2% PBS-T
4) Washing was repeated with PBS
5) 100µl of equilibration buffer was placed on the sections for 10 minutes
6) 50µl of rTdT solution was then added to the slides
7) The sections were then incubated at 37°C within a humidified environment for 1 hour
8) 2×SSC was placed on the section for 15 minutes at room temperature
9) Washing was repeated with PBS
10) 0.5µg/ml of propidium iodide was used to stain the slides for 15 minutes
11) Washing was repeated with distilled water
12) Coverslips were placed using Mowiol as a mountant

2.1.13 Image analysis

The sections were imaged utilising a variety of modalities depending on whether the samples had be stained with fluorescent antibodies or not.

TUNEL stained sections were analysed using Volocity software. The software measures the level of green fluorescence created by DNA nicks and indicative of apoptosis, compared to the background level of fluorescence produced by PI staining.

The Volocity software (PerkinElmer, Massachusetts USA) was also used to measure the level of fluorescence created with immunohistochemistry. As described previously, a red fluorescent secondary antibody was used for the immunohistochemistry analysis. The background level of blue fluorescence produced by DAPI was compared to the specific

level of red fluorescence created by the conjugated secondary antibody. Image J software (National Institute of Health, Maryland, USA) was used to analyse the sections stained with the BCIP/NBT kit. Image J utilised a similar principle whereby pixel concentrations for an area of interest are compared to the background levels.

2.1.14 Statistical analysis

All results are presented as mean ± SEM (standard error of the mean), unless otherwise stated, n represents the number of replicates. For normally distributed data, statistical comparisons were made using an unpaired student's t-test, with a significance threshold of $p < 0.05$. For comparison of more than two groups a one way analysis of variance (ANOVA) was used with a Bonferroni multiple comparisons test, with a significance threshold of $p < 0.05$. GraphPad Prism Software (GraphPad San Diego, USA) was used for statistical analysis. Excel and GraphPad Prism were used for graph production.

2.2 Pharmacogenomic correlations in age related macular degeneration (AMD) study design

2.2.1 Identification of research sites

The eye departments of Southampton General Hospital (SGH) and Frimley Park Hospital (FPH) were the two sites involved in the study. Prof Andrew Lotery was the Chief Investigator (CI) for the study and Principal Investigator (PI) for SGH. Mrs Geeta Menon, Consultant Ophthalmologist at FPH was the PI for FPH.

2.2.2 Obtaining study approval

Ethical, followed by Research and Development (R & D) approval for each site, had to be obtained before initiation of the study (REC reference: 11/SC/0106; Protocol number: RHM OPH0156). The first step in the process was protocol development for the observational study. The initial completed protocol (Version 1) was submitted for internal peer review, performed by Mr Parwez Hossain Consultant Ophthalmologist at Southampton General Hospital.

Essential study documents were created in a detailed online submission process using the Integrated Research Application System (IRAS) portal, to the local Research Ethics Committee (REC) and R & D committees. These included a patient information leaflet (PIL), consent form (ICF), patient reply slip, patient invitation letter and proforma. Examples of these documents are supplied in the Appendix.

A review panel of the REC requested a more detailed presentation of planned investigations, method of storage of patients' samples and safeguards to ensure confidentiality. The study was approved by the REC in late 2010 and later submitted to the University Hospitals of Southampton (UHS) R & D for approval. The final stage of the application process was to request R & D approval for the study to begin in FPH. This was gained in mid-2012.

2.2.3 Patient selection

The inclusion criteria for the main observational study titled "Pharmacogenetic Correlations in Age Related Macular Degeneration" were:

1. Patients of a Caucasian origin
2. Aged greater than 50 years

3. Receiving Lucentis© treatment for a subretinal neovascular membrane (SRNVM) in one eye

Patients were excluded if they:

1. Had both eyes treated simultaneously with an anti VEGF agent
2. Had a macular co-pathology
3. Had poor venous access
4. Were unable to provide informed consent

Patient selection began with a weekly review of all notes of patients receiving their second or third Lucentis© intravitreal injection. This information was collated by the secretarial staff at SGH. All eligible patients on their second intravitreal injection were approached with a PIL and invited to enrol in 1 month at their third injection. Patients on their third injection were eligible for enrolment.

2.2.4 Screening and follow-up visits

Visual acuity (VA) change is maximal after 3 monthly injections, and to achieve a comparable and standardized evaluation of the response to Ranibizumab treatment, only data obtained after 3 consecutive Ranibizumab (Novartis, Frimley UK) injections was used. All patients were recruited for six 6 months follow-up. This consisted of an initial baseline visit followed by six further research appointments. The patients at baseline first had their informed consent obtained. Their past ophthalmic history, past medical history, recent record of any acute medical illnesses, drug history, smoking status and family history of eye disease were recorded in a proforma. The baseline LogMAR visual acuity, number of intravitreal injections, a record of any investigations at the visit, height and weight were noted. Each patient was assigned a unique study code which was placed on the consent form, vacutainer tubes (Becton Dickinson, Oxford UK) and proforma.

The details, including linked identifiable information were entered into a recruitment log and secured in the research office. 10ml of blood was taken for serum, 10mls for plasma and 10mls for DNA analysis. The samples were transported in sealed vacutainers at room temperature in containers conforming to UN3373 regulations for the transport of biological materials. All samples were processed by either myself or a member of the Vision Research team in the University of Southampton Vision Research Laboratory at SGH.

Patients were given a copy of their signed consent form and a patient information leaflet (PIL). A copy of the PIL and signed consent form were placed in the patients' medical

notes. Follow up visits required only a review of systems from the prior month, a record of investigations performed, LogMAR visual acuity, any further intravitreal injections at the visit and confirmation that blood tests for plasma and serum analysis were performed.

2.2.5 Eye unit investigations

All patients attending the Eye Unit for a clinical appointment received an initial fundus fluorescein angiogram (FFA). Information provided by this investigation allows for classification of the various types of subretinal neovascular membranes (SRNVMs) and assessment of activity/leakage.

FFA requires the injection of sodium fluorescein into the venous circulation. Light in the blue spectrum, approximately 490nm, excites the dye leading to fluorescence in the yellow-green spectrum (520-530nm). Emitted light within this wavelength range passes through a barrier filter and the image is digitally recorded.

All patients had as part of their routine standard of care, an optical coherence tomography (OCT) scan (Topcon, Berkshire UK). This provides an objective measurement of any leakage from the SRNVM as well as central macular thickness (CMT), a key indicator of potential visual acuity outcome.

The CMT values, OCT and FFA images are stored in a central database. These indicators will be correlated with my survey questionnaire and blood investigation results to give a comprehensive evaluation of SRNVM response to Lucentis® treatment.

2.2.6 Tracking patients

All patients enrolled had their clinic review appointments tracked via the e-Camis system. This allowed research review appointments to be scheduled monthly alongside monthly NHS appointments without requiring extra onerous visits.

2.2.7 Processing of samples

Blood was collected at the initial visit in two EthyleneDiamineTetraacetic acid (EDTA) vacutainer tubes (Becton and Dickinson (BD), Oxford UK) and a plain tube (BD, Oxford UK). One of the EDTA tubes was stored immediately at -20 degrees Celsius (°C) for future DNA analysis. There was no patient identifiable data recorded on the vacutainer tubes.

2.2.8 Processing of plasma

Blood from the EDTA container was centrifuged (Eppendorf Centrifuge 5810r, Stevenage UK) at 2600rpm for 10 minutes at 21°C. The plasma was pipetted into five 200µl

aliquots and the remainder into 1000µl aliquots. The plastic tubes (Fisher Scientific, Loughborough UK) were labelled with the patient's unique ID number, visit number and the plasma volume. The samples were then stored at -80°C.

2.2.9 Processing of serum

The serum processing protocol followed a similar procedure. However, a review of the literature suggested an adaptation to the protocol may be necessary. Lachman *et al*. described in their review paper "Preparing serum for functional complement assays[140]" a two stage process. In their review, they advised that blood be transported at room temperature and left standing for at least 20 minutes until clot retraction had taken place. The initial spin cycle was considerably faster at 3900rpm at room temperature for 5-10 minutes. Following this, the supernatant was pipetted into microcentrifuge tubes (Fisher Scientific, Loughborough UK) and spun at 14000rpm for 2-5 minutes. This was done to remove any remaining cell fragments, believed to lead to complement activation and subsequent inaccuracies when measuring functional complement activity levels.

My samples were prepared using both a single spin cycle at 2600rpm and a two stage spin cycle as described above. The results from the in house assay of complement activity showed no difference in the two methods of preparation. We therefore maintained my original protocol of a single spin cycle. Copies of the two protocols are supplied in the Appendix.

2.2.10 DNA extraction

The steps for DNA extraction followed the protocol of Miller *et al*.[141]. The main modification was the use of erythrocyte lysis buffer (ELB) (Fisher Scientific, Loughborough UK) to obtain white blood cells as opposed to buffy coats. See Appendix 5 for full details.

The Nanodrop ND1000 spectrophotometer (Thermo Scientific, Wilmington USA) was used to measure DNA concentrations. The machine measures absorbance of light at 260 and 280nm from a pulse Xenon lamp to calculate nucleic acid concentrations in a 1.5µl sample. It also highlights the relative purity of the sample based on the absorbance levels of light from the emitted pulse. This is measured as a 260/280 ratio whereby samples at 1.80 are considered pure DNA and 2.0, pure RNA.

The steps involved in DNA processing were as follows:

1. Samples were first defrosted and vortexed
2. The ND 1000 software was initialised by selecting "nucleic acid"
3. The pedestal of the machine was cleaned with 100% ethanol and allowed to dry

4. 1.5µl of water was placed on the pedestal to initialise analysis
5. 1.5µl of TE buffer (Sigma-Aldrich, Dorset UK) was used as a blank
6. Once completed, 1.5µl of each patient's DNA sample was processed

The calculated DNA concentrations were used to standardise sample concentrations to 50ng/µl and subsequently stored at -20□. The calculation to produce diluted samples is:

$$\frac{1}{\frac{Current\ conc.}{(ng\ per\ \mu l)}} \times required\ volume\ (\mu l) \times required\ conc.\ (ng\ per\ \mu l) = X$$

Amount of DNA to use = *X*

2.2.11 High resolution melt (HRM) Analysis

Patient samples of DNA, diluted to 10ng/µl, were used for HRM analysis. The process involved pipetting 10µl of each sample into a 96-well plate (Fisher Scientific, Loughborough UK). A programmed robot (Corbett robotics, Manchester UK) completed the mixture for each sample using a mastermix based on volumes as per the guidelines (based on 12 samples per plate):

1. Water=24µl
2. Forward and reverse primers=12µl
3. Sensimix=70µl
4. Syto 9=12µl

9µl of the mastermix was combined with 1µl of DNA (10ng/µl) for HRM analysis.

The primer selected was for the *SERPNG1* gene due to its previous in-house testing and validation. The samples were analysed in the Rotor Gene 6000 (Qiagen, Manchester UK).

2.2.12 Genotyping

Genotyping of samples was performed by a commercial service, LGC Genomics (Hoddesdon, UK). The considerably reduced costs and standardised quality assurance associated with the company made this the most effective method for genotyping. Stock DNA samples were diluted to 10ng/µl and placed into 96-well plates. These were subsequently sealed and shipped on dry ice to the company's processing unit.

The following SNPs were analysed:

SNP	Genotype
rs429358	Apolipoprotein E (ApoE),
rs3732378	CX3 chemokine receptor 1(CX3CR1),
rs10490924	Age-related maculopathy susceptibility protein 2 (ARMS2)
RS1061170	Complement factor H (CFH)
rs10033900	Complement factor I (CFI)
rs2511989	Serpin peptidase inhibitor, clade G (C1 inhibitor), member 1 (SERPING1)
rs641153	Complement factor B (CFB)
rs9332739	Complement component 2 (C2)
rs2230199	Complement component 3 (C3)

Table 12 Table of SNPs and associated genotypes examined for in the study. The main genotypes assessed are: Apolipoprotein E (ApoE) (rs429358), CX3 chemokine receptor 1(CX3CR1 (rs3732378), Age-related maculopathy susceptibility protein 2 (ARMS2) (rs10490924), Complement factor H (CFH) (rs1061170), Complement factor I (CFI) (rs10033900), Serpin peptidase inhibitor, clade G (C1 inhibitor), member 1 (SERPING1) (rs2511989), Complement factor B (CFB) (rs641153), Complement component 2 (C2) (rs9332739), Complement component 3 (C3) (rs2230199)

2.2.13 Storage of samples

All serum and plasma samples were stored in distinctly labelled 1.5ml plastic containers at 80°C. Green topped containers were chosen for plasma samples and yellow for serum.

The samples were grouped according to visit number for easier reference. Blood for DNA analysis was stored in a -20°C freezer.

2.2.14 Inflammatory marker analysis

The plasma and serum samples were analysed using semi quantitative assays with kits supplied by MesoScale Discovery (MSD) (Meso Scale Discovery, Rockville USA) for cytokine quantification and EuroDiagnostica (Malmo, Sweden) for individual complement pathway activation levels.

2.2.15 MSD analysis

MSD (Meso Scale Discovery, Rockville USA) products utilised kits based on sandwich immunoassays detection methods. The underlying principle is based on specific wells lined with capture antibodies on the base. The samples are added and the antigen of interest bound to the plate surface. A series of washes and diluents reduces nonspecific binding. A detection antibody is then added followed by a solution containing an electroluminescent fluorophore. The plate is placed in a sector reader and an electric current applied to the base. The level of luminescence produced is directly proportional to the amount of bound antigen within the analyte.

The process varied for the 3 types of investigations i.e. Cytokine 5-plex (IL-1, -2, -6, -8 and TNF), Eotaxin-2 and CRP plates. However, all steps involved a series of incubations and washes. The protocol for the cytokine 5-plex plate as an example:

1. Diluent 2 added to MSD (Meso Scale Discovery, Rockville USA) plate and incubated for 30 minutes on a rotary mixer
2. 25µl of serum was added to each well and the mixture incubated for 2 hours on the rocker followed by 3 cycles of washing with phosphate buffered saline/tween (PBS-T)
3. 25µl of detection antibody was added and incubated for 2 hours followed by washing with PBS-T
4. 150µl of read buffer was placed in each well and the plate read with the MSD (Meso Scale Discovery, Rockville USA) spectrophotometer

A 7 point standard curve using 4 fold dilutions was used for all concentration calculations and was a major determinant in overall quality control of the experiment. The MSD spectrophotometer was preprogrammed with individual patient specific identification and analysis parameters.

2.2.16 Complement analysis

The activated complement levels for the classical and alternative pathways were analysed with kits supplied by EuroDiagnostica (Malmo, Sweden).

The wells of each plate contain specific activators of either the alternative or the classical complement pathways. The serum samples were incubated with diluents designed to inhibit complement pathways not involved in the testing process. The plates were washed and incubated with an alkaline phosphatase labelled enzyme specific for C5b-9. A solution containing alkaline phosphatase substrate was added and the plates analysed in a plate reader spectrophotometer (BMG Labtech, Aylesbury UK) (at 405nm) to measure the optical density of the solution.

The results were measured as a percentage compared to complement activation in the supplied positive control.

2.2.17 Statistical analysis

All results are presented as mean ± SEM (standard error of the mean), unless otherwise stated, n represents the number of replicates. For normally distributed data, statistical comparisons were made using an unpaired student's t-test, with a significance threshold of$p< 0.05$. For comparison of more than two groups a one way analysis of variance (ANOVA) was used with a Bonferroni multiple comparisons test, with a significance threshold of $p< 0.05$. Statistical Package for Social Sciences (SPSS Version 21) (IBM, Portsmouth UK) and Excel were used for statistical analysis and graph production.

3 Results

This chapter presents my results investigating the role of SERPING1 in CNV pathogenesis. The first section deals with the role of C1Inh in the development of CNV utilising 2 groups of mice, the C57BL/6 and $Ccl2^{-/-}/Cx3cr1^{-/-}$ mice.

3.1 C57BL/6 and $Ccl2^{-/-}/Cx3cr1^{-/-}$ mice photographed 12, 24 and 52 weeks post subretinal injection of C1Inh

This section presents fundus photographs of C57BL/6 mice at 12 weeks following injection of C1Inh. This explores at a macroscopic level whether SERPING1 influences the development of AMD.

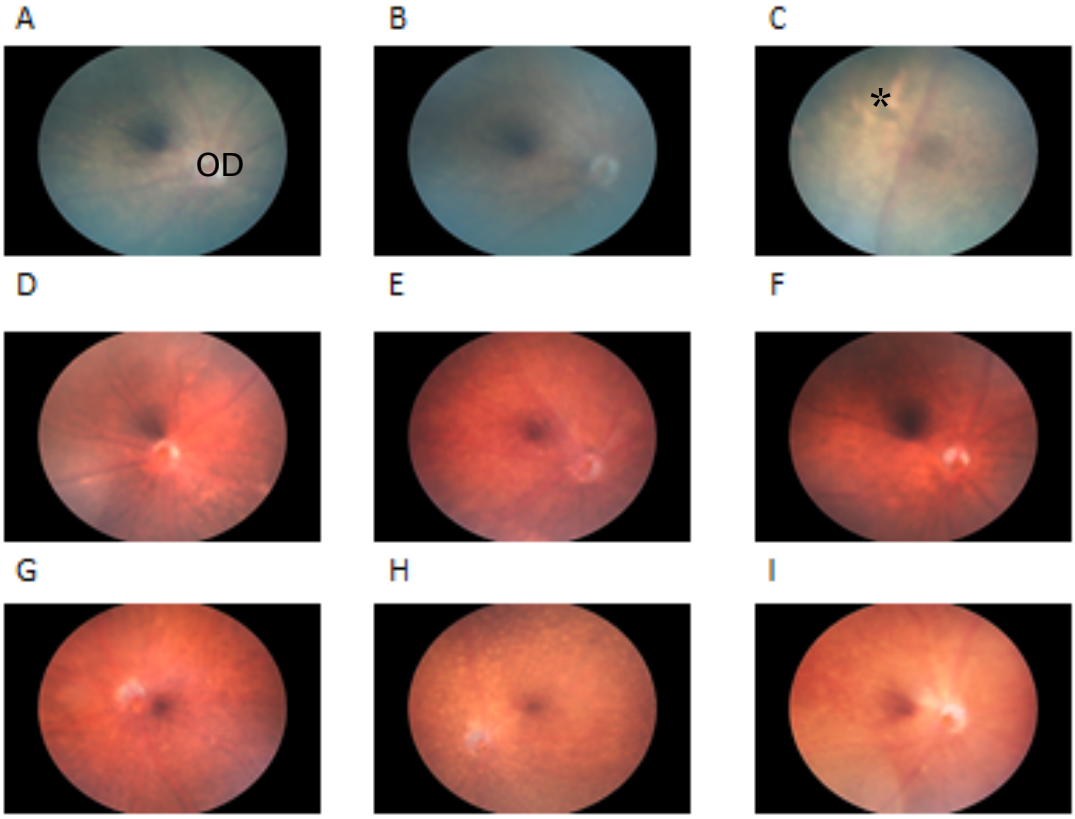

Figure 19 Fundus photographs of three examples of treated right eyes of C57BL/6 mice from each timepoint. Fundus photos of the right eye of three C57BL/6 mice (n=10) that received a subretinal injection of C1Inh. The first row (A-C) represents timepoint 1 (t=12 weeks post injection), the second row (D-F) represents timepoint 2 (t=24 weeks post subretinal injection) and the third row (G-I) represents timepoint 3 (t=52 weeks post subretinal injection of C1Inh. *- Area of retinal pigmentary change created by the induced retinal detachment. OD- Optic disc with radiating retinal blood vessels.

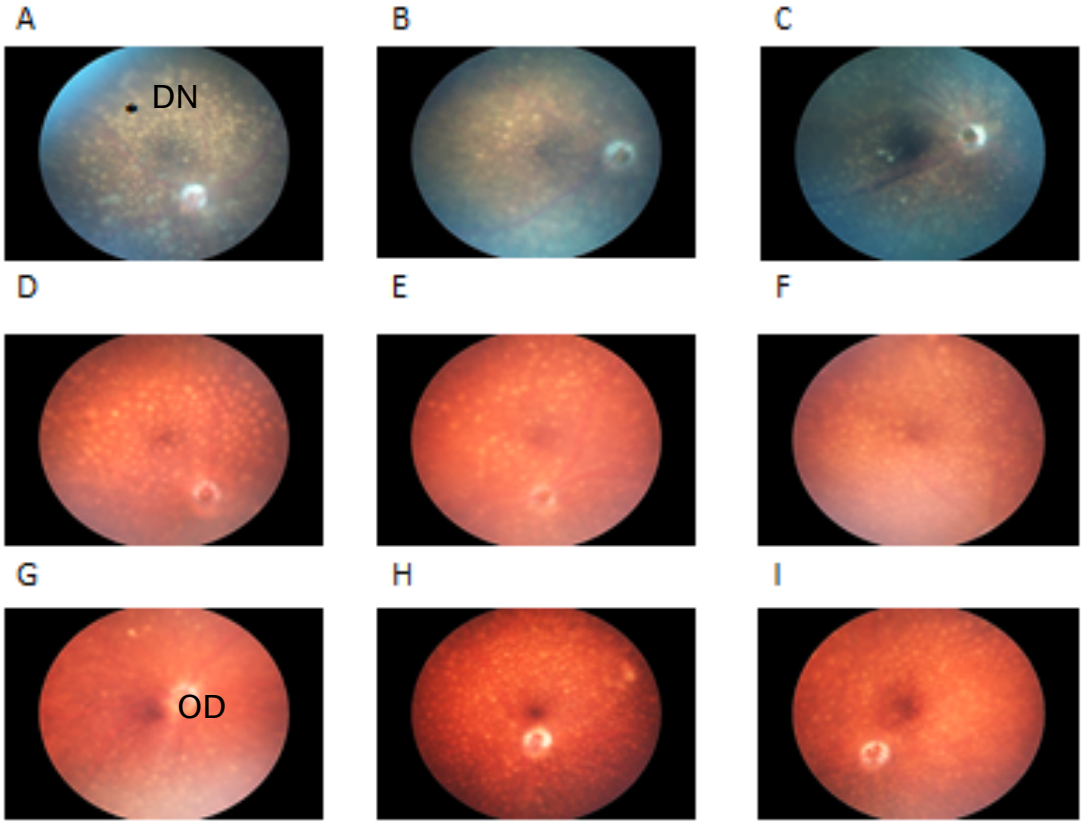

Figure 20 Fundus photographs of three examples treated right eyes of $Ccl2^{-/-}/Cx3cr1^{-/-}$ mice from each timepoint. Fundus photos of the right eye of three $Ccl2^{-/-}/Cx3cr1^{-/-}$ mice (n=10) that received a subretinal injection of C1Inh. The first row (A-C) represents timepoint 1 (t=12 weeks post injection), the second row (D-F) represents timepoint 2 (t=24 weeks post subretinal injection) and the third row (G-I) represents timepoint 3 (t=52 weeks post subretinal injection of C1Inh. DN- Area of phenotypic drusen-like deposits. OD- Optic disc with radiating retinal blood vessels.

3.1.1 Summary

The fundus photographs showed no gross phenotypic changes suggestive of AMD development in the C57/Bl6 mice (Figure 19). This work provided the basis for investigations into the effect of C1Inh utilising immunohistochemistry and staining techniques to examine photoreceptor function and architecture as well as the integrity of Bruch's membrane.

Photographed fundi of the $Ccl2^{-/-}/Cx3cr1^{-/-}$ mice demonstrated hypopigmented discrete spots reminiscent of drusen (Figure 20). However, as discussed previously these spots are not drusen but rather a result of an underlying retinal degeneration mutation (Crb1, rd8) on the background C57BL/6 murine strain[172-174]. There were no other significant gross fundal changes noted.

3.2 Histology of the C57BL/6 and Ccl2$^{-/-}$/Cx3cr1$^{-/-}$ mice at timepoints 1, 2 and 3 following injection of C1Inh

The two groups of mice were examined with light and transmission electron microscopy and with varying staining techniques to identify any differences in histological architecture suggestive of AMD. This related to the hypothesis that C1Inh inhibited the development of AMD.

3.2.1 Haematoxylin and eosin (H&E) stains of retinal sections from C57BL/6 mice

I examined H&E stained retinal sections of mice from the C57BL/6 cohort from 12, 24 and 52 weeks post injection of C1Inh, for any signs suggestive of AMD development. Specifically, sub RPE deposits, new vessel formation or abnormally thickened sub RPE basement membrane were investigated.

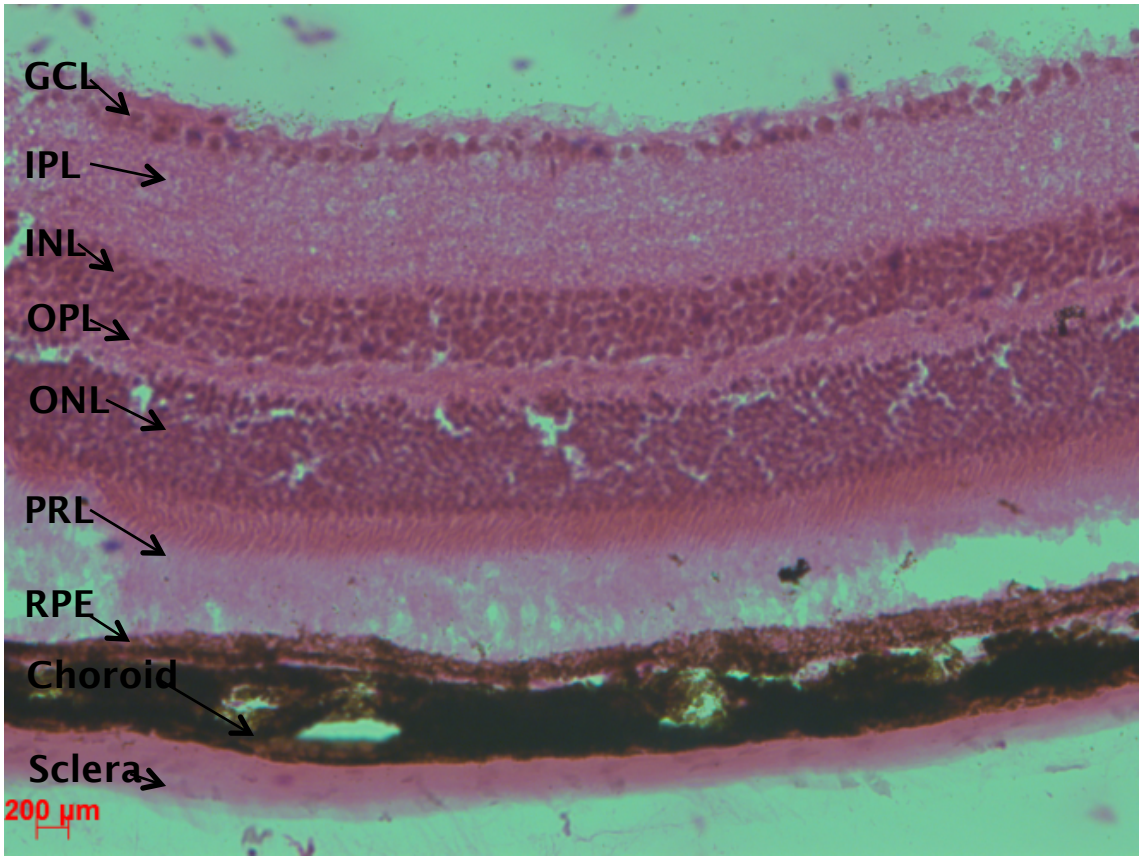

Figure 21 Representative photomicrographs of a C57BL/6 mouse stained with H & E at magnification X20. The retinal layers are ganglion cell layer (GCL), inner plexiform layer (IPL), inner nuclear layer (INL), outer plexiform layer (OPL), outer nuclear layer (ONL), photoreceptor layer (PRL), retinal pigment epithelium (RPE), choroid and sclera.

3.2.2 Haematoxylin and eosin (H&E) stains of retinal sections from $Ccl2^{-/-}$/$Cx3cr1^{-/-}$ mice

I examined H&E stained retinal sections of mice from the $Ccl2^{-/-}$/$Cx3cr1^{-/-}$ cohort from 12, 24 and 52 weeks post injection of C1Inh, for any signs suggestive of AMD development. Specifically, sub RPE deposits, new vessel formation or abnormally thickened sub RPE basement membrane were investigated.

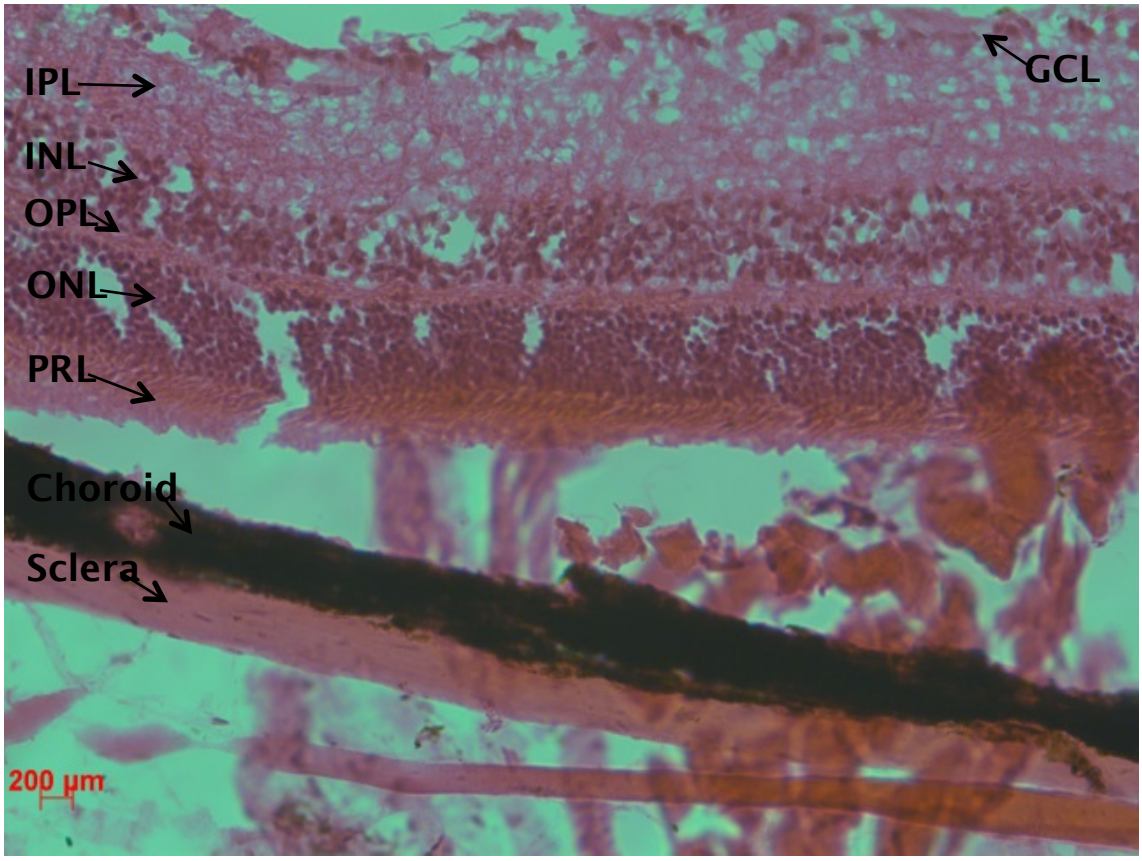

Figure 22 Representative photomicrograph of a $Ccl2^{-/-}/Cx3cr1^{-/-}$ mouse stained with H & E at magnification X20. The retinal layers are ganglion cell layer (GCL), inner plexiform layer (IPL), inner nuclear layer (INL), outer plexiform layer (OPL), outer nuclear layer (ONL), photoreceptor layer (PRL), choroid and sclera.

3.2.2.1 Summary

Light microscopic examination of H & E stained sections did not detect any gross histological difference in the two groups of mice under investigation. There were no obvious drusenoid deposits phenotypically characteristic of the $Ccl2^{-/-}/Cx3cr1^{-/-}$ mice.

3.2.3 Transmission electron microscopy (TEM) images of C57BL/6 and Ccl2$^{-/-}$/Cx3cr1$^{-/-}$ mice at timepoint three

I investigated at the nanoscopic level whether there were detectable differences between the C57/BL6 and Ccl2$^{-/-}$/Cx3cr1$^{-/-}$ mice at 52 weeks post injection of C1Inh. This examined for differences at the sub RPE basement membrane in aged mice suggestive of AMD.

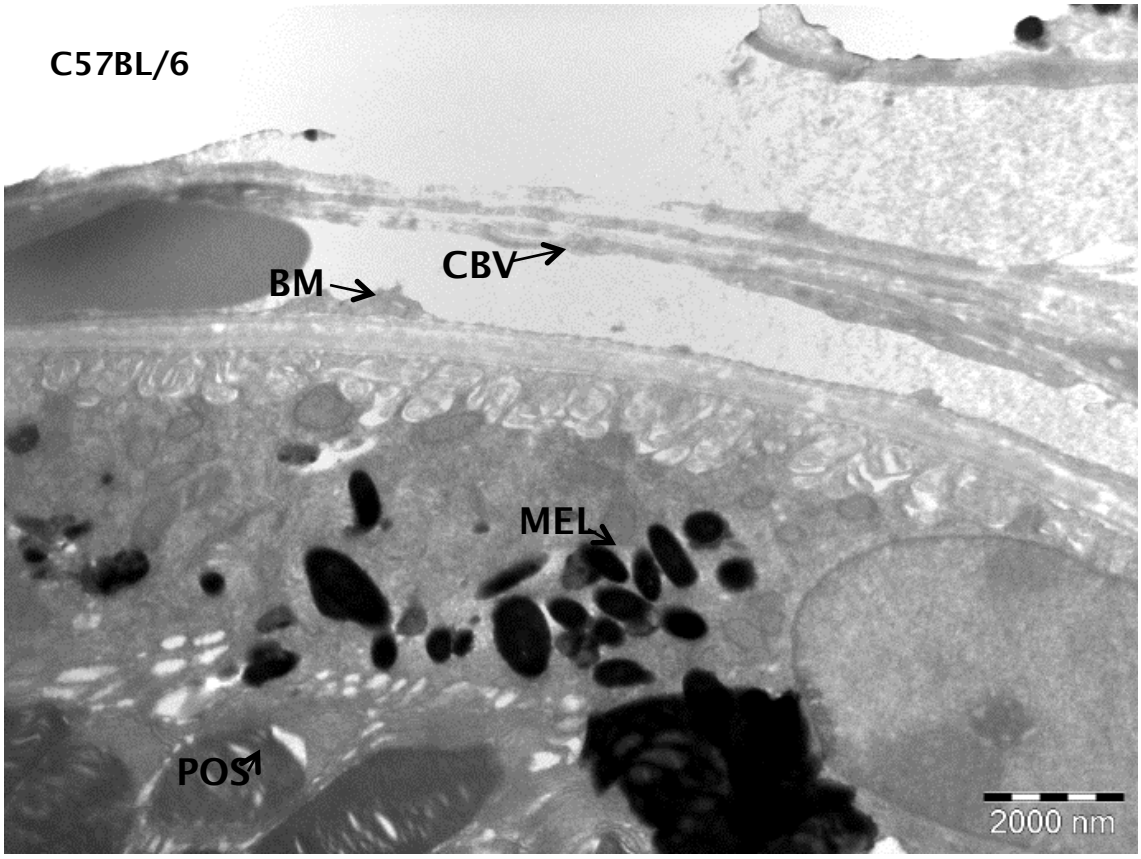

Figure 23 TEM image of the outer retina and choroid from a C57BL/6 mouse harvested 52 weeks post subretinal injection of C1Inh. (POS) photoreceptor outer segments (MEL) melanosomes from the RPE (BM) Basement membrane (CBV) vessel in the choriocapillaris.

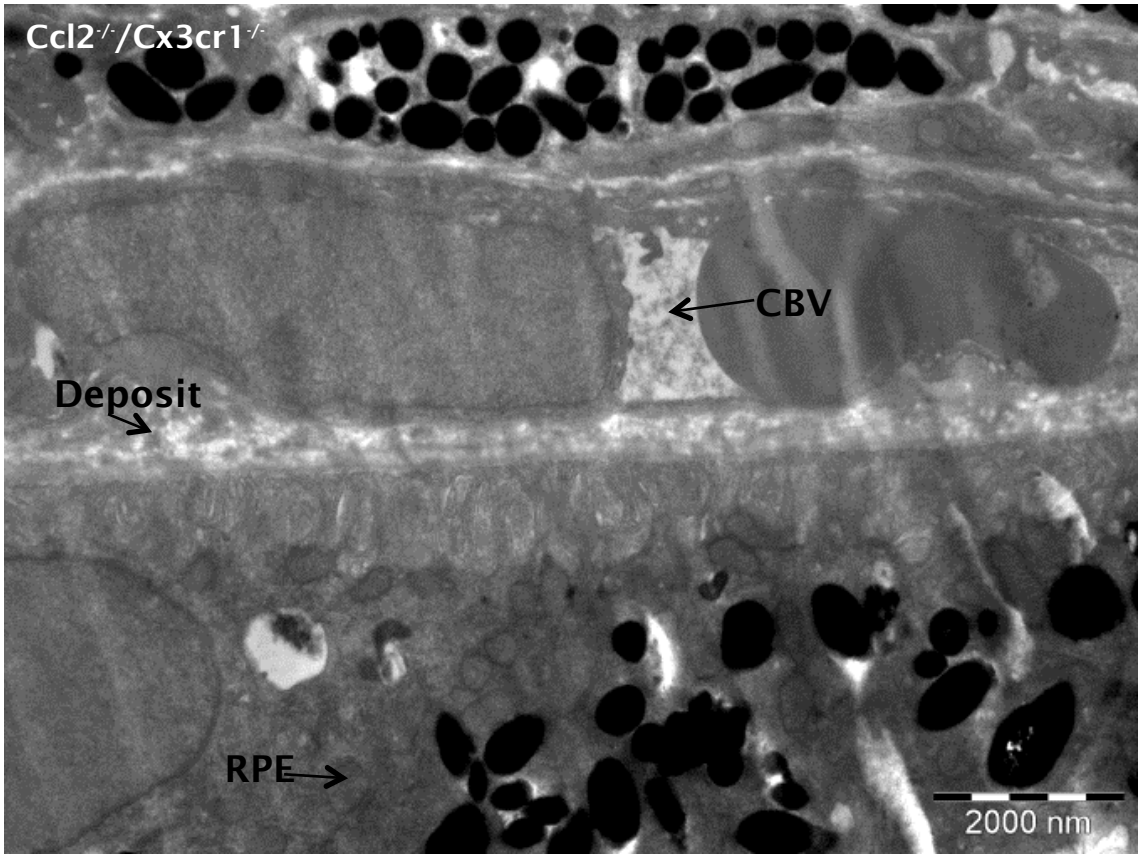

Figure 24 TEM image of the outer retina and choroid from a $Ccl2^{-/-}/Cx3cr1^{-/-}$ mouse harvested 52 weeks post subretinal injection of C1Inh. The image identified a drusenoid deposit in the sub-RPE layer within the basement membrane. (CBV) vessel in the choriocapillaris

3.2.3.1 Summary

The main anatomical difference noted between the two groups of mice from timepoint 3 was the drusenoid deposit present in the sub RPE basement membrane. Further histochemical analysis would be necessary to determine the composition of the structure.

3.2.4 (5-bromo-4-chloro-1H-indol-3-yl) dihydrogen phosphate and nitro blue tetrazolium chloride (BCIP/NBT) stains of C57BL/6 mice at all timepoints

This experiment continued the investigations into AMD development. BCIP/NBT was used to detect signs of neovascularization, specifically subretinal neovascularization characteristic of CNV development. I examined BCIP/NBT stained retinal sections of mice from the C57/BL6 cohort from 12, 24 and 52 weeks post injection of C1Inh, for any signs suggestive of CNV formation.

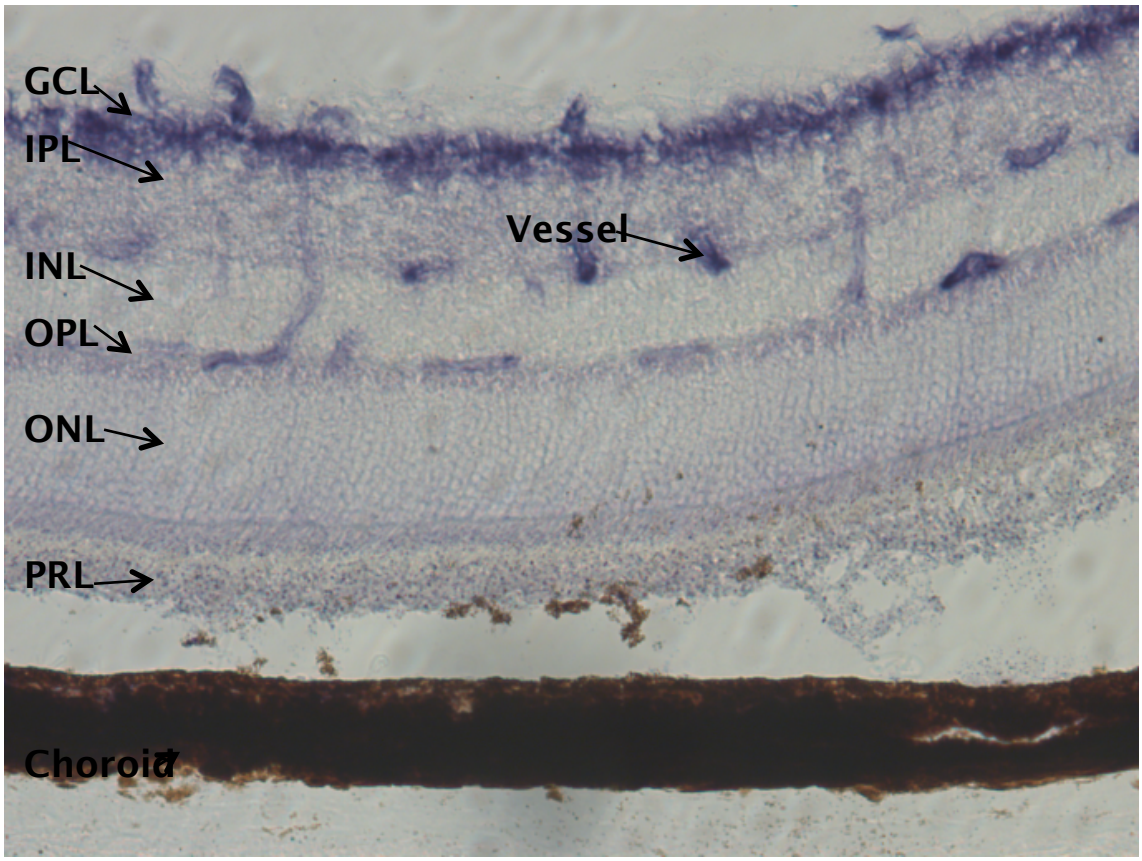

Figure 25 Representative photomicrographs of a C57BL/6 mouse stained with (BCIP/NBT) at magnification X20. The retinal layers are ganglion cell layer (GCL), inner plexiform layer (IPL), inner nuclear layer (INL), outer plexiform layer (OPL), outer nuclear layer (ONL), photoreceptor layer (PRL) and choroid. Retinal blood vessels stained with BCIP/NBT are also identified.

3.2.5 (5-bromo-4-chloro-1H-indol-3-yl) dihydrogen phosphate and nitro blue tetrazolium chloride (BCIP/NBT) stains of $Ccl2^{-/-}$/$Cx3cr1^{-/-}$ mice at all timepoints

This experiment continued the investigations into AMD development. BCIP/NBT was used to detect signs of neovascularizationv (through its ability to identify blood vessels), specifically subretinal neovascularization characteristic of CNV development. I examined BCIP/NBT stained retinal sections of mice from the $Ccl2^{-/-}$/$Cx3cr1^{-/-}$ cohort from 12, 24 and 52 weeks post injection of C1Inh, for any signs suggestive of CNV formation.

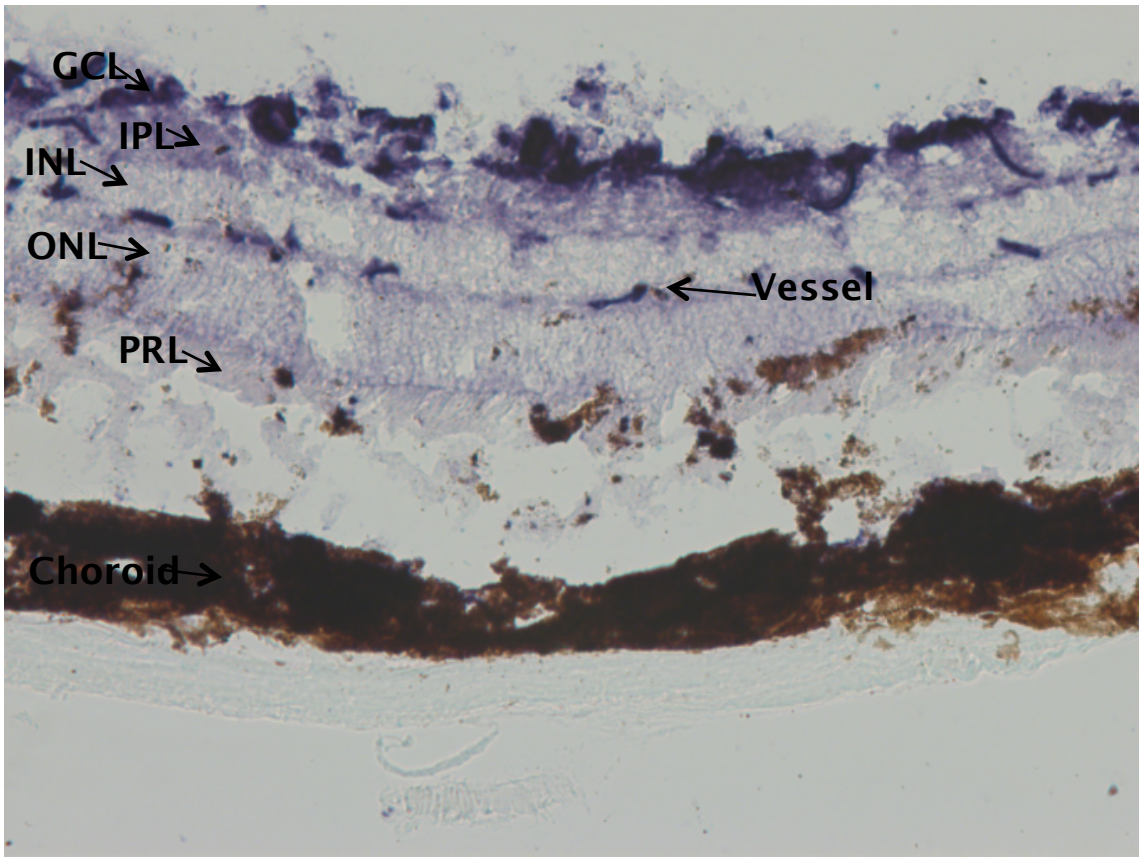

Figure 26 Representative photomicrographs of a $Ccl2^{-/-}$/$Cx3cr1^{-/-}$ mouse stained with (BCIP/NBT) at magnification X20. The retinal layers are ganglion cell layer (GCL), inner plexiform layer (IPL), inner nuclear layer (INL), outer nuclear layer (ONL), photoreceptor layer (PRL) and choroid. A blood vessel within the inner retina is also highlighted.

3.2.5.1 Summary

BCIP/NBT utilizes the endogenous alkaline phosphatase activity in blood vessels to produce the intense dark blue stain. Angiogenesis is the key feature of CNV development. There was no detectable difference in the levels of angiogenesis between the two groups at all timepoints.

3.2.6 Oil red O (OrO) combined with eosin stains of C57BL/6 mice

This experiment continued the investigations into AMD development and the relationship to the main hypothesis of the thesis. OrO stains lipids, a component of both basement membranes and drusen. I examined OrO stained retinal sections of mice from the C57BL/6 cohort from 12, 24 and 52 weeks post injection of C1Inh, for any signs suggestive of AMD development.

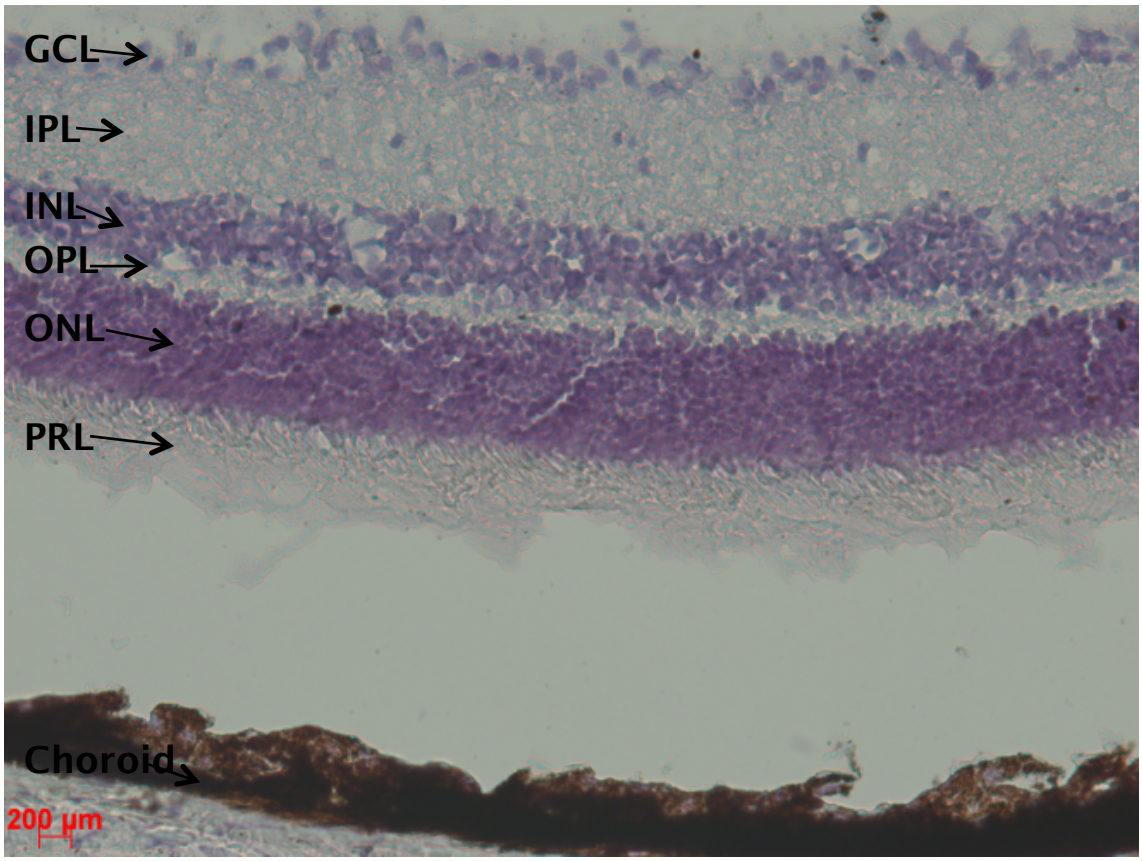

Figure 27 Representative photomicrographs of a C57BL/6 mouse stained with OrO at magnification X20. The retinal layers are ganglion cell layer (GCL), inner plexiform layer (IPL), inner nuclear layer (INL), outer plexiform layer (OPL), outer nuclear layer (ONL), photoreceptor layer (PRL) and choroid.

3.2.7 Oil red O (OrO) combined with eosin stains of $Ccl2^{-/-}$/$Cx3cr1^{-/-}$ mice

This experiment continued the investigations into AMD development. OrO stains lipids, a component of drusen. I examined OrO stained retinal sections of mice from the $Ccl2^{-/-}$/$Cx3cr1^{-/-}$ cohort from 12, 24 and 52 weeks post injection of C1Inh, for any signs suggestive of AMD development.

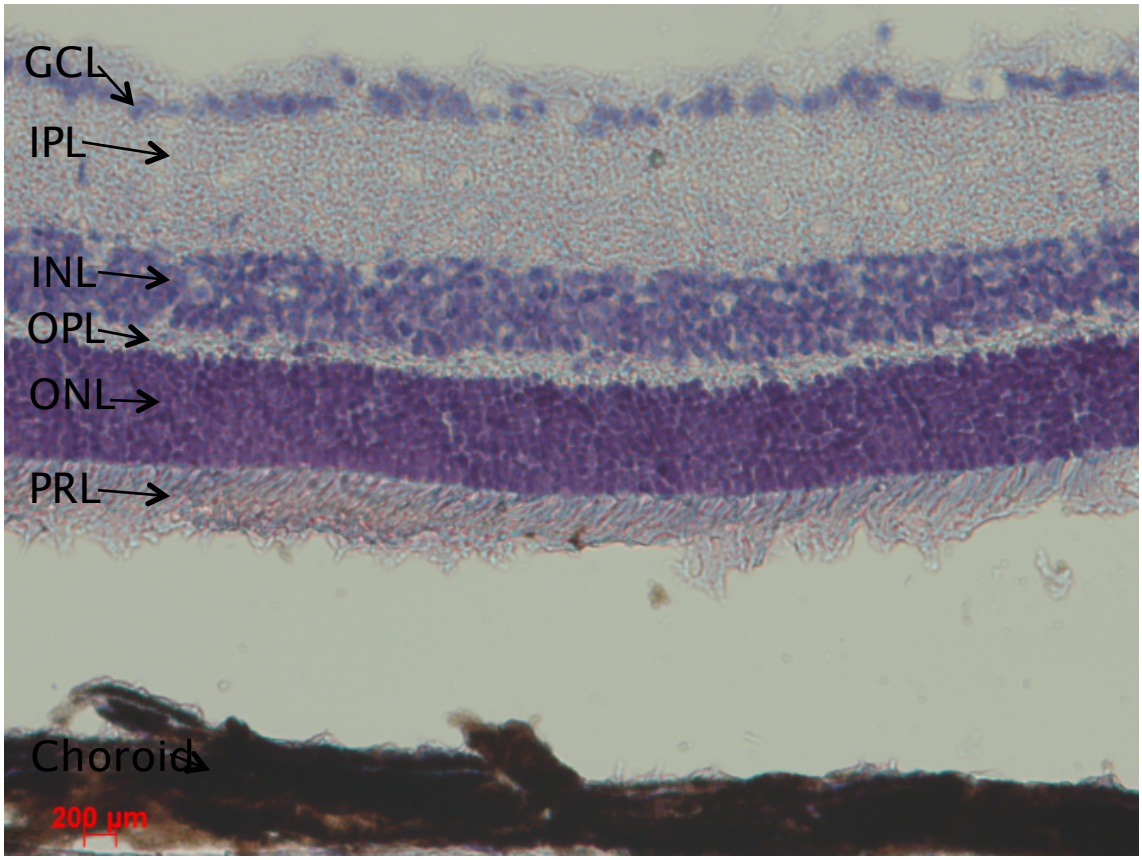

Figure 28 Representative photomicrographs of a $Ccl2^{-/-}$/$Cx3cr1^{-/-}$ mouse stained with OrO at magnification X20. The retinal layers are ganglion cell layer (GCL), inner plexiform layer (IPL), inner nuclear layer (INL), outer plexiform layer (OPL), outer nuclear layer (ONL), photoreceptor layer (PRL) and choroid.

3.2.7.1 Summary

OrO has been used to stain for lipid deposits, a common feature of AMD with both deposition in Bruch's membrane and drusen. There was no gross difference in the level of staining produced with OrO in either the knockout or wild type mice.

3.3 Immunohistochemical imaging and analysis of the retina of C57BL/6 and $Ccl2^{-/-}$/$Cx3cr1^{-/-}$ mice at timepoints 1, 2 and 3 following subretinal injection of C1Inh, examining known components of drusen and Bruch's membrane

I utilised immunohistochemistry to complete a semi-quantitative analysis of known components of Bruch's membrane and drusen. This provided data comparing the levels of these components in wild type and knockout mice (AMD model) at specific timepoints post subretinal injection of C1Inh. I also investigated the level of apoptosis and retinal thickness of the two groups at 52 weeks post treatment knowing the relationship of the classical complement pathway with GA.

3.3.1 Analysis of immunohistochemical results.

This section examined any differences in fluorescent staining intensity for rhodpsin (a component of rod photoreceptor outer segments), laminin (an extracellular matrix protein found in retinal basement membrane), vitronectin (an extracellular matrix protein found in drusen) and complement components 5 and C5b-9 (found in drusen).

3.3.1.1 Laminin deposition within the study cohorts

Laminin is an extracellular matrix protein found in human Bruch's membrane and expressed in CNV[175, 176]. I investigated whether there was a significant difference in deposition at the three timepoints for the two groups.

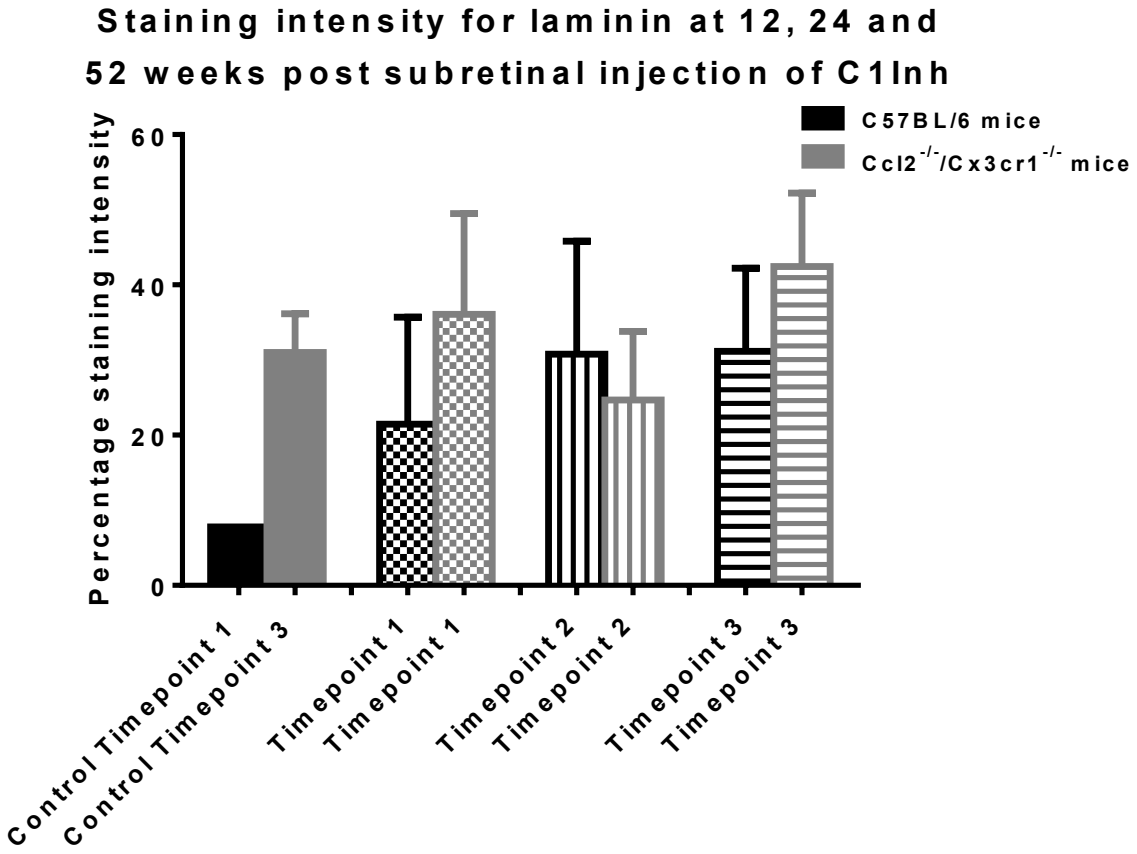

Figure 29 This figure represents sections stained with an antibody directed against laminin an extracellular matrix protein found throughout the basement membranes of retina. Mice were culled at 12, 24 and 52 weeks post subretinal injection of humanized C1Inh and the level of fluorescent intensity calculated using Volocity software. Values calculated are mean ± SEM (n=49)

3.3.1.1.1 ***Summary***

Analysis of the three timepoints demonstrated no statistically significant difference between the 2 groups of mice at each timepoint (Timepoint 1, p=0.0578 with 95% CI of-0.5566 to 29.80) (Timepoint 2, p=0.3681 with 95% CI of -20.23 to 8.032) (Timepoint 3, p=0.4391 with 95% CI of -10.11 to 22.20). One way ANOVA analysis for significance between all timepoints demonstrated no significant result (p=0.0739, with an F statistic of 0.4477 (95% CI 5, 43)). The non-significant result from this experiment may be due to the relatively small sample size.

3.3.1.2 Rhodopsin fluorescent staining intensity within the study cohorts

Rhodopsin is an integral compound in the phototransduction cycle and is found in rod outer segments[177]. Advanced AMD leads to photoreceptor cell death with an associated reduction in pigment concentration. I investigated whether there was a significant difference in fluorescent staining at the three timepoints for the two groups.

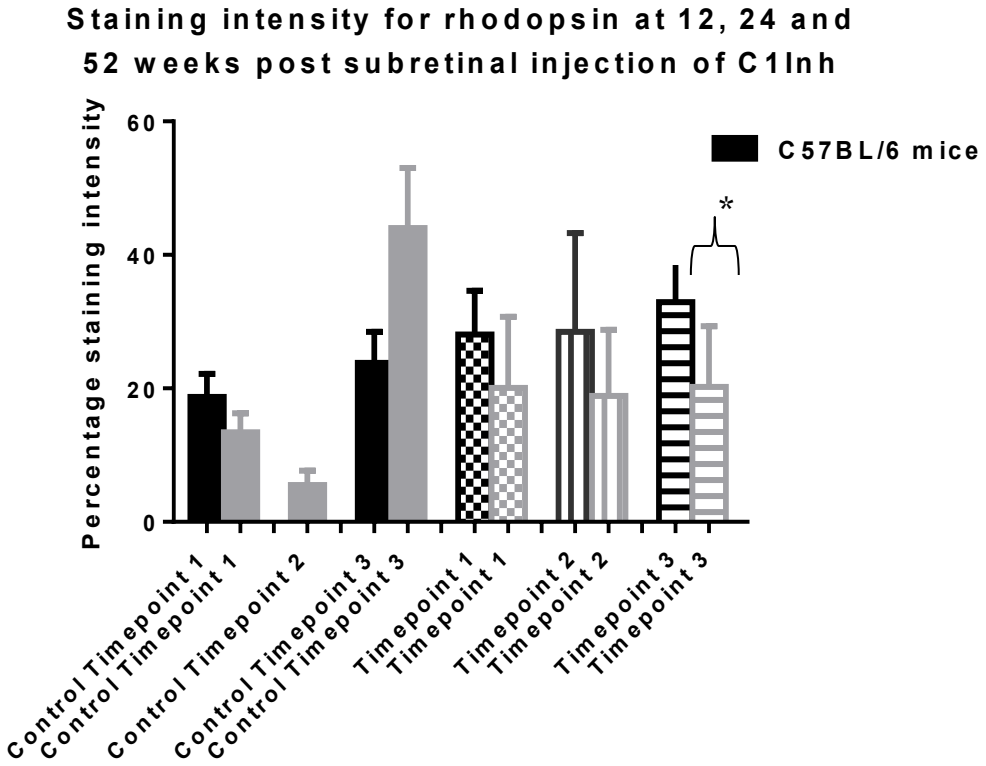

Figure 30 This figure represents sections stained with an antibody directed against rhodopsin, a photoreactive pigment protein found in rod photoreceptors. Mice were culled at 12, 24 and 52 weeks post subretinal injection of humanized C1Inh and the level of fluorescent intensity calculated using Volocity software. Values calculated are mean ± SEM (n=49). *- represented a statistically significant difference between two groups.

3.3.1.2.1 *Summary*

Analysis of the three timepoints demonstrated a statistically significant difference between the 2 groups of mice at timepoint 3 (Timepoint 1, p= 0.9622 with 95% CI of -21.10 to 20.16) (Timepoint 2, p= 0.0761 with 95% CI of -20.28 to 1.098) (Timepoint 3, p= 0.0161 with 95% CI of -22.79 to -2.619). C57BL/6 mice at timepoint 3 had a mean percentage staining intensity of 32.94 ± 4.278 (N=10) compared to those in the AMD model for the same timepoint (mean=20.23 ± 2.617 (N=12)). There was however no statistical significant difference between timepoints 1 and 3 for the two groups. This suggests the photoreceptors are preserved to a greater extent in the wild type as compared to the AMD model.

3.3.1.3 Complement component 5 (C5) fluorescent staining intensity within the study cohorts

C5 has previously been isolated from drusen in early AMD[54, 55, 175]. I investigated whether there was a significant difference in fluorescent staining at the three timepoints for the two groups.

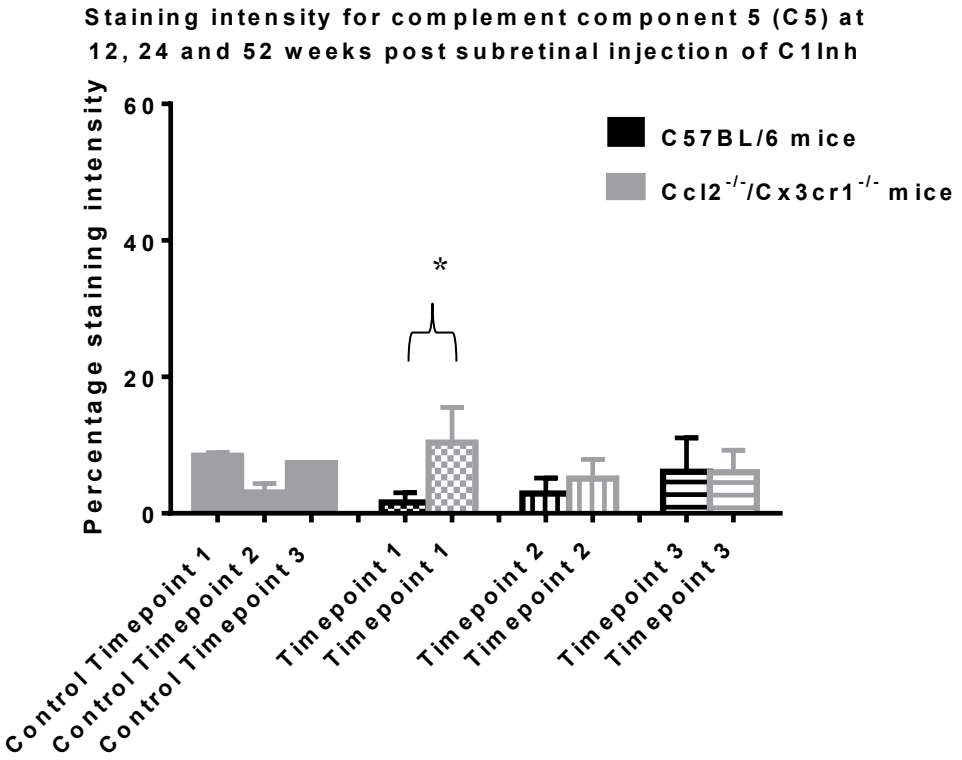

Figure 31 This figure represents sections stained with an antibody directed against C5. Complement components have been isolated from drusen and play a key role in AMD development and progression. Mice were culled at 12, 24 and 52 weeks post subretinal injection of humanized C1Inh and the level of fluorescent intensity calculated using Volocity software. Values calculated are mean ± SEM (n=49). *- represented a statistically significant difference between two groups.

3.3.1.3.1 ***Summary***

Analysis of the three timepoints demonstrated a statistically significant difference between the 2 groups of mice at timepoint 1 only (Timepoint 1, p=0.0003 with 95% CI of 4.716 to 12.81). There was a statistically significant difference in the mean percentage staining intensity of C57BL/6 mice in timepoints 1 and 3 (p=0.0265). This was replicated in the

$Ccl2^{-/-}/Cx3cr1^{-/-}$ mice (p= 0.0404). The results demonstrate that in spite of the higher level of C5 present initially in the AMD model, at 52 weeks the levels have decreased to the same level as wild type mice. In contrast, the wild type mice have an increase in C5 levels over the time of the experiment.

3.3.1.4 C5b-9 fluorescent staining intensity within the study cohorts

C5-9 is the terminal pathway for all three components of the complement cascade. C5b-9 has been isolated from drusen[54, 55, 178, 179], suggesting a role in the development of AMD.

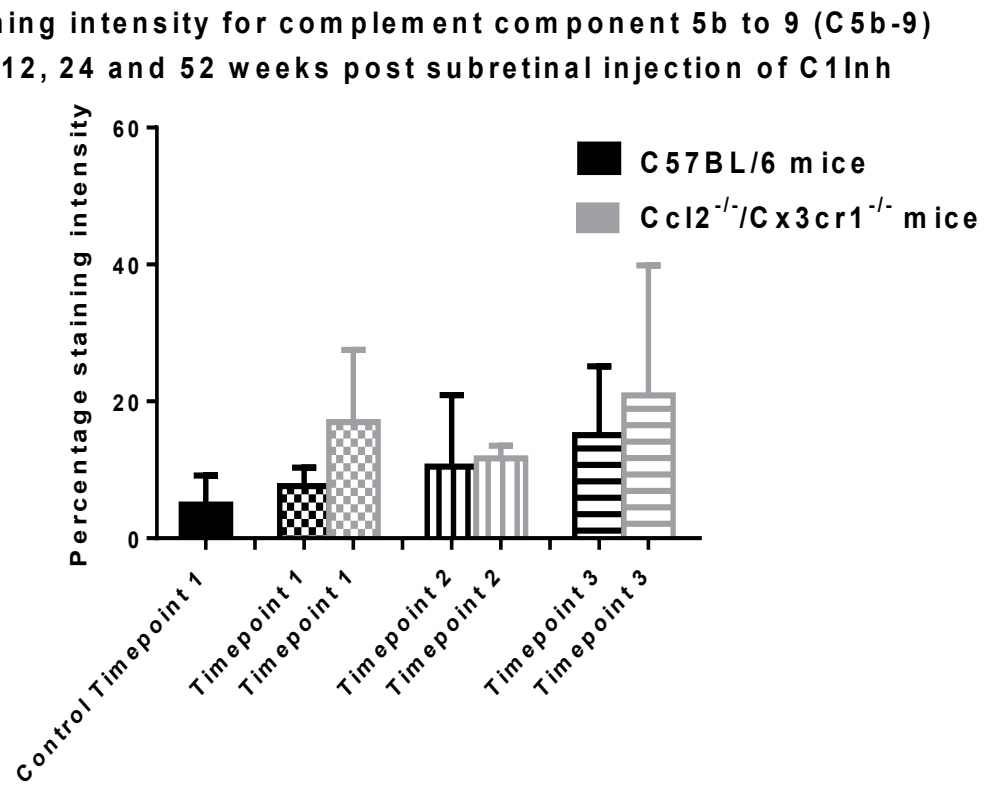

Figure 32 This figure represents sections stained with an antibody directed against C5b-9. Complement membrane attack complex (MAC) components have been isolated from drusen and play a key role in AMD development and progression. Mice were culled at 12, 24 and 52 weeks post subretinal injection of humanized C1Inh and the level of fluorescent intensity calculated using Volocity software. Values calculated are mean ± SEM (n=39).

3.3.1.4.1 *Summary*

Analysis of the three timepoints demonstrated no statistically significant difference between the 2 groups of mice at any of the 3 timepoints (utilising a student's t test of independent samples) ($p>0.05$). There was also no significant difference between timepoints 1 and 3 ($p>0.05$). This may suggest a sustained protective effect for C1Inh in preventing MAC formation.

3.3.1.5 Vitronectin fluorescent staining intensity within the study cohorts

Vitronectin has been isolated from drusen[22, 180], suggesting a role in the development of AMD. Fluorescent immunohistochemistry was performed to determine any difference between the 2 groups of mice at the 3 timepoints.

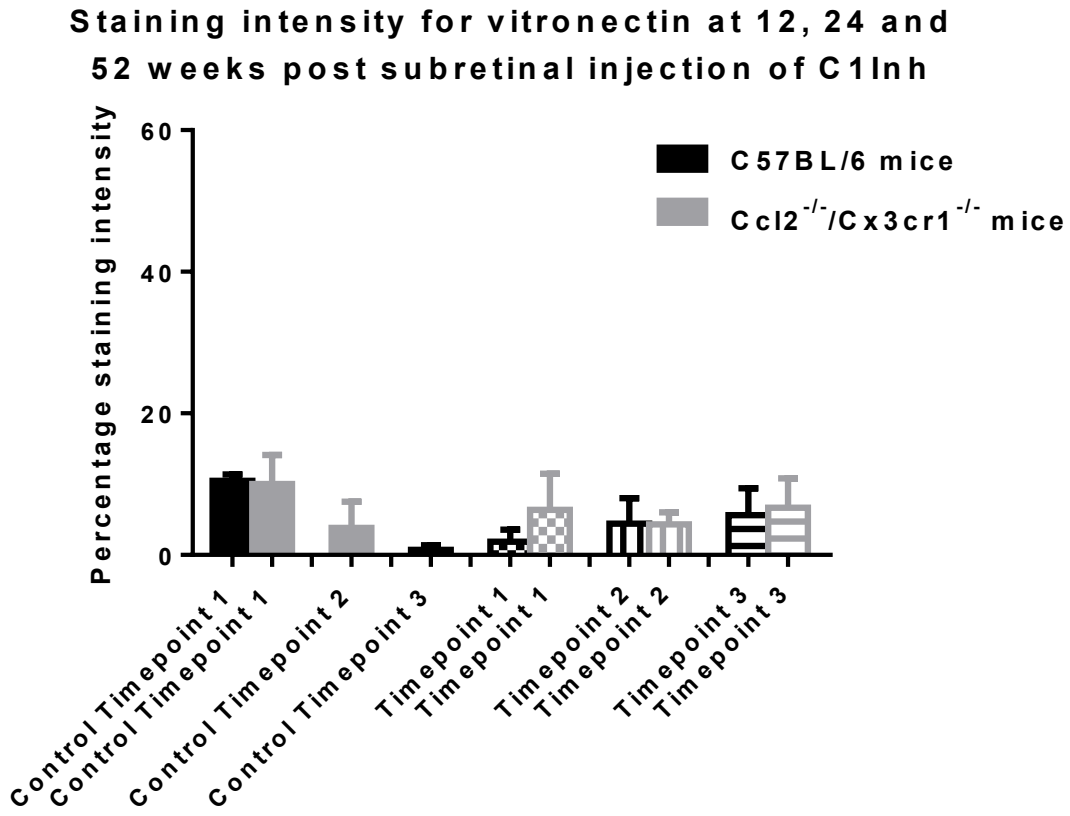

Figure 33 This figure represents sections stained with an antibody directed against vitronectin. Vitronectin has been isolated from drusen and may play a role in early AMD pathogenesis. Mice were culled at 12, 24 and 52 weeks post subretinal injection of humanized C1Inh and the level of fluorescent intensity calculated using Volocity software. Values calculated are mean ± SEM (n=50).

3.3.1.5.1 *Summary*

Analysis of the three timepoints demonstrated no statistically significant difference between the 2 groups of mice at any of the 3 timepoints (utilising a student's t test of independent samples) ($p>0.05$). There was also no significant difference between timepoints 1 and 3 ($p>0.05$). This may suggest a protective effect of C1Inh in preventing drusen formation or signs of retinal degeneration.

3.4 Assessment of apoptosis levels and retinal thickness of the C57BL/6 and $Ccl2^{-/-}/Cx3cr1^{-/-}$ mice at timepoints 1, 2 and 3 following subretinal injection of C1Inh

Based on the hypothesis that C1Inh has a role in AMD pathogenesis and that it is likely protective via inhibition of complement 1 (essential component of the classical complement pathway), I analysed the apoptosis levels (by TUNEL stains) occurring in the two cohorts following intervention with subretinal C1Inh. The retinal thickness measurements also provided a quantification of retinal cell viability.

3.4.1 Apoptosis levels within the cohorts

AMD is associated with higher levels of cell death[121, 181]. I investigated with TUNEL analysis whether significant differences existed in my study population between groups.

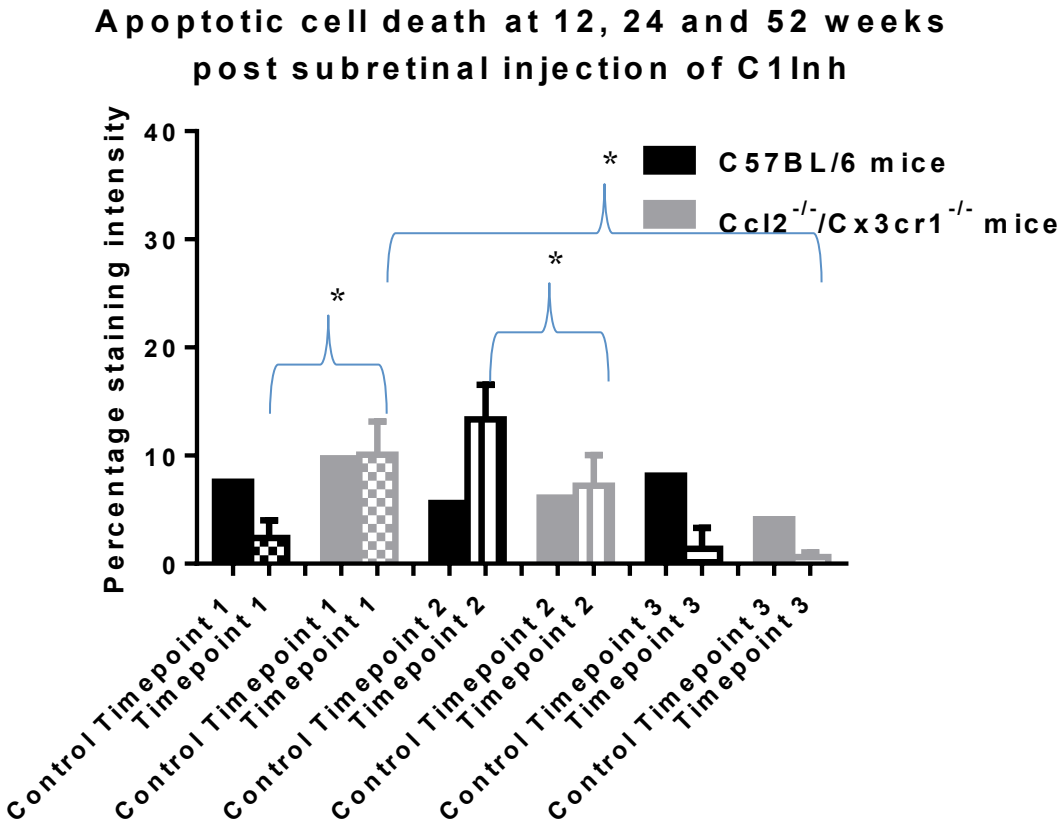

Figure 34 Terminal deoxynucleotidyl transferase dUTP nick end labelling (TUNEL) analysis measures the percentage of stained apoptotic cells within a sample utilising Volocity software. There is an increase in apoptosis in AMD retina compared to unaffected. Mice were culled at 12, 24 and 52 weeks post subretinal injection of humanized C1Inh and the level of fluorescent intensity calculated using Volocity software. Values calculated are mean ± SEM (n=26). *- represented a statistically significant difference between two groups.

3.4.1.1 Summary

Analysis of the three timepoints demonstrated a statistically significant difference between the 2 groups of mice at timepoints 1 and 2 (Timepoint 1, p=0.0023 with 95% CI of 3.950 to 11.47) (Timepoint 2, p=0.0284 with 95% CI of -11.41 to -0.9107). There was a statistically significant difference in the mean percentage staining intensity of $Ccl2^{-/-}$ /$Cx3cr1^{-/-}$ mice in timepoints 1 and 3 (p= 0.0019). These results demonstrate a higher rate of cell death initially in the $Ccl2^{-/-}$/$Cx3cr1^{-/-}$ mice as compared to wild type mice. However, at 1 year the amount of measured apoptosis is not statistically different.

3.4.2 Retinal thickness measurement levels within the cohorts

Advanced AMD in its two forms of GA or CNV produces correspondingly thin or thicker than average retinal measurements. I examined the characteristics of retinal thickness measurements in this section of the study.

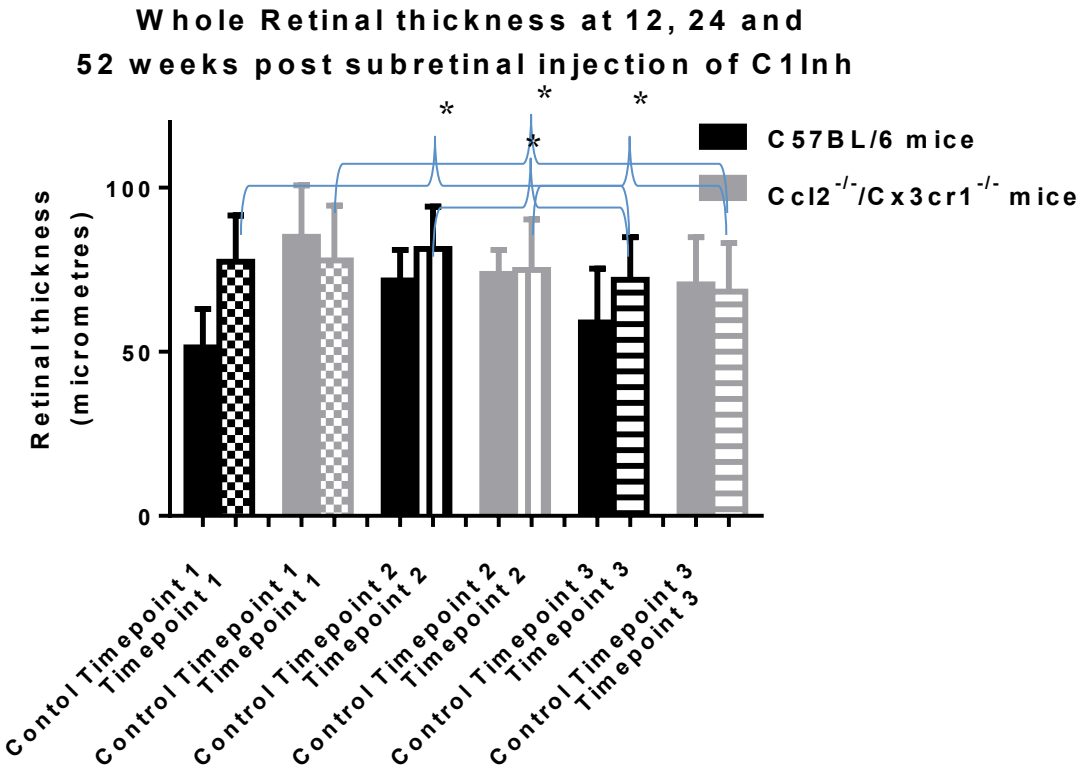

Figure 35 Whole retinal thickness measurements utilising Volocity software. Measurements were made from ILM to the sub RPE basement membrane. Mice were culled at 12, 24 and 52 weeks post subretinal injection of humanized C1Inh. Values calculated are mean ± SEM (n=2040). *- represented a statistically significant difference between two groups.

3.4.2.1 Summary

Analysis of the three timepoints demonstrated a statistically significant difference between the 2 groups of mice at timepoints 2 and 3 (Timepoint 2, p< 0.0001 with 95% CI of -8.528 to -4.174) (Timepoint 3, p=0.0007 with 95% CI of -5.659 to -1.506). There was a statistically significant difference in the mean retinal thickness change from timepoints 1 to 3 for both groups of mice ($Ccl2^{-/-}$/$Cx3cr1^{-/-}$ p < 0.0001; C57BL/6, p < 0.0001). There was a progressive thinning of the retina with time (a feature of advanced AMD-geographic atrophy) which also correlates with the lower level of apoptosis with senescence. The AMD model group developed thinner retinas with initially the higher rate of apoptosis. Further experiments may be necessary to investigate whether C1Inh accelerates initial levels of apoptosis.

3.5 Pharmacogenetic associations for AMD and potential biomarkers for predicting treatment outcome

This section of my results explores the hypothesis that possession of the adverse genotype of *SERPING1* reduces CNV response to anti VEGF treatment with ranibizumab. This is measured both with CMT and VAS changes from baseline and the number of intravitreal injections of ranibizumab. The section also explores whether known predictors of progression from early to advanced AMD can be applied to prediction of treatment outcome.

3.5.1 Demographic data obtained from the Pharmacogenetic cohort of patients

This section examines the relationship between patient demographics, behavioural factors (eg. smoking) and baseline examination characteristics (eg. baseline VAS and CMT) and the response to treatment with ranibizumab.

3.5.1.1 The relationship of gender to treatment outcome measures (CMT, VAS and administered injections of anti VEGF)

The incidence of progression to advanced AMD was previously believed to be higher in women than men[182]. This has now been shown to be incorrect with a meta-analysis by Chakravarthy *et al*.[60]. The difference in outcomes was mainly associated with variation in longevity. This result was replicated in our study where there was no significant difference in clinician administered anti-VEGF injections for active CNV per patient visit. This was the same for objective measures of change in CMT and VAS from baseline.

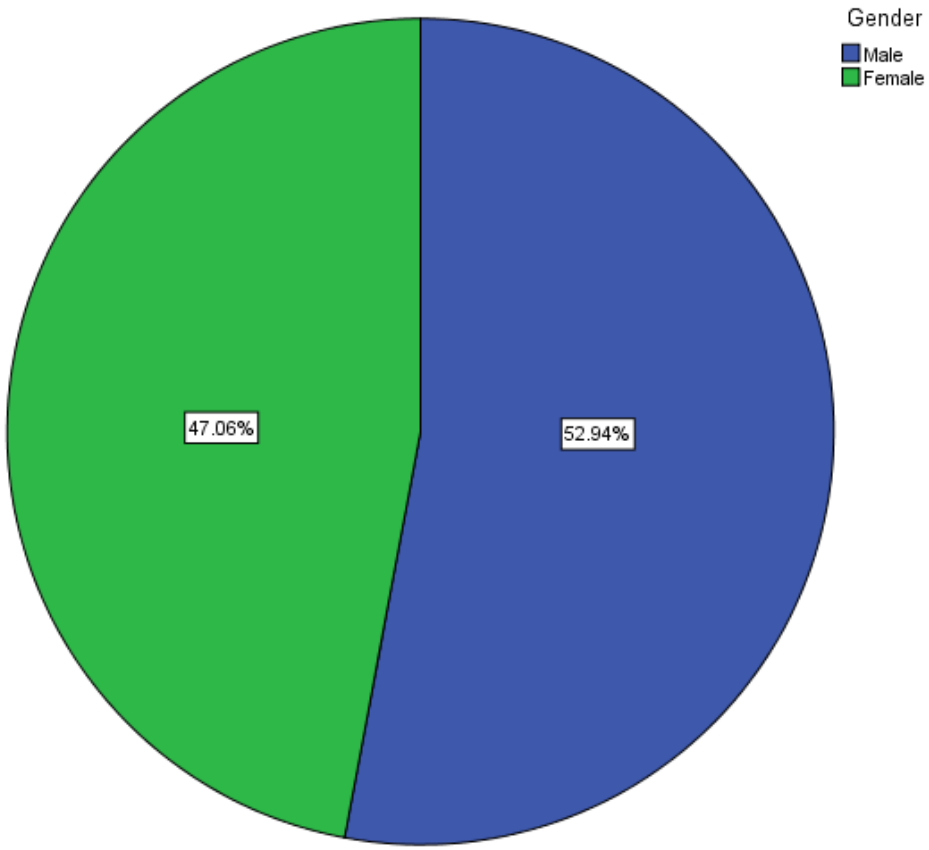

Figure 36 Gender distribution. A pie chart illustrating the distribution of study participants (n=99) according to gender.

A) Independent Samples Test				
Visit		t-test for Equality of Means		
		Sig. (2-tailed)	95% Confidence Interval of the Difference	
			Lower	Upper
2	VAS change	0.728	-4.428	3.115
3	VAS change	0.297	-4.548	1.407
4	VAS change	0.446	-4.904	2.183
5	VAS change	0.171	-7.299	1.326
6	VAS change	0.139	-9.074	1.295
7	VAS change	0.056	-10.824	0.140

B) Independent Samples Test				
Visit		t-test for Equality of Means		
		Sig. (2-tailed)	95% Confidence Interval of the Difference	
			Lower	Upper
2	CMT Change	0.634	-29.499	48.145
3	CMT Change	0.758	-38.951	53.157
4	CMT Change	0.834	-46.445	57.378
5	CMT Change	0.763	-52.478	38.665
6	CMT Change	0.926	-46.797	51.397
7	CMT Change	0.610	-66.588	39.465

Table 13 An independent samples t tests comparing mean change from baseline of central macular thickness (CMT Change) (B) in microns and visual acuity score change (VAS Change) (A) in letters according to gender.

Chi-Square Tests		
Visit		Exact Sig. (2-sided)
1	Fisher's Exact Test	0.621
2	Fisher's Exact Test	1.000
3	Fisher's Exact Test	0.615
4	Fisher's Exact Test	0.452
5	Fisher's Exact Test	1.000
6	Fisher's Exact Test	0.573
7	Fisher's Exact Test	0.770

Table 14. A Chi-square test to investigate the relationship at each visit between injection of anti VEGF for active CNV and gender using Fisher's test of significance.

3.5.1.1.1 ***Summary***

Analysis demonstrated no significant difference in the gender composition of the population cohort (47% female, 53% male in Figure 36). Unusually there were more males than females in the study whereas the population demographic would suggest a higher proportion of female participants. Independent samples t test for an association between CMT change and VAS change by gender at each participant visit demonstrated no significant association (Table 13). There was also no significant difference in means between the two genders for the administration of an injection at each participant visit when analysed by Chi-squared testing (Table 14).

3.5.1.2 The relationship of the study eye to treatment outcome measures (CMT, VAS and administered injections of anti VEGF)

This investigation explored any association of treatment outcomes with left or right treated eye.

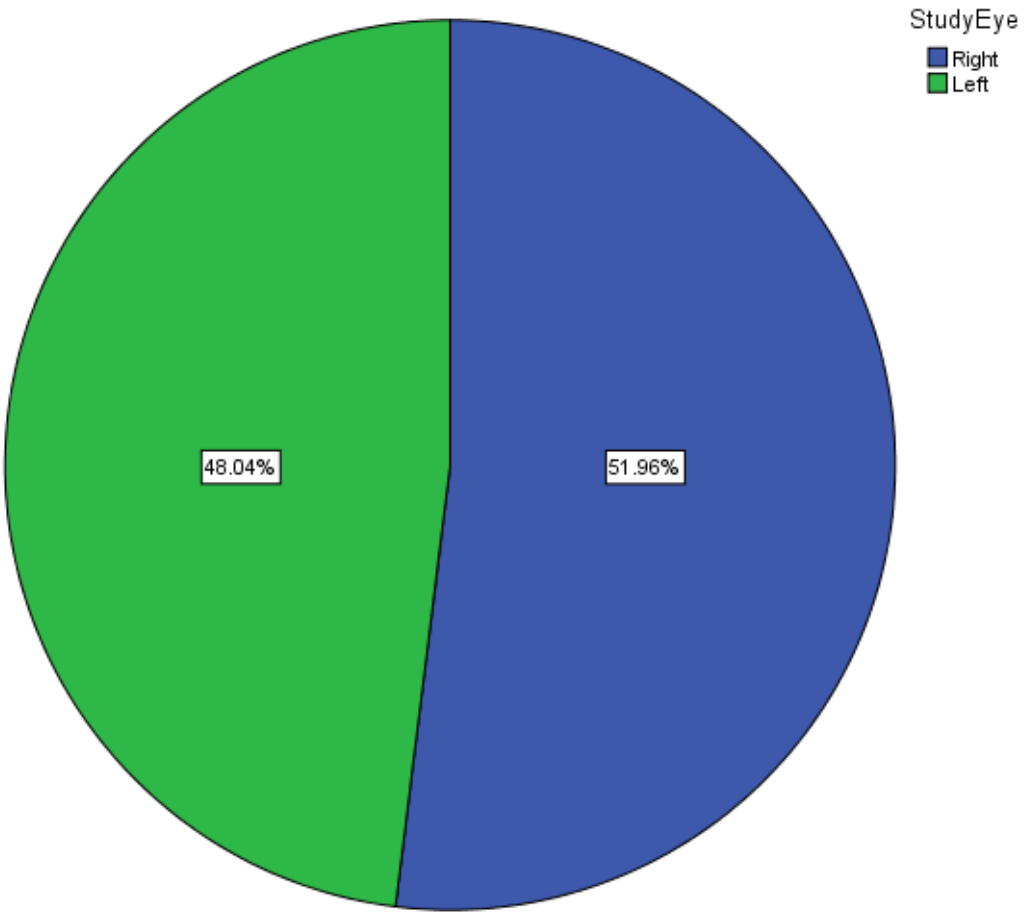

Figure 37. Percentage distribution of the study (treated) eye within the cohort (n=99)

A) Independent Samples Test						
Visit		t-test for Equality of Means				
		t	df	Sig. (2-tailed)	95% Confidence Interval of the Difference	
					Lower	Upper
2	VAS change	2.040	68.690	*0.045	0.080	7.274
3	VAS change	1.264	82.709	0.210	-1.056	4.738
4	VAS change	1.116	73.777	0.268	-1.523	5.401
5	VAS change	0.735	68.258	0.465	-2.636	5.710
6	VAS change	0.159	65.546	0.874	-4.575	5.369
7	VAS change	0.606	55.020	0.547	-3.889	7.261

B) Independent Samples Test				
Visit		t-test for Equality of Means		
		Sig. (2-tailed)	95% Confidence Interval of the Difference	
			Lower	Upper
2	CMT Change	0.522	-51.364	26.287
3	CMT Change	0.184	-75.717	14.888
4	CMT Change	0.307	-81.446	26.110
5	CMT Change	0.227	-76.613	18.622
6	CMT Change	0.623	-61.145	36.931
7	CMT Change	0.800	-46.807	60.400

Table 15 An independent samples t test comparing mean change of central macular thickness (CMT Change) (B) in microns and visual acuity score change (VAS Change) (A) in letters from baseline between treated eyes at each visit.

Chi-Square Tests		
Visit		Exact Sig. (2-sided)
1	Fisher's Exact Test	0.341
2	Fisher's Exact Test	0.230
3	Fisher's Exact Test	0.615
4	Fisher's Exact Test	1.000
5	Fisher's Exact Test	0.773
6	Fisher's Exact Test	0.577
7	Fisher's Exact Test	0.236

Table 16 A table of Chi-square values using the Fisher's exact test comparing the relationship between injections and study eye at each visit.

3.5.1.2.1 ***Summary***

Analysis demonstrated no significant difference in the study eye composition of the population cohort (48% left, 52% right in Figure 37). Independent samples t test for an association between CMT change and VAS change by study eye at each participant visit demonstrated no significant difference between the means (Table 15). There was also no significant difference in means between the study eyes for the administration of an injection at each participant visit when analysed by Chi-squared testing (Table 16).

3.5.1.3 The relationship of the age of participants to treatment outcome measures (CMT, VAS and administered injections of anti VEGF)

Phase 3 multicentre clinical trials have established increasing age as a predictor of poor outcome[183-185]. In our study this correlative effect was only demonstrated at the 6 month visit.

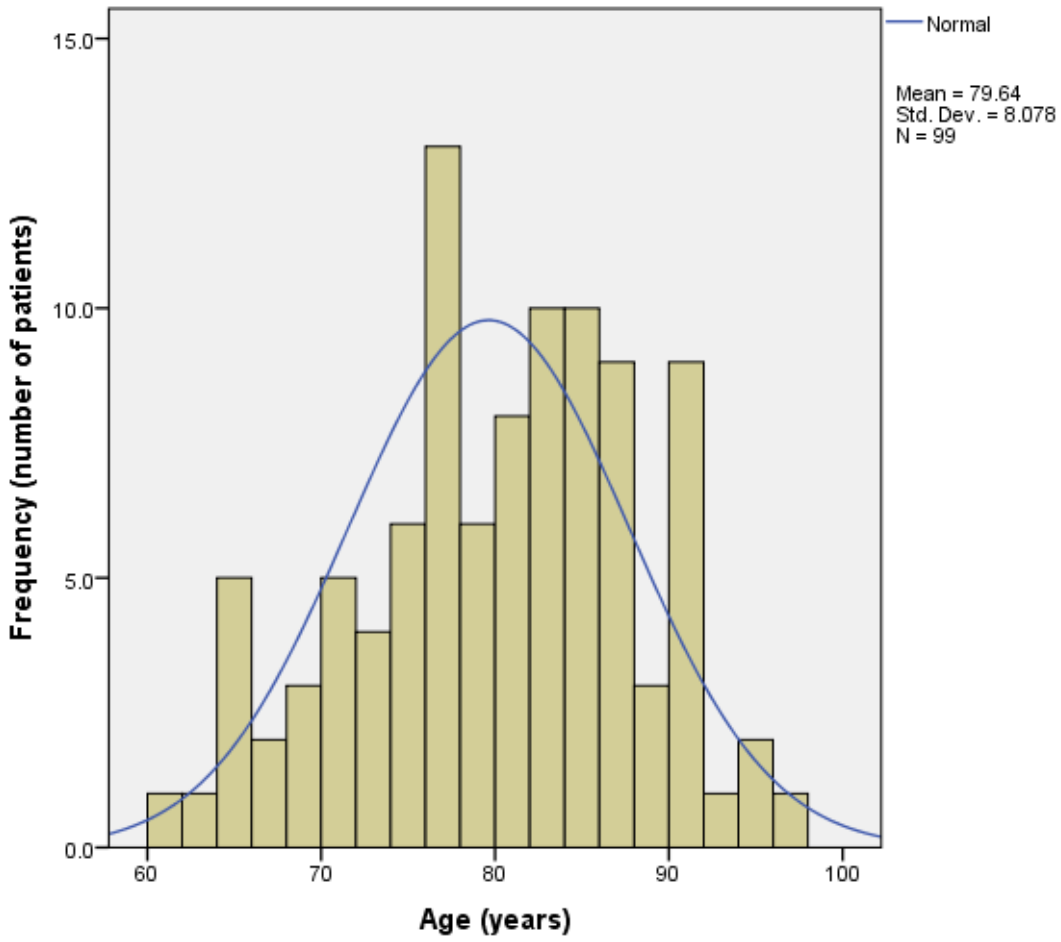

Figure 38 Age distribution of patients in the Pharmacogenetics cohort. The mean age was 79.64 years with a normally distributed population and standard deviation of 8.078 years. (N=99)

Visit	A) VAS change		
2	Gender & BMI & Pack Years	Correlation	0.013
		Significance (2-tailed)	0.913
		df	69
3	Gender & BMI & Pack Years	Correlation	-0.064
		Significance (2-tailed)	0.598
		df	69
4	Gender & BMI & Pack Years	Correlation	-0.117
		Significance (2-tailed)	0.358
		df	62
5	Gender & BMI & Pack Years	Correlation	-0.115
		Significance (2-tailed)	0.366
		df	62
6	Gender & BMI & Pack Years	Correlation	-0.245
		Significance (2-tailed)	0.055
		df	60
7	Gender & BMI & Pack Years	Correlation	-0.391
		Significance (2-tailed)	*0.005
		df	48

Visit	B) CMT Change		
2	Gender & BMI & Pack Years	Correlation	0.018
		Significance (2-tailed)	0.879
		df	70
3	Gender & BMI & Pack Years	Correlation	0.010
		Significance (2-tailed)	0.942
		df	50
4	Gender & BMI & Pack Years	Correlation	0.093
		Significance (2-tailed)	0.526
		df	47
5	Gender & BMI & Pack Years	Correlation	0.135
		Significance (2-tailed)	0.307
		df	57
6	Gender & BMI & Pack Years	Correlation	0.008
		Significance (2-tailed)	0.960
		df	43
7	Gender & BMI & Pack Years	Correlation	0.309
		Significance (2-tailed)	*0.039
		df	43

Table 17 Tables comparing change in CMT (CMT Change) (B) in microns and VA score (VAS Change) (A) in letters from baseline utilising Pearson's correlation coefficient (Correlation) and controlling for gender, pack years and body mass index (BMI). Df = degrees of freedom. *-significant result with a p value <0.05

Independent Samples Test						
Visit		t-test for Equality of Means				
		t	df	Sig. (2-tailed)	95% Confidence Interval of the Difference	
					Lower	Upper
1	Age	0.672	3.139	0.548	-14.007	21.745
2	Age	-1.404	1.038	0.388	-85.720	67.295
3	Age	-0.946	23.884	0.354	-7.592	2.822
4	Age	-1.615	37.989	0.115	-7.218	0.812
5	Age	0.090	15.607	0.930	-5.297	5.763
6	Age	-1.182	23.524	0.249	-7.424	2.020
7	Age	-2.455	16.491	*0.026	-11.658	-0.868

Table 18 T test establishing correlations between injections administered and age at each visit. T- test statistic df-degrees of freedom *-significant result with a p value <0.05

3.5.1.3.1 ***Summary***

The population of the study had a normally distributed age range (mean=79.64, standard deviation=8.078) as demonstrated in Figure 38. There was a significant correlation in visit 7 for both CMT change and VAS change and increasing age (Table 17). The correlation coefficient was -0.391 when corrected for gender, BMI and pack years (p=0.005) for VAS change. This suggests increasing age has a negative correlation on the number of letters read by patients receiving active treatment for CNV with ranibizumab at visit 7 only. The correlation coefficient was 0.309 when corrected for gender, BMI and pack years (p=0.039) for CMT change. Increasing age therefore correlated with increased CMT at visit 7.

Visit 7 demonstrated a statistically significant difference (p=0.026) (Table 18) in the mean age of patients receiving injections (73.83 years old) and those who did not (80.10

years old). This may be due to the fact that older patients had poorer vision with more macula oedema (higher CMT) and were clinically judged to be treatment failures.

3.5.1.4 The relationship of the BMI of participants to treatment outcome measures (CMT, VAS and administered injections of anti VEGF)

There have been no reports of BMI as a predictor of response to therapy. Increased BMI has been demonstrated in a meta-analysis to be associated with progression from early to advance AMD[52, 60, 186]. This may have been influenced by confounders such as hypertension.

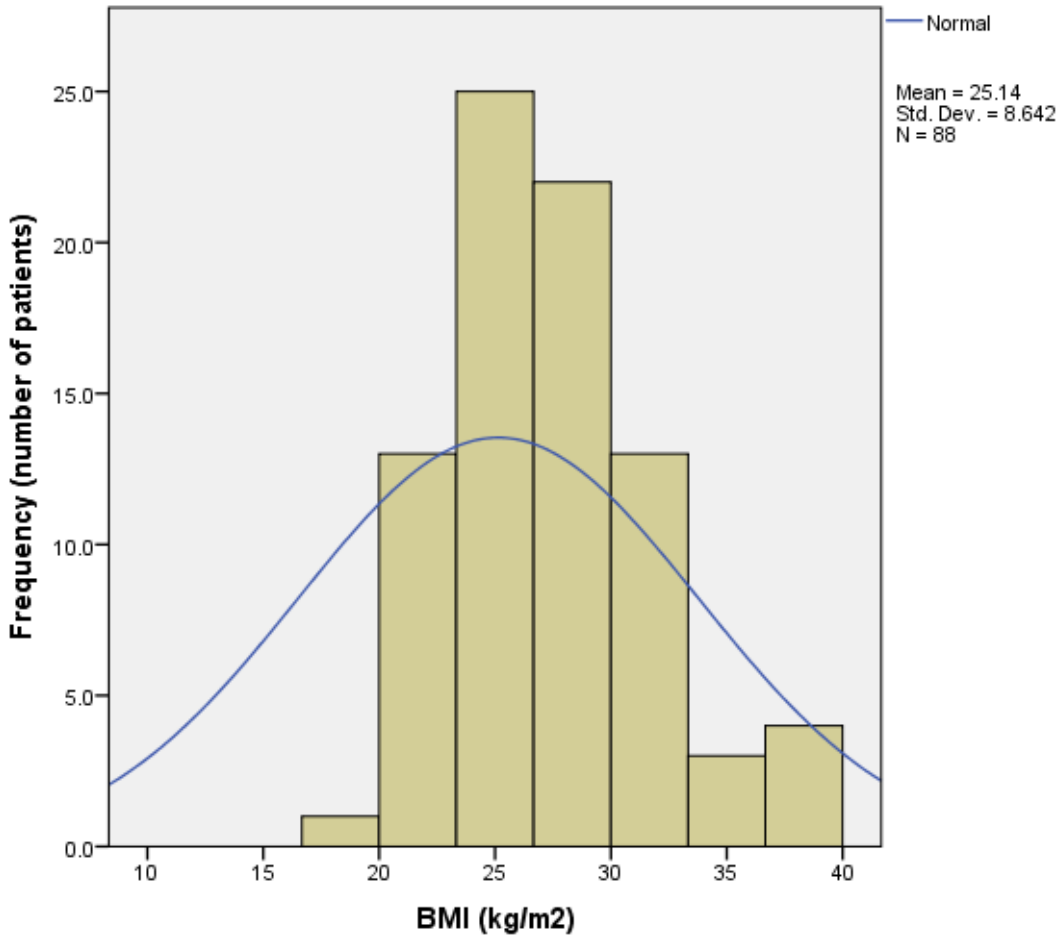

Figure 39 BMI distribution of patients in the Pharmacogenetics cohort. The mean BMI was 25.14 kg/m^2 with a normally distributed population and standard deviation of 8.642. (N=88)

Visit	A) VAS change		
2	Gender & Pack Years & Age	Correlation	0.124
		Significance (2-tailed)	0.303
		df	69
3	Gender & Pack Years & Age	Correlation	0.008
		Significance (2-tailed)	0.948
		df	69
4	Gender & Pack Years & Age	Correlation	0.064
		Significance (2-tailed)	0.614
		df	62
5	Gender & Pack Years & Age	Correlation	-0.074
		Significance (2-tailed)	0.563
		df	62
6	Gender & Pack Years & Age	Correlation	-0.160
		Significance (2-tailed)	0.214
		df	60
7	Gender & Pack Years & Age	Correlation	-0.112
		Significance (2-tailed)	0.437
		df	48

Visit	B) CMT Change		
2	Gender & Pack Years & Age	Correlation	-0.152
		Significance (2-tailed)	0.204
		df	70
3	Gender & Pack Years & Age	Correlation	-0.169
		Significance (2-tailed)	0.232
		df	50
4	Gender & Pack Years & Age	Correlation	-0.259
		Significance (2-tailed)	0.073
		df	47
5	Gender & Pack Years & Age	Correlation	-0.008
		Significance (2-tailed)	0.955
		df	57
6	Gender & Pack Years & Age	Correlation	0.110
		Significance (2-tailed)	0.470
		df	43
7	Gender & Pack Years & Age	Correlation	-0.112
		Significance (2-tailed)	0.463
		df	43

Table 19 Tables comparing change in CMT (CMT Change) (B) in microns and VA score (VAS Change) (A) in letters from baseline utilising Pearson's correlation coefficient (correlation) and controlling for gender, pack years and age. Df = degrees of freedom.

Independent Samples Test						
Visit		t-test for Equality of Means				
		t	df	Sig. (2-tailed)	95% Confidence Interval of the Difference	
					Lower	Upper
1	BMI	0.608	80	0.545	-6.279	11.807
2	BMI	-0.422	76	0.674	-15.351	9.981
3	BMI	-1.384	77	0.170	-7.912	1.422
4	BMI	-0.241	69	0.811	-5.428	4.259
5	BMI	-1.311	67	0.194	-9.460	1.958
6	BMI	-3.413	67	*0.001	-13.752	-3.603
7	BMI	0.857	60	0.395	-3.408	8.522

Table 20 Independent samples t Test establishing correlations between injections administered and BMI at each visit. t- t Test statistic, df-degrees of freedom, *-significant result with a p value <0.05

3.5.1.4.1 ***Summary***

The population of the study had a normally distributed BMI range (mean=25.14, standard deviation=8.642) as demonstrated in Figure 39. There was no significant correlation in any visit for CMT change or VAS change and BMI (Table 19).

Visit 6 (Table 20) demonstrated a significant difference in the mean BMI of patients receiving an anti VEGF injection (18.33kg/m^2) versus those who did not (27.01kg/m^2). This result was not repeated for any other visit and may be a statistical anomaly.

3.5.1.5 The relationship of participants' smoking history to treatment outcome measures (CMT, VAS and administered injections of anti VEGF)

The association between smoking and progression from early to advance AMD has been well documented[41, 42, 87, 187]. However there is no conclusive evidence demonstrating pack years and response to therapy.

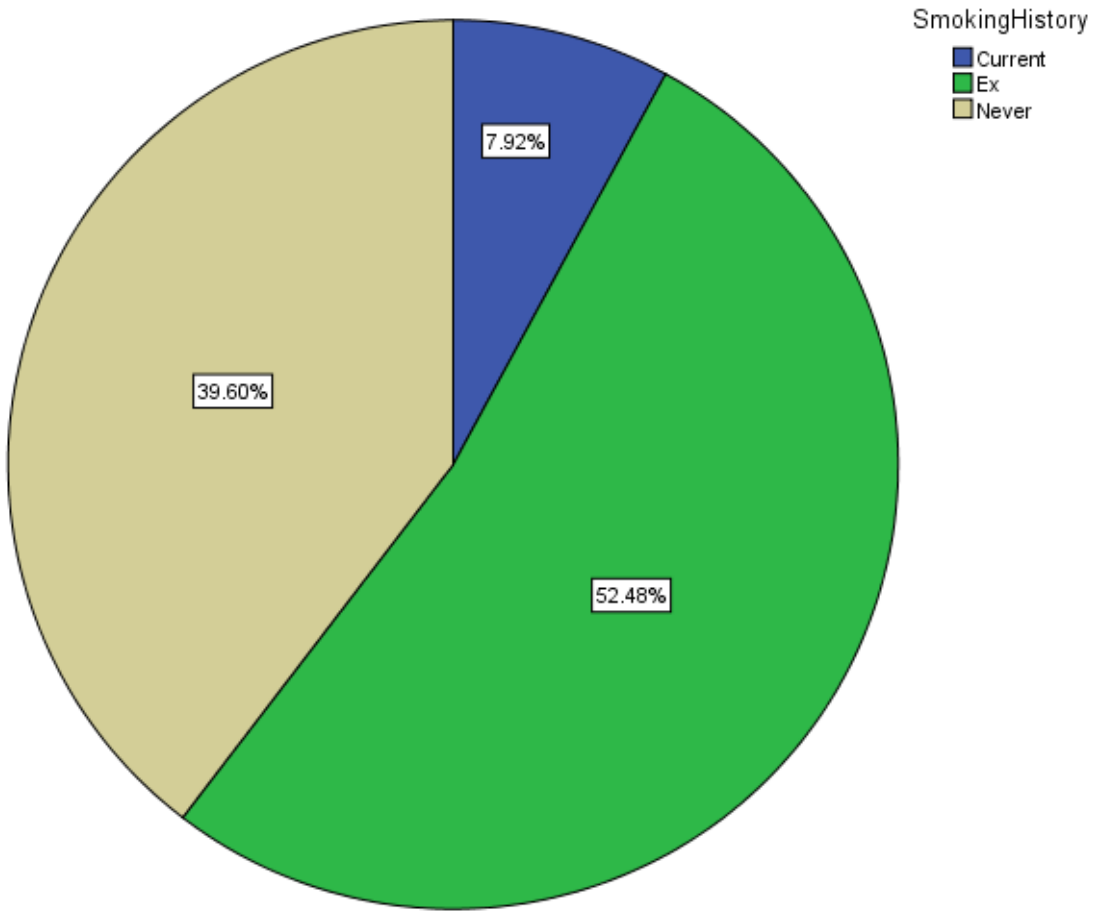

Figure 40 Smoking distribution within the cohort. 39.60% of patients reported never smoking, 52.48% had a past history of smoking and 7.92% were current smokers. (N=99)

A) Multiple Comparisons					
Dependent Variable: VAS change					
Bonferroni					
Visit	(I) Smoking History	(J) Smoking History	Sig.	95% Confidence Interval	
				Lower Bound	Upper Bound
2	Current	Ex	0.101	-16.528	1.012
		Never	0.244	-15.190	2.451
	Ex	Current	0.101	-1.020	16.528
		Never	1.000	-3.186	5.956
	Never	Current	0.244	-2.451	15.190
		Ex	1.000	-5.956	3.186
3	Current	Ex	1.000	-5.037	7.858
		Never	1.000	-4.832	8.268
	Ex	Current	1.000	-7.858	5.037
		Never	1.000	-3.518	4.132
	Never	Current	1.000	-8.268	4.832
		Ex	1.000	-4.132	3.518
4	Current	Ex	1.000	-10.626	4.908
		Never	1.000	-9.101	6.704
	Ex	Current	1.000	-4.908	10.626
		Never	1.000	-2.909	6.231
	Never	Current	1.000	-6.704	9.101
		Ex	1.000	-6.231	2.909

A cont'd) Multiple Comparisons					
Dependent Variable: VAS change					
Bonferroni					
Visit	(I) Smoking History	(J) Smoking History	Sig.	95% Confidence Interval	
				Lower Bound	Upper Bound
5	Current	Ex	1.000	-12.850	5.967
		Never	.538	-15.043	4.329
	Ex	Current	1.000	-5.967	12.850
		Never	1.000	-7.593	3.762
	Never	Current	0.538	-4.329	15.043
		Ex	1.000	-3.762	7.593
6	Current	Ex	1.000	-11.310	13.002
		Never	1.000	-13.358	11.507
	Ex	Current	1.000	-13.002	11.310
		Never	1.000	-8.568	5.025
	Never	Current	1.000	-11.507	13.358
		Ex	1.000	-5.025	8.568
7	Current	Ex	1.000	-17.163	11.001
		Never	1.000	-20.068	8.797
	Ex	Current	1.000	-11.001	17.163
		Never	1.000	-9.748	4.638
	Never	Current	1.000	-8.797	20.068
		Ex	1.000	-4.638	9.748

B) Multiple Comparisons

Dependent Variable: CMT Change

Bonferroni

Visit	(I) Smoking History	(J) Smoking History	Sig.	95% Confidence Interval	
				Lower Bound	Upper Bound
2	Current	Ex	1.000	-79.72	99.17
		Never	1.000	-109.15	72.58
	Ex	Current	1.000	-99.17	79.72
		Never	0.523	-77.97	21.95
	Never	Current	1.000	-72.58	109.15
		Ex	0.523	-21.95	77.97
3	Current	Ex	1.000	-115.94	157.43
		Never	1.000	-133.97	142.79
	Ex	Current	1.000	-157.43	115.94
		Never	1.000	-75.46	42.79
	Never	Current	1.000	-142.79	133.97
		Ex	1.000	-42.79	75.46
4	Current	Ex	1.000	-160.74	89.20
		Never	0.749	-183.92	66.02
	Ex	Current	1.000	-89.20	160.74
		Never	1.000	-91.97	45.62
	Never	Current	0.749	-66.02	183.92
		Ex	1.000	-45.62	91.97

B cont'd) Multiple Comparisons					
Dependent Variable: CMT Change					
Bonferroni					
Visit	(I) Smoking History	(J) Smoking History	Sig.	95% Confidence Interval	
				Lower Bound	Upper Bound
5	Current	Ex	1.000	-111.95	89.20
		Never	0.744	-150.30	53.59
	Ex	Current	1.000	-89.20	111.95
		Never	0.370	-95.20	21.25
	Never	Current	0.744	-53.59	150.30
		Ex	0.370	-21.25	95.20
6	Current	Ex	1.000	-160.78	110.65
		Never	0.932	-195.33	80.96
	Ex	Current	1.000	-110.65	160.78
		Never	0.630	-94.69	30.46
	Never	Current	0.932	-80.96	195.33
		Ex	0.630	-30.46	94.69
7	Current	Ex	1.000	-85.47	149.54
		Never	1.000	-75.86	166.16
	Ex	Current	1.000	-149.54	85.47
		Never	1.000	-57.74	83.97
	Never	Current	1.000	-166.16	75.86
		Ex	1.000	-83.97	57.74

Table 21 Tables examining the relationship between VAS (A) and CMT (B) change from baseline using one-way ANOVA analysis with Bonferroni correction for multiple comparisons. Current- current smokers, ex- participants who smoked previously, never- participants who had never smoked. *-significant result with a p value <0.05

Chi-Square Tests				
Visit		Value	df	Asymp. Sig. (2-sided)
1	Pearson Chi-Square	0.458	2	0.795
	N of Valid Cases	91		
2	Pearson Chi-Square	6.382	2	*0.041
	N of Valid Cases	85		
3	Pearson Chi-Square	3.776	2	0.151
	N of Valid Cases	87		
4	Pearson Chi-Square	2.424	2	0.298
	N of Valid Cases	77		
5	Pearson Chi-Square	0.929	2	0.628
	N of Valid Cases	74		
6	Pearson Chi-Square	2.146	2	0.342
	N of Valid Cases	75		
7	Pearson Chi-Square	0.178	2	0.915
	N of Valid Cases	67		

Table 22 Chi square analysis comparing smoking groups within the cohort and administered injections for active CNV. Df- degrees of freedom, *-significant result with a p value <0.05

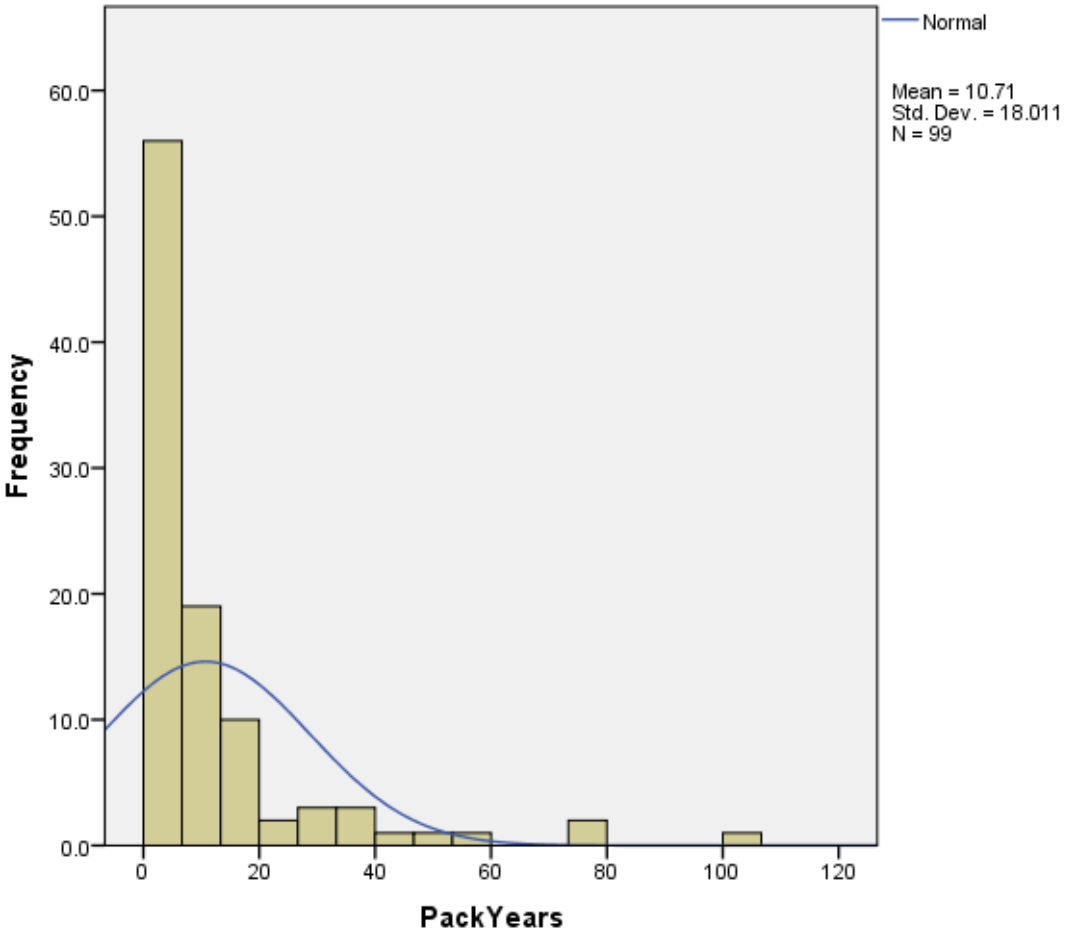

Figure 41 Graph demonstrating the distribution of pack years (Number of pack-years = (number of *cigarettes* smoked per day × number of years smoked)/20 (1 pack has 20 cigarettes)) within the cohort. Mean=10.71 pack years, SD=18.011 pack years (n=99)

A) Correlations				
Visit	Control Variables			Pack Years
2	Gender & Age & BMI	VAS change	Correlation	0.093
			Significance (2-tailed)	0.442
			df	69
3	Gender & Age & BMI	VAS change	Correlation	0.016
			Significance (2-tailed)	0.893
			df	69
4	Gender & Age & BMI	VAS change	Correlation	0.023
			Significance (2-tailed)	0.859
			df	62
5	Gender & Age & BMI	VAS change	Correlation	-0.329
			Significance (2-tailed)	*0.008
			df	62
6	Gender & Age & BMI	VAS change	Correlation	-0.258
			Significance (2-tailed)	*0.043
			df	60
7	Gender & Age & BMI	VAS change	Correlation	-0.368
			Significance (2-tailed)	*0.009
			df	48

B) Correlations				
Visit	Control Variables			CMT Change
2	Gender & Age & BMI	Pack Years	Correlation	-0.114
			Significance (2-tailed)	0.342
			df	70
3	Gender & Age & BMI	Pack Years	Correlation	-0.021
			Significance (2-tailed)	0.884
			df	50
4	Gender & Age & BMI	Pack Years	Correlation	-0.055
			Significance (2-tailed)	0.706
			df	47
5	Gender & Age & BMI	Pack Years	Correlation	-0.028
			Significance (2-tailed)	0.830
			df	57
6	Gender & Age & BMI	Pack Years	Correlation	0.091
			Significance (2-tailed)	0.553
			df	43
7	Gender & Age & BMI	Pack Years	Correlation	0.112
			Significance (2-tailed)	0.463
			df	43

Table 23 Tables comparing change in CMT (CMT Change) (B) in microns and VA score (VAS Change) (A) in letters from baseline utilising Pearson's correlation coefficient (correlation) and controlling for gender, BMI and age. Df = degrees of freedom. *-significant result with a p value <0.05

Independent Samples Test						
Visit		t-test for Equality of Means				
		t	df	Sig. (2-tailed)	95% Confidence Interval of the Difference	
					Lower	Upper
1	Pack Years	3.115	15.432	0.007	2.690	14.263
2	Pack Years	-0.355	1.157	0.777	-74.959	69.441
3	Pack Years	0.519	29.032	0.607	-7.899	13.278
4	Pack Years	1.647	23.895	0.113	-2.725	24.255
5	Pack Years	-1.100	42.978	0.277	-11.912	3.503
6	Pack Years	0.687	19.153	0.500	-9.864	19.511
7	Pack Years	0.183	17.496	0.857	-14.551	17.324

Table 24 Independent samples t Test establishing correlations between injections administered and pack years at each visit. t- t Test statistic, df-degrees of freedom

3.5.1.5.1 ***Summary***

Figure 40 illustrates the distribution of patients' smoking status at baseline (Current=7.92%, Ex smokers=39.60%, Never smoked=52.48%). There was no significant difference in VAS change or CMT change from baseline of the 3 groups at each visit ($p>0.05$) with Bonferroni correction for multiple comparisons (Table 21). Visit 2 (Table 22) demonstrated a significant result ($p=0.041$) however there was only 1 (out of a total of 6) current smokers receiving an injection versus 36 in the never smoked subgroup (out of a total of 37) who did not require an injection. This may have been a statistical anomaly.

Figure 41 demonstrates the distribution of pack years within the study cohort (mean=10.71, standard deviation=18.011). There was significant correlation between VAS change and pack years at visits 5, 6 and 7 ($p=0.008$, $=0.043$ and $=0.005$ respectively). There was a negative correlation suggesting an increased number of pack years produced a loss of letters compared to baseline while on treatment with ranibizumab. This result was not repeated in any other outcome measures however (Table 24 and Table 23).

3.5.1.6 The relationship of patient reported acute inflammatory events to treatment outcome measures (CMT, VAS and administered injections of anti VEGF)

This section explored whether patient reported systemic illnesses within the previous month was associated with treatment outcome measures.

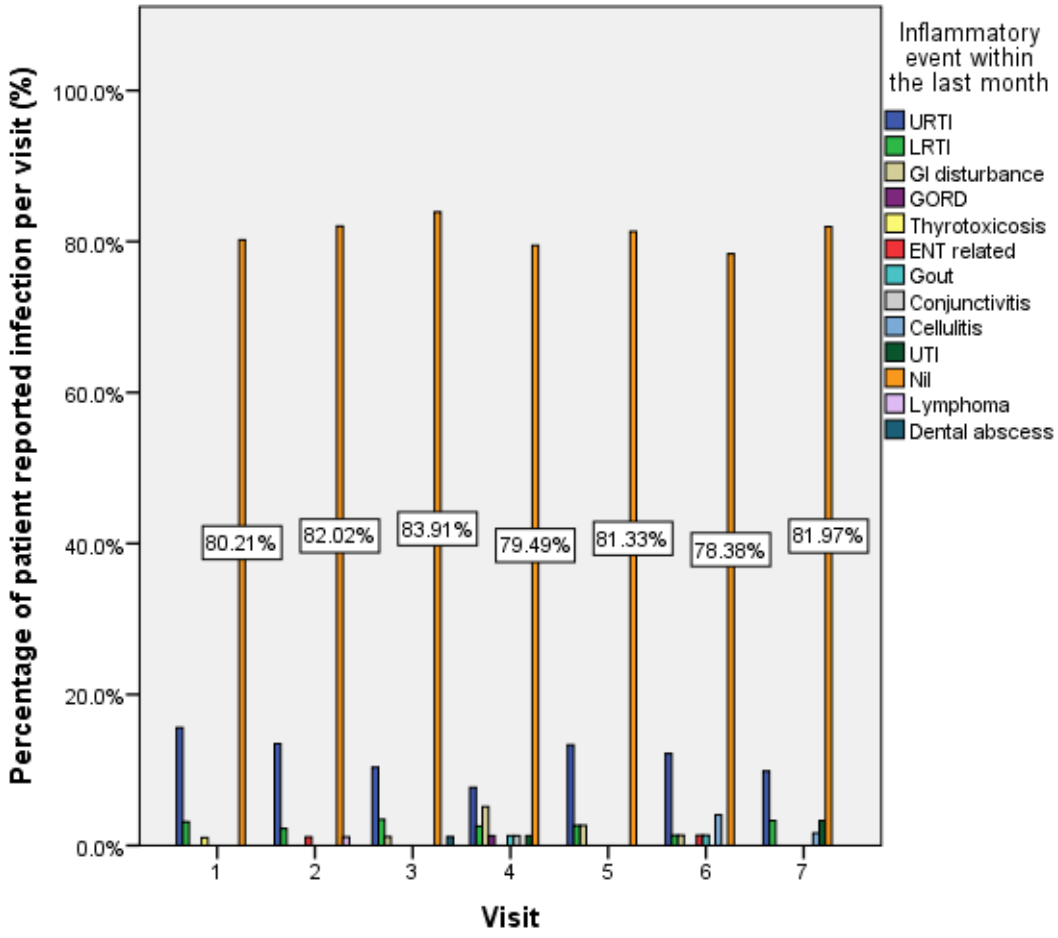

Figure 42 Distribution of patient reported infections. URTI- upper respiratory tract infection, LRTI- lower respiratory tract infection, GI- gastrointestinal, GORD-gastro oesophageal regurge disease, ENT- ear, nose and throat, UTI- urinary tract infection

Chi-Square Tests		
Visit		Exact Sig. (2-sided)
1	Fisher's Exact Test	0.572
2	Fisher's Exact Test	1.000
3	Fisher's Exact Test	0.724
4	Fisher's Exact Test	0.752
5	Fisher's Exact Test	0.721
6	Fisher's Exact Test	1.000
7	Fisher's Exact Test	0.206

Table 25 A table of Chi-square values using the Fisher's exact test comparing the relationship between injections and patient reported illness groups at each visit.

3.5.1.6.1 ***Summary***

Figure 42 illustrates the distribution of patient reported illnesses within the previous month. There was no relationship within the cohort between mean number of injections and the different patient reported illnesses (Table 25). However, the majority of patients with significant acute illnesses would not have attended an outpatient appointment for treatment.

3.5.1.7 The relationship of past ophthalmic history to treatment outcome measures (CMT, VAS and administered injections of anti VEGF)

AMD in the fellow eye is a known risk factor for progression to advanced AMD[60]. However in our cohort there was no association with administered intravitreal therapy and past ophthalmic history including AMD in the fellow eye.

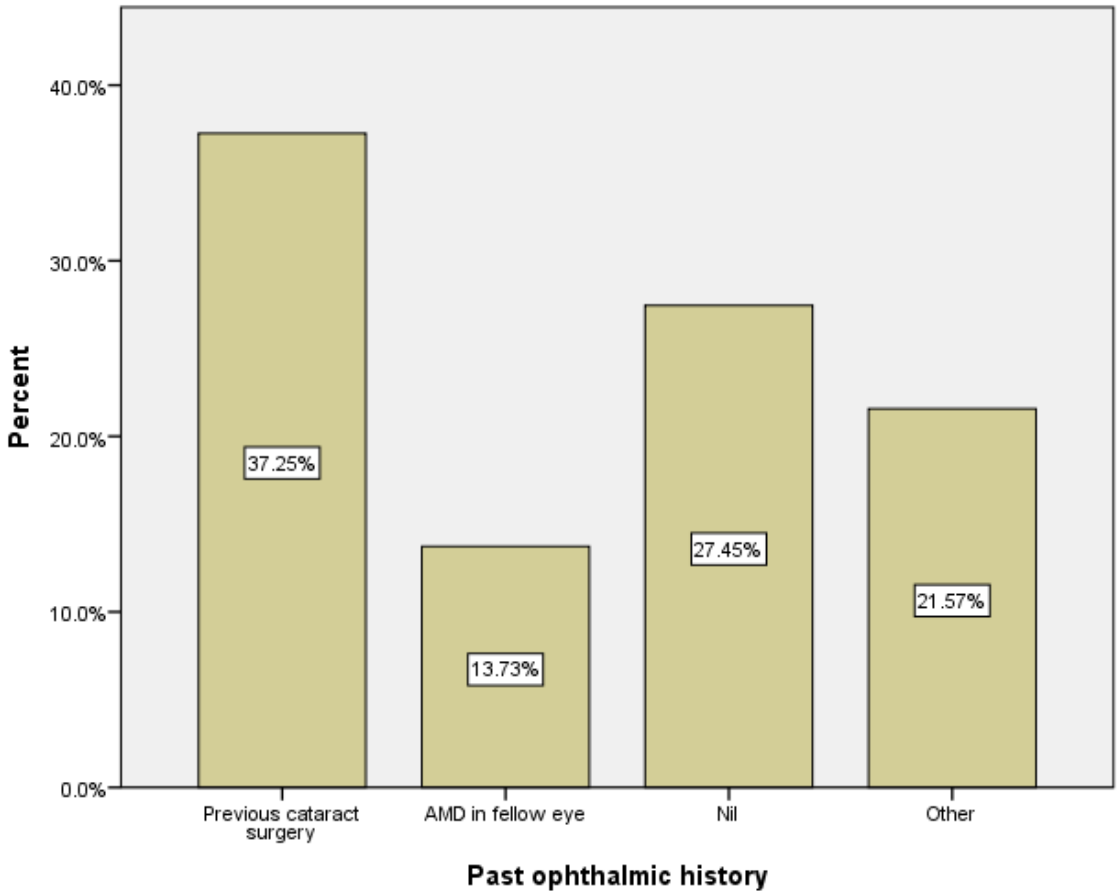

Figure 43 Past ophthalmic history within cohort. Histogram of patient reported ophthalmic disease/surgery. 37.25% of patients reported prior cataract surgery (study eye), 13.73% had AMD in the non-study eye and 27.45% of patients had no reported ophthalmic complaint (Nil category). 21.57% of the cohort had diseases of lesser frequency (Other category) including retinal vessel occlusion, ischaemic optic neuropathies and prior squint surgery.

3.5.1.7.1 ***Summary***

Figure 43 demonstrates the distribution of ophthalmic conditions within the cohort. Chi squared analysis demonstrated no significant association ($p>0.05$) between administered injections and categories of past ophthalmic history.

3.5.1.8 The relationship of chronic illnesses to treatment outcome measures (CMT, VAS and administered injections of anti VEGF)

Hypertension has been previously demonstrated to be a risk factor for AMD progression[188, 189] and may also influence CNV response to therapy. Subgroup analysis on a larger cohort would be necessary.

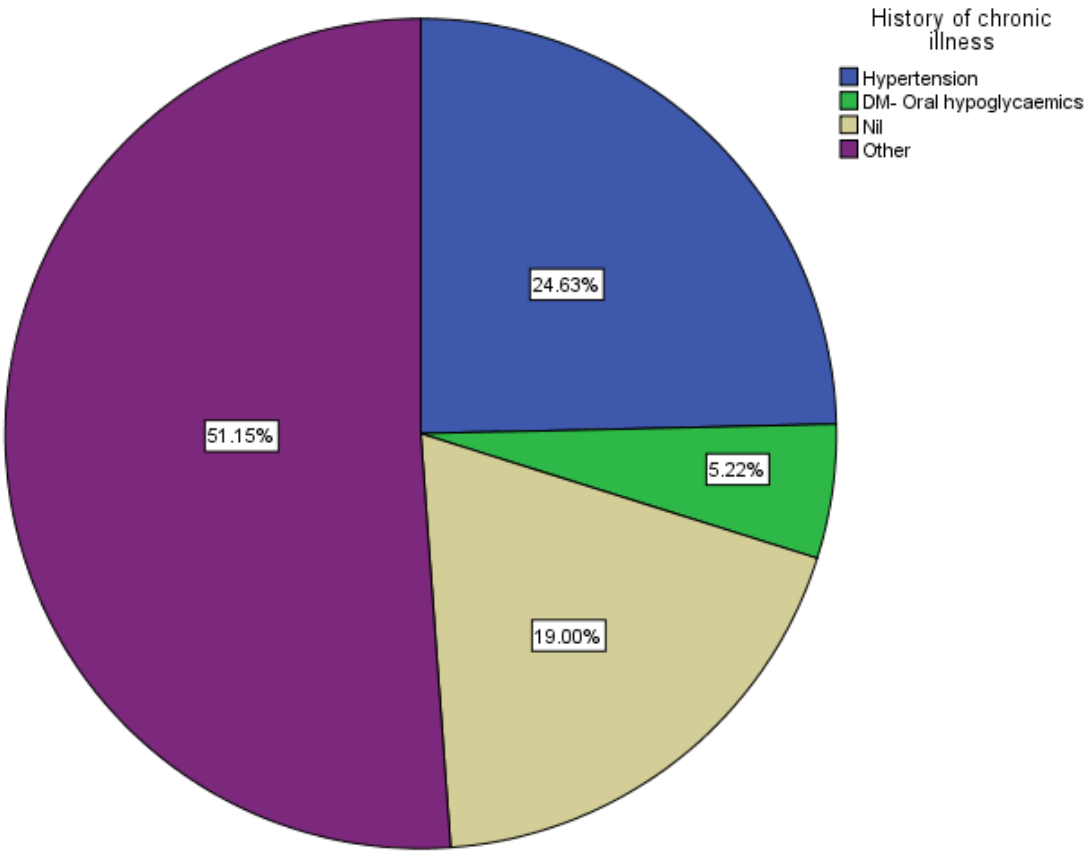

Figure 44 Past medical history. A pie chart of chronic medical illnesses described by patients in the Pharmacogenetics cohort. The most frequent illness was hypertension (24.63%), followed by Type 2 diabetes (DM) (5.22%). The "other" category was composed

of lesser reported illnesses such as gout, Type 1 diabetes, osteoarthritis and mental illnesses. The Nil category reflected patients with no systemic illnesses.

ANOVA				
A) VAS Change				
Visit		df	F	Sig.
2	Between Groups	25	0.515	0.965
	Within Groups	57		
	Total	82		
3	Between Groups	20	0.929	0.556
	Within Groups	44		
	Total	64		
4	Between Groups	16	1.252	0.295
	Within Groups	27		
	Total	43		
5	Between Groups	13	1.704	0.122
	Within Groups	25		
	Total	38		
6	Between Groups	16	1.342	0.257
	Within Groups	22		
	Total	38		
7	Between Groups	12	1.174	0.375
	Within Groups	16		
	Total	28		

ANOVA				
B) CMT Change				
Visit		df	F	Sig.
2	Between Groups	24	1.373	0.161
	Within Groups	60		
	Total	84		
3	Between Groups	15	0.522	0.909
	Within Groups	32		
	Total	47		
4	Between Groups	12	1.514	0.189
	Within Groups	23		
	Total	35		
5	Between Groups	9	1.158	0.365
	Within Groups	23		
	Total	32		
6	Between Groups	12	0.807	0.641
	Within Groups	19		
	Total	31		
7	Between Groups	11	1.630	0.187
	Within Groups	15		
	Total	26		

Table 26 Tables examining the relationship between VAS (A) and CMT (B) change from baseline using one-way ANOVA analysis (without Bonferroni correction for multiple comparisons due to small group size). Df-degrees of freedom, F-F statistic

Chi-Square Tests				
Visit		Value	df	Asymp. Sig. (2-sided)
2	Pearson Chi-Square	3.041	25	1.000
	N of Valid Cases	85		
3	Pearson Chi-Square	36.280	20	*0.014
	N of Valid Cases	67		
4	Pearson Chi-Square	19.632	16	0.237
	N of Valid Cases	45		
5	Pearson Chi-Square	18.387	13	0.143
	N of Valid Cases	39		
6	Pearson Chi-Square	15.445	16	0.492
	N of Valid Cases	40		
7	Pearson Chi-Square	15.031	12	0.240
	N of Valid Cases	32		

Table 27 Chi square analysis comparing chronic illness groups within the cohort and administered injections for active CNV. Df- degrees of freedom. *-significant result with a p value <0.05.

3.5.1.8.1 ***Summary***

Figure 44 illustrates the distribution of patients' reported chronic illnesses at baseline (hypertension=24.63%, Type 2 diabetes (DM)=5.22%, Nil=19%. The "other" category was composed of lesser reported illnesses such as gout, Type 1 diabetes, osteoarthritis and mental illnesses=51.15%). There was no significant difference in VAS change or CMT change at each visit (p>0.05) from baseline with ANOVA (Table 26). Visit 3 (Table 27) demonstrated a significant result (p=0.014).

3.5.1.9 The relationship of participants' mean baseline CMT to treatment outcome measures (CMT, VAS and administered injections of anti VEGF)

The Comparison of AMD Treatments Trials (CATT) discovered no correlation between baseline CMT and response to anti VEGF therapy[190]. I investigated whether the same findings were relevant in my study.

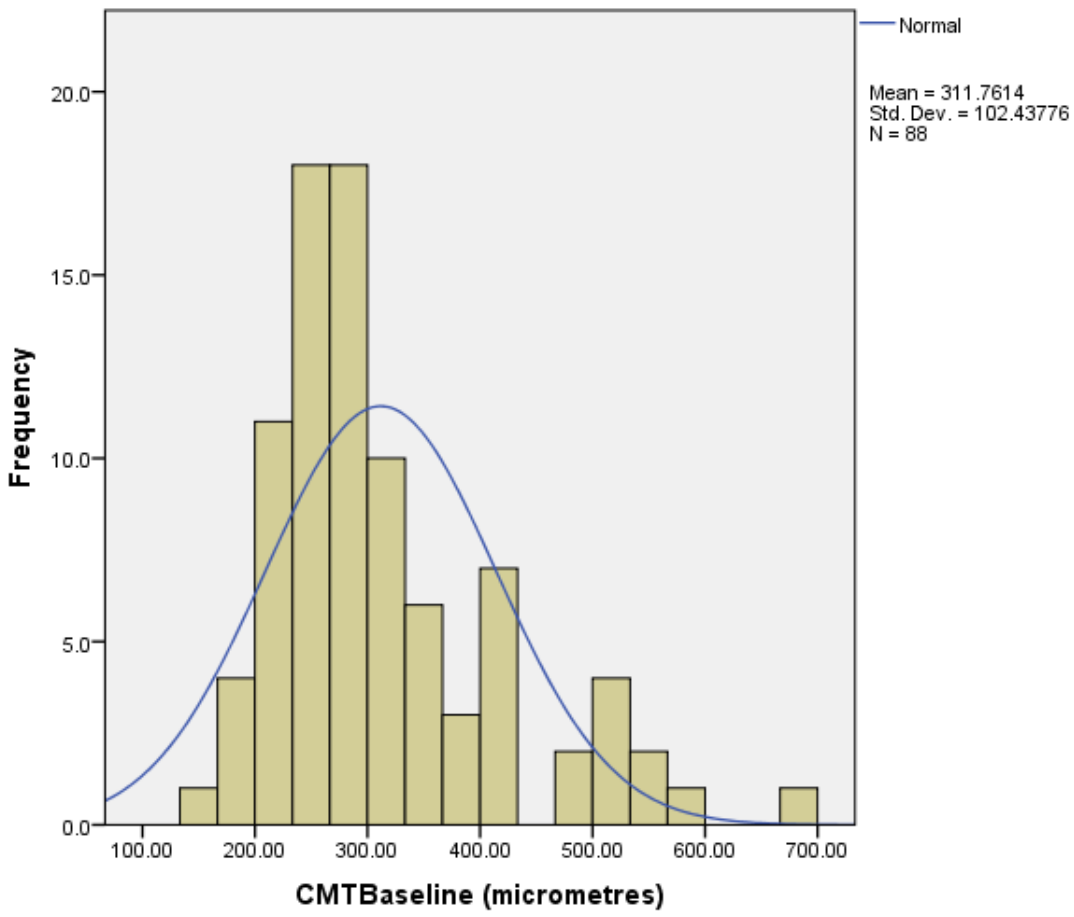

Figure 45 Distribution of measured baseline central macular thickness (CMTBaseline) within the study population. The mean central macular thickness measured 311.76µm at baseline with a standard deviation of 102.43µm and population of n=88.

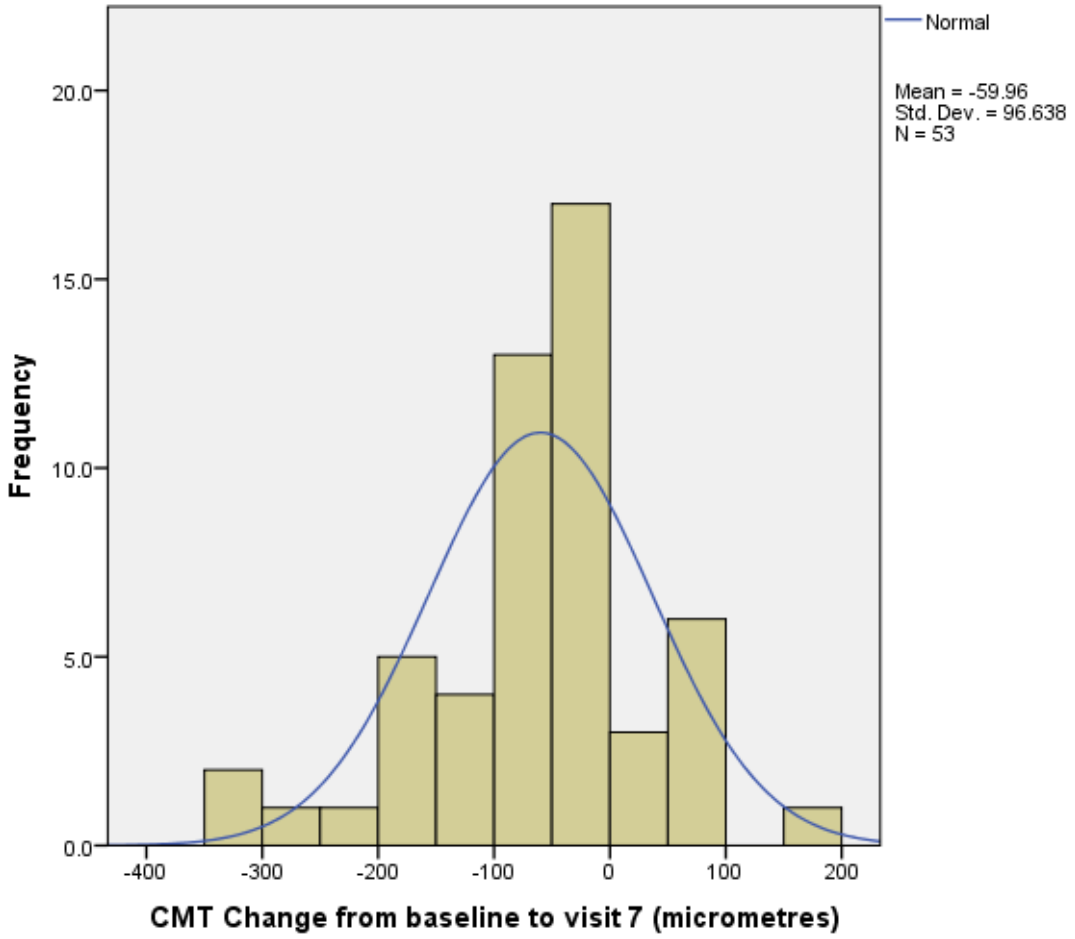

Figure 46 Distribution of central macular thickness (CMT) change from baseline measurement to visit 7. The mean central macular thickness change measured -59.96µm from baseline to visit 7 with a standard deviation of 96.64µm and population of n=53.

Independent Samples Test						
Visit		t-test for Equality of Means				
		t	df	Sig. (2-tailed)	95% Confidence Interval of the Difference	
					Lower	Upper
1	CMT Baseline	-0.884	3.089	0.440	-355.558	198.962
2	CMT Baseline	0.712	1.005	0.606	-2515.118	2817.315
3	CMT Baseline	-0.383	40.944	0.704	-53.921	36.725
4	CMT Baseline	0.586	43.567	0.561	-36.119	65.700
5	CMT Baseline	-1.366	22.627	0.185	-93.658	19.196
6	CMT Baseline	-0.715	59.028	0.477	-50.792	24.042
7	CMT Baseline	-0.309	22.653	0.760	-73.370	54.336

Table 28 Independent samples t Test establishing correlations between injections administered and baseline central macular thickness (CMT Baseline) at each visit. t- t Test statistic, df-degrees of freedom

3.5.1.9.1 ***Summary***

Figure 45 demonstrates the distribution of measured baseline CMT within the cohort (mean=311.76µm, standard deviation=102.44µm) suggesting a wide range in baseline macular thickness.

Figure 46 illustrates the change in CMT from baseline to the 6 month end of study marker. There was a mean decrease in CMT of 59.96µm suggesting an overall reduction in macula oedema with therapy. Baseline CMT was not a predictor of clinical activity in this study (Table 28).

3.5.1.10 The relationship of participants' mean baseline VAS to treatment outcome measures (CMT, VAS and administered injections of anti VEGF)

A previous report in the literature[184, 191] suggested that baseline VA predicts response to anti VEGF therapy for AMD. I explored whether the baseline VAS could predict treatment outcome in my study.

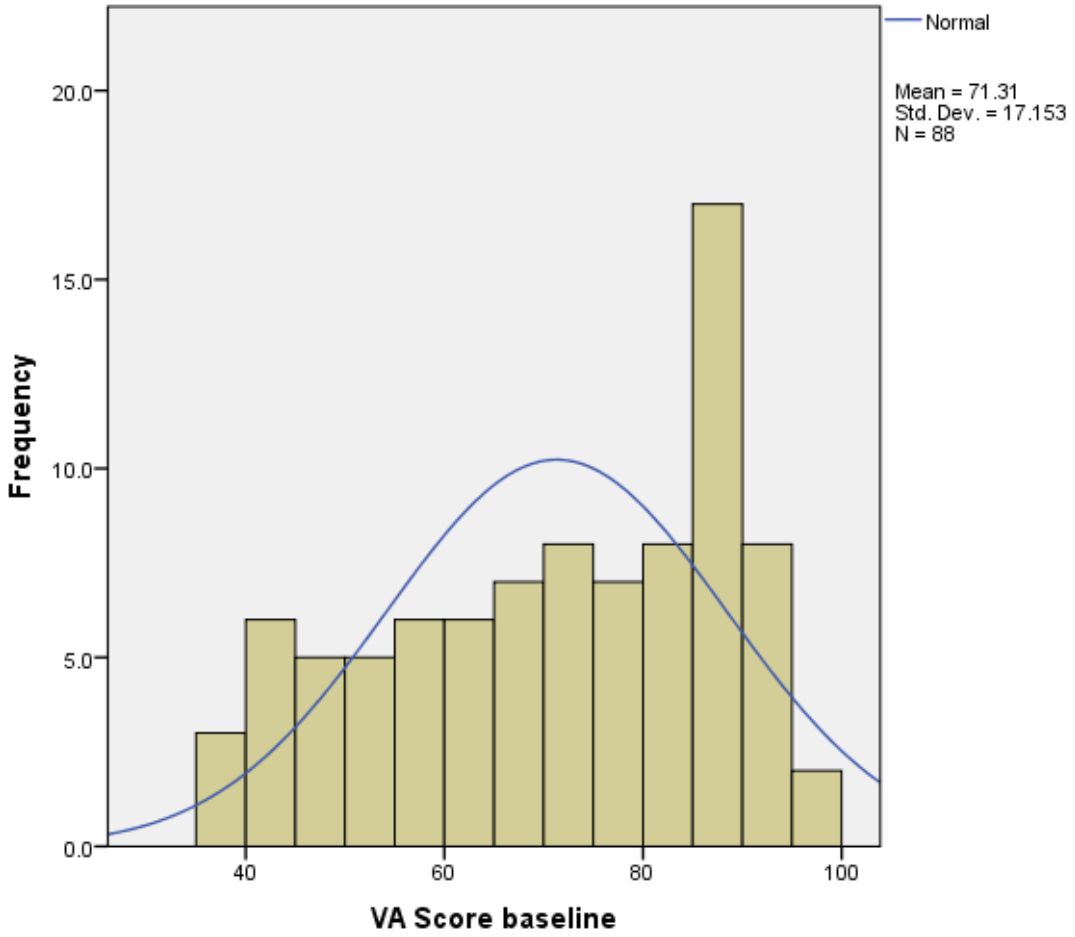

Figure 47 Distribution of measured baseline visual acuity score (VAS) in ETDRS letters within the study population. The mean VA score measured 71 letters at baseline with a standard deviation of 17 letters and population of n=88.

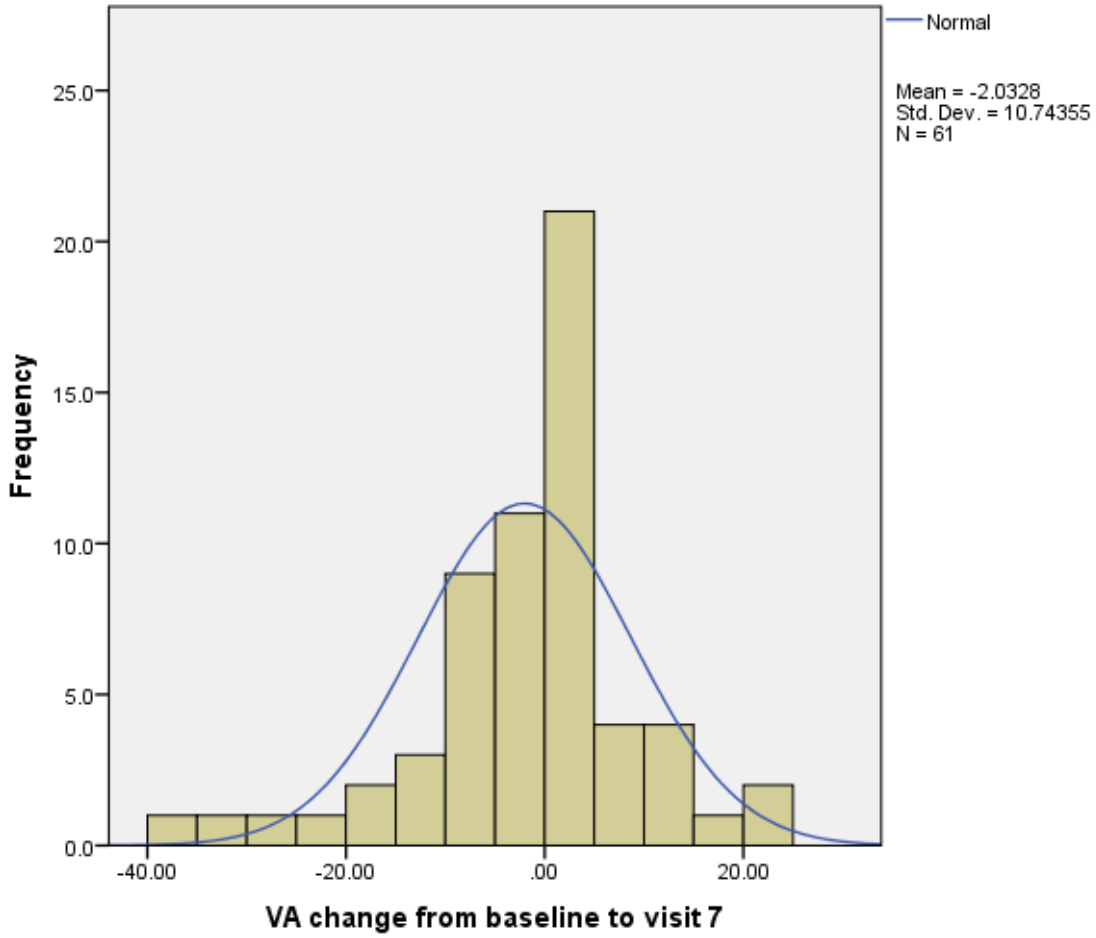

Figure 48 Distribution of visual acuity score (VAS) change from baseline measurement to visit 7. The change in VA score measured -2 letters from baseline to visit 7 with a standard deviation of 11 letters and population of n=61.

Independent Samples Test						
Visit		t-test for Equality of Means				
		t	df	Sig. (2-tailed)	95% Confidence Interval of the Difference	
					Lower	Upper
1	VAS Baseline	-0.524	3.470	0.632	-24.804	17.328
2	VAS Baseline	0.385	1.029	0.765	-188.294	200.893
3	VAS Baseline	1.731	34.697	0.092	-1.190	14.935
4	VAS Baseline	1.665	57.006	0.101	-1.244	13.537
5	VAS Baseline	0.334	18.757	0.742	-8.993	12.405
6	VAS Baseline	2.962	37.261	*0.005	3.197	17.034
7	VAS Baseline	0.436	29.244	0.666	-7.184	11.073

Table 29 Independent samples t Test establishing correlations between injections administered and baseline visual acuity score (VASBaseline) at each visit. t- t Test statistic, df-degrees of freedom, *-significant result with a p value <0.05

3.5.1.10.1 ***Summary***

Figure 47 demonstrates the distribution of measured baseline VA within the cohort (mean=71.31 letters, standard deviation=17.15 letters) suggesting a wide range in baseline visual acuity.

Figure 48 illustrates the change in VA from baseline to the 6 month end of study marker. There was a mean decrease in VA of approximately 2 letters with therapy. This suggests treatment is maintaining visual acuity over the 6 month period.

A significant difference in baseline VA between those receiving therapy (mean=81.72 letters) and those not receiving therapy (mean=71.60 letters) was evident at solely visit 6 (Table 29).

3.5.1.11 Examination of SNPs reported to be involved in AMD progression from early to advanced stages and their role in predicting the outcome of CNV treatment with ranvibizumab

This section examines some of the known SNPs previously found to be involved in AMD progression. This directly explores the hypothesis that the genotype *SERPING1* affects AMD response to treatment.

3.5.1.11.1 *DNA extraction analysis within the study*

I extracted the DNA for genotyping from study participants. Below is a summary table of the results.

Patient ID Number	DNA Concentration (ng/µl)	260/280 ratio
PA041	373.52	1.74
PA030	271.16	1.75
PA046	351.4	1.66
PA047	698.22	1.87
PA049	233.03	1.73
PA051	509.34	1.76
PA053	347.34	1.76
PA054	228.47	1.67
PA057	131.91	1.66
PA058	562.49	1.76
PA059	914.24	1.83
PA060	1020.47	1.84
PA063	515.1	1.76
PA069	708.74	1.81
PA070	492.69	1.74
PA071	417.76	1.75
PA073	761.11	1.87
PA074	1206.8	1.8
PA076	736.86	1.77
PA077	805.47	1.88
PA078	843.8	1.84
PA079	1334.58	1.82
PA080	495.92	1.73
PA081	855.01	1.8
PA082	493.42	1.77
PA083	537.56	1.76

Patient Id Number	DNA Concentration (ng/µl)	260/280 ratio
PA084	940.46	1.76
PA086	729.65	1.86
PA087	313.45	1.77
PA088	531.87	1.78
PA089	812.95	1.89
PA090	660.92	1.88
PA091	827.07	1.85
PA092	479.77	1.74
PA093	820.86	1.84
PA094	699.02	1.81
PA095	737.25	1.8
PA096	829.99	1.84
PA097	789.18	1.86
PA098	947.08	1.78
PA099	674.18	1.89
PA100	560.64	1.74
PA101	716.27	1.81
PA102	532.31	1.81
PA103	534.36	1.75
PA105	552.73	1.77
PA106	445.73	1.8
PA107	654.46	1.83

Table 30 DNA concentration values for individual patients. 260/280 ratio is a measure of sample purity defined by the absorbance level at 260 and 280nm. Individual amino acids have varying 260/280 ratios with uracil displaying the highest. Therefore, samples high in RNA content have a higher 260/280 ratio.

3.5.1.11.2 ***Summary***

Processed samples showed a high concentration and purity of DNA. The samples were genotyped in house for *SERPING1* and by a commercial company (LGC Genomics; Hoddesdon, UK).

3.5.1.12 HRM analysis within the study

HRM analysis was performed using the SERPING1 (rs2511989) SNP. This was in preparation for further investigation of the gene in predicting AMD outcome measures.

A

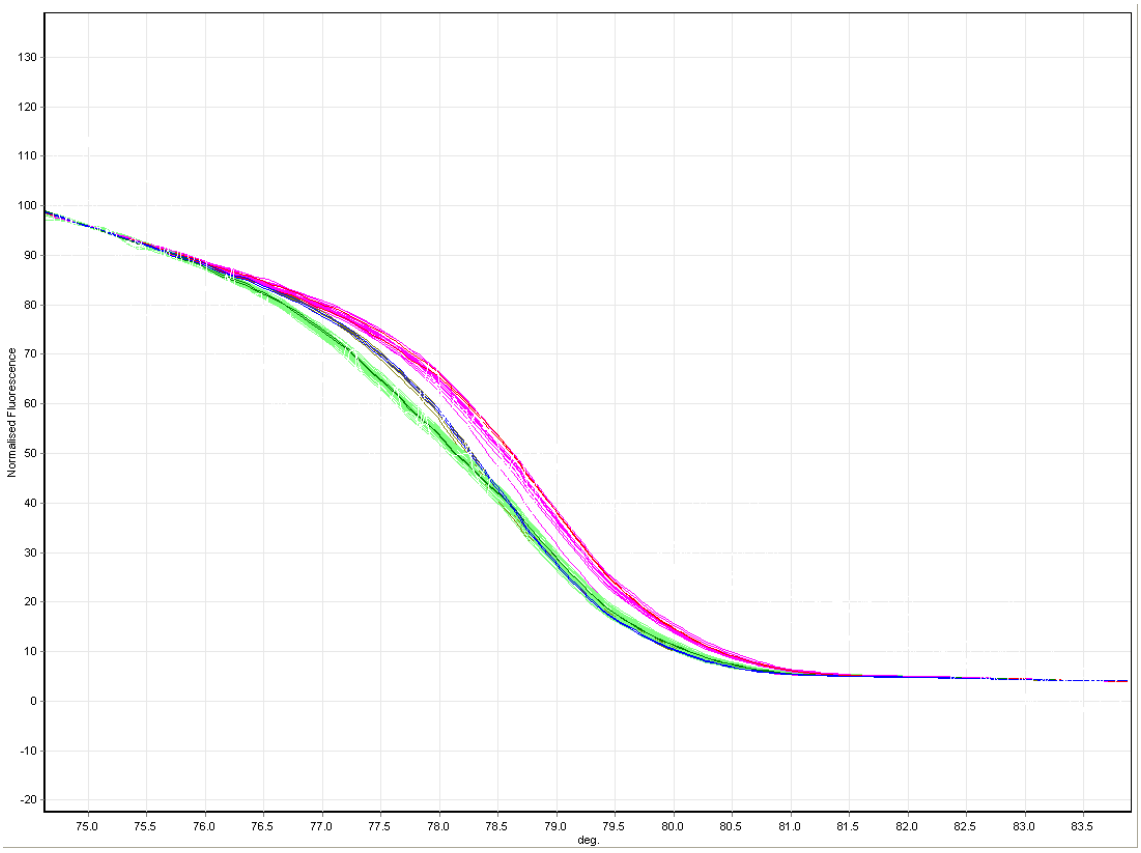

B

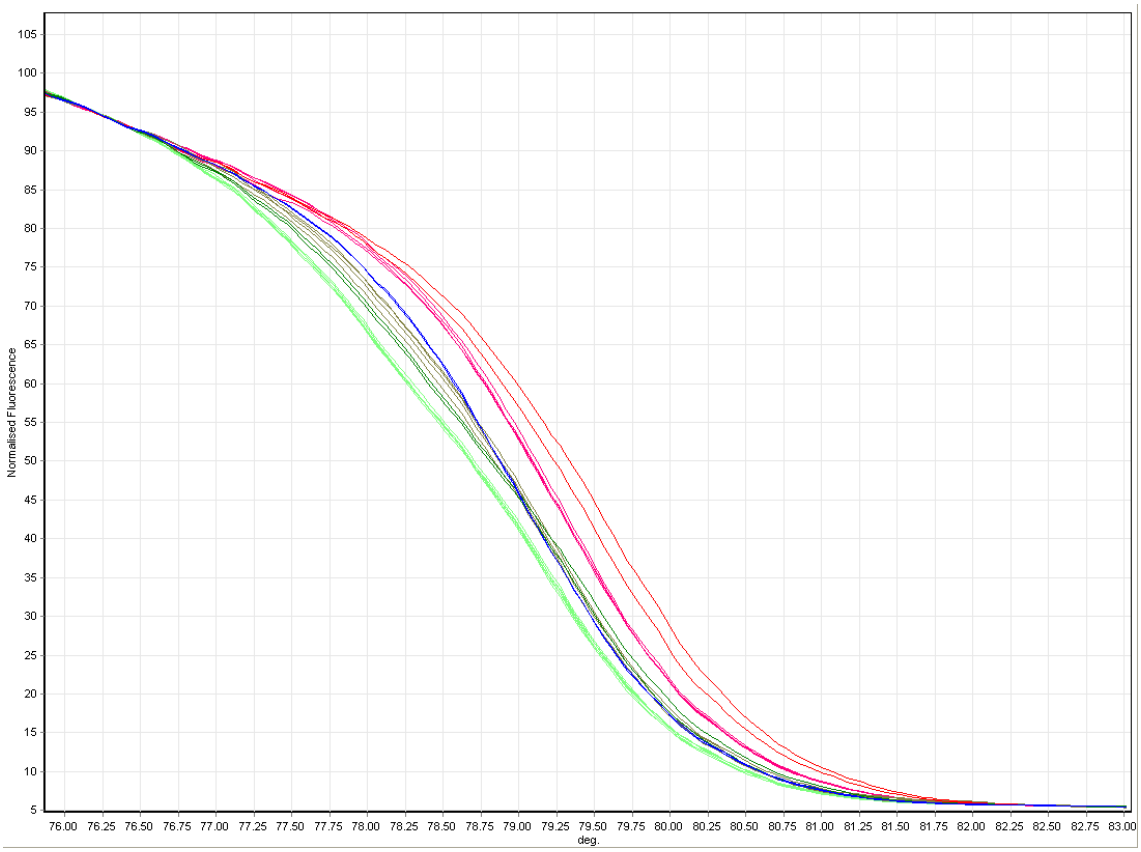

Figure 49 HRM results from 2 example plates (A and B) analysing the genotype of SERPING1 (rs2511989) in the cohort. (Wild type, heterozygote, mutant) (29 Wild type (29.29%), 14 Homozygote (14.14%), 35 Heterozygote (35.35%) participants were isolated).

3.5.1.12.1 *Summary*

The results of the in-house HRM analysis were not dissimilar from the commercial genotyping results. This was a proof of concept and provided validation of the in-house analysis.

3.5.1.13 The relationship of SERPING1 to treatment outcome measures (CMT, VAS and administered injections of anti VEGF)

My hypothesis suggests an association with SERPING1 and outcome measures for CNV treatment with ranibizumab. There have been no previous trials to demonstrate SERPING1 as a reliable biomarker of CNV response to anti VEGF therapy. MY study results however did not indicate the genotype would be a reliable predictor for outcome measures.

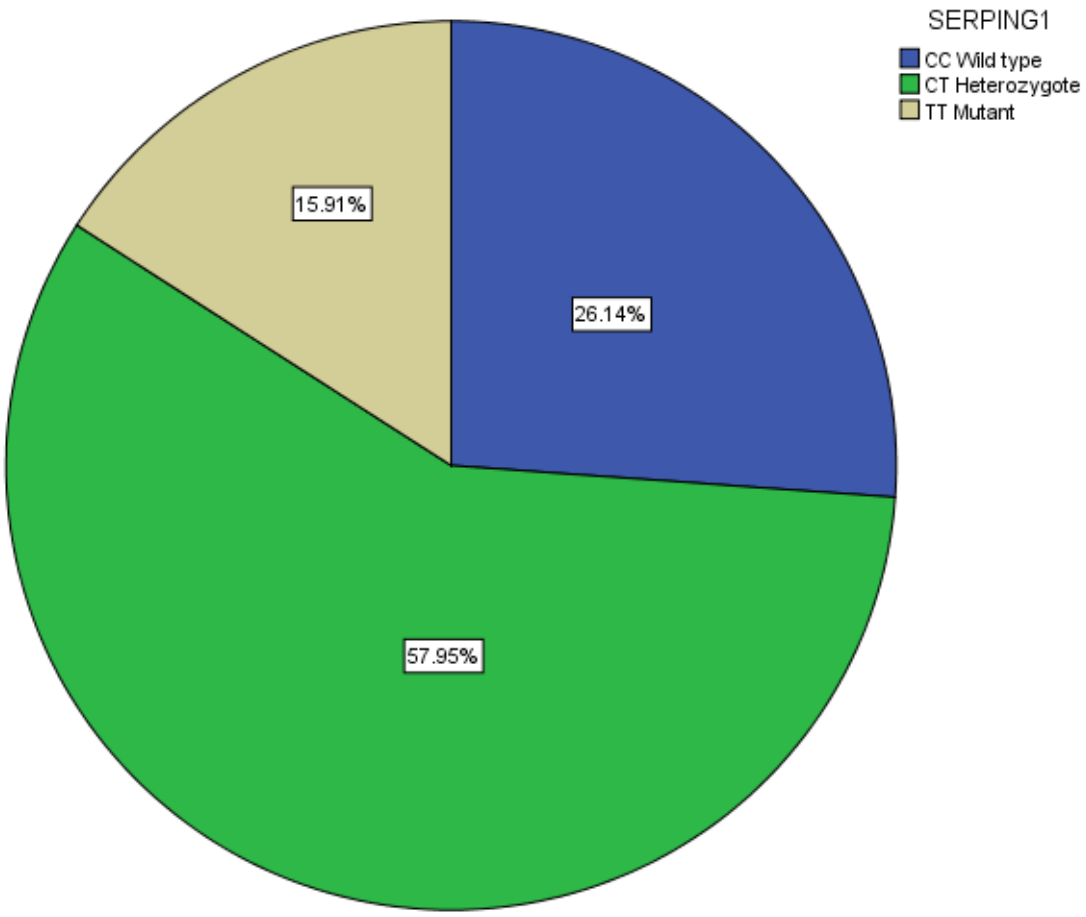

Figure 50 Distribution of the serpin peptidase inhibitor, clade G (C1 inhibitor), member 1 (*SERPING1*) genotype (rs2511989) within the study population (n=99). 15.9% percent of the population were identified as TT genotype (mutant), 57.9% were CT (heterozygous) and 26.1% were CC (wild type).

A) Multiple Comparisons

Dependent Variable: VAS change

Bonferroni

Visit	(I) SERPING1	(J) SERPING1	Sig.	95% Confidence Interval	
				Lower Bound	Upper Bound
2	CC Wild type	CT Heterozygote	1.000	-4.8914	7.0786
		TT Mutant	1.000	-8.0792	7.3643
	CT Heterozygote	CC Wild type	1.000	-7.0786	4.8914
		TT Mutant	1.000	-8.0670	5.1649
	TT Mutant	CC Wild type	1.000	-7.3643	8.0792
		CT Heterozygote	1.000	-5.1649	8.0670
3	CC Wild type	CT Heterozygote	1.000	-5.4834	3.8326
		TT Mutant	1.000	-4.7888	6.9951
	CT Heterozygote	CC Wild type	1.000	-3.8326	5.4834
		TT Mutant	1.000	-3.1740	7.0312
	TT Mutant	CC Wild type	1.000	-6.9951	4.7888
		CT Heterozygote	1.000	-7.0312	3.1740
4	CC Wild type	CT Heterozygote	1.000	-5.7903	5.4755
		TT Mutant	1.000	-4.9813	9.5156
	CT Heterozygote	CC Wild type	1.000	-5.4755	5.7903
		TT Mutant	1.000	-3.9620	8.8111
	TT Mutant	CC Wild type	1.000	-9.5156	4.9813
		CT Heterozygote	1.000	-8.8111	3.9620

A cont'd) Multiple Comparisons

Dependent Variable: VAS change

Bonferroni

Visit	(I) SERPING1	(J) SERPING1	Sig.	95% Confidence Interval	
				Lower Bound	Upper Bound
5	CC Wild type	CT Heterozygote	0.864	-9.9285	3.9044
		TT Mutant	1.000	-11.0993	8.3146
	CT Heterozygote	CC Wild type	0.864	-3.9044	9.9285
		TT Mutant	1.000	-6.9955	10.2348
	TT Mutant	CC Wild type	1.000	-8.3146	11.0993
		CT Heterozygote	1.000	-10.2348	6.9955
6	CC Wild type	CT Heterozygote	1.000	-8.2538	7.1950
		TT Mutant	1.000	-8.8388	10.7702
	CT Heterozygote	CC Wild type	1.000	-7.1950	8.2538
		TT Mutant	1.000	-7.2364	10.2266
	TT Mutant	CC Wild type	1.000	-10.7702	8.8388
		CT Heterozygote	1.000	-10.2266	7.2364
7	CC Wild type	CT Heterozygote	1.000	-11.1519	6.5269
		TT Mutant	0.474	-20.9313	5.5980
	CT Heterozygote	CC Wild type	1.000	-6.5269	11.1519
		TT Mutant	0.816	-17.3107	6.6024
	TT Mutant	CC Wild type	0.474	-5.5980	20.9313
		CT Heterozygote	0.816	-6.6024	17.3107

B) Multiple Comparisons

Dependent Variable: CMT Change

Bonferroni

Visit	(I) SERPING1	(J) SERPING1	Sig.	95% Confidence Interval	
				Lower Bound	Upper Bound
2	CC Wild type	CT Heterozygote	0.661	-30.42	92.31
		TT Mutant	0.158	-15.28	140.49
	CT Heterozygote	CC Wild type	0.661	-92.31	30.42
		TT Mutant	0.781	-36.78	100.11
	TT Mutant	CC Wild type	0.158	-140.49	15.28
		CT Heterozygote	0.781	-100.11	36.78
3	CC Wild type	CT Heterozygote	1.000	-62.47	95.77
		TT Mutant	0.767	-54.78	149.51
	CT Heterozygote	CC Wild type	1.000	-95.77	62.47
		TT Mutant	1.000	-57.33	118.75
	TT Mutant	CC Wild type	0.767	-149.51	54.78
		CT Heterozygote	1.000	-118.75	57.33
4	CC Wild type	CT Heterozygote	1.000	-55.88	112.42
		TT Mutant	1.000	-97.20	120.07
	CT Heterozygote	CC Wild type	1.000	-112.42	55.88
		TT Mutant	1.000	-114.00	80.33
	TT Mutant	CC Wild type	1.000	-120.07	97.20
		CT Heterozygote	1.000	-80.33	114.00

B cont'd) Multiple Comparisons					
Dependent Variable: CMT Change					
Bonferroni					
Visit	(I) SERPING1	(J) SERPING1	Sig.	95% Confidence Interval	
				Lower Bound	Upper Bound
5	CC Wild type	CT Heterozygote	1.000	-56.80	106.10
		TT Mutant	0.775	-56.99	154.83
	CT Heterozygote	CC Wild type	1.000	-106.10	56.80
		TT Mutant	1.000	-63.80	112.34
	TT Mutant	CC Wild type	0.775	-154.83	56.99
		CT Heterozygote	1.000	-112.34	63.80
6	CC Wild type	CT Heterozygote	1.000	-98.60	71.83
		TT Mutant	0.615	-51.33	161.24
	CT Heterozygote	CC Wild type	1.000	-71.83	98.60
		TT Mutant	0.184	-20.30	156.98
	TT Mutant	CC Wild type	0.615	-161.24	51.33
		CT Heterozygote	0.184	-156.98	20.30
7	CC Wild type	CT Heterozygote	1.000	-60.74	96.00
		TT Mutant	1.000	-99.23	151.60
	CT Heterozygote	CC Wild type	1.000	-96.00	60.74
		TT Mutant	1.000	-111.36	128.48
	TT Mutant	CC Wild type	1.000	-151.60	99.23
		CT Heterozygote	1.000	-128.48	111.36

Table 31 Tables examining the relationship between VAS (A) and CMT (B) change from baseline using one-way ANOVA analysis with Bonferroni correction for multiple comparisons.

Chi-Square Tests				
Visit		Value	df	Asymp. Sig. (2-sided)
1	Pearson Chi-Square	0.835	2	0.659
		0.801	2	0.670
		0.030	1	0.862
	N of Valid Cases	78		
2	Pearson Chi-Square	1.068	2	0.586
	N of Valid Cases	75		
3	Pearson Chi-Square	0.456	2	0.796
	N of Valid Cases	76		
4	Pearson Chi-Square	2.276	2	0.321
	N of Valid Cases	67		
5	Pearson Chi-Square	10.286	2	*0.006
	N of Valid Cases	64		
6	Pearson Chi-Square	1.766	2	0.414
	N of Valid Cases	64		
7	Pearson Chi-Square	5.590	2	0.061
	N of Valid Cases	57		

Table 32 Chi square analysis comparing SERPING1 genotypes within the cohort and administered injections for active CNV. Df- degrees of freedom, *-significant result with a p value <0.05

3.5.1.13.1 *Summary*

The results demonstrated no significant difference between the wild type and mutant alleles for change in either VA score or CMT (Table 31). There was however a significant association at visit 5 (p=0.006) for administered injections (Table 32). The heterozygote allele was associated with a significantly lower number of injections at this visit.

Figure 50 demonstrates the distribution of alleles within the study population.

3.5.1.14 The relationship of CFI to treatment outcome measures (CMT, VAS and administered injections of anti VEGF)

A recent Nature Genetics paper[192] implicated a rare highly penetrant variant of CFI (p.Gly119Arg) as conferring a high risk of developing (P = 3.79 × 10□6; odds ratio (OR) = 22.20, 95% confidence interval (CI) = 2.98–164.49). There have however been no studies that implicate CFI as a predictor of CNV response to therapy.

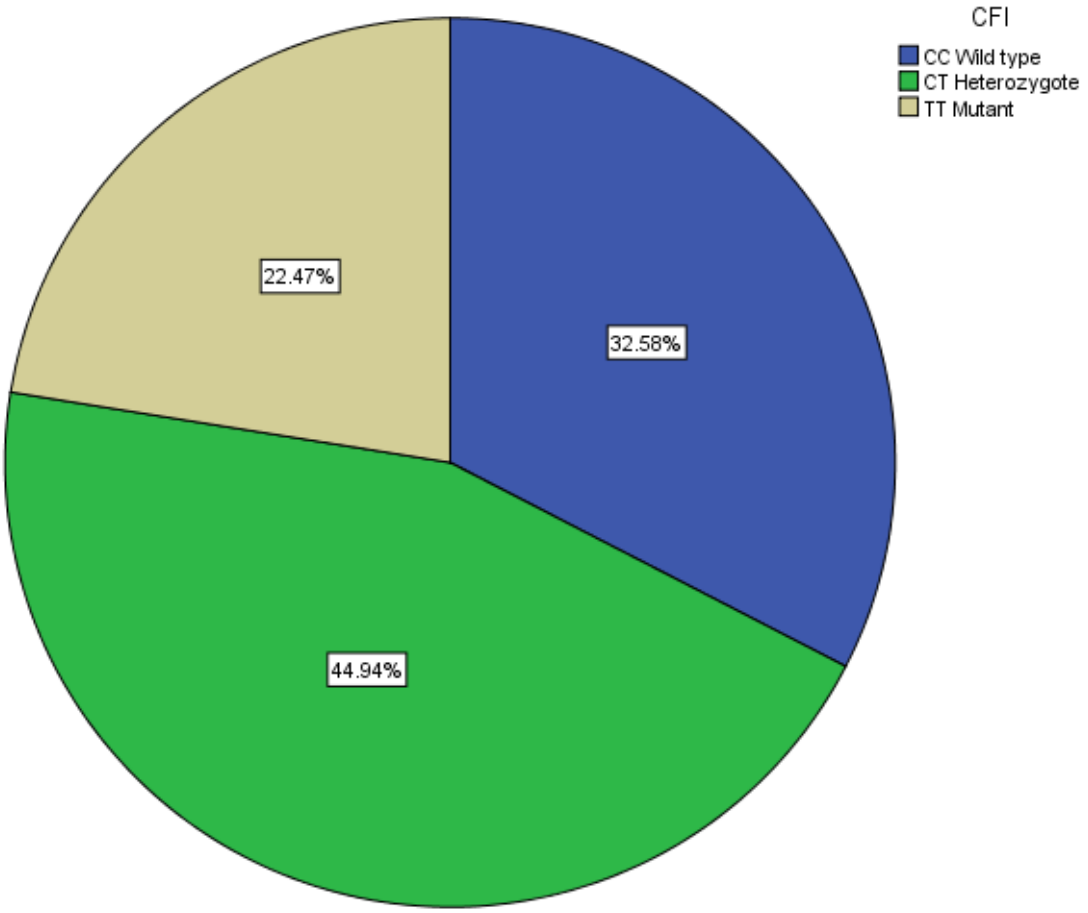

Figure 51 Distribution of the complement factor I (CFI) genotype (rs10033900) within the study population (n=99). 22.5% percent of the population were identified as TT genotype (mutant), 44.9% were CT (heterozygous) and 22.5% were CC (wild type).

A) Multiple Comparisons

Dependent Variable: VAS change

Bonferroni

Visit	(I) CFI	(J) CFI	Sig.	95% Confidence Interval	
				Lower Bound	Upper Bound
2	CC Wild type	CT Heterozygote	1.000	-4.6349	6.7102
		TT Mutant	1.000	-6.3839	6.8687
	CT Heterozygote	CC Wild type	1.000	-6.7102	4.6349
		TT Mutant	1.000	-6.8425	5.2520
	TT Mutant	CC Wild type	1.000	-6.8687	6.3839
		CT Heterozygote	1.000	-5.2520	6.8425
3	CC Wild type	CT Heterozygote	0.521	-1.9974	7.0984
		TT Mutant	1.000	-4.5219	6.3320
	CT Heterozygote	CC Wild type	0.521	-7.0984	1.9974
		TT Mutant	1.000	-6.5910	3.3002
	TT Mutant	CC Wild type	1.000	-6.3320	4.5219
		CT Heterozygote	1.000	-3.3002	6.5910
4	CC Wild type	CT Heterozygote	1.000	-5.0670	6.1193
		TT Mutant	1.000	-8.9606	4.7146
	CT Heterozygote	CC Wild type	1.000	-6.1193	5.0670
		TT Mutant	0.867	-8.7424	3.4441
	TT Mutant	CC Wild type	1.000	-4.7146	8.9606
		CT Heterozygote	0.867	-3.4441	8.7424

A cont'd) Multiple Comparisons					
Dependent Variable: VAS change					
Bonferroni					
Visit	(I) CFI	(J) CFI	Sig.	95% Confidence Interval	
				Lower Bound	Upper Bound
5	CC Wild type	CT Heterozygote	1.000	-5.5878	8.5510
		TT Mutant	0.993	-5.0430	11.7180
	CT Heterozygote	CC Wild type	1.000	-8.5510	5.5878
		TT Mutant	1.000	-5.3720	9.0837
	TT Mutant	CC Wild type	0.993	-11.7180	5.0430
		CT Heterozygote	1.000	-9.0837	5.3720
6	CC Wild type	CT Heterozygote	1.000	-6.6330	8.7997
		TT Mutant	1.000	-5.8982	12.1982
	CT Heterozygote	CC Wild type	1.000	-8.7997	6.6330
		TT Mutant	1.000	-6.1177	10.2511
	TT Mutant	CC Wild type	1.000	-12.1982	5.8982
		CT Heterozygote	1.000	-10.2511	6.1177
7	CC Wild type	CT Heterozygote	1.000	-7.6174	10.2617
		TT Mutant	1.000	-9.9234	10.2673
	CT Heterozygote	CC Wild type	1.000	-10.2617	7.6174
		TT Mutant	1.000	-10.8199	8.5196
	TT Mutant	CC Wild type	1.000	-10.2673	9.9234
		CT Heterozygote	1.000	-8.5196	10.8199

B) Multiple Comparisons					
Dependent Variable: CMT Change					
Bonferroni					
Visit	(I) CFI	(J) CFI	Sig.	95% Confidence Interval	
				Lower Bound	Upper Bound
2	CC Wild type	CT Heterozygote	0.856	-87.92	34.26
		TT Mutant	0.556	-110.46	32.46
	CT Heterozygote	CC Wild type	0.856	-34.26	87.92
		TT Mutant	1.000	-76.39	52.06
	TT Mutant	CC Wild type	0.556	-32.46	110.46
		CT Heterozygote	1.000	-52.06	76.39
3	CC Wild type	CT Heterozygote	1.000	-61.95	89.60
		TT Mutant	1.000	-112.76	56.93
	CT Heterozygote	CC Wild type	1.000	-89.60	61.95
		TT Mutant	0.562	-119.14	35.65
	TT Mutant	CC Wild type	1.000	-56.93	112.76
		CT Heterozygote	0.562	-35.65	119.14
4	CC Wild type	CT Heterozygote	1.000	-86.12	79.39
		TT Mutant	1.000	-123.81	83.04
	CT Heterozygote	CC Wild type	1.000	-79.39	86.12
		TT Mutant	1.000	-112.62	78.59
	TT Mutant	CC Wild type	1.000	-83.04	123.81
		CT Heterozygote	1.000	-78.59	112.62

B cont'd) Multiple Comparisons					
Dependent Variable: CMT Change					
Bonferroni					
Visit	(I) CFI	(J) CFI	Sig.	95% Confidence Interval	
				Lower Bound	Upper Bound
5	CC Wild type	CT Heterozygote	1.000	-91.18	61.89
		TT Mutant	0.856	-126.95	49.80
	CT Heterozygote	CC Wild type	1.000	-61.89	91.18
		TT Mutant	1.000	-100.46	52.61
	TT Mutant	CC Wild type	0.856	-49.80	126.95
		CT Heterozygote	1.000	-52.61	100.46
6	CC Wild type	CT Heterozygote	1.000	-90.63	62.79
		TT Mutant	0.429	-143.91	36.06
	CT Heterozygote	CC Wild type	1.000	-62.79	90.63
		TT Mutant	0.781	-127.29	47.29
	TT Mutant	CC Wild type	0.429	-36.06	143.91
		CT Heterozygote	0.781	-47.29	127.29
7	CC Wild type	CT Heterozygote	1.000	-102.77	64.95
		TT Mutant	0.665	-152.25	51.06
	CT Heterozygote	CC Wild type	1.000	-64.95	102.77
		TT Mutant	1.000	-123.23	59.86
	TT Mutant	CC Wild type	0.665	-51.06	152.25
		CT Heterozygote	1.000	-59.86	123.23

Table 33 Tables examining the relationship between VAS (A) and CMT (B) change from baseline using one-way ANOVA analysis with Bonferroni correction for multiple comparisons.

Chi-Square Tests				
Visit		Value	df	Asymp. Sig. (2-sided)
2	Pearson Chi-Square	0.758	2	0.685
	N of Valid Cases	76		
3	Pearson Chi-Square	2.588	2	0.274
	N of Valid Cases	77		
4	Pearson Chi-Square	1.290	2	0.525
	N of Valid Cases	67		
5	Pearson Chi-Square	1.030	2	0.598
	N of Valid Cases	65		
6	Pearson Chi-Square	1.099	2	0.577
	N of Valid Cases	64		
7	Pearson Chi-Square	1.175	2	0.556
	N of Valid Cases	57		

Table 34 Chi square analysis comparing CFI genotypes within the cohort and administered injections for active CNV. Df- degrees of freedom

3.5.1.14.1 *Summary*

No significant correlation was established between treatment (CMT and VA score change from baseline) or CNV activity (administered injections) as seen in Table 29 and Table 34.

Figure 51 demonstrates the distribution of alleles within the study population.

3.5.1.15 The relationship of CFH to treatment outcome measures (CMT, VAS and administered injections of anti VEGF)

There have been many studies investigating the role of CFH in predicting treatment response with conflicting results. Studies that reported an association between CFH and treatment outcomes, varied with respect to the influence of genotype. The CC allele was found to be associated with worse outcome in some reports[193, 194], whereas the protective TT allele was found to be detrimental in 1 report[195]. There were also many reported studies which found no association between CFH and treatment outcomes[190, 196-198].

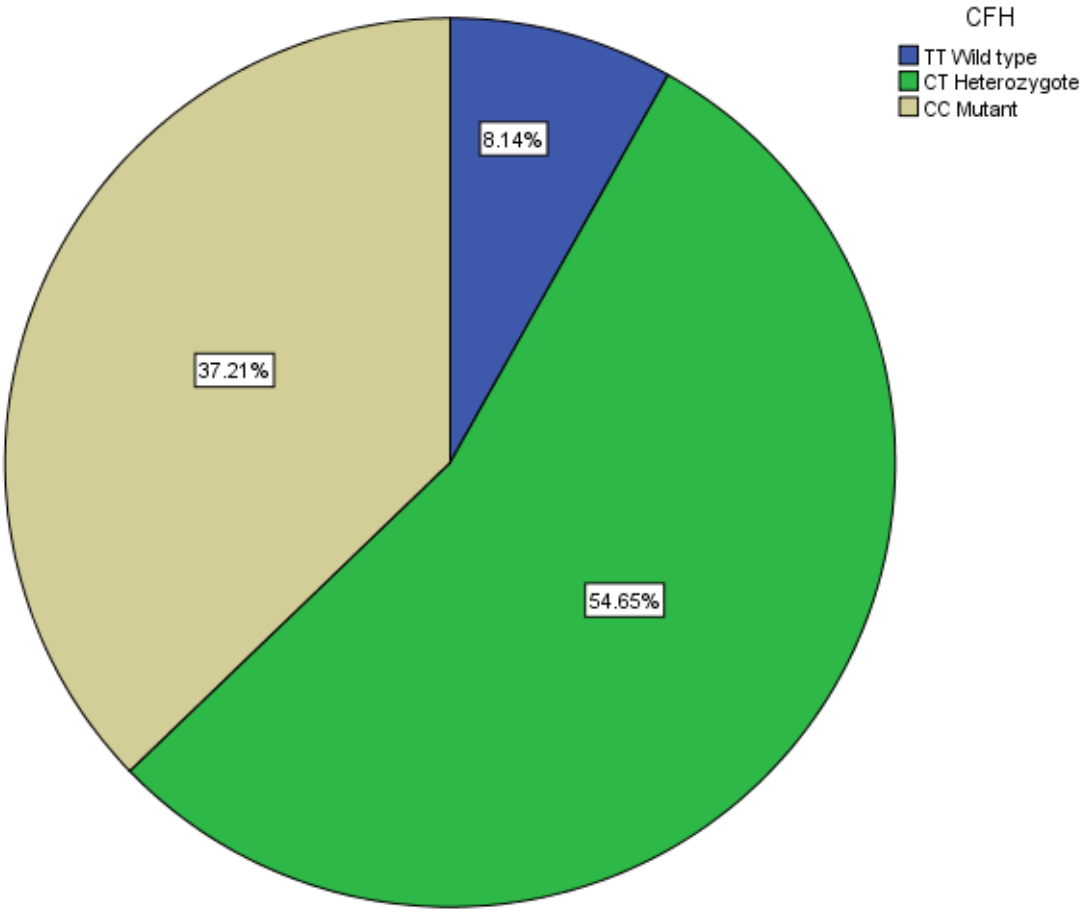

Figure 52 Distribution of the complement factor H (CFH) genotype (rs1061170) within the study population (n=99). 8.1% percent of the population were identified as TT genotype (mutant), 54.6% were CT (heterozygous) and 37.2% were CC (wild type).

A) Multiple Comparisons

Dependent Variable: VAS change

Bonferroni

Visit	(I) CFH	(J) CFH	Sig.	95% Confidence Interval	
				Lower Bound	Upper Bound
2	TT Wild type	CT Heterozygote	1.000	-7.5956	10.0241
		CC Mutant	1.000	-7.7100	10.6433
	CT Heterozygote	TT Wild type	1.000	-10.0241	7.5956
		CC Mutant	1.000	-4.8467	5.3515
	CC Mutant	TT Wild type	1.000	-10.6433	7.7100
		CT Heterozygote	1.000	-5.3515	4.8467
3	TT Wild type	CT Heterozygote	1.000	-7.9965	6.5679
		CC Mutant	1.000	-7.3071	7.8071
	CT Heterozygote	TT Wild type	1.000	-6.5679	7.9965
		CC Mutant	1.000	-3.1995	5.1280
	CC Mutant	TT Wild type	1.000	-7.8071	7.3071
		CT Heterozygote	1.000	-5.1280	3.1995
4	TT Wild type	CT Heterozygote	1.000	-6.2206	11.7817
		CC Mutant	0.873	-5.2395	13.2395
	CT Heterozygote	TT Wild type	1.000	-11.7817	6.2206
		CC Mutant	1.000	-3.6906	6.1295
	CC Mutant	TT Wild type	0.873	-13.2395	5.2395
		CT Heterozygote	1.000	-6.1295	3.6906

A cont'd) Multiple Comparisons					
Dependent Variable: VAS change					
Bonferroni					
Visit	(I) CFH	(J) CFH	Sig.	95% Confidence Interval	
				Lower Bound	Upper Bound
5	TT Wild type	CT Heterozygote	1.000	-9.1306	11.4584
		CC Mutant	1.000	-9.3319	12.0410
	CT Heterozygote	TT Wild type	1.000	-11.4584	9.1306
		CC Mutant	1.000	-5.6465	6.0278
	CC Mutant	TT Wild type	1.000	-12.0410	9.3319
		CT Heterozygote	1.000	-6.0278	5.6465
6	TT Wild type	CT Heterozygote	1.000	-13.1984	13.6150
		CC Mutant	1.000	-12.5956	14.9652
	CT Heterozygote	TT Wild type	1.000	-13.6150	13.1984
		CC Mutant	1.000	-5.8138	7.7667
	CC Mutant	TT Wild type	1.000	-14.9652	12.5956
		CT Heterozygote	1.000	-7.7667	5.8138
7	TT Wild type	CT Heterozygote	1.000	-16.4326	23.0533
		CC Mutant	1.000	-13.5525	26.5025
	CT Heterozygote	TT Wild type	1.000	-23.0533	16.4326
		CC Mutant	0.967	-4.6846	11.0139
	CC Mutant	TT Wild type	1.000	-26.5025	13.5525
		CT Heterozygote	0.967	-11.0139	4.6846

B) Multiple Comparisons

Dependent Variable: CMT Change

Bonferroni

Visit	(I) CFH	(J) CFH	Sig.	95% Confidence Interval	
				Lower Bound	Upper Bound
2	TT Wild type	CT Heterozygote	1.000	-71.32	123.02
		CC Mutant	1.000	-115.54	85.13
	CT Heterozygote	TT Wild type	1.000	-123.02	71.32
		CC Mutant	0.216	-96.15	14.04
	CC Mutant	TT Wild type	1.000	-85.13	115.54
		CT Heterozygote	0.216	-14.04	96.15
3	TT Wild type	CT Heterozygote	1.000	-111.40	109.75
		CC Mutant	1.000	-152.30	76.65
	CT Heterozygote	TT Wild type	1.000	-109.75	111.40
		CC Mutant	0.545	-104.69	30.70
	CC Mutant	TT Wild type	1.000	-76.65	152.30
		CT Heterozygote	0.545	-30.70	104.69
4	TT Wild type	CT Heterozygote	0.117	-17.74	229.60
		CC Mutant	0.766	-67.99	186.18
	CT Heterozygote	TT Wild type	0.117	-229.60	17.74
		CC Mutant	0.358	-120.01	26.34
	CC Mutant	TT Wild type	0.766	-186.18	67.99
		CT Heterozygote	0.358	-26.34	120.01

B cont'd) Multiple Comparisons					
Dependent Variable: CMT Change					
Bonferroni					
Visit	(I) CFH	(J) CFH	Sig.	95% Confidence Interval	
				Lower Bound	Upper Bound
5	TT Wild type	CT Heterozygote	1.000	-81.21	167.71
		CC Mutant	1.000	-116.23	141.97
	CT Heterozygote	TT Wild type	1.000	-167.71	81.21
		CC Mutant	0.822	-98.35	37.59
	CC Mutant	TT Wild type	1.000	-141.97	116.23
		CT Heterozygote	0.822	-37.59	98.35
6	TT Wild type	CT Heterozygote	1.000	-121.94	138.01
		CC Mutant	1.000	-158.68	105.29
	CT Heterozygote	TT Wild type	1.000	-138.01	121.94
		CC Mutant	0.753	-109.11	39.65
	CC Mutant	TT Wild type	1.000	-105.29	158.68
		CT Heterozygote	0.753	-39.65	109.11
7	TT Wild type	CT Heterozygote	1.000	-156.15	195.39
		CC Mutant	1.000	-207.37	149.70
	CT Heterozygote	TT Wild type	1.000	-195.39	156.15
		CC Mutant	0.323	-121.90	25.00
	CC Mutant	TT Wild type	1.000	-149.70	207.37
		CT Heterozygote	0.323	-25.00	121.90

Table 35 Tables examining the relationship between VAS (A) and CMT (B) change from baseline using one-way ANOVA analysis with Bonferroni correction for multiple comparisons.

Chi-Square Tests				
Visit		Value	df	Asymp. Sig. (2-sided)
2	Pearson Chi-Square	1.566	2	0.457
	N of Valid Cases	74		
3	Pearson Chi-Square	2.327	2	0.312
	N of Valid Cases	76		
4	Pearson Chi-Square	2.283	2	0.319
	N of Valid Cases	67		
5	Pearson Chi-Square	2.962	2	0.227
	N of Valid Cases	63		
6	Pearson Chi-Square	0.345	2	0.841
	N of Valid Cases	64		
7	Pearson Chi-Square	2.200	2	0.333
	N of Valid Cases	57		

Table 36 Chi square analysis comparing CFH genotypes within the cohort and administered injections for active CNV. Df- degrees of freedom

3.5.1.15.1 *Summary*

No significant correlation was established between treatment (CMT and VA score change from baseline) or CNV activity (administered injections) as seen in Table 35 and Table 36. Figure 52 demonstrates the distribution of alleles within the study population.

3.5.1.16 The relationship of ARMS2/HTRA1 to treatment outcome measures (CMT, VAS and administered injections of anti VEGF)

One study[197] provided evidence of poor VA score outcomes as a response to treatment in the TT allele. There was also evidence in the literature which suggested a higher mean number of injections were administered in the TT mutant subgroup[161] during the study period. Our study did not provide conclusive evidence of the benefit of the ARMS2/HTRA1 genotype as a biomarker for disease response to treatment.

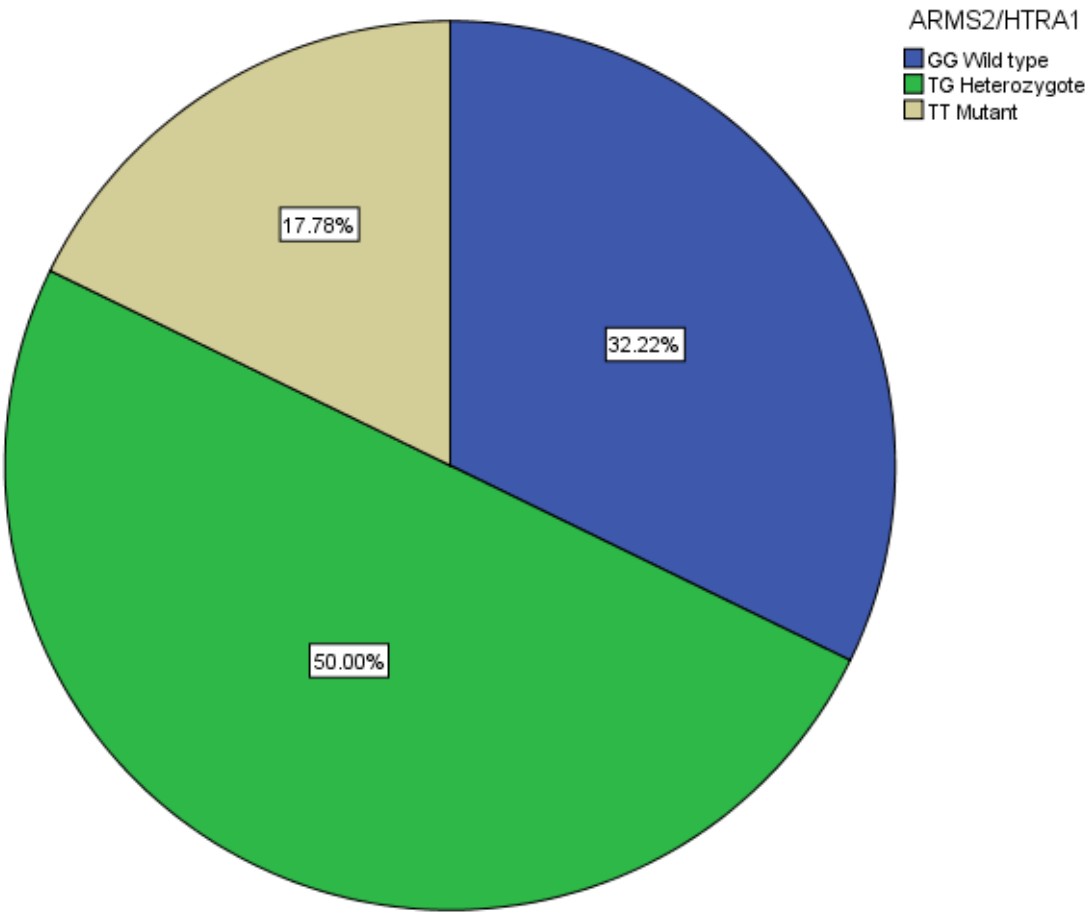

Figure 53 Distribution of the Age-related maculopathy susceptibility protein 2/ High temperature requirement (ARMS2/HTRA1) genotype (rs10490924) within the study population (n=99). 17.8% percent of the population were identified as TT genotype (mutant), 50.0% were GT (heterozygous) and 32.2% were GG (wild type).

A) Multiple Comparisons					
Dependent Variable: VAS change					
Bonferroni					
Visit	(I) ARMS2/HTRA1	(J) ARMS2/HTRA1	Sig.	95% Confidence Interval	
				Lower Bound	Upper Bound
2	GG Wild type	TG Heterozygote	0.132	-9.7221	0.8689
		TT Mutant	1.000	-5.8562	7.4441
	TG Heterozygote	GG Wild type	0.132	-0.8689	9.7221
		TT Mutant	0.112	-0.8135	11.2545
	TT Mutant	GG Wild type	1.000	-7.4441	5.8562
		TG Heterozygote	0.112	-11.2545	0.8135
3	GG Wild type	TG Heterozygote	0.072	-8.2839	0.2480
		TT Mutant	*0.008	-11.8371	-1.3731
	TG Heterozygote	GG Wild type	0.072	-0.2480	8.2839
		TT Mutant	0.557	-7.3328	2.1584
	TT Mutant	GG Wild type	*0.008	1.3731	11.8371
		TG Heterozygote	0.557	-2.1584	7.3328
4	GG Wild type	TG Heterozygote	1.000	-6.4098	4.1000
		TT Mutant	0.090	-12.6253	0.6496
	TG Heterozygote	GG Wild type	1.000	-4.1000	6.4098
		TT Mutant	0.155	-10.8225	1.1565
	TT Mutant	GG Wild type	0.090	-0.6496	12.6253
		TG Heterozygote	0.155	-1.1565	10.8225
5	GG Wild type	TG Heterozygote	0.104	-12.5249	0.8106
		TT Mutant	0.215	-14.5023	2.1177
	TG Heterozygote	GG Wild type	0.104	-0.8106	12.5249
		TT Mutant	1.000	-7.6609	6.9906
	TT Mutant	GG Wild type	0.215	-2.1177	14.5023
		TG Heterozygote	1.000	-6.9906	7.6609

A cont'd) Multiple Comparisons

Dependent Variable: VAS change

Bonferroni

Visit	(I) ARMS2/HTRA1	(J) ARMS2/HTRA1	Sig.	95% Confidence Interval	
				Lower Bound	Upper Bound
6	GG Wild type	TG Heterozygote	0.086	-13.4887	0.6265
		TT Mutant	0.172	-16.6821	1.9883
	TG Heterozygote	GG Wild type	0.086	-0.6265	13.4887
		TT Mutant	1.000	-9.4626	7.6311
	TT Mutant	GG Wild type	0.172	-1.9883	16.6821
		TG Heterozygote	1.000	-7.6311	9.4626
7	GG Wild type	TG Heterozygote	0.958	-11.8837	5.0239
		TT Mutant	0.443	-18.5454	4.7288
	TG Heterozygote	GG Wild type	0.958	-5.0239	11.8837
		TT Mutant	1.000	-14.0936	7.1367
	TT Mutant	GG Wild type	0.443	-4.7288	18.5454
		TG Heterozygote	1.000	-7.1367	14.0936

B) Multiple Comparisons

Dependent Variable: CMT Change

Bonferroni

Visit	(I) ARMS2/HTRA1	(J) ARMS2/HTRA1	Sig.	95% Confidence Interval	
				Lower Bound	Upper Bound
2	GG Wild type	TG Heterozygote	1.000	-60.44	55.93
		TT Mutant	1.000	-79.87	74.59
	TG Heterozygote	GG Wild type	1.000	-55.93	60.44
		TT Mutant	1.000	-72.21	71.44
	TT Mutant	GG Wild type	1.000	-74.59	79.87
		TG Heterozygote	1.000	-71.44	72.21
3	GG Wild type	TG Heterozygote	0.418	-117.58	28.81
		TT Mutant	1.000	-126.54	59.71
	TG Heterozygote	GG Wild type	0.418	-28.81	117.58
		TT Mutant	1.000	-71.51	93.45
	TT Mutant	GG Wild type	1.000	-59.71	126.54
		TG Heterozygote	1.000	-93.45	71.51
4	GG Wild type	TG Heterozygote	1.000	-83.76	72.02
		TT Mutant	1.000	-86.63	124.92
	TG Heterozygote	GG Wild type	1.000	-72.02	83.76
		TT Mutant	1.000	-77.67	127.69
	TT Mutant	GG Wild type	1.000	-124.92	86.63
		TG Heterozygote	1.000	-127.69	77.67
5	GG Wild type	TG Heterozygote	1.000	-88.21	54.52
		TT Mutant	1.000	-96.43	84.38
	TG Heterozygote	GG Wild type	1.000	-54.52	88.21
		TT Mutant	1.000	-71.92	93.55
	TT Mutant	GG Wild type	1.000	-84.38	96.43
		TG Heterozygote	1.000	-93.55	71.92

B cont'd) Multiple Comparisons					
Dependent Variable: CMT Change					
Bonferroni					
Visit	(I) ARMS2/HTRA1	(J) ARMS2/HTRA1	Sig.	95% Confidence Interval	
				Lower Bound	Upper Bound
6	GG Wild type	TG Heterozygote	1.000	-100.01	57.42
		TT Mutant	1.000	-106.83	86.83
	TG Heterozygote	GG Wild type	1.000	-57.42	100.01
		TT Mutant	1.000	-78.54	101.13
	TT Mutant	GG Wild type	1.000	-86.83	106.83
		TG Heterozygote	1.000	-101.13	78.54
7	GG Wild type	TG Heterozygote	0.634	-120.72	39.22
		TT Mutant	1.000	-113.59	98.77
	TG Heterozygote	GG Wild type	00.634	-39.22	120.72
		TT Mutant	1.000	-63.98	130.65
	TT Mutant	GG Wild type	1.000	-98.77	113.59
		TG Heterozygote	1.000	-130.65	63.98

Table 37 Tables examining the relationship between VAS (A) and CMT (B) change from baseline using one-way ANOVA analysis with Bonferroni correction for multiple comparisons. *-significant result with a p value <0.05

Chi-Square Tests				
Visit		Value	df	Asymp. Sig. (2-sided)
2	Pearson Chi-Square	2.300	2	0.317
	N of Valid Cases	77		
3	Pearson Chi-Square	0.415	2	0.813
	N of Valid Cases	78		
4	Pearson Chi-Square	4.035	2	0.133
	N of Valid Cases	68		
5	Pearson Chi-Square	1.034	2	0.596
	N of Valid Cases	65		
6	Pearson Chi-Square	0.194	2	0.908
	N of Valid Cases	65		
7	Pearson Chi-Square	3.755	2	0.153
	N of Valid Cases	58		

Table 38 Chi square analysis comparing ARMS2/HTRA1 genotypes within the cohort and administered injections for active CNV. Df- degrees of freedom

3.5.1.16.1 ***Summary***

The results demonstrated a significant difference (p=0.008) between the wild type and mutant alleles for change in VA score at visit 3 with a small Chi-square value of 1.3731 (Table 37). No significant correlation was established between administered injections (Table 38).

Figure 53 demonstrates the distribution of alleles within the study population.

3.5.1.17 The relationship of C3 to treatment outcome measures (CMT, VAS and administered injections of anti VEGF)

There has been one prospective trial[199] that provided evidence of an association between the wild type allele and decreased CMT after 1 year of treatment. Other trials have not shown an association between the C3 genotype and treatment outcomes[190, 193, 200].

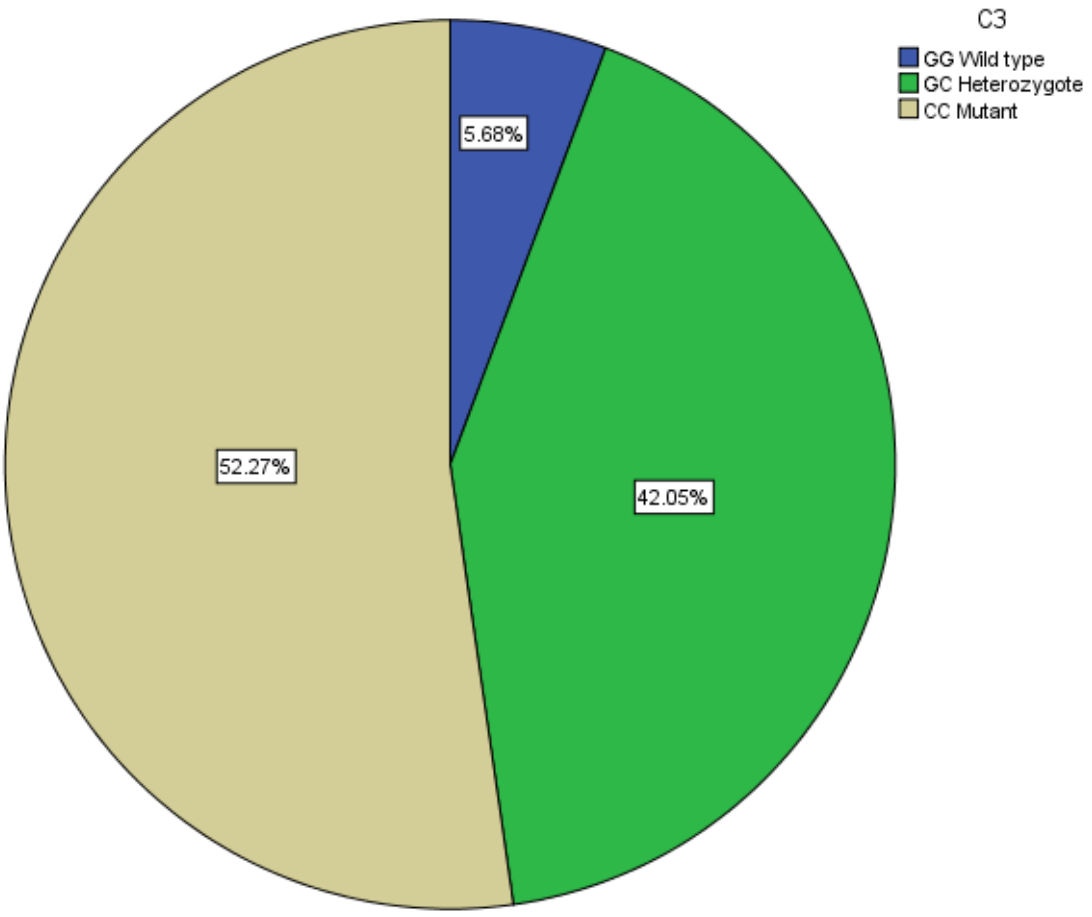

Figure 54 Distribution of the complement component 3 (C3) genotype (rs2230199) within the study population (n=99). 52.3% percent of the population were identified as CC genotype (mutant), 42.1% were GC (heterozygous) and 5.7% were GG (wild type).

A) Multiple Comparisons					
Dependent Variable: VAS change					
Bonferroni					
Visit	(I) C3	(J) C3	Sig.	95% Confidence Interval	
				Lower Bound	Upper Bound
2	GG Wild type	GC Heterozygote	1.000	-12.2203	12.2506
		CC Mutant	1.000	-16.5410	7.7953
	GC Heterozygote	GG Wild type	1.000	-12.2506	12.2203
		CC Mutant	0.087	-9.2159	0.4400
	CC Mutant	GG Wild type	1.000	-7.7953	16.5410
		GC Heterozygote	0.087	-0.4400	9.2159
3	GG Wild type	GC Heterozygote	1.000	-11.0314	9.6071
		CC Mutant	1.000	-11.8283	8.6967
	GC Heterozygote	GG Wild type	1.000	-9.6071	11.0314
		CC Mutant	1.000	-4.9255	3.2182
	CC Mutant	GG Wild type	1.000	-8.6967	11.8283
		GC Heterozygote	1.000	-3.2182	4.9255
4	GG Wild type	GC Heterozygote	1.000	-17.3614	10.8130
		CC Mutant	1.000	-17.4553	10.6674
	GC Heterozygote	GG Wild type	1.000	-10.8130	17.3614
		CC Mutant	1.000	-4.9494	4.7099
	CC Mutant	GG Wild type	1.000	-10.6674	17.4553
		GC Heterozygote	1.000	-4.7099	4.9494

A cont'd) Multiple Comparisons					
Dependent Variable: VAS change					
Bonferroni					
Visit	(I) C3	(J) C3	Sig.	95% Confidence Interval	
				Lower Bound	Upper Bound
6	GG Wild type	GC Heterozygote	0.287	-20.9137	3.8767
		CC Mutant	0.141	-22.4178	2.1782
	GC Heterozygote	GG Wild type	0.287	-3.8767	20.9137
		CC Mutant	1.000	-6.9236	3.7211
	CC Mutant	GG Wild type	0.141	-2.1782	22.4178
		GC Heterozygote	1.000	-3.7211	6.9236
7	GG Wild type	GC Heterozygote	0.051	-35.0392	0.0776
		CC Mutant	*0.047	-35.5357	-0.1916
	GC Heterozygote	GG Wild type	0.051	-0.0776	35.0392
		CC Mutant	1.000	-7.3144	6.5487
	CC Mutant	GG Wild type	0.047	0.1916	35.5357
		GC Heterozygote	1.000	-6.5487	7.3144

B) Multiple Comparisons					
Dependent Variable: CMT Change					
Bonferroni					
Visit	(I) C3	(J) C3	Sig.	95% Confidence Interval	
				Lower Bound	Upper Bound
2	GG Wild type	GC Heterozygote	0.304	-43.10	224.00
		CC Mutant	0.241	-36.83	229.39
	GC Heterozygote	GG Wild type	0.304	-224.00	43.10
		CC Mutant	1.000	-46.85	58.51
	CC Mutant	GG Wild type	0.241	-229.39	36.83
		GC Heterozygote	1.000	-58.51	46.85
4	GG Wild type	GC Heterozygote	0.832	-107.31	278.31
		CC Mutant	0.461	-79.53	303.96
	GC Heterozygote	GG Wild type	0.832	-278.31	107.31
		CC Mutant	1.000	-46.16	99.59
	CC Mutant	GG Wild type	0.461	-303.96	79.53
		GC Heterozygote	1.000	-99.59	46.16
7	GG Wild type	GC Heterozygote	0.256	-50.89	296.19
		CC Mutant	0.127	-27.68	316.76
	GC Heterozygote	GG Wild type	0.256	-296.19	50.89
		CC Mutant	1.000	-48.95	92.74
	CC Mutant	GG Wild type	0.127	-316.76	27.68
		GC Heterozygote	1.000	-92.74	48.95

Table 39 Tables examining the relationship between VAS (A) and CMT (B) change from baseline using one-way ANOVA analysis with Bonferroni correction for multiple comparisons. *-significant result with a p value <0.05

Chi-Square Tests				
Visit		Value	df	Asymp. Sig. (2-sided)
2	Pearson Chi-Square	2.615	2	0.270
	N of Valid Cases	75		
3	Pearson Chi-Square	3.139	2	0.208
	N of Valid Cases	76		
4	Pearson Chi-Square	0.790	2	0.674
	N of Valid Cases	67		
5	Pearson Chi-Square	0.578	2	0.749
	N of Valid Cases	64		
6	Pearson Chi-Square	0.238	2	0.888
	N of Valid Cases	63		
7	Pearson Chi-Square	1.456	2	0.483
	N of Valid Cases	56		

Table 40 Chi square analysis comparing C3 genotypes within the cohort and administered injections for active CNV. Df- degrees of freedom.

3.5.1.17.1 ***Summary***

The results demonstrated a significant difference (p=0.047) between the wild type and mutant alleles for change in VA score at visit 7 (Table 39). No significant correlation was established for administered injections (Table 40).

Figure 54 demonstrates the distribution of alleles within the study population.

3.5.1.18 The relationship of CX3/CR1 to treatment outcome measures (CMT, VAS and administered injections of anti VEGF)

CX3/CR1 genotypes have not been shown to predict CNV treatment response to anti VEGF therapy in an examination of the literature[201]. I examined whether the genotype was a significant biomarker in this section of the study.

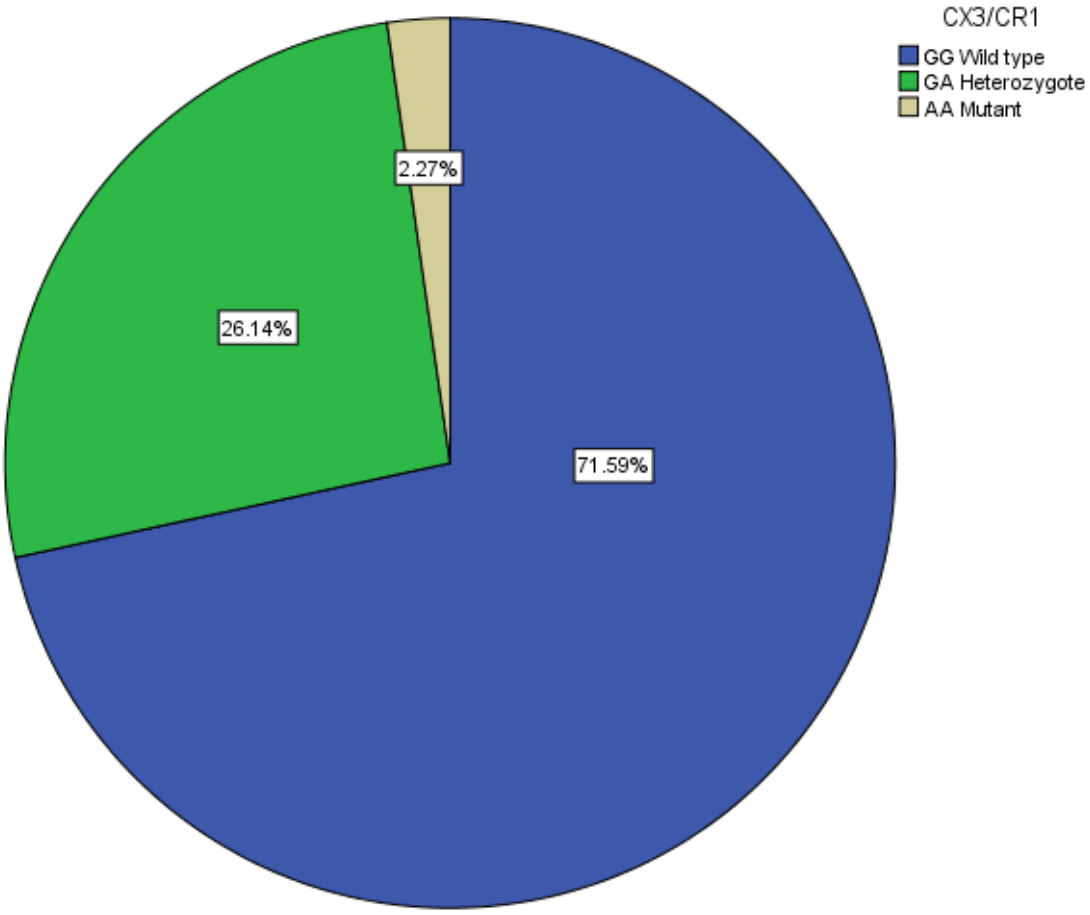

Figure 55 Distribution of the CX3C chemokine receptor (CX3/CR1) (rs3732378) within the study population (n=99). 2.3% percent of the population was identified as AA genotype (mutant), 26.1% were GA (heterozygous) and 71.6% were CC (wild type).

A) ANOVA			
VAS Change			
Visit		F	Sig.
2	Between Groups	0.066	0.936
3	Between Groups	0.381	0.685
4	Between Groups	0.147	0.863
5	Between Groups	0.686	0.508
6	Between Groups	0.155	0.857
7	Between Groups	0.217	0.806

B) ANOVA			
CMT Change			
Visit		F	Sig.
2	Between Groups	0.787	0.459
3	Between Groups	5.478	*0.023
4	Between Groups	0.529	0.592
5	Between Groups	0.904	0.411
6	Between Groups	2.870	0.097
7	Between Groups	0.000	0.988

Table 41 Tables examining the relationship between VAS (A) and CMT (B) change from baseline using one-way ANOVA analysis (without Bonferroni correction for multiple comparisons) F-F statistic, *-significant result with a p value <0.05

Chi-Square Tests				
Visit		Value	df	Asymp. Sig. (2-sided)
2	Pearson Chi-Square	0.837	2	0.658
	N of Valid Cases	76		
3	Pearson Chi-Square	11.538	2	*0.003
	N of Valid Cases	76		
4	Pearson Chi-Square	1.445	2	0.486
	N of Valid Cases	67		
5	Pearson Chi-Square	0.264	2	0.876
	N of Valid Cases	63		
6	Pearson Chi-Square	3.259	2	0.196
	N of Valid Cases	64		
7	Pearson Chi-Square	0.421	2	0.810
	N of Valid Cases	57		

Table 42 Chi square analysis comparing CX3/CR1 genotypes within the cohort and administered injections for active CNV. Df- degrees of freedom

3.5.1.18.1 ***Summary***

The results demonstrated a significant difference (p=0.023) between the wild type and mutant allele for the mean change in CMT at visit 3 (Table 41). There was also a significant association at visit 3 (p=0.003) for administered injections (Table 42). The

heterozygote allele was associated with a significantly lower number of injections at this visit. Bonferroni correction was not applied due to small sample subgroups.
Figure 55 demonstrates the distribution of alleles within the study population.

3.5.1.19 The relationship of APOE to treatment outcome measures (CMT, VAS and administered injections of anti VEGF)

There has been one study which showed an increase risk of treatment failure with the □4 variant as compared to the protective □2 allele[202] (odds ratio (OR) of 4.04 (95% confidence interval [CI], 1.11-14.70) for a 2-line gain in vision from baseline to month 3). Due to the limitations in sample size within subgroups, our study cannot conclusively state whether APOE is a potential biomarker of disease progression.

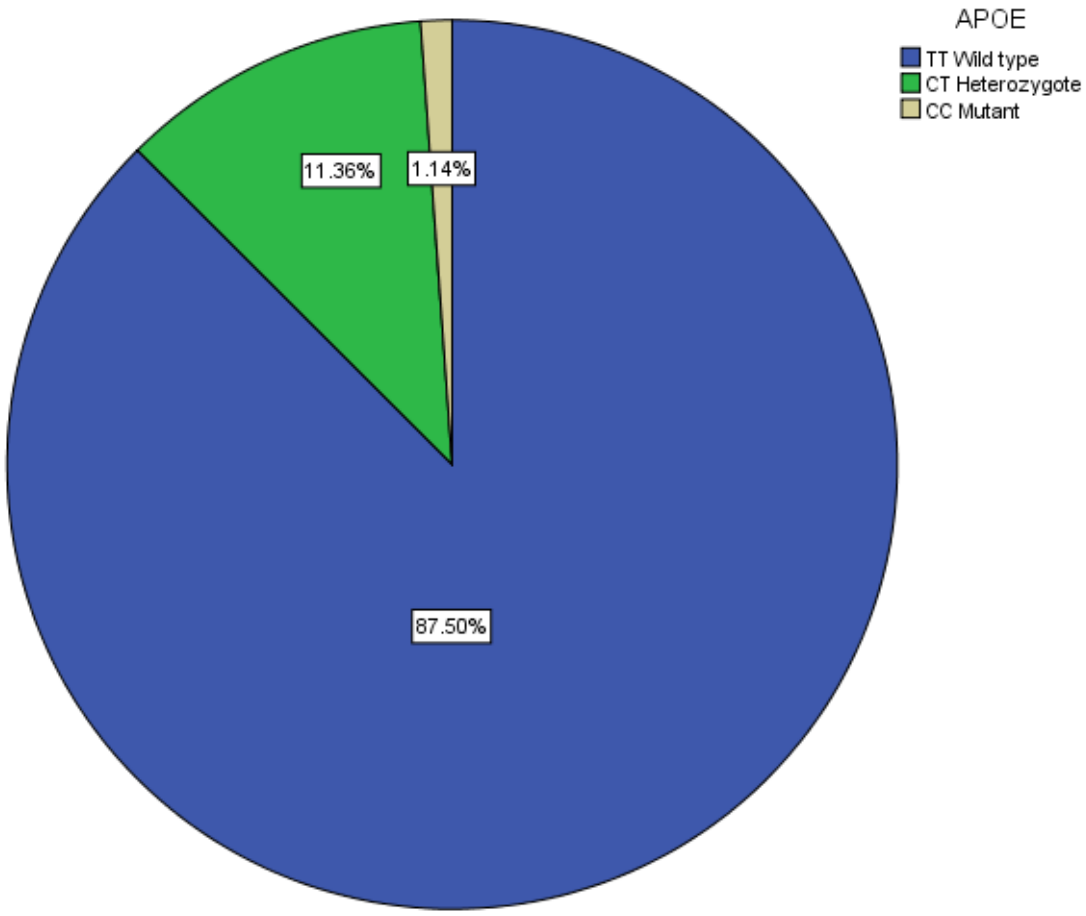

Figure 56 Distribution of the apolipoprotein E (APOE) (rs429358) within the study population (n=99). 1.1% percent of the population was identified as CC genotype (mutant), 11.4% were CT (heterozygous) and 87.5% were TT (wild type).

A) ANOVA				
APOE VAS Change				
Visit		df	F	Sig.
2	Between Groups	28	1.265	0.236
	Within Groups	45		
	Total	73		
3	Between Groups	31	2.431	*0.004
	Within Groups	42		
	Total	73		
4	Between Groups	38	1.031	0.473
	Within Groups	28		
	Total	66		
5	Between Groups	31	1.013	0.484
	Within Groups	32		
	Total	63		
6	Between Groups	35	0.783	0.755
	Within Groups	27		
	Total	62		
7	Between Groups	32	.	.
	Within Groups	19		
	Total	51		

B) ANOVA				
APOE CMT Change				
Visit		df	F	Sig.
2	Between Groups	64	2.854	*0.046
	Within Groups	9		
	Total	73		
3	Between Groups	48	.	.
	Within Groups	3		
	Total	51		
4	Between Groups	49	.	.
	Within Groups	5		
	Total	54		
5	Between Groups	51	0.882	0.649
	Within Groups	4		
	Total	55		
6	Between Groups	42	0.589	0.818
	Within Groups	3		
	Total	45		
7	Between Groups	46	.	.
	Within Groups	0		
	Total	46		

Table 43 Table examining the relationship between VAS (A) and CMT (B) change from baseline with one-way ANOVA analysis (without Bonferroni correction for multiple comparisons). The small sample size in some subgroups prevented ANOVA calculations. F-F statistic, *-significant result with a p value <0.05

3.5.1.19.1 *Summary*

The results demonstrated a significant difference (p=0.004) between the wild type and mutant allele for the mean change in VA score at visit 3 (Table 43). There was also a significant association at visit 2 (p=0.046) between wild and mutant alleles at visit 2 for CMT change. Chi square testing for an association with treatment was not applied due to small sample subgroups. Figure 56 demonstrates the distribution of alleles within the study population.

3.5.1.20 The relationship of complement factor B (CFB) to treatment outcome measures (CMT, VAS and administered injections of anti VEGF)

CFB was the only tested genotype in the cohort that produced multiple significant results for both change in CMT and VA between mutant and wild type alleles making it a strong candidate as a biomarker. Previous studies have found no association with CFB alleles and treatment outcomes[190, 193, 200].

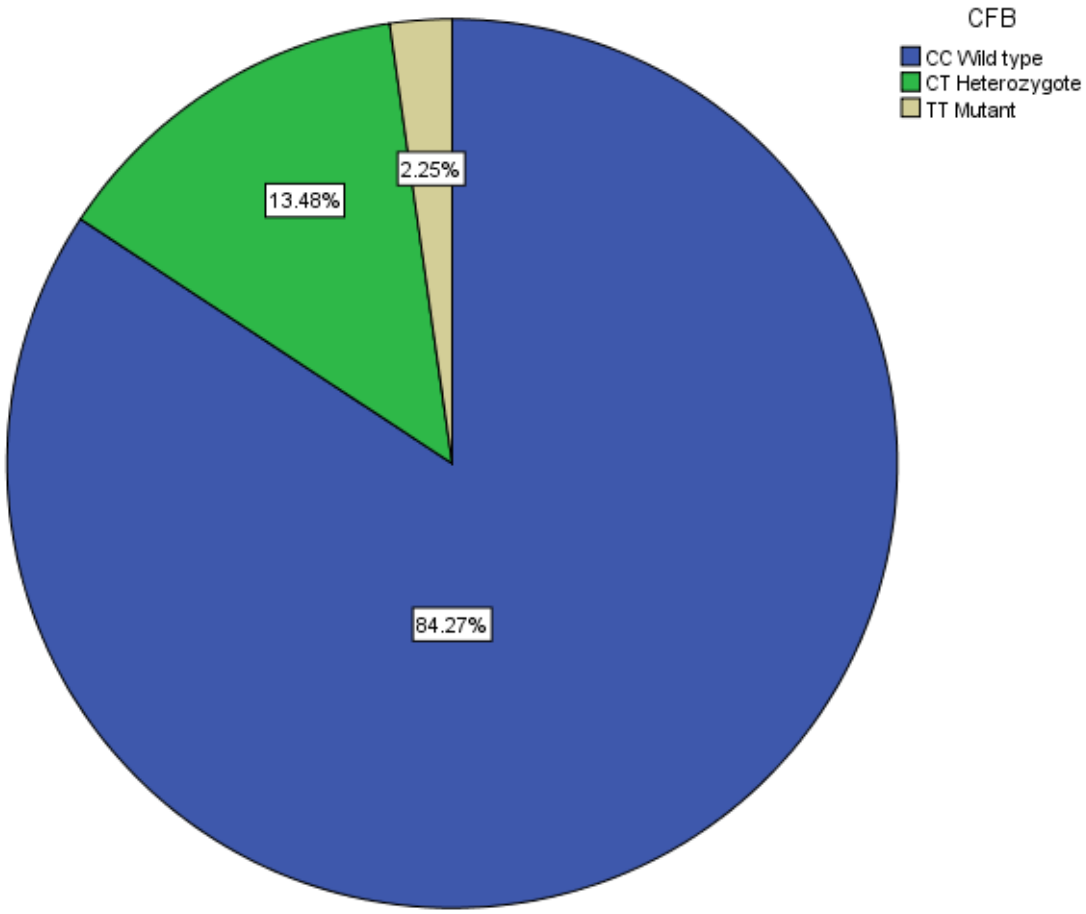

Figure 57 Distribution of the complement factor B (CFB) (rs641153) within the study population (n=99). 2.2% percent of the population was identified as TT genotype (mutant), 13.5% were CT (heterozygous) and 84.3% were CC (wild type).

A) ANOVA				
CFB VAS Change				
Visit		df	F	Sig.
2	Between Groups	28	0.671	0.868
	Within Groups	46		
	Total	74		
3	Between Groups	31	1.031	0.456
	Within Groups	43		
	Total	74		
4	Between Groups	37	3.060	*0.001
	Within Groups	29		
	Total	66		
5	Between Groups	30	0.490	0.974
	Within Groups	33		
	Total	63		
6	Between Groups	34	1.841	*0.049
	Within Groups	29		
	Total	63		
7	Between Groups	32	7.445	*0.000
	Within Groups	19		
	Total	51		

B) ANOVA		
CMT Change		
Visit	F	Sig.
2	0.996	0.374
3	8.844	*0.004
4	5.303	*0.008
5	1.744	0.185
6	0.911	0.345
7	1.250	0.297

Table 44 Tables examining the relationship between VAS (A) and CMT (B) change from baseline using one-way ANOVA analysis (without Bonferroni correction for multiple comparisons) F-F statistic, *-significant result with a p value <0.05

3.5.1.20.1 ***Summary***

CFB produced highly significant results for change in mean CMT at visits 3 and 4 (p=0.004 and 0.008 respectively) when wild type and mutant alleles were compared. There were also significant results for change in VA score at visits 4, 6 and 7 (p=0.001, 0.0049 and 0.000 respectively) when mutant and wild type alleles were compared (Table 44). There was no relationship by Chi-square testing for administered injections due to limited subgroup sample size. Figure 57 illustrates the distribution of alleles across the study population.

3.5.1.21 The relationship of C2 to treatment outcome measures (CMT, VAS and administered injections of anti VEGF)

Previous studies have found no association with C2 alleles and treatment outcomes[190, 193, 203]. I investigated whether C2 was a potential biomarker.

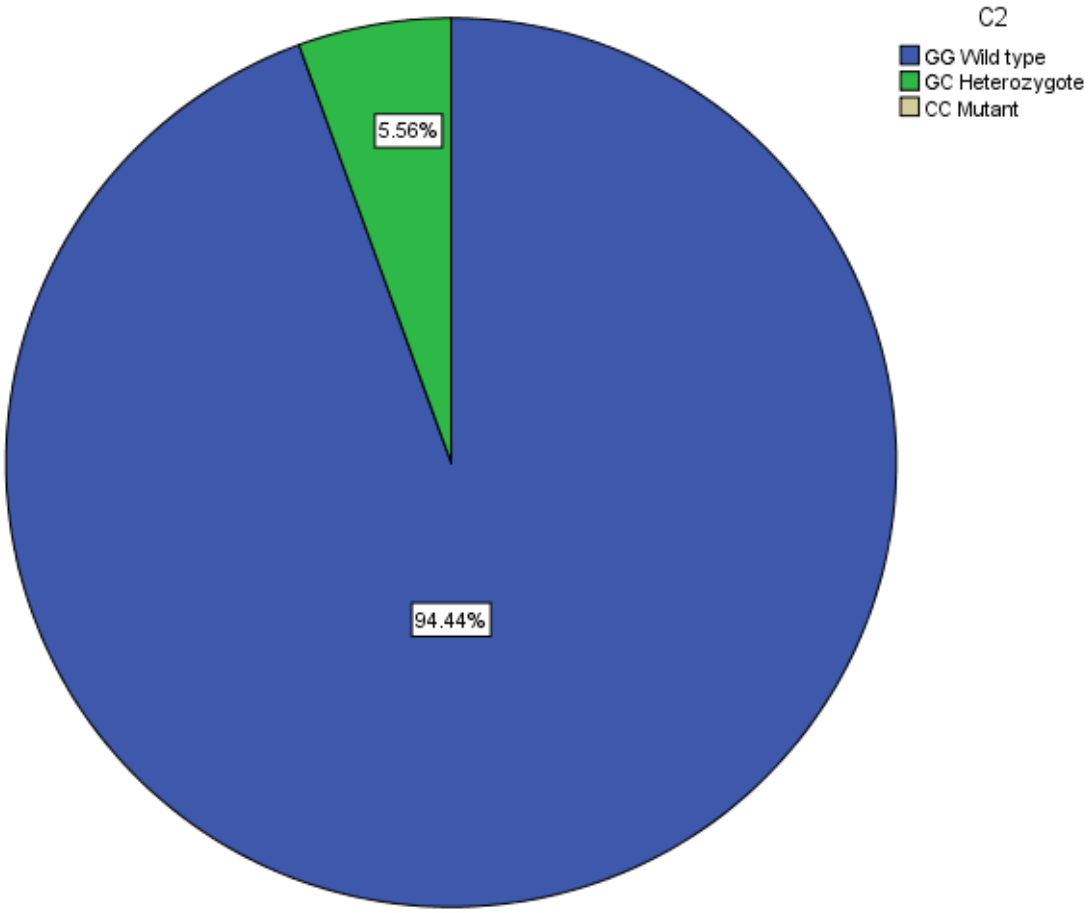

Figure 58 Distribution of the complement component 2 (C2) (rs9332739) within the study population (n=99). 5.6% percent of the population was identified as GC genotype (heterozygous) and 94.4% were GG (wild type).

A) ANOVA				
C2 VAS Change				
Visit		df	F	Sig.
2	Between Groups	28	0.380	0.996
	Within Groups	47		
	Total	75		
3	Between Groups	31	0.809	0.729
	Within Groups	44		
	Total	75		
4	Between Groups	38	0.428	0.993
	Within Groups	29		
	Total	67		
5	Between Groups	31	1.826	*0.046
	Within Groups	33		
	Total	64		
6	Between Groups	35	1.871	*0.044
	Within Groups	29		
	Total	64		
7	Between Groups	32	1.153	0376
	Within Groups	20		
	Total	52		

B) ANOVA		
CMT Change		
Visit	F	Sig.
2	0.224	0.637
3	0.046	0.832
4	0.261	0.612
5	0.411	0.524
6	0.006	0.938
7	0.691	0.410

Table 45 Tables examining the relationship between VAS (A) and CMT (B) change from baseline using one-way ANOVA analysis (without Bonferroni correction for multiple comparisons) F-F statistic, *-significant result with a p value <0.05

3.5.1.21.1 ***Summary***

C2 produced significant results for change in mean VA score at visits 5 and 6 (p=0.046 and 0.044 respectively) when wild type and mutant alleles were compared (Table 45). There was no relationship by Chi-square testing for administered injections due to limited subgroup sample size. Figure 58 illustrates the distribution of alleles across the study population. Limitations in sample size and the significant result in only one outcome measure prevent us from proposing C2 genotype as a reliable biomarker.

3.5.1.22 The relationship of TIMP3 to treatment outcome measures (CMT, VAS and administered injections of anti VEGF)

In this section I examined whether the genotype TIMP3 was a viable predictive biomarker of CNV response to treatment.

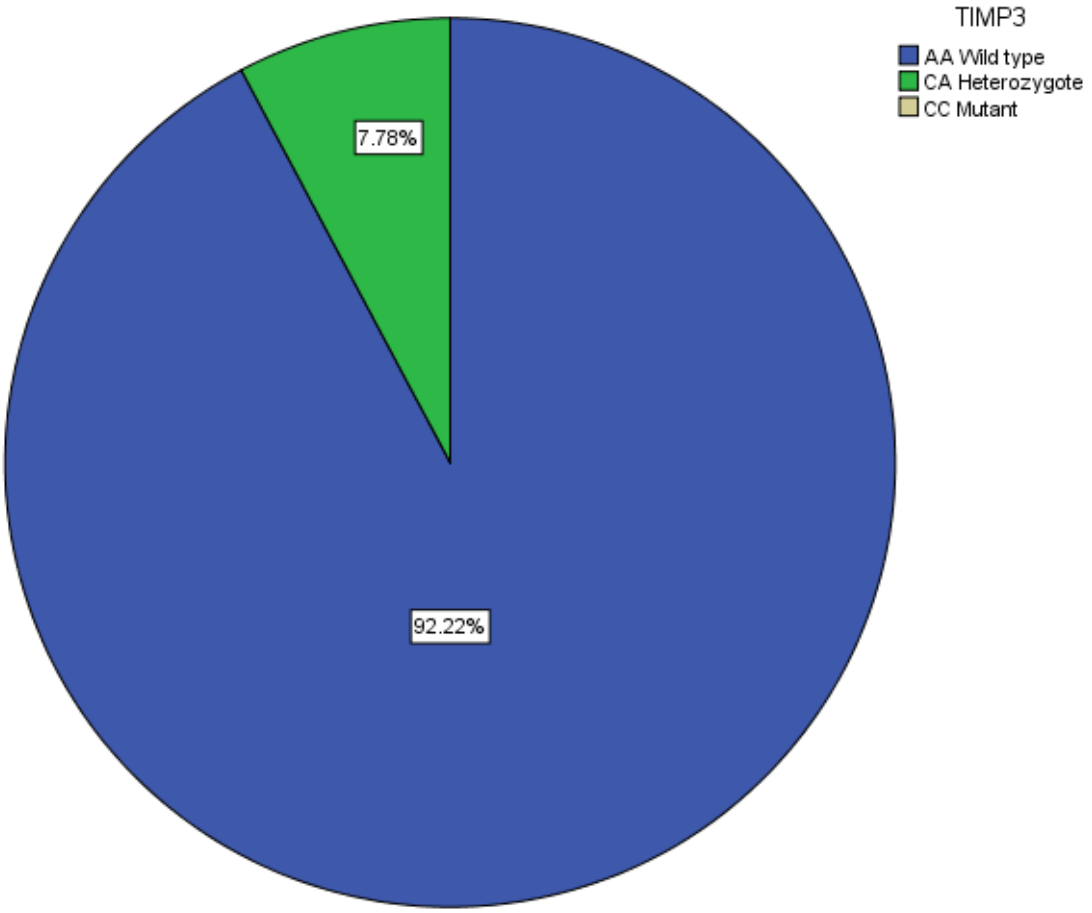

Figure 59 Distribution of the tissue inhibitor of metalloproteinases-3 (TIMP3) (rs9621532) within the study population (n=99). 7.8% percent of the population was identified as CA genotype (heterozygous) and 92.2% were AA (wild type).

A) ANOVA		
CMT Change		
Visit	F	Sig.
2	1.021	0.316
3	1.681	0.201
4	2.115	0.152
5	2.714	0.105
6	2.719	0.106
7	0.354	0.555

B) ANOVA		
VAS change		
Visit	F	Sig.
2	1.829	0.180
3	1.083	0.301
4	0.118	0.732
5	0.390	0.535
6	0.000	0.988
7	0.075	0.785

Table 46 Tables examining the relationship between VAS (B) and CMT (A) change from baseline using one-way ANOVA analysis (without Bonferroni correction for multiple comparisons) F-F statistic

3.5.1.22.1 ***Summary***

TIMP3 produced no significant results for change in mean VA score or CMT at any visit. There was no relationship by Chi-square testing for administered injections due to limited subgroup sample size.

Figure 59 illustrates the distribution of alleles across the study population.

3.5.2 Examination of inflammatory markers reported to be involved in AMD progression from early to advanced stages and their role in predicting the outcome of CNV treatment with ranvibizumab

This section explores known inflammatory markers associated with the development of AMD. It further investigates the hypothesis that C1Inh, via the classical complement pathway, influences CNV response to anti VEGF therapy.

3.5.2.1 The relationship of the activated classical complement pathway to treatment outcome measures (CMT, VAS and administered injections of anti VEGF)

The classical pathway is activated via C1q binding to CRP, immune complexes or components of microbial cell membranes. The majority of research has not implicated the classical pathway in wet AMD pathogenesis.

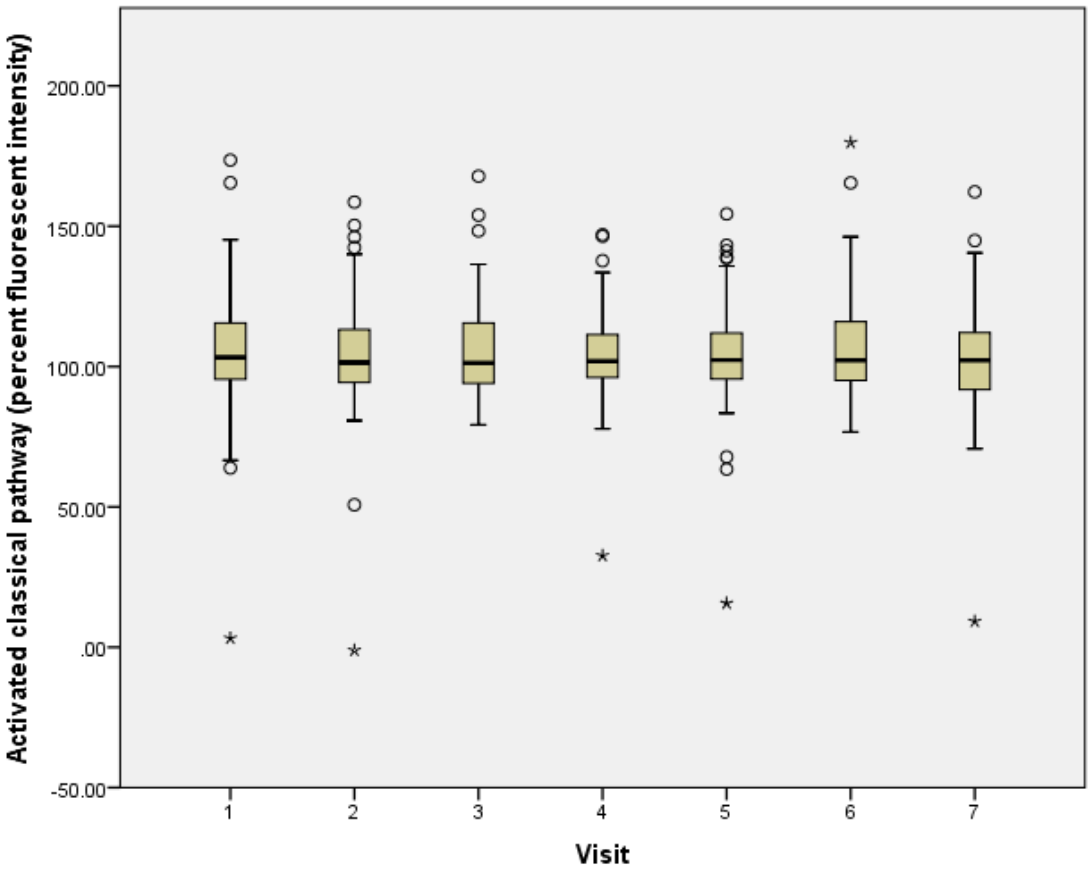

Figure 60 Figure demonstrating mean +/- 2 standard deviations of measured fluorescent activity within the classical pathway at each patient visit. o-values more than 1.5X interquartile (IQ) range, *-values more than 3X IQ range

A) Correlations				
Visit	Control Variables			CP
2	Gender & Age & BMI & Pack Years	CMT Change	Correlation	0.218
			Significance (2-tailed)	0.079
			df	64
3	Gender & Age & BMI & Pack Years	CMT Change	Correlation	-0.085
			Significance (2-tailed)	0.580
			df	43
4	Gender & Age & BMI & Pack Years	CMT Change	Correlation	-0.112
			Significance (2-tailed)	0.486
			df	39
5	Gender & Age & BMI & Pack Years	CMT Change	Correlation	0.109
			Significance (2-tailed)	0.472
			df	44
6	Gender & Age & BMI & Pack Years	CMT Change	Correlation	0.031
			Significance (2-tailed)	0.859
			df	33
7	Gender & Age & BMI & Pack Years	CMT Change	Correlation	0.016
			Significance (2-tailed)	0.933
			df	28

B) Correlations				
Visit	Control Variables			VAS change
2	Gender & Age & BMI & Pack Years	CP	Correlation	-0.032
			Significance (2-tailed)	0.797
			df	65
3	Gender & Age & BMI & Pack Years	CP	Correlation	0.028
			Significance (2-tailed)	0.829
			df	61
4	Gender & Age & BMI & Pack Years	CP	Correlation	0.027
			Significance (2-tailed)	0.840
			df	55
5	Gender & Age & BMI & Pack Years	CP	Correlation	-0.165
			Significance (2-tailed)	0.234
			df	52
6	Gender & Age & BMI & Pack Years	CP	Correlation	-0.041
			Significance (2-tailed)	0.770
			df	50
7	Gender & Age & BMI & Pack Years	CP	Correlation	0.124
			Significance (2-tailed)	0.444
			df	38

Table 47 Tables comparing change in CMT (CMT change) (A) in microns and VA score (VAS change) (B) in letters from baseline utilising Pearson's correlation coefficient (correlation) and controlling for gender, BMI, pack years and age. Df = degrees of freedom, CP- classical complement pathway.

Independent Samples Test						
Visit		t-test for Equality of Means				
		t	df	Sig. (2-tailed)	95% Confidence Interval of the Difference	
					Lower	Upper
1	CP	0.297	3.679	0.783	-20.22872	24.88280
2	CP	-7.139	10.574	*0.000	-26.77421	-14.10801
3	CP	-0.250	22.245	0.805	-12.81550	10.05954
4	CP	0.503	42.998	0.618	-6.19337	10.30837
5	CP	0.511	10.978	0.620	-14.59275	23.41180
6	CP	1.718	16.859	0.104	-2.55786	24.89818
7	CP	-0.208	28.658	0.837	-12.95264	10.56008

Table 48 Independent samples t Test establishing correlations between injections administered and classical pathway activation at each visit. t- t Test statistic, df-degrees of freedom, CP- classical complement pathway, *-significant result with a p value <0.05

3.5.2.1.1 ***Summary***

Figure 60 provides a summary of the mean level of classical complement pathway activation at each visit (as a percentage fluorescent intensity versus the positive control). There was no statistically significant difference in means ($p>0.05$) between visits.

Table 47 demonstrated no significant relationship between the level of classical complement pathway activation and the change in CMT and VA score from baseline at each visit correcting for gender, age, BMI and pack years. Table 48 revealed a highly significant difference in mean percentage activity between patients receiving and not receiving injections. However, only 2 patients received injections at visit 2 compared to 78 who did not. This is likely a statistical error.

3.5.2.2 The relationship of the activated alternative complement pathway to treatment outcome measures (CMT, VAS and administered injections of anti VEGF)

The alternative complement pathway is activated via spontaneous hydrolysis of C3. The pathway is regulated via a group of intermediary components including CFH, CFI and CFB. It ultimately leads to formation of the MAC. The majority of research has strongly implicated the alternative complement pathway in AMD pathogenesis[56, 204] and elevated levels of the components have been detected in the blood of patients with advanced AMD[205]. I examine its role as a potential biomarker.

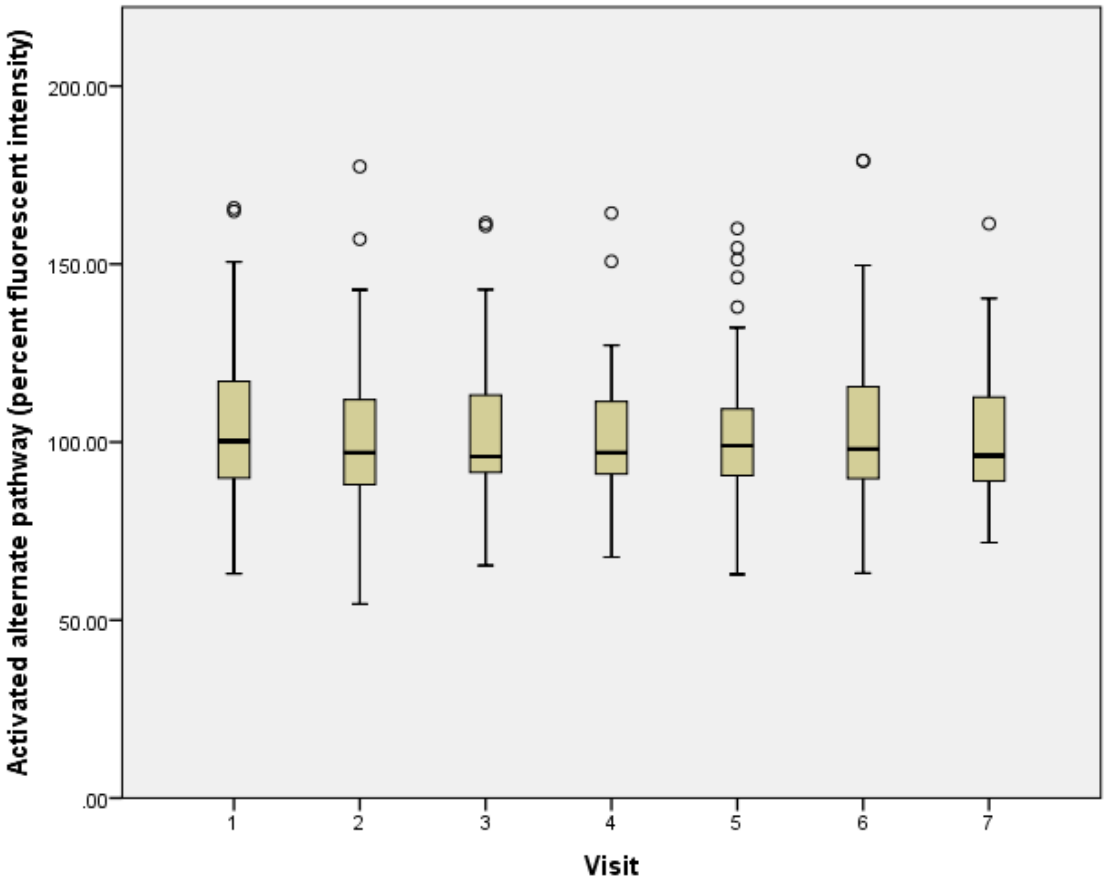

Figure 61 Figure demonstrating mean+/- 2 standard deviations of measured fluorescent activity within the alternative pathway at each patient visit. . o-values more than 1.5X interquartile (IQ) range

A) Correlations				
Visit	Control Variables			AP
2	Gender & Age & BMI & Pack Years	VAS change	Correlation	0.095
			Significance (2-tailed)	0.444
			df	65
3	Gender & Age & BMI & Pack Years	VAS change	Correlation	0.156
			Significance (2-tailed)	0.223
			df	61
4	Gender & Age & BMI & Pack Years	VAS change	Correlation	0.097
			Significance (2-tailed)	0.477
			df	54
5	Gender & Age & BMI & Pack Years	VAS change	Correlation	0.093
			Significance (2-tailed)	0.508
			df	51
6	Gender & Age & BMI & Pack Years	VAS change	Correlation	0.071
			Significance (2-tailed)	0.619
			df	50
7	Gender & Age & BMI & Pack Years	VAS change	Correlation	0.051
			Significance (2-tailed)	0.757
			df	38

B) Correlations				
Visit	Control Variables			CMT Change
2	Gender & Age & BMI & Pack Years	AP	Correlation	0.124
			Significance (2-tailed)	0.322
			df	64
3	Gender & Age & BMI & Pack Years	AP	Correlation	-0.104
			Significance (2-tailed)	0.497
			df	43
4	Gender & Age & BMI & Pack Years	AP	Correlation	-0.100
			Significance (2-tailed)	0.537
			df	38
5	Gender & Age & BMI & Pack Years	AP	Correlation	-0.147
			Significance (2-tailed)	0.335
			df	43
6	Gender & Age & BMI & Pack Years	AP	Correlation	-0.021
			Significance (2-tailed)	0.906
			df	33
7	Gender & Age & BMI & Pack Years	AP	Correlation	-0.085
			Significance (2-tailed)	0.654
			df	28

Table 49 Tables comparing change in CMT (CMT change) (B) in microns and VA score (VAS change) (A) in letters from baseline utilising Pearson's correlation coefficient (correlation) and controlling for gender, BMI, pack years and age. Df=degrees of freedom, AP- alternative complement pathway.

Independent Samples Test						
Visit		t-test for Equality of Means				
		t	df	Sig. (2-tailed)	95% Confidence Interval of the Difference	
					Lower	Upper
1	AP	-0.576	3.218	0.602	-43.84486	29.96928
2	AP	-2.475	1.049	0.235	-194.89486	125.32710
3	AP	0.509	23.611	0.616	-8.30657	13.73681
4	AP	-0.155	52.968	0.878	-7.82999	6.70822
5	AP	1.084	10.202	0.303	-11.21112	32.57548
6	AP	1.731	18.232	0.100	-2.65244	27.62557
7	AP	0.222	27.765	0.826	-9.25373	11.50114

Table 50 Independent samples t Test establishing correlations between injections administered and alternative pathway activation at each visit. t- t Test statistic, df- degrees of freedom, AP- Alternative complement pathway

3.5.2.2.1 ***Summary***

Figure 61 provides a summary of the mean level of alternative complement pathway activation at each visit (as a percentage fluorescent intensity versus the positive control). There was no statistically significant difference in means ($p>0.05$) between visits.

Table 49 demonstrated no significant relationship between the level of classical complement pathway activation and the change in CMT and VA score from baseline at each visit correcting for gender, age, BMI and pack years. Table 50 revealed no significant difference in mean percentage activity between patients receiving and not receiving injections.

3.5.2.3 The relationship of eotaxin concentration to treatment outcome measures (CMT, VAS and administered injections of anti VEGF)

Eotaxin 2 (CCl24) is a chemokine important in eosinophil trafficking to sites of chronic inflammation[206]. It has been implicated as a biomarker of disease progression in a case control study comparing subjects with early and advanced AMD and age-matched controls[207]. The case control study demonstrated higher levels of serum eotaxin in patients with advanced AMD compared to early AMD and controls. My significant result was found at only 1 visit and would need further investigation to determine whether a correlation exists.

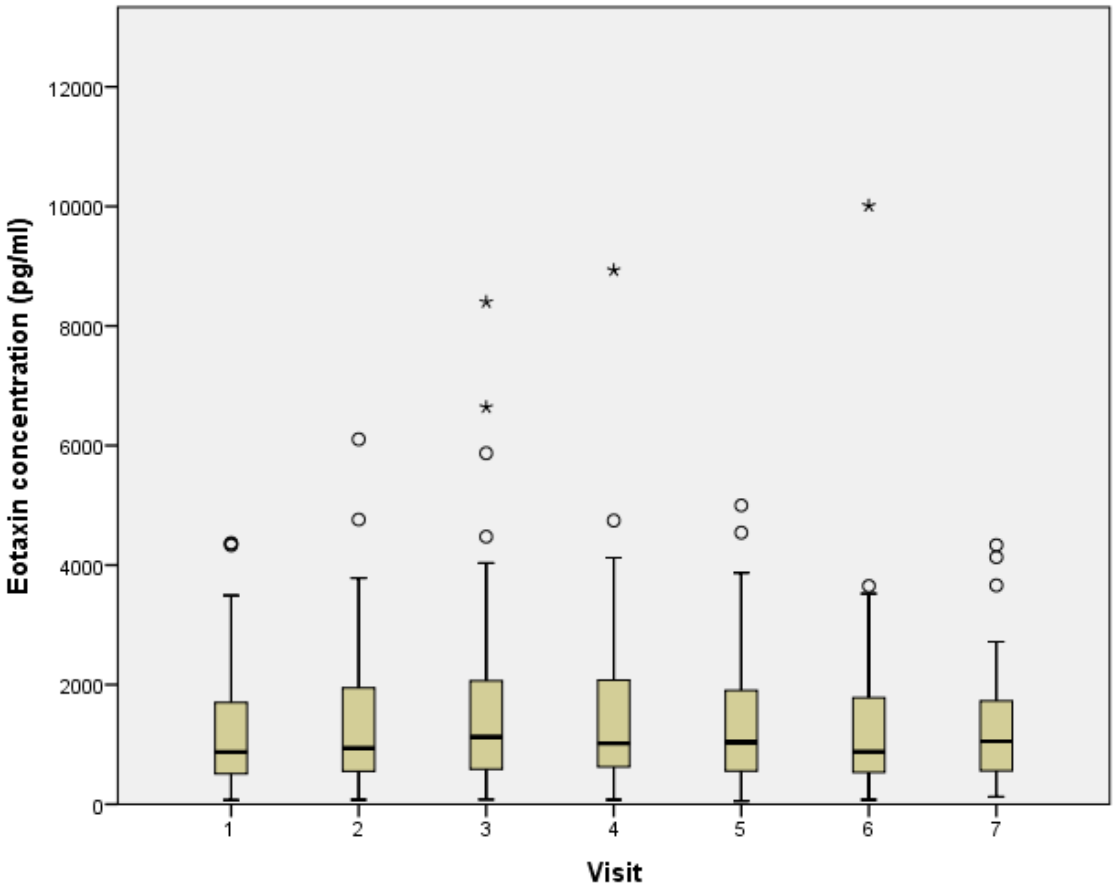

Figure 62 Figure demonstrating mean +/- 2 standard deviation of eotaxin concentration. o-values more than 1.5X interquartile (IQ) range, *-values more than 3X IQ range

A) Correlations				
Visit	Control Variables			Eotaxin
2	Gender & Age & BMI & Pack Years	CMT Change	Correlation	-0.138
			Significance (2-tailed)	0.278
			df	62
3	Gender & Age & BMI & Pack Years	CMT Change	Correlation	-0.071
			Significance (2-tailed)	0.624
			df	48
4	Gender & Age & BMI & Pack Years	CMT Change	Correlation	-0.456
			Significance (2-tailed)	*0.002
			df	40
5	Gender & Age & BMI & Pack Years	CMT Change	Correlation	-0.114
			Significance (2-tailed)	0.424
			df	49
6	Gender & Age & BMI & Pack Years	CMT Change	Correlation	-0.190
			Significance (2-tailed)	0.253
			df	36
7	Gender & Age & BMI & Pack Years	CMT Change	Correlation	-0.059
			Significance (2-tailed)	0.749
			df	30

B) Correlations				
Visit	Control Variables			VAS change
2	Gender & Age & BMI & Pack Years	Eotaxin	Correlation	-0.198
			Significance (2-tailed)	0.117
			df	62
3	Gender & Age & BMI & Pack Years	Eotaxin	Correlation	-0.172
			Significance (2-tailed)	0.171
			df	63
4	Gender & Age & BMI & Pack Years	Eotaxin	Correlation	0.061
			Significance (2-tailed)	0.647
			df	56
5	Gender & Age & BMI & Pack Years	Eotaxin	Correlation	0.034
			Significance (2-tailed)	0.797
			df	58
6	Gender & Age & BMI & Pack Years	Eotaxin	Correlation	-0.110
			Significance (2-tailed)	0.427
			df	52
7	Gender & Age & BMI & Pack Years	Eotaxin	Correlation	-0.115
			Significance (2-tailed)	0.469
			df	40

Table 51 Tables comparing change in CMT (CMT Change) (A) in microns and VA score (VAS change) (B) in letters from baseline utilising Pearson's correlation coefficient (correlation) and controlling for gender, BMI, pack years and age. Df=degrees of freedom, *-significant result with a p value <0.05

Independent Samples Test						
Visit		t-test for Equality of Means				
		t	df	Sig. (2-tailed)	95% Confidence Interval of the Difference	
					Lower	Upper
1	Eotaxin	-0.779	3.488	0.485	-1713.698	996.449
2	Eotaxin	0.624	1.030	0.642	-12199.482	13555.065
3	Eotaxin	-0.501	18.984	0.622	-997.174	612.197
4	Eotaxin	-2.531	61.511	*0.014	-1281.845	-150.520
5	Eotaxin	0.344	15.868	0.735	-614.155	852.054
6	Eotaxin	-0.115	26.194	0.909	-792.904	708.727
7	Eotaxin	-1.417	22.004	0.171	-958.623	180.430

Table 52 Independent samples t Test establishing correlations between injections administered and eotaxin concentrations at each visit. t- t Test statistic, df-degrees of freedom, *-significant result with a p value <0.05

3.5.2.3.1 ***Summary***

Figure 62 provides a summary of the mean level of eotaxin concentration at each visit. There was no statistically significant difference (p>0.05) between visits when measured by ANOVA. Table 51 demonstrated no significant relationship between the concentration of eotaxin and the change in VA score. There was a significant relationship for CMT change from baseline and visit 4 correcting for gender, age, BMI and pack years (p=0.002) with a correlation coefficient of -0.456.

Table 52 also revealed a significant difference in mean concentrations of eotaxin between patients receiving and not receiving injections (p=0.014) with a t test statistic of -2.531. This suggests patients with a lower concentration were associated with clinical activity requiring an anti VEGF injection and had a higher CMT.

3.5.2.4 The relationship of IL-1□ concentration to treatment outcome measures (CMT, VAS and administered injections of anti VEGF)

IL-1□ is a key component of drusen[72]. It has therefore been implicated in the progression of early to advanced AMD[208, 209]. There are no studies that demonstrate a relationship between systemic levels and response to treatment. Our study would suggest local production may have a greater impact.

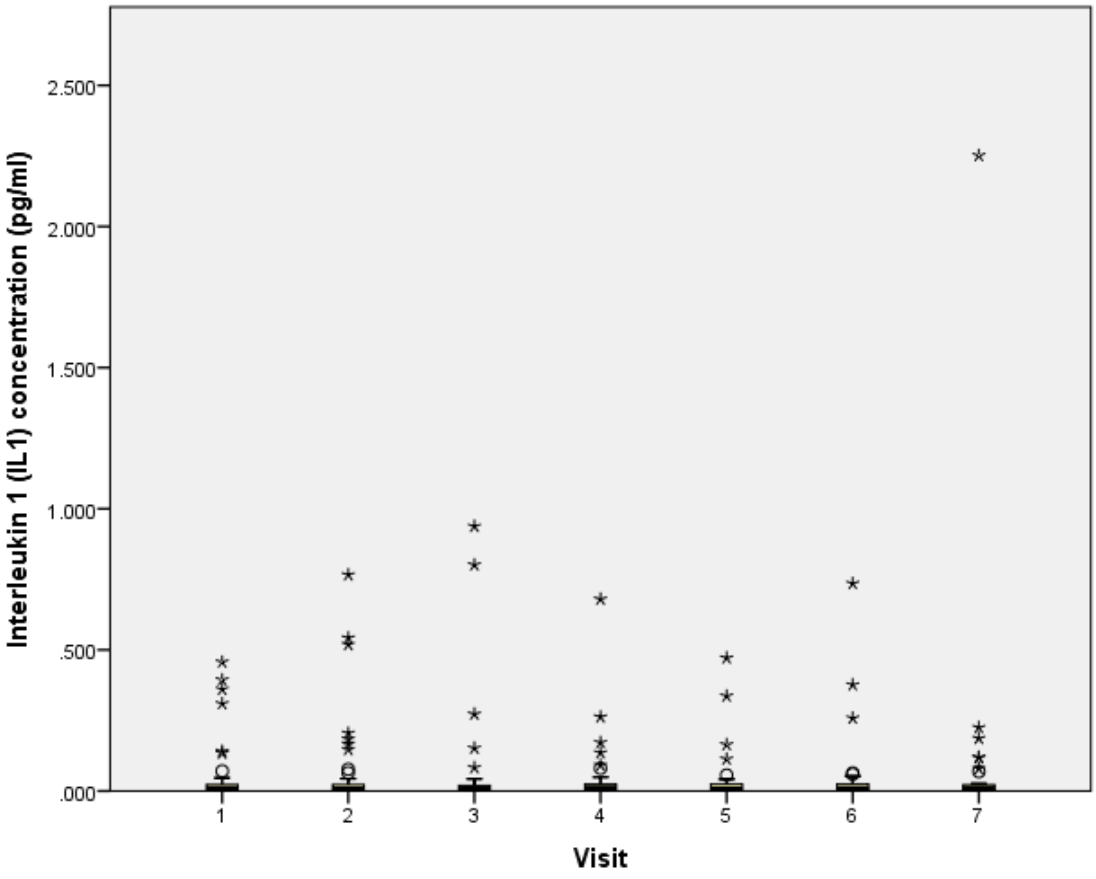

Figure 63 Figure demonstrating mean+/- 2 standard deviations of measured IL1 at each patient visit. o-values more than 1.5X interquartile (IQ) range, *-values more than 3X IQ range

A) Correlations				
Visit	Control Variables			IL1
2	Gender & Age & BMI & Pack Years	VAS change	Correlation	-0.170
			Significance (2-tailed)	0.295
			df	38
3	Gender & Age & BMI & Pack Years	VAS change	Correlation	0.034
			Significance (2-tailed)	0.824
			df	44
4	Gender & Age & BMI & Pack Years	VAS change	Correlation	0.093
			Significance (2-tailed)	0.527
			df	46
5	Gender & Age & BMI & Pack Years	VAS change	Correlation	0.047
			Significance (2-tailed)	0.793
			df	32
6	Gender & Age & BMI & Pack Years	VAS change	Correlation	0.381
			Significance (2-tailed)	*0.024
			df	33
7	Gender & Age & BMI & Pack Years	VAS change	Correlation	0.089
			Significance (2-tailed)	0.658
			df	25

B) Correlations				
Visit	Control Variables			CMT Change
2	Gender & Age & BMI & Pack Years	IL1	Correlation	0.098
			Significance (2-tailed)	0.552
			df	37
3	Gender & Age & BMI & Pack Years	IL1	Correlation	-0.211
			Significance (2-tailed)	0.240
			df	31
4	Gender & Age & BMI & Pack Years	IL1	Correlation	-0.047
			Significance (2-tailed)	0.786
			df	34
5	Gender & Age & BMI & Pack Years	IL1	Correlation	-0.006
			Significance (2-tailed)	0.976
			df	28
6	Gender & Age & BMI & Pack Years	IL1	Correlation	0.081
			Significance (2-tailed)	0.720
			df	20
7	Gender & Age & BMI & Pack Years	IL1	Correlation	-0.037
			Significance (2-tailed)	0.874
			df	19

Table 53 Tables comparing change in CMT (CMT Change) (B) in microns and VA score (VAS Change) (A) in letters from baseline utilising Pearson's correlation coefficient (correlation) and controlling for gender, BMI, pack years and age. Df=degrees of freedom, *-significant result with a p value <0.05.

Independent Samples Test						
Visit		t-test for Equality of Means				
		t	df	Sig. (2-tailed)	95% Confidence Interval of the Difference	
					Lower	Upper
1	IL1	0.690	2.076	0.559	-0.073911	0.103345
3	IL1	0.574	13.459	0.575	-0.116063	0.200445
4	IL1	0.772	15.898	0.451	-0.057623	0.123598
5	IL1	-1.480	38.940	0.147	-0.056724	0.008781
6	IL1	1.127	9.319	0.288	-0.083766	0.251958
7	IL1	-1.270	28.066	0.214	-0.256384	0.060121

Table 54 Independent samples t Test establishing correlations between injections administered and IL1 concentrations at each visit. t- t Test statistic, df-degrees of freedom

3.5.2.4.1 ***Summary***

Figure 63 provides a summary of the mean level of IL-1 concentration at each visit. There was no statistically significant difference ($p>0.05$) between visits when measured by ANOVA.

Table 53 demonstrated no significant relationship between the concentration of IL-1 and the change in CMT. There was a significant relationship for VA score change from baseline and visit 6 correcting for gender, age, BMI and pack years ($p=0.024$) with a correlation coefficient of 0.381. Table 54 also revealed no significant difference in mean concentrations of IL-1 between patients receiving and not receiving injections. This result is likely a statistical anomaly.

3.5.2.5 The relationship of IL-2 concentration to treatment outcome measures (CMT, VAS and administered injections of anti VEGF)

This section examined the role of IL-2 as a potential biomarker for CNV response to anti VEGF therapy.

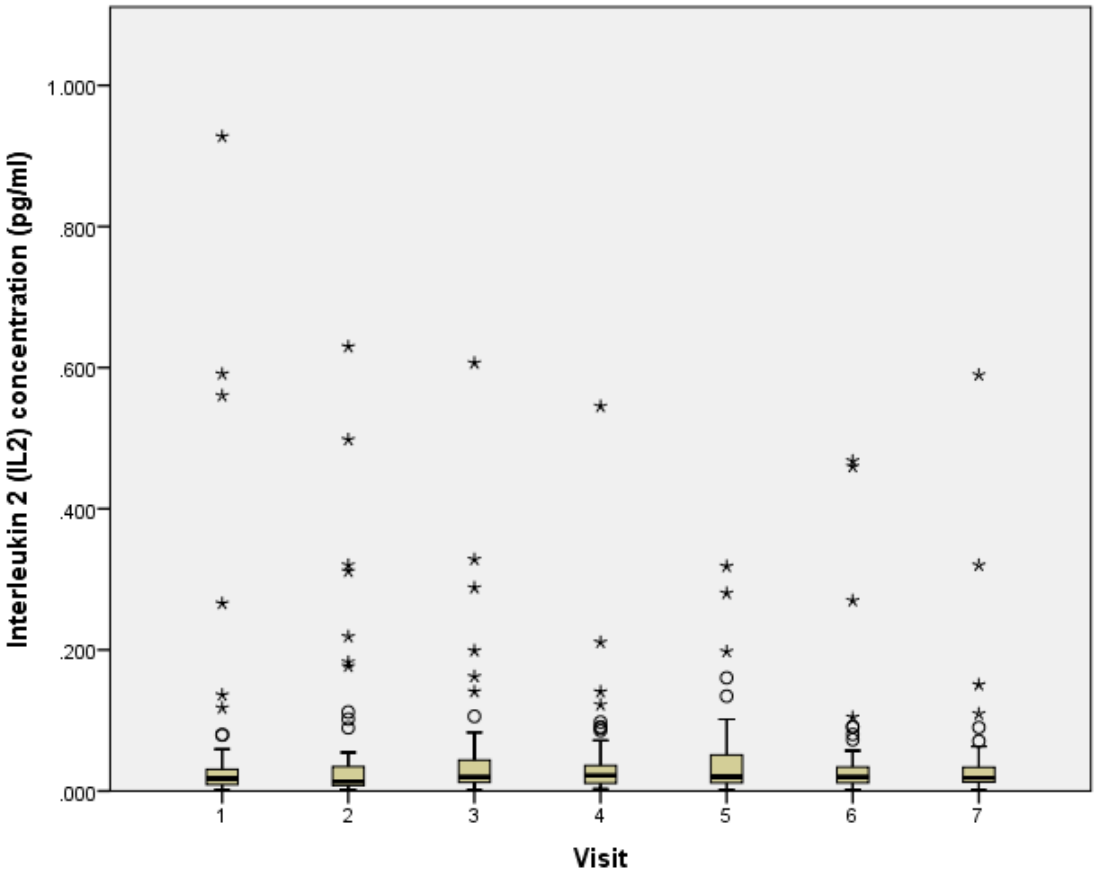

Figure 64 Figure demonstrating mean+/- 2 standard deviations of measured IL2 at each patient visit. o-values more than 1.5X interquartile (IQ) range, *-values more than 3X IQ range

A) Correlations				
Visit	Control Variables			IL2
2	Gender & Age & BMI & Pack Years	CMT Change	Correlation	-0.047
			Significance (2-tailed)	0.702
			df	66
3	Gender & Age & BMI & Pack Years	CMT Change	Correlation	-0.057
			Significance (2-tailed)	0.695
			df	48
4	Gender & Age & BMI & Pack Years	CMT Change	Correlation	-0.084
			Significance (2-tailed)	0.593
			df	41
5	Gender & Age & BMI & Pack Years	CMT Change	Correlation	-0.027
			Significance (2-tailed)	0.850
			df	48
6	Gender & Age & BMI & Pack Years	CMT Change	Correlation	-0.057
			Significance (2-tailed)	0.738
			df	35
7	Gender & Age & BMI & Pack Years	CMT Change	Correlation	-0.069
			Significance (2-tailed)	0.709
			df	30

B) Correlations				
Visit	Control Variables			VAS change
2	Gender & Age & BMI & Pack Years	IL2	Correlation	-0.045
			Significance (2-tailed)	0.716
			df	67
3	Gender & Age & BMI & Pack Years	IL2	Correlation	-0.033
			Significance (2-tailed)	0.790
			df	67
4	Gender & Age & BMI & Pack Years	IL2	Correlation	0.021
			Significance (2-tailed)	0.875
			df	58
5	Gender & Age & BMI & Pack Years	IL2	Correlation	-0.047
			Significance (2-tailed)	0.728
			df	56
6	Gender & Age & BMI & Pack Years	IL2	Correlation	0.139
			Significance (2-tailed)	0.313
			df	53
7	Gender & Age & BMI & Pack Years	IL2	Correlation	0.249
			Significance (2-tailed)	0.111
			df	40

Table 55 Tables comparing change in CMT (CMT Change) (A) in microns and VA score (VAS Change) (B) in letters from baseline utilising Pearson's correlation coefficient (correlation) and controlling for gender, BMI, pack years and age. Df = degrees of freedom.

Independent Samples Test						
Visit		t-test for Equality of Means				
		t	df	Sig. (2-tailed)	95% Confidence Interval of the Difference	
					Lower	Upper
1	IL2	2.301	38.846	0.027	0.004668	0.072672
2	IL2	-2.134	81.705	*0.036	-0.046491	-0.001630
3	IL2	-1.295	68.420	0.200	-0.047699	0.010153
4	IL2	-0.484	69.514	0.630	-0.032158	0.019606
5	IL2	-0.709	20.942	0.486	-0.042937	0.021103
6	IL2	0.951	15.958	0.356	-0.040085	0.105327
7	IL2	-1.985	43.249	0.053	-0.062953	0.000489

Table 56 Independent samples t Test establishing correlations between injections administered and IL2 concentrations at each visit. t- t Test statistic, df-degrees of freedom, *-significant result with a p value <0.05

3.5.2.5.1 ***Summary***

Figure 64 provides a summary of the mean level of IL-2 concentration at each visit. There was no statistically significant difference (p>0.05) between visits when measured by ANOVA.

Table 55 demonstrated no significant relationship between IL-2 concentration and the change in CMT and VA score from baseline at each visit correcting for gender, age, BMI and pack years. Table 56 revealed a significant difference in mean IL-2 concentration between patients receiving and not receiving an injection at Visit 2. However, only 2 patients received injections at this visit compared to 78 who did not. This significant result is likely a statistical error due to the small group size.

3.5.2.6 The relationship of IL-6 concentration to treatment outcome measures (CMT, VAS and administered injections of anti VEGF)

Seddon *et al.* concluded that an elevated level of serum IL-6 was a marker to predict progression of early AMD[210] to advanced AMD in a prospective case controlled study

using age-matched controls. Our study did not however provide evidence of a significant correlation when between serum levels and treatment outcome measures.

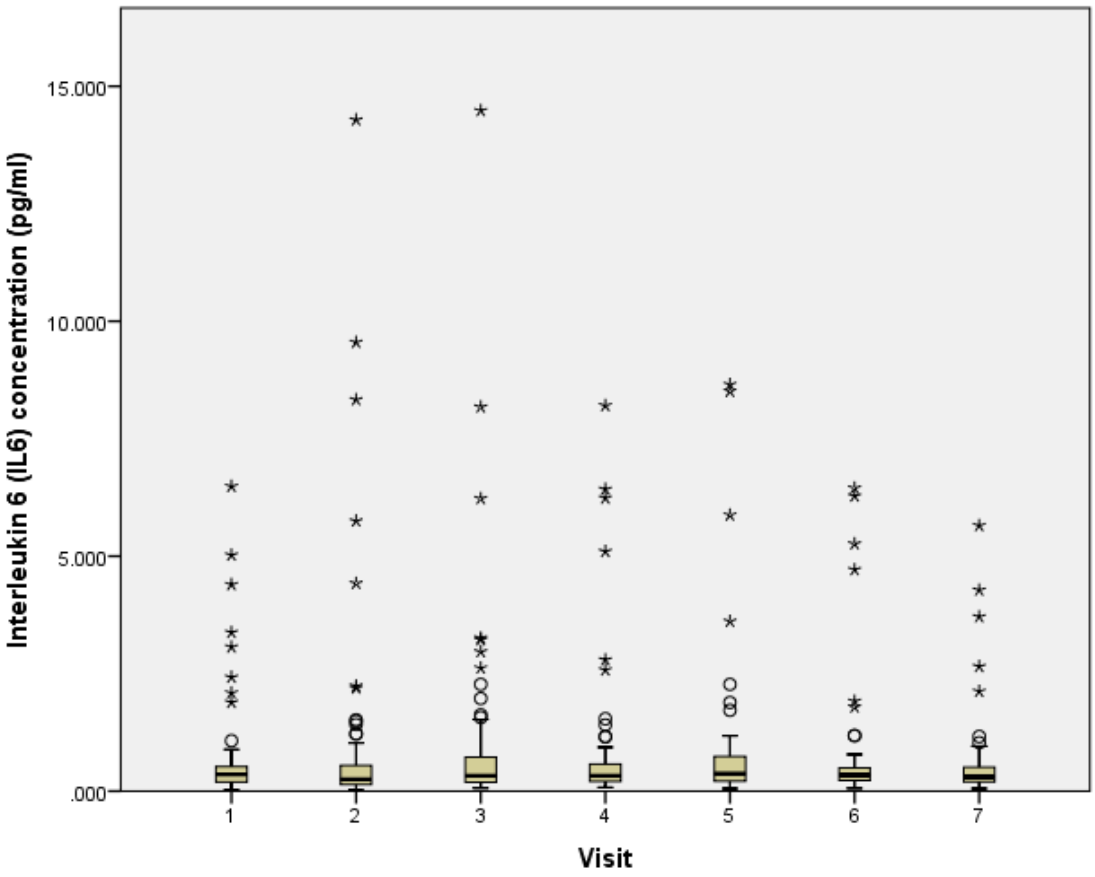

Figure 65 Figure demonstrating mean+/- 2 standard deviations of measured IL6 at each patient visit. o-values more than 1.5X interquartile (IQ) range, *-values more than 3X IQ range

A) Correlations				
Visit	Control Variables			IL6
2	Gender & Age & BMI & Pack Years	VAS change	Correlation	0.058
			Significance (2-tailed)	0.636
			df	67
3	Gender & Age & BMI & Pack Years	VAS change	Correlation	0.033
			Significance (2-tailed)	0.787
			df	68
4	Gender & Age & BMI & Pack Years	VAS change	Correlation	0.143
			Significance (2-tailed)	0.271
			df	59
5	Gender & Age & BMI & Pack Years	VAS change	Correlation	0.001
			Significance (2-tailed)	0.995
			df	58
6	Gender & Age & BMI & Pack Years	VAS change	Correlation	0.144
			Significance (2-tailed)	0.291
			df	54
7	Gender & Age & BMI & Pack Years	VAS change	Correlation	0.347
			Significance (2-tailed)	*0.024
			df	40

B) Correlations				
Visit	Control Variables			CMT Change
2	Gender & Age & BMI & Pack Years	IL6	Correlation	0.103
			Significance (2-tailed)	0.401
			df	66
3	Gender & Age & BMI & Pack Years	IL6	Correlation	0.061
			Significance (2-tailed)	0.673
			df	48
4	Gender & Age & BMI & Pack Years	IL6	Correlation	0.042
			Significance (2-tailed)	0.785
			df	42
5	Gender & Age & BMI & Pack Years	IL6	Correlation	-0.016
			Significance (2-tailed)	0.911
			df	49
6	Gender & Age & BMI & Pack Years	IL6	Correlation	-0.088
			Significance (2-tailed)	0.598
			df	36
7	Gender & Age & BMI & Pack Years	IL6	Correlation	-0.102
			Significance (2-tailed)	0.579
			df	30

Table 57 Tables comparing change in CMT (CMT Change) (B) in microns and VA score (VAS Change) (A) in letters from baseline utilising Pearson's correlation coefficient (correlation) and controlling for gender, BMI, pack years and age. Df = degrees of freedom, *-significant result with a p value <0.05.

Independent Samples Test						
Visit		t-test for Equality of Means				
		t	df	Sig. (2-tailed)	95% Confidence Interval of the Difference	
					Lower	Upper
1	IL6	3.448	33.324	*0.002	0.197763	0.766487
2	IL6	-3.514	81.955	*0.001	-1.321324	-0.366115
3	IL6	-1.863	82.778	0.066	-1.130308	0.036986
4	IL6	-0.417	55.505	0.678	-0.794137	0.520293
5	IL6	-0.598	33.208	0.554	-0.902708	0.492706
6	IL6	1.494	15.357	0.155	-0.355966	2.036124
7	IL6	-0.702	38.242	0.487	-0.649870	0.315122

Table 58 Independent samples t Test establishing correlations between injections administered and IL2 concentrations at each visit. t- t Test statistic, df-degrees of freedom, *-significant result with a p value <0.05

3.5.2.6.1 ***Summary***

Figure 65 provides a summary of the mean level of IL-6 concentration at each visit. There was no statistically significant difference (p>0.05) between visits when measured by ANOVA.

Table 57 demonstrated no significant relationship between IL-6 concentration and the change in CMT. Visit 7 for VA score was significant (p=0.024) with a correlation coefficient of 0.347. The analysis was corrected for gender, age, BMI and pack years. Table 58 revealed no significant difference in mean IL-6 concentration between patients who were treated and those were not. The isolated significant result may not be a valid biomarker to predict disease response to treatment.

3.5.2.7 The relationship of CRP concentration to treatment outcome measures (CMT, VAS and administered injections of anti VEGF)

CRP has a local role in early AMD development as it is a constituent both of drusen and the thickened Bruch's membrane pathognomonic of the disease[21, 54, 211]. Higher concentrations of CRP are also present in excised CNV membranes compared to age matched control retinal tissue[72]. Seddon *et al.* demonstrated that elevated serum CRP levels could be used as marker of progression from early to advanced AMD. I investigated its role as a biomarker of treatment response.

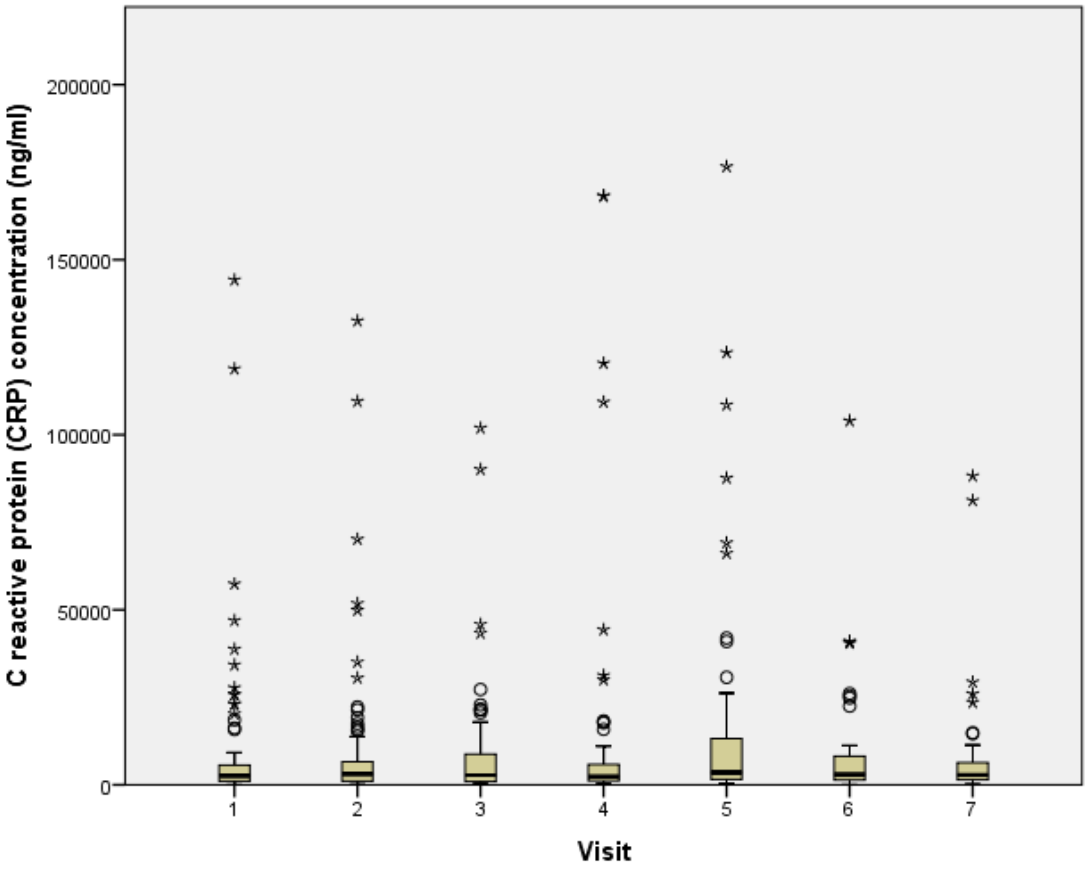

Figure 66 Figure demonstrating mean+/- 2 standard deviations of measured CRP at each patient visit. o-values more than 1.5X interquartile (IQ) range, *-values more than 3X IQ range

A) Correlations				
Visit	Control Variables			CRP
2	Gender & Age & BMI & Pack Years	VAS change	Correlation	0.030
			Significance (2-tailed)	0.810
			df	67
3	Gender & Age & BMI & Pack Years	VAS change	Correlation	0.038
			Significance (2-tailed)	0.756
			df	68
4	Gender & Age & BMI & Pack Years	VAS change	Correlation	0.129
			Significance (2-tailed)	0.323
			df	59
5	Gender & Age & BMI & Pack Years	VAS change	Correlation	-0.099
			Significance (2-tailed)	0.454
			df	57
6	Gender & Age & BMI & Pack Years	VAS change	Correlation	0.037
			Significance (2-tailed)	0.787
			df	54
7	Gender & Age & BMI & Pack Years	VAS change	Correlation	0.217
			Significance (2-tailed)	0.167
			df	40

B) Correlations				
Visit	Control Variables			CMT Change
2	Gender & Age & BMI & Pack Years	CRP	Correlation	0.121
			Significance (2-tailed)	0.323
			df	67
3	Gender & Age & BMI & Pack Years	CRP	Correlation	-0.106
			Significance (2-tailed)	0.466
			df	48
4	Gender & Age & BMI & Pack Years	CRP	Correlation	-0.165
			Significance (2-tailed)	0.285
			df	42
5	Gender & Age & BMI & Pack Years	CRP	Correlation	0.002
			Significance (2-tailed)	0.991
			df	48
6	Gender & Age & BMI & Pack Years	CRP	Correlation	0.039
			Significance (2-tailed)	0.818
			df	36
7	Gender & Age & BMI & Pack Years	CRP	Correlation	0.135
			Significance (2-tailed)	0.460
			df	30

Table 59 Tables comparing change in CMT (CMT Change) (B) in microns and VA score (VAS Change) (A) in letters from baseline utilising Pearson's correlation coefficient (correlation) and controlling for gender, BMI, pack years and age. Df=degrees of freedom.

Independent Samples Test						
Visit		t-test for Equality of Means				
		t	df	Sig. (2-tailed)	95% Confidence Interval of the Difference	
					Lower	Upper
1	CRP	3.546	83.148	*0.001	3171.756	11274.552
2	CRP	-4.172	81.061	*0.000	-14573.104	-5161.684
3	CRP	0.032	25.859	0.975	-9788.738	10100.667
4	CRP	-2.187	54.964	*0.033	-22694.343	-988.347
5	CRP	-2.423	66.307	*0.018	-22729.371	-2194.261
6	CRP	-0.779	61.501	0.439	-7606.495	3339.671
7	CRP	0.707	12.824	0.492	-10885.499	21460.909

Table 60 Independent samples t Test establishing correlations between injections administered and CRP concentrations at each visit. t- t Test statistic, df-degrees of freedom, *-significant result with a p value <0.05

3.5.2.7.1 ***Summary***

Figure 66 provides a summary of the mean level of CRP concentration at each visit. There was no statistically significant difference (p>0.05) between visits when measured by ANOVA.

Table 59 demonstrated no significant relationship between IL-6 concentration and the change in CMT or VA score. The analysis was corrected for gender, age, BMI and pack years. Table 60 however revealed significant difference in mean CRP concentration between patients who were treated and those were not at visits 1, 2, 4 and 5. The results from visits can be discounted as all patients received an injection at this visit. Visit 2 had a very small subgroup of patients (n=2) who received an injection. Visits 4 and 5 counterintuitively showed a higher mean concentration of CRP for patients not receiving an injection (16809 and 18212 ng/ml respectively) versus mean concentration

for patients who received an injection (4248 and 5251 ng/ml respectively). This was significant ($p<0.05$) but may have been due to the influence of outliers and the smaller sample size of patients receiving an injection compared to those who did not receive treatment at the visits.

3.5.2.8 The relationship of IL-8 concentration to treatment outcome measures (CMT, VAS and administered injections of anti VEGF)

This section is a summary of the investigation of IL-8 as a biomarker of CNV response to therapy with ranibizumab.

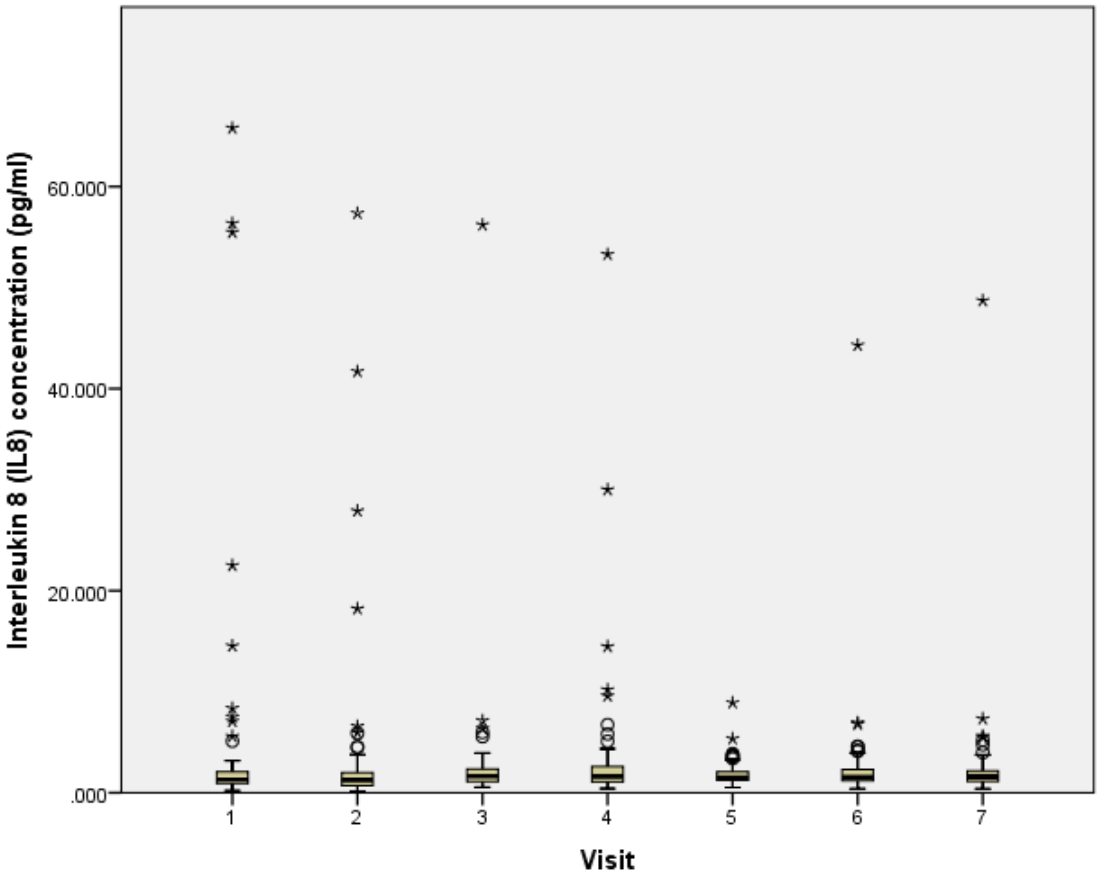

Figure 67 Figure demonstrating mean+/- 2 standard deviations of measured IL8 at each patient visit. o-values more than 1.5X interquartile (IQ) range, *-values more than 3X IQ range

A) Correlations				
Visit	Control Variables			IL8
2	Gender & Age & BMI & Pack Years	CMT Change	Correlation	-0.062
			Significance (2-tailed)	0.618
			df	66
3	Gender & Age & BMI & Pack Years	CMT Change	Correlation	-0.108
			Significance (2-tailed)	0.455
			df	48
4	Gender & Age & BMI & Pack Years	CMT Change	Correlation	0.013
			Significance (2-tailed)	0.933
			df	42
5	Gender & Age & BMI & Pack Years	CMT Change	Correlation	-0.074
			Significance (2-tailed)	0.608
			df	49
6	Gender & Age & BMI & Pack Years	CMT Change	Correlation	-0.034
			Significance (2-tailed)	0.839
			df	36
7	Gender & Age & BMI & Pack Years	CMT Change	Correlation	-0.173
			Significance (2-tailed)	0.343
			df	30

B) Correlations				
Visit	Control Variables			VAS change
2	Gender & Age & BMI & Pack Years	IL8	Correlation	-0.082
			Significance (2-tailed)	0.501
			df	67
3	Gender & Age & BMI & Pack Years	IL8	Correlation	-0.157
			Significance (2-tailed)	0.194
			df	68
4	Gender & Age & BMI & Pack Years	IL8	Correlation	0.113
			Significance (2-tailed)	0.385
			df	59
5	Gender & Age & BMI & Pack Years	IL8	Correlation	-0.011
			Significance (2-tailed)	0.933
			df	58
6	Gender & Age & BMI & Pack Years	IL8	Correlation	-0.004
			Significance (2-tailed)	0.975
			df	54
7	Gender & Age & BMI & Pack Years	IL8	Correlation	-0.050
			Significance (2-tailed)	0.755
			df	40

Table 61 Tables comparing change in CMT (CMT Change) (A) in microns and VA score change (VAS change) (B) in letters from baseline utilising Pearson's correlation coefficient (correlation) and controlling for gender, BMI, pack years and age. Df = degrees of freedom.

Independent Samples Test						
Visit		t-test for Equality of Means				
		t	df	Sig. (2-tailed)	95% Confidence Interval of the Difference	
					Lower	Upper
1	IL8	3.046	83.364	*0.003	1.301592	6.197960
2	IL8	-2.240	54.776	*0.029	-4.075689	-0.226037
3	IL8	-1.198	78.920	0.234	-2.837441	0.704755
4	IL8	-1.495	56.293	0.141	-4.150283	0.603208
5	IL8	0.224	19.573	0.825	-0.476667	0.591108
6	IL8	0.873	14.114	0.397	-3.629812	8.616630
7	IL8	-0.713	51.495	0.479	-3.381161	1.607980

Table 62 Independent samples t Test establishing correlations between injections administered and IL8 concentrations at each visit. t- t Test statistic, df-degrees of freedom, *-significant result with a p value <0.05

3.5.2.8.1 ***Summary***

Figure 67 provides a summary of the mean level of IL-8 concentration at each visit. There was no statistically significant difference (p>0.05) between visits when measured by ANOVA.

Table 61 demonstrated no significant relationship between IL-8 concentration and the change in CMT and VA score from baseline at each visit correcting for gender, age, BMI and pack years.

Table 62 revealed a significant difference in mean IL-8 concentration between patients receiving and not receiving an intravitreal injection of ranibizumab at Visits 1 and 2. However, all patients received an injection at visit 1 while only 2 patients received injections at visit 2. These significant results are likely statistical errors due to small group size.

3.5.2.9 The relationship of TNF concentration to treatment outcome measures (CMT, VAS and administered injections of anti VEGF)

Holmes *et al.* discovered in his recent paper that patients with Alzheimer's disease (a neurodegenerative disease with similar histopathological characteristics to AMD) who experienced acute systemic inflammatory events, developed an increase in the serum levels of TNF-□ and a 2-fold increase in the rate of cognitive decline over a 6-month period[212, 213]. Our study however, did no not provide strong evidence for the role of systemic TNF levels as a biomarker of AMD response to treatment.

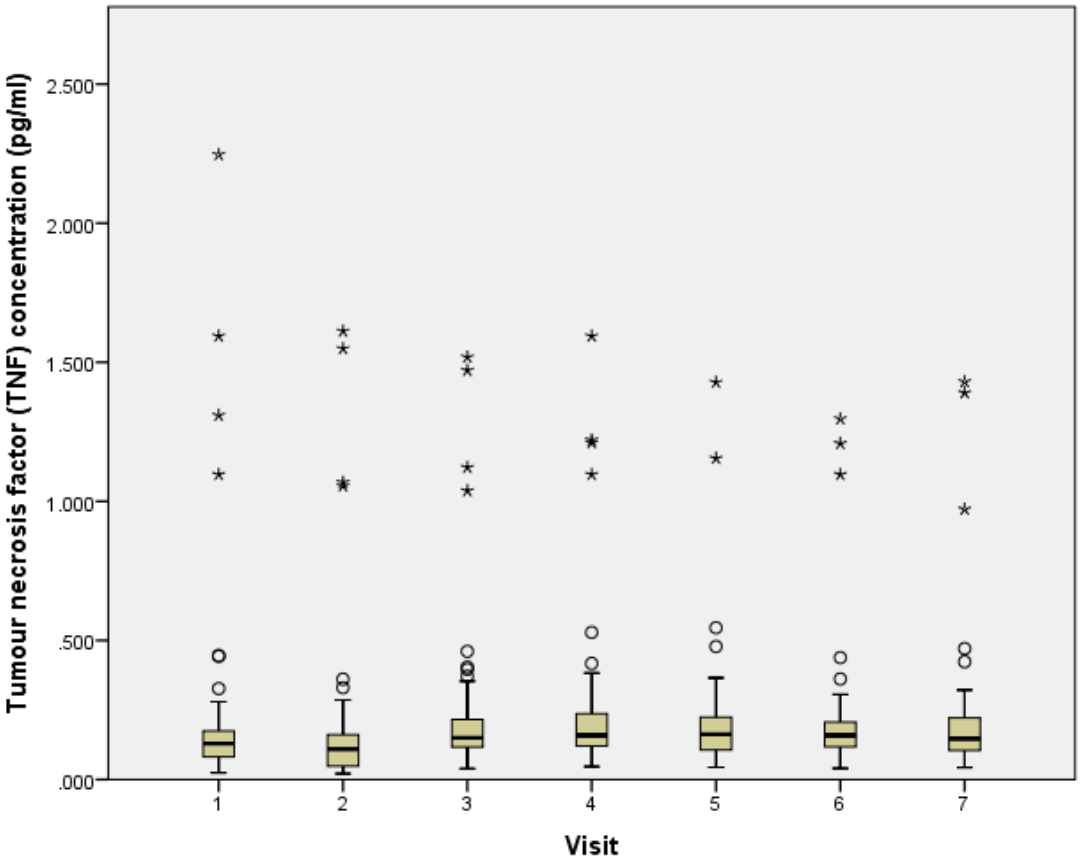

Figure 68 Figure demonstrating mean+/- 2 standard deviations of measured TNF at each patient visit. o-values more than 1.5X interquartile (IQ) range, *-values more than 3X IQ range

A) Correlations				
Visit	Control Variables			TNF
2	Gender & Age & BMI & Pack Years	VAS change	Correlation	0.084
			Significance (2-tailed)	0.492
			df	67
3	Gender & Age & BMI & Pack Years	VAS change	Correlation	0.056
			Significance (2-tailed)	0.644
			df	68
4	Gender & Age & BMI & Pack Years	VAS change	Correlation	0.055
			Significance (2-tailed)	0.671
			df	59
5	Gender & Age & BMI & Pack Years	VAS change	Correlation	0.023
			Significance (2-tailed)	0.862
			df	58
6	Gender & Age & BMI & Pack Years	VAS change	Correlation	0.110
			Significance (2-tailed)	0.420
			df	54
7	Gender & Age & BMI & Pack Years	VAS change	Correlation	0.272
			Significance (2-tailed)	0.081
			df	40

B) Correlations				
Visit	Control Variables			CMT Change
2	Gender & Age & BMI & Pack Years	TNF	Correlation	0.011
			Significance (2-tailed)	0.930
			df	66
3	Gender & Age & BMI & Pack Years	TNF	Correlation	-0.006
			Significance (2-tailed)	0.967
			df	48
4	Gender & Age & BMI & Pack Years	TNF	Correlation	0.034
			Significance (2-tailed)	0.828
			df	42
5	Gender & Age & BMI & Pack Years	TNF	Correlation	-0.053
			Significance (2-tailed)	0.709
			df	49
6	Gender & Age & BMI & Pack Years	TNF	Correlation	-0.026
			Significance (2-tailed)	0.876
			df	36
7	Gender & Age & BMI & Pack Years	TNF	Correlation	-0.122
			Significance (2-tailed)	0.505
			df	30

Table 63 Tables comparing change in CMT (CMT Change) (B) in microns and VA score (VAS Change) (A) in letters from baseline utilising Pearson's correlation coefficient (correlation) and controlling for gender, BMI, pack years and age. Df=degrees of freedom.

Independent Samples Test						
Visit		t-test for Equality of Means				
		t	df	Sig. (2-tailed)	95% Confidence Interval of the Difference	
					Lower	Upper
1	TNF	3.363	31.147	*0.002	0.056543	0.230769
2	TNF	-1.939	2.110	0.185	-0.330401	0.118006
3	TNF	-0.551	38.373	0.585	-0.150184	0.085886
4	TNF	0.634	32.220	0.530	-0.107257	0.204284
5	TNF	-3.257	67.703	*0.002	-0.172481	-0.041419
6	TNF	0.802	15.011	0.435	-0.139651	0.308129
7	TNF	-1.448	49.669	0.154	-0.160760	0.026091

Table 64 Independent samples t Test establishing correlations between injections administered and TNF concentrations at each visit. t- t Test statistic, df-degrees of freedom, *-significant result with a p value <0.05

3.5.2.9.1 ***Summary***

Figure 68 provides a summary of the mean level of TNF concentration at each visit. There was no statistically significant difference (p>0.05) between visits when measured by ANOVA.

Table 63 demonstrated no significant relationship between mean TNF concentration and the change in CMT and VA score from baseline at each visit correcting for gender, age, BMI and pack years.

Table 64 revealed a significant difference in mean TNF concentration between patients receiving and not receiving an intravitreal injection of ranibizumab at Visits 1 and 5. As previously stated, all patients received an injection at visit 1. Patients who did not receive an injection had a statistically significant (p=0.002) higher mean TNF concentration compared to those receiving an injection at visit 5.

3.5.3 Multilevel linear regression model for CFB genotype and CRP

I examined the impact of CRP levels to predict CNV response with known CFB alleles in a multilevel linear regression model. CFB was the genotype chosen as it had the greatest number of visits and outcome measures where there was a significant association with treatment outcome. CRP was chosen for this reason from the inflammatory markers examined.

A)

Visit	Adjusted R Square	Change Statistics
		R Square Change
2	-0.007	0.003
3	0.016	0.001
4	0.158	0.002
5	0.017	0.002
6	0.025	0.000
7	0.234	0.035

B)

ANOVA				
Visit	Model	df	F	Sig.
2	Regression	2	0.735	0.483
3	Regression	2	1.621	0.205
4	Regression	2	6.901	*0.002
5	Regression	2	1.505	0.231
6	Regression	2	1.745	0.184
7	Regression	2	7.100	*0.002

Table 65 A multilevel logistic regression model investigating the relationship between CFB and VAS (Visual acuity score) Change from baseline in letters with CRP as a second order correlate. Df-Degrees of freedom, F statistic for the ANOVA analysis, *-significant result with a p value <0.05, A-R^2 change statistic table, B-table of significance of the regression model at each visit

A)

Visit	Adjusted R Square	Change Statistics
		R Square Change
2	0.006	0.010
3	0.139	0.024
4	0.000	0.007
5	0.074	0.000
6	-0.022	0.002
7	0.136	0.015

B)

ANOVA				
Visit	Model	df	F	Sig.
2	Regression	2	1.235	0.297
3	Regression	2	5.197	*0.009
4	Regression	2	0.990	0.379
5	Regression	2	2.919	0.064
6	Regression	2	0.541	0.586
7	Regression	2	3.511	*0.043

Table 66 A multilevel logistic regression model investigating the relationship between CFB and CMT (central macular thickness) change from baseline in microns with CRP as a second order correlate. Df-Degrees of freedom, F statistic for the ANOVA analysis, *-significant result with a p value <0.05, A-R^2 change statistic table, B-table of significance of the regression model at each visit

3.5.3.1 Summary

The linear regression model above produced significant results (p=0.009 for visit 3 and 0.043 for visit 7) for a correlation of CRP levels with CMT Change in a population of known CFB genotype. The increased predictive capacity was indicated by an R^2 change value of 2.4% and 1.5% in visits 3 and 7 respectively. Visits 7 and 4 also produced significant results for VAS Change (p=0.002 at both visits). The R^2 change for CRP in the predictive model was 3.5% and 0.2% respectively.

There have been no studies utilising this model to predict outcome measures of patients undergoing anti VEGF treatment for CNV.

4 Discussion and future planned work

The investigation into predictors of CNV response to treatment with the anti VEGF agent ranibizumab (Lucentis) provided new insights into possible biomarkers for disease response and described significant clinical prognostic indicators.

The first significant finding was no difference in the outcome measures (change in CMT and VA score from baseline and the number of intravitreal injections for active CNV) between males and females. There has been a report in the literature supporting males having a worse outcome than females[146] in treatment response for AMD. My study found no difference between the genders, agreeing with the meta-analysis by Chakravarty *et al.*[149] which recorded no evidence for higher risk of developing AMD.

Age of participants in the study proved a significant association for poor outcomes in CMT and VAS during treatment. This may be related to the hypothesis that increasing age leads to Bruch's membrane becoming thicker and more dysfunctional with accumulated byproducts of oxidative stress[172]. This pathological process may create a micro environment at the RPE-Bruch's membrane interface which antagonizes the effects of Ranibizumab. The resulting treatment failure leads to a clinical indication to withhold therapy due to limited benefit. This is a possible explanation as to why older patients were receiving fewer injections whereas objective measures of visual function worsened with age.

High BMI values[149] have been associated with the development of advanced AMD. Elevated BMI was not found to be associated with poor outcome measures when assessed by CMT and VAS change from treatment baseline. This finding was similar to a prospective trial investigating responders versus non responders on treatment with anti VEGF therapy[173].

Oxidative stress at the level of Bruch's membrane, leading to pro inflammatory deposits in drusen and complement dysregulation is a posited theory for CNV pathogenesis[127]. There have been many studies implicating smoking in the development of AMD via the mechanism of increased free radical production and subsequent oxidation end-product deposition[174-176]. The literature however has not demonstrated a conclusive relationship between smoking and response to treatment[173].

Baseline measures of foveal thickness have been found in the CATT trial to predict a poor treatment outcome[120] (whereas large CNV area is a predictor of poor response[177]). My study did not demonstrate this correlation. One possible explanation is the NICE guidance that patients be treated within 2 weeks of presentation. This minimizes structural anatomical damage to the macula through early treatment. The early intervention with therapy may mask the predictive value of baseline CMT and visual acuity.

A review of the literature revealed that genotypes confirmed in the development of AMD or progression of early to advanced AMD have not been established as having a Pharmacogenetic association for CNV[178]. This trend was followed in my study where the only genotype with multiple significant results in VAS change and CMT change was complement factor B (rs641153). The significant results were not replicated for an association between administered injections and the genotype.

Complement dysregulation has been found in numerous studies to be associated with AMD development and progression from early to advanced stages[72, 179, 180]. The evidence for treatment response either relating to CMT and VA values or mean number of injections has been less conclusive.

Contrary to my hypothesis of SERPING1 influencing treatment outcomes, there was no evidence in my study of an association between the mutant allele (TT) and outcome measures of VAS and CMT. Only visit 5 produced a difference in mean number of injections ($p=0.006$) between the heterozygote and wild type alleles (CT and CC). Patients with the wild type allele had significantly more injections than heterozygotes. This result at only one visit and in one outcome measure would suggest it is not highly meaningful.

The CFH Y402H allele (rs1061170) has been associated in some studies with poor treatment response of CNV to anti VEGF therapy[66, 155, 156]. Paradoxically, some studies have not demonstrated an association between CFH Y402H and treatment outcomes[158-160]. My study did not produce definitive evidence of an association. The intervention with anti VEGF therapy likely counteracts the natural history of the disease process and the influence of adverse genotypes.

The main findings related to the Pharmacogenetic section of the study were significant associations at 2 visits for change in CMT from baseline (visit 3, $p=0.004$; visit 4, $p=0.008$) and significant associations at 3 visits for change in VAS from baseline (visit 4, $p=0.001$; visit 6, $p=0.005$; visit 7, $p<0.001$) for CFB genotype (rs641153). These results

were between the wild type (CC) and mutant allele (TT) with the CC allele group having a lower mean CMT and higher mean VAS compared to the TT allele group. There were no visits with significant associations for CFB genotypes and therapeutic intervention. Previous studies have not found an association between treatment outcome and this SNP[181, 182].

CFB is involved in the regulation of the alternative complement pathway through formation of C3b (regulated by Factor D) and the C3 convertase enzyme. This critical role in complement regulation may influence the response of CNV to anti VEGF therapy. The results of my study suggest that the mutant allele of the CFB genotype investigated is associated with a worse treatment outcome with ranibizumab.

SERPING1, via the protein product C1Inh, is involved in regulating the classical complement pathway[48]. If the hypothesis of the study was correct, a higher level of complement activation in the classical pathway would be expected in patient with worse VAS and CMT. There were no consistent results in my analysis to suggest a greater level classical pathway activity. The alternative pathway activity also did not correlate with treatment response.

The only inflammatory marker with significant results at multiple visits and in more than one outcome measure was CRP. This systemic marker of acute inflammation was comparatively elevated in patients who did not receive an injection. The VAS and CMT outcome measures were non-significant for all visits. This may suggest that high levels of CRP are associated with a clinical indication not to treat. A sub analysis of the participants in this group would be necessary to determine the exact causal relationship.

4.1 Limitations

1. Small sample size. There is ongoing recruitment at Frimley Park Hospital to increase the population size.
2. Short follow-up. Blood samples will be collected at the 1 and 2 year marker from willing participants to further investigate any pharmacogenetic or inflammatory biomarkers
3. Inter visit variability. The time interval between visits varied considerably. The appointment times within the NHS clinical setting varied from 4-6 weeks thus making statistical analysis less reliable
4. Lack of negative control mice. There was unfortunately a limited number of negative control mice (injected with subretinal saline) to compare the effects of the procedure. This resulted from a combination of animal death

compounded by the design of the study where fewer control animals were selected than study population.

5. Small sample populations. The $Ccl2^{-/-}/Cx3cr1^{-/-}$ mice proved difficult to breed in house. This led to a limitation of sample size within the time constraints of the experiment.

We undertook a series of investigations into the function of the gene SERPING1, via its protein product C1Inh, to corroborate the hypothesis that it influences AMD development.

The fundoscopic images at the three timepoints for the two groups of mice did not demonstrate any signs of CNV formation. There were phenotypic changes in the $Ccl2^{-/-}/Cx3cr1^{-/-}$ fundi suggestive of drusen. These deposits result from dysfunctional microglia within the retina and are not true drusen.

The H&E stained sections did not show any gross difference on light microscopy between timepoints and groups of mice. OrO and BCIP/NBT images showed no discernible difference between timepoints or between wild type and knockout mice. One possible theory is subretinal C1Inh was protecting the $Ccl2^{-/-}/Cx3cr1^{-/-}$ mice from developing signs of CNV.

Immunohistochemistry analysis demonstrated a number of interesting findings. Rod photoreceptors as demonstrated by rhodopsin staining intensity, were more preserved in the wild type mice at 52 weeks post subretinal injection compared to the $Ccl2^{-/-}/Cx3cr1^{-/-}$ mice (there was no statistically significant difference in controls at this timepoint within each group $p>0.05$) as evidenced by the higher level of fluorescent staining intensity.

C5 levels are higher initially in $Ccl2^{-/-}/Cx3cr1^{-/-}$ mice compared to C57/BL6 ($p=0.0003$ with 95% CI of 4.716 to 12.81) but decrease to no significant difference at 52 weeks. Levels in the C57/BL6 mice increase from timepoint 1 to 3 ($p=0.0265$) and decrease significantly in the $Ccl2^{-/-}/Cx3cr1^{-/-}$ group ($p=0.0404$). This high initial complement activity in the knockout mice may be responsible for photoreceptor loss. This is counterintuitive to the injection of a complement inhibitor.

The results from the TUNEL analysis demonstrated an initial higher level of apoptosis as measured by the statistically significant difference in mean percentage staining intensity at timepoints 1 and 2, between the 2 groups of mice (timepoint 1, $p=0.0023$ with 95% CI of 3.950 to 11.47 and timepoint 2, $p=0.0284$ with 95% CI of -11.41 to -0.9107). There

was also a statistically significant difference in the $Ccl2^{-/-}$/$Cx3cr1^{-/-}$ mice in their level of apoptosis at timepoints 1 and 3 (p= 0.0019) with a higher rate initially. This corresponded to the findings of retinal thickness, where the C57/BL6 mice had statistically significant thicker retinas at timepoints 2 and 3 (timepoint 2, p< 0.0001 with 95% CI of -8.528 to -4.174 and timepoint 3, p=0.0007 with 95% CI of -5.659 to -1.506). Both groups of mice demonstrated statistically significant thinner retinas comparing timepoints 1 and 3.

Further investigations would have to be performed to investigate whether the higher level of complement deposition, high level of initial apoptosis and loss of rod photoreceptors are related.

4.2 Future planned work

Relating to the patient investigations:

1. Subanalysis to determine any associations with outcome for:
    (1) Angiographic phenotype (Classic, occult)
    (2) Medications for systemic illnesses
    (3) Type of macula oedema (SRF, IRF)

2. Further genotyping of patients for new SNPs of relevance to AMD development or predictors of outcome

Relating to the animal model:

1. Further investigation of the effect of intravitreal C1Inh on laser induced CNV in wild-type mice

5 Conclusion

Hypothesis: *SERPING1* influences the pathogenesis of AMD and the clinical response of CNV to therapeutic intervention with the anti VEGF drug ranibizumab.

5.1.1 Does SERPING1 influence the pathogenesis of AMD?

Utilising a rodent model of AMD ($Ccl2^{-/-}$/$Cx3cr1^{-/-}$) the main conclusions are:

1. There were no signs of choroidal neovascularization on the fundi of both C57/BL6 and $Ccl2^{-/-}$/$Cx3cr1^{-/-}$ mice up to 52 weeks when examined with light microscopy.
2. H&E staining demonstrated no histological difference; TEM demonstrated a solitary sub RPE deposit in a 52 week old $Ccl2^{-/-}$/$Cx3cr1^{-/-}$ mouse.
3. OrO demonstrated no difference in lipid deposition; BCIP/NBT demonstrated no difference in vascularization.
4. Rhodopsin immunohistochemistry demonstrated photoreceptors are preserved to a greater extent in the C57BL/6 as compared to the $Ccl2^{-/-}$/$Cx3cr1^{-/-}$ mice at 52 weeks.
5. C5 levels are higher initially in $Ccl2^{-/-}$/$Cx3cr1^{-/-}$ mice compared to C57/BL6 but decrease to the same at 52 weeks. Levels in the C57/BL6 increase from timepoint 1 to 3. This high initial complement activity in the knockout mice may be responsible for photoreceptor loss.
6. The above result corresponded to the higher rate of apoptosis in the $Ccl2^{-/-}$/$Cx3cr1^{-/-}$ mice at timepoint 1. The apoptosis rate was similar at timepoint 3.
7. Both groups of mice develop thinner retinas with time. However, the $Ccl2^{-/-}$/$Cx3cr1^{-/-}$ mice have statistically significant thinner retinas at timepoints 2 and 3 compared to C57/BL6.

This suggests that subretinal injection of C1Inh may lead to increased complement deposition and subsequent photoreceptor loss via apoptosis in a murine model of AMD compared to wild type mice. This may correspond to the GA equivalent of advanced AMD.

5.1.2 Does SERPING1 influence the response of active CNV to treatment with ranibizumab?

On a cohort of patients (106 patients receiving treatment with intravitreal ranibizumab, evenly divided between males and females) examined by genotype and serum inflammatory marker analysis, the main results are:

1. There was no statistically significant difference in the outcome measures of change in VAS or CMT for the three alleles. This was replicated for the outcome measure of number of injections (there was one visit that was significant for the heterozygote group).
2. There was no correlation between classical complement pathway activity and any outcome measure.

This suggests, similar to many genotypes implicated in AMD progression from early to advanced, that SERPING1 is not a candidate gene to predict CNV response to treatment with ranibizumab.

6 Appendix

6.1 Documents related to the Pharmacogenetics study

6.1.1 Protocol for Pharmacogenetics study

Pharmacogenetic correlations in Age Related Macular Degeneration

A study to identify specific genetic variations and serum/plasma proteins related to age related macular degeneration (AMD) including its association with vascular endothelial growth factor (VEGF) biology.

Funder
Macula Disease Society

Sponsor
Southampton University Hospital Trust

Chief Investigator
Professor Andrew Lotery
Southampton Eye Unit
Southampton General Hospital
Tremona Road
Southampton
SO16 6YD
Tel: 02380 795049
Fax: 02380 796085
Email: a.j.lotery@soton.ac.uk

Co-Investigator
Mr Charles Pierce
Southampton Eye Unit
Southampton General Hospital
Tremona Road
Southampton
SO16 6YD
Tel: 02380 795049
Fax: 02380 796085
Email: cop1e10@soton.ac.uk

Principal Investigator
Ms Geeta Menon
Eye Unit
Frimley Park Hospital
Portsmouth Road
Frimley **geeta.menon@fph-tr.nhs.uk**

Objective

1) Record the main choroidal neovascular membrane (CNV) sub-types presenting to clinic and their response to anti-VEGF treatment.
2) Record the changes in visual acuity as a response to anti-VEGF treatment.
3) Measure the response of the CNV to anti-VEGF therapy by optical coherence tomography (OCT).
4) Look for any systemic markers that indicate a reactivation of the CNV or poor prognosis to treatment.
5) To look for specific genes involved in AMD which may influence treatment response to anti-VEGF drugs.

Summary

VEGF is a protein molecule important for blood vessel growth in the body. Conditions such as macular degeneration are characterised by inappropriate production of VEGF leading to abnormal blood vessel growth and leakiness of the new vessels[1].

Neovascular age-related macular degeneration (nvAMD) is an eye condition in which there is abnormal growth of blood vessels and secondary leakage at the macula of the eye. This leads to severe deterioration of central vision. VEGF blocking drugs have been

shown to improve the eyesight of patients with nvAMD[1;2]. However, some patients become resistant to the treatment leading to a deterioration of vision.

The specific genes and proteins that cause this variation in treatment response are currently unknown. The objective of this study is to collect samples of blood from nvAMD patients undergoing anti-VEGF treatment to study how variations in their DNA or serum / plasma proteins could account for the treatment response.

Identifying these genes or serum/plasma proteins would allow better targeting of treatment and possible novel drugs. This should lead to better visual outcomes when applied to AMD.

Hypothesis

1. Variations in genotype determine choroidal neovascularisation subtypes (CNV).
2. Variations in the VEGF gene alter VEGF expression levels and thus alter response to therapy.
3. Systemic pro-inflammatory changes influence local VEGF expression and thus CNV reactivation.

Background to the project:

Age related macular degeneration is a complex disease and is the leading cause of blindness in the developed world[1]. There are multifactorial causes associated with its development.

We plan to undertake a gene based study to look at polymorphic variations which exist in AMD, especially those involved in VEGF biology. The response to treatment may be linked to the level of VEGF expression[2].

There is considerable evidence that complement has a significant role in the development and response to treatment of AMD[4-7]. Therefore, we will look at the genetic variation in the region coding for C3 and other complement related genes including complement factor HR1 and HR3 and SERPING1[8].

Recent evidence has shown that serum complement factor H and the factor H Tyr402His polymorphic variant may act as a biomarker for disease progression in multiple sclerosis[4]. We therefore plan to investigate whether serum complement factors and other inflammatory markers, can identify CNV subtypes more responsive to anti VEGF treatments. They may also provide an early indication of disease relapse and act as a biomarker.

Proposed research plan including methodology

We plan to perform a retrospective study to identify 50 patients from Frimley Park Hospital and 100 from Southampton General Hospital who have received 12 months of anti VEGF treatment. Patients' notes who have received 12 months of anti VEGF treatment will be identified and evaluated for their response to treatment. They will then be sub classified based on OCT and VA findings into responders and non responders. Patients will be invited to have a single episode of blood taking at one of their routine clinic appointments for genotyping and plasma/serum analysis.

The prospective aspect of the study consists of collecting blood samples for differential full blood count (dFBC),C-RP, DNA and serum/ plasma analyses from **200** patients who are under the care of the Southampton Eye Unit medical retinal team for treatment of AMD and 50 age matched control patients attending the Southampton Eye unit for a non-medical retinal condition. We will also recruit 100 patients from the Eye Unit at Frimley Park Hospital. The inclusion criteria are age greater than 50 years and Caucasian origin. Anyone with known retinal pathology, other than AMD, will be excluded. The research will last for 36 months and the length of time each participant is involved, will depend on their time of entry.

Demographic details will be collected and questionnaires administered to determine smoking habits, as well as ophthalmic and general medical history.

They will then have the following investigations by members of the research team:

1. Distance logMAR visual acuity will be measured in a vision tunnel.
2. A full slit lamp eye examination including dilated fundoscopy.
3. CNV phenotyping using fundus fluorescein angiography (FFA) and OCT.
4. Four sets of 10ml blood samples will be collected for differential full blood count (dFBC), DNA analysis, serum and plasma at the initial visit.
5. We will then repeat the tests for dFBC, inflammatory markers and OCT investigations at monthly clinic visits. A general systemic enquiry will also take place.
6. Any clinical evidence of CNV reactivation will be documented by a fundus photograph, OCT and FFA.

Statistical considerations and sample size justification

We will estimate the extent to which treatment effects are associated with particular polymorphisms (such as CFH, LOC387715, HTRA1, C3, CRP, C2/BF, VEGF, VEGFR1, VEGFR2 or CFH deletion). These are all possible contributors to the pathogenesis of CNV in AMD. This will be achieved by analyses of the effect of the specified polymorphisms on visual acuity and other quantitative outcomes, including CNV morphology.

The assumptions required for sample size calculations are based on previous analyses performed for the IVAN trial (of which Prof Lotery is a co-investigator) and accepted by the HTA Clinical Trials commissioning board. The power of the analysis is the ability of this sample to detect the stated difference in outcome between exposed and unexposed groups, given the prevalence of genotypic sub-groups. For SNPs in CFH (Y402H) and HTRA1 (rs11200638) which have prevalences averaging 35%, a sample size of 300 will allow the study to have >90% power to detect a difference of 6 letters on the EDTRS eye chart (for other outcomes, equivalent to a standardised difference ~0.30 standard deviations) at a significance level of 5%, assuming that different polymorphisms have independent effects (supported by the existing literature).

For serum /plasma biomarkers, the way in which associations of biomarker levels with cumulative treatment will ultimately be modelled will depend on the nature of the associations. In previous papers a sample size of 350 was able to detect a significant difference in CFH protein levels in MS patients[10] while a sample size of 300 was sufficient to detect a significant difference in TNF-□ in Alzheimer patients[11].

Ethical Issues

Genetic analysis may reveal a gene mutation linked with an adverse prognosis for treatment with anti VEGF agents. This fact will be highlighted in the patient information sheet. Samples will be linked anonymised. The linked data will be kept confidentially by Professor Lotery. We do not plan to inform individual patients, however the patient may contact Professor Lotery in the future to obtain further information if required.

Data Protection and Anonymity

Data will be collected and retained in accordance with the Data Protection Act 1998. Linked anonymised data will be used. Patients will be allocated a study number when initially recruited into the study. Proformas, photos and blood samples for DNA extraction, plasma and serum samples will only be labelled with this study number. This study number will be linked to patient identifiers only on the consent form and within

the patient recruitment log which will be kept securely in a locked filing cabinet in Professor Lotery's office.

No report / publication / presentation will contain patient identifiers.

Dissemination of results

We plan to publish the results in peer reviewed scientific journals and present the findings at regional and international meetings eg. The Association for Research in Vision and Ophthalmology (ARVO).

References

(1) Siemerink MJ, Augustin AJ, Schlingemann RO. Mechanisms of ocular angiogenesis and its molecular mediators. *Dev Ophthalmol* 2010;46:4-20.

(2) Folk JC, Stone EM. Ranibizumab therapy for neovascular age-related macular degeneration. *N Engl J Med* 2010;363:1648-1655.

(3) Galan A, Ferlin A, Caretti L *et al*. Association of Age-related Macular Degeneration with Polymorphisms in Vascular Endothelial Growth Factor and Its Receptor. *Ophthalmology* 2010;117:1769-1774.

(4) Chen Y, Bedell M, Zhang K. Age-related macular degeneration: genetic and environmental factors of disease. *Mol Interv* 2010;10:271-281.

(5) Seddon JM, Gensler G, Milton RC, Klein ML, Rifai N. Association between C-reactive protein and age-related macular degeneration. *JAMA* 2004;291:704-710.

(6) Yates JR, Sepp T, Matharu BK *et al*. Complement C3 variant and the risk of age-related macular degeneration. *N Engl J Med* 2007;357:553-561.

(7) Edwards AO, Ritter R, III, Abel KJ, Manning A, Panhuysen C, Farrer LA. Complement factor H polymorphism and age-related macular degeneration. *Science* 2005;308:421-424.

(8) Klein RJ, Zeiss C, Chew EY *et al*. Complement factor H polymorphism in age-related macular degeneration. *Science* 2005;308:385-389.

(9) Li H.-L., Yu R.-G., Wu R.-X. Hemodynamic changes of central retinal artery and posterior ciliary artery in patients with age-related macular degeneration. International Journal of Ophthalmology. 8 (2) (pp 321-322), 2008

(10) Ingram G, Hakobyan S, Hirst CL, Harris CL, Pickersgill TP, Cossburn MD et al. Complement regulator factor H as a serum biomarker of multiple sclerosis disease state. Brain 2010 June;133(Pt 6):1602-11.

(11) Aisen PS. Inflammation and Alzheimer disease. [Review] [37 refs]. Molecular & Chemical Neuropathology 1996 May;28(1-3):83-8.

6.1.2 Consent form

Study title: "Pharmacogenetic correlations in age related macular degeneration (Prospective arm)" (Ref: Protocol V1.1 10/Aug/2011)

Patient sticker

Patient Identification Number for this study: _____

Chief Investigator: Professor Andrew Lotery, Southampton Eye Unit, Tremona Road, Southampton SO16 6YD Tel: 02380 795049

PART A: Consent for the current study

(Samples to be destroyed on study completion unless part B completed)

PLEASE INITIAL THE BOXES IF YOU AGREE WITH EACH SECTION:

1. I confirm that I have read and understand the information sheet dated for the above study and have been given a copy to keep. I have been able to ask questions about the study and I understand why the research is being done and any risks involved. ☐

2. I agree to give samples of blood for research in this project. I understand how the samples will be collected, that giving samples for this research is voluntary and that I am free to withdraw my approval for use of the samples at any time without my medical treatment or legal rights being affected. ☐

3. I give permission for sections of my medical notes to be looked at by responsible individuals where it is relevant to this study. I expect that my medical notes will b treated confidentially at all times. ☐

4. I understand that I will not benefit financially if this research leads to th development of a new treatment or test. ☐

5. I know how to contact the research team if I need to. ☐

6. I agree to take part in the above study ☐

_____ _____ _____

Name of Patient Signature Date

_____ _____ _____

Name of person taking consent/Researcher Signature Date

When completed, 1 for patient; 1 for researcher site file; 1 (original) to be kept in hospital; medical notes

PART B: Samples for storage and use in possible future studies - Linked anonymised samples

7. I give permission for my samples and the information gathered about me to be stored by Professor Andrew Lotery at the University of Southampton Eye Laboratory, Southampton General Hospital, for possible use in future projects, as described in the information sheet. I understand that some of these projects may be carried out by other researchers, including researchers working for commercial companies. I understand that future studies will be reviewed and approved by a Research Ethics Committee prior to my samples being used, and that I can alter these decisions at any stage by letting the research team know. ☐

a. I give permission for the samples to be used for research about eye disease

b. I give permission for the samples to be used for other unrelated research studies the precise nature of which will depend upon future scientific advances. ☐

8. I want to be told the results of any future test which may have healt implications for me. Yes ☐ No ☐

9. I give permission for sections of my medical notes to be looked at by responsible individuals where it is relevant to such future study. I expect that my medical notes will be treated confidentially at all times. ☐

10. I give permission for the continued storage of my samples and data in the event I lose the capacity to consent. ☐

11. I have informed the researchers of my participation in any other research study ☐

_____ _____ _____

Name of Patient Signature Date

_____ _____ _____

Name of person taking consent/Researcher Signature Date

When completed, 1 (copy) for patient; 1 (original) for researcher site file; 1 (copy) to be kept in hospital medical notes.

6.1.3 Patient invitation letter

PATIENT INVITATION LETTER

Study title: "Pharmacogenetic correlations in AMD"

Ref:

Dear Sir / Madam,

We would like to invite you to participate in a research project being carried out with eye doctors from Southampton University and Southampton Eye Unit. You have been sent this letter since you have either started treatment for age related macular degeneration or you have been found to be free of any retinal disease.
The project is looking at what factors predispose people to develop this eye condition and how it affects treatment.

If you kindly agree to take part, then this research project will take place during your next routine visit to the eye department, and will take about 30 minutes altogether.

As part of the research:

1. We will ask you some questions about your general health.
2. We will take a blood sample from you.

If your english is not adequate, it would be very useful to bring an english-speaking relative or friend with you to help you.

Please take time to read the enclosed information sheet. If you decide to take part in this study, could you please complete and send the enclosed reply slip back to us in the addressed envelope. You will then be referred to the research team. The research team will consist of eye doctors and nurses from the University of Southampton and Southampton Eye Unit.

Yours sincerely,

Professor Andrew Lotery
Consultant Ophthalmologist
Southampton Eye Unit
Tremona Road
Southampton
SO16 6YD
Tel: 02380 795049

6.1.4 Patient reply slip

REPLY SLIP

Study title: "Pharmacogenetic correlations in AMD"

Ref:

Name:

Address:

Please tick the box below if you wish to take part:

	Yes, I would be happy to take part in the research project

Please send completed reply slip in the enclosed addressed envelope.

Thank you for your interest in this study

Yours Sincerely,

Professor Andrew Lotery
Consultant Ophthalmologist
Southampton Eye Unit
Tremona Road
Southampton
SO16 6YD
Tel: 02380 794590

(Mailing address: LD74, MP806, Clinical Neurosciences, South Academic and Path Block, Southampton General Hospital, Southampton SO16 6YD)

6.1.5 Patient information sheet

STUDY: "Pharmacogenetic correlations in age related macular degeneration" (Ref: protocol V1.1, 10 Aug 11)

CHIEF INVESTIGATOR: Professor Andrew Lotery, Southampton Eye Unit, Southampton General Hospital, Tremona Road, Southampton, SO16 6YD. Tel: 02380 795049

We would like to invite you to take part in a research study. Before you decide you need to understand why the research is being done and what it would involve for you. Please take time to read the following information carefully. Talk to others about the study if you wish. Ask us if there is anything that is not clear or if you would like more information. Take time to decide whether or not you wish to take part.

What is the purpose of this study?

- We would like to understand more about the types of genes and proteins that lead to macular degeneration and why some people respond better to our treatment than others.
- We hope the results of this study will increase our understanding of the underlying processes occurring. In future this could mean that better, more effective therapy could be developed.

Why have I been invited to take part in this study?

- You have been chosen to take part in this study because you have recently started treatment for macular degeneration or have been identified as never having suffered from the disease.
- We hope to look at 350 patients altogether. 300 with macular degeneration and 50 healthy participants.
-

Do I have to take part?

- It is up to you. If you do not want to take part then you will continue to receive the normal medical care from your doctor.

What will happen to me if I take part?

- We would like to carry out the following:
    1. **Medical history**: We would like to ask about your medical history.

2. **Clinical examination: This will be part of your routine clinical care and will involve photographic investigations of your eyes.**
3. **Blood test**: We would like to take 40ml (about 8 teaspoons) of blood, to look at your DNA, cells in your blood, plasma and serum (the liquid part of blood). These will be analysed in the laboratory later.

How much of my time will the study take?

- **The research will take about 30 minutes of your time, and will take place during each of your routine visits to the eye unit for up to 12 months**.

Expenses and payments

- We are unable to offer any expenses or payments for taking part in the study.

Will taking part in the study affect my daily life? Is there anything I am not allowed to do while taking part in the study?

- This study will not affect your daily life, and there are no restrictions.

What are the possible benefits of taking part?

- We cannot promise the study will help you. However information obtained from this study may help to improve the management of people with retinal conditions in the future.

What are the possible disadvantages and risks of taking part?

Discovering changes in your genes

- There is the potential that we may find something new which was not previously known about you. If it is found that you have a changed gene in your DNA, it is possible that you and family members may be more likely to develop certain retinal conditions in the future, which may affect your vision. In some situations, certain lifestyle changes could help to reduce the risk of developing visual problems in the future.
- If you or your relatives wish to discuss any the results of your gene analysis further, then please contact Professor Lotery (details on top of page 1).
- You may also request to be informed in the eventuality that we find any significant gene change.
- We can then arrange an outpatient appointment at the eye unit to provide more information on the implications of these gene changes, and offer advice on preventative measures. We can also offer genetic counselling if required.
- Please note that any personal information about you will be kept confidentially by Professor Lotery (see below).

Provision of a blood sample

- The risks of providing a blood sample are mild bruising of the skin and mild discomfort from the needle.

What happens at the end of the study?

- You will continue to receive the usual medical care from your doctor.
- We may also contact you in the future regarding other research studies.

Will my taking part in this study be kept confidential?

- Yes. All information and samples which is collected about you during the course of the research will be kept strictly confidential. Our procedures for handling, processing, storage and destruction of your data match the Data Protection Act 1998.
- Your data and samples will be kept in an anonymised state, linked only to your personal information by a single record kept locked in Professor Lotery's office at Southampton General Hospital.
- Your confidential data will be accessible only to the study personnel, and to the Research Departments of Southampton University Hospital NHS Trust (the sponsors) and the local NHS trust for monitoring the quality of the study.
- Your data and samples may be shared with external scientists, but any information about you which leaves the hospital will be completely anonymous, so that you cannot be recognised
- Your data will be retained for a minimum of 15 years, and if not required will be disposed of securely.
- You may have your data or samples removed at any time by contacting us.

What will happen to any samples I give?

- Your samples will be stored in a freezer in Professor Lotery's eye research laboratory at Southampton General Hospital. This laboratory has restricted access to members of the research team only.
- After this project, your samples will be kept in this same place or in a bank with others like it, so that Professor Lotery can continue to study eye conditions for many years to come. Your samples will only be used for other projects if full ethical permission has been granted.

What will happen in the unlikely event that I might lose the ability to consent after the study?

- We would like to still retain the samples and personal data collected already and use this confidentially in connection with this project. We also may use this information for further research in future, for projects which are ethically approved.

Will my GP know I am taking part in this study?

- We do not plan to inform your GP as the research will have no impact on your routine care. You can however, ask us to do so.

What if I am already taking part in another study?

- Please let us know if you are involved in another study, as you may not be able to take part in this study.

What will happen to the results of the research study?

- We aim to analyse the results of the research and publish them in leading eye research journals in three years from now – these should be accessible by contacting Professor Lotery's secretary (details on top of page 1). You will not be identified in any report/publication

Who is organising and funding the research?

- This research is being organised by a research group at the University of Southampton lead by Professor Lotery, and is being carried out as part of a PhD project. Funding will be from charities or government organisations.

Who has reviewed the study?

- All research in the NHS is looked at by independent group of people, called a Research Ethics Committee to protect your safety, rights, wellbeing and dignity. This study has been reviewed and given a favourable opinion by Southampton and South West Hampshire Research Ethics Committee.

Where can I obtain further information?

- **For specific information about this research project**: Please contact Professor Lotery's secretary (contact details on top of page 1)
- **For independent advice on this particular research study:** You may contact the Research department at Southampton University Hospitals NHS Trust: R&D Office, Duthie Building (Trust), Ground Floor, MP 138, Southampton General Hospital, Tremona Road, Southampton SO16 6YD. Tel: 02380 795078. You may also contact your hospital's Patient Advice and Liaison Service.
- **For independent advice on research in general:** Please refer to the NHS Research Ethics Service website: www.nres.npsa.nhs.uk

Who can I contact if I am unhappy?

- Any complaint about the way you have been dealt with during the study or any possible harm you might suffer will be addressed. If you have a concern about any aspect of this study, you should ask to speak to the researchers who will do their best to answer your questions (contact details on top of page 1). If you remain unhappy and wish to complain formally, you can do this through the NHS Complaints Procedure (or Private Institution). Details can be obtained from the hospital.
- We are legally bound to tell you the following: "In the event that something does go wrong and you are harmed during the research and this is due to someone's negligence then you may have grounds for a legal action for compensation against Southampton University Hospital NHS Trust (the sponsor) or your local NHS Trust but you may have to pay your legal costs. The normal National Health Service complaints mechanisms will still be available to you (if appropriate)"

How long do I have to decide if I want to take part in the study?

- You have as long as you wish to decide. If you change your mind later then we can always remove your data and samples.

Thank you for reading this information leaflet and for considering taking part in this study. You may keep this leaflet with you.

6.1.6 Screening visit proforma

PROFORMA

STUDY ID: PA_ _

SCREENING VISIT

Study title:
"Pharmacogenetic correlations in AMD" (Retrospective arm) (Ref: protocol V1.1, 10 Aug 11)

REC ref: 11/SC/0106
CI: Professor Andrew Lotery,
Consultant Ophthalmologist,
Southampton General Hospital

Date	
Consent taken?	o
Site	Southampton
Consultant	
Gender	Male o Female o
Age	

LogMAR VA	RightEye: Left Eye:
Family history of eye disease	
Past ophthalmic history including any previous treatment for AMD:	
Recent systemic illnesses	
Medical history	

Concomitant Medications	
Smoking status	Current / Ex / Never If current / ex: No of years: ____ Average no per day: ______
Bloods taken	o 3 bottles (10ml each): Plasma, DNA, serum, (x2 purple top , x1 red top)
Documentation to be placed in Medical Notes	o Copy of consent form o Patient Information Sheet, o Study details sticker o Archive sticker
Number of Lucentis injections up to but not including this visit	Right Eye: Left Eye:
Lucentis injection at this visit?	Right Eye: Yes/ No Left Eye: Yes/ No

Proforma completed by (Print name, sign and date):

……

6.1.7 Vision sciences DNA extraction protocol

DNA Extraction from blood – LD79

1. Read and sign all appropriate risk assessments.
2. Never attempt procedure if you have not been shown how to do it first. You will need to be signed of for this procedure.
3. The procedure must be conducted in LD79 (and access to this room must have been granted first, see Lab manager).
4. The procedure takes 2 consecutive days to complete, do not start day 1 if day 2 cannot be done the following day.
5. Gloves, lab coat and goggles must be worn.

DNA extraction from 10ml whole blood - Day 1

All instructions below are for 10ml of blood or close to (≥8ml). For less than 8mls of blood, adjust the volumes of solutions used as mentioned in part C and D (see volume chart).

A; Preparation

- Turn on water incubator and set temperature to 37˚C.
- Turn on enviro-genie machine on the bench to the right and set the temperature to 4˚C and the rocking speed is set to 22/44.
- Note down the ID's of the blood samples to be extracted in your lab book (12 blood samples can be easily be processed over the 2 consecutive days; alternatively 24 samples could be processed by alternating 2 batches of 12 on the pieces of equipment).
- Label 1 x 50ml and two 15ml conical tubes per sample for later use.

- Make a 1% virkon solution in the squeasy bottle for the use to regularly clean the workspace and to clean any minor blood spills. To do this add one scoop of virkon and fill with warm tap water to ¾ full.
- Make a 1% virkon solution and for soaking used tips in (large plastic beaker on bench for this).
- Make up in the large bucket 1 litre of 1% virkon by add 4 level scoops of virkon to hot tap water. Use the glass stirrer to mix.

B; Defrosting blood samples

- Place the frozen vacutainer blood samples into the water incubator at 37˚C for ~20 minutes with the shaker set on a medium speed.
- Remove the defrosted blood samples from the water incubator then carefully transfer the blood by inversion into a 50ml conical tube using a peg to hold the vacutainer over the conical tube. Dispose of the emptied vacutainer tubes in a blue autoclave bin
- Place the 12 tubes into the 4 suitably sized metal racks for the enviro-genie machine. Then put the samples in the enviro-genie at 4˚C for 1 hr on the rock function (speed 22/44).
- At the end of the 1hr, briefly (~20 sec) spin the blood tubes in large centrifuge @ 1500rpm to ensure any blood is spun down away from the lid of the tube.

C; ELB wash x3 (all blood samples should now be in 50ml conical tubes)

Wash 1

1) **Add 35ml cold ELB** by pouring directly from the bottle (located in fridge) to the 10mls of blood, replace lids and **mix** by inversion.
2) **Place all the tubes in the inviro-genie for 20-30 mins @ 4˚C** on the rock function at a speed of **22/44** (This first ELB wash can be done for up to an hour).
3) **Spin the blood tubes** in the large centrifuge at **1500rpm for 10 mins at 4□C**.

4) **Pour the supernatant** from each tube into the 1% Virkon solution in the large bucket, leaving the pellet of white blood cells at bottom of each tube undisturbed.

Wash 2

5) **Add another 30ml cold ELB,** mix vigorously so as to resuspend as much of the pellet as possible.
6) Place the samples back into the **inviro-genie at 4□ for a further 15 mins**.
7) **Spin again at 1500rpm for 10 mins at 4□**. Pour off supernatant leaving pellet at bottom undisturbed as before.

Wash 3

8) Add final **30ml cold ELB,** mix vigorously so as to resuspend as much of the pellet as possible.
9) Place the samples back into the incubator at 4□ for the last 15 mins.
10) Remove **2 tubes of protease** from the freezer located in a blue box. Leave on bench to defrost.
11) Spin blood tubes at **1500rpm for 10 mins at 4□.**

12) Put a line of paper towels several layers thick on the left of the workspace. Pour off all supernatant into the virkon**,** and **keeping** the **tube upside down, carefully** put the tubes onto tissues to dry for a minute or so. If you see the pellet slipping down the tube as it is inverted, stop and leave the tube upright, but use a 1ml pipette to try and remove as much of the supernatant as possible. If the pellet falls onto the tissue, that area of tissue may be cut out and put back into the tube along with the pellet. Lids of the tubes can be discarded.

D; Overnight Protein Digestion

1) Return the tubes upright into the rack. Using the large purple pipette add **3ml NLB** to all tubes (no.4 on pipette 3 times), **250µl 10% SDS** (no.5 on pipette once) and **150µl** 40mg/ml **Protease** (no.3 on pipette once, add yellow tip to the end) to each of the tubes.

2) Swirl each tube and then pour each pellet into a fresh 15ml labelled conical tube. Put lids on (turn anti-clockwise until it clicks, then clockwise tightly). Dispose of the 50ml tubes into a plastic bag and put in the blue autoclave bin.
3) Put into the correctly sized metal racks and incubate at **37□ overnight** in the enviro-genie machine, set function to rock (speed 11/22). Check tubes for leakage before leaving for the day.

DNA extraction from 10ml whole blood - Day 2

Ethanol Precipitation of DNA

1) Remove tubes from incubator, spin briefly in large centrifuge to clear the lids. Allow to **cool to room temperature** (approximately 30 minutes). Dispose of virkon from yesterday in the sink by putting the grey tube (found by the sink) into the plug hole firmly, stir and pour the virkon waste directly down the tube. Clean out the bucket with a little cream cleaner found by the sink, dry and return bucket to the shelf.
2) Remove all lids of the 15ml tubes and **add 1ml** saturated **NaCl solution** (no.4 on pipette), replace lids and **shake** tubes vigorously (6 in each hand) for **15 seconds**, and then **spin at 4000rpm** for **20mins** at room temperature in large centrifuge.
3) Using a P1000 pipette, take as much as possible (3-4ml) of the **supernatant** into the **fresh, labelled 15ml tubes**. If the last ml of supernatant is not clear, transfer it to a 1.5ml eppendorf tube, label it clearly and spin in the microcentrifuge at 14,000rpm for 5mins. Then pour this into the corresponding 15ml tube.
4) Using the 5ml Gilson pipette, **add** exactly **twice the volume** of **cold Absolute Ethanol** found in the fridge (Example: If tube contains 4ml supernatant, add **2x** 4 ml absolute ethanol), invert the tube gently until the DNA precipitates out and forms a fluffy pellet.
5) **Add 1ml** of **70% Ethanol** to labelled 1.5ml eppendorfs.
6) Remove the sticky pellet using a yellow tip on a 200µl pipette and place it in the corresponding eppendorf (pour remaining ethanol into glass beaker found on shelf or by sink). This may be left in the 70% ethanol for several hours. Repeat the wash if the DNA looks very brown.
7) Then **pulse spin** the eppendorfs in microcentrifuge (hold pulse button for 10-15seconds), **pour off** the **ethanol** (making sure the DNA stays in the tube), blot the end of the tube, rest on its side on the bench and **allow the DNA to nearly dry** (~15mins).
8) **Add 500µl TE Buffer** (adjust if DNA yield is low) and allow DNA to dissolve overnight at room temperature, then put in fridge or freezer depending on your needs the following day.

Solution volume chart for DNA extraction from whole blood

Solution	**tube**	**10ml blood**	**tube**	**5ml blood**	**tube**	**2.5ml blood**
ELB wash	50ml	20-30 mins 35ml	50ml	20-30 mins 30ml	15ml	20-30 mins 12.5ml
ELB wash		15 mins 30ml		15 mins 30ml		15 mins 12.5ml
ELB wash		15 mins 30ml		15 mins 30ml		15 mins 12.5ml
NLB	15ml	3ml	15ml	2ml	15ml	1.5ml
10% SDS		250µl		200µl		150µl
40mg/ml protease		150µl		100µl		75µl
Saturated NaCl		1.0ml		750µl		500µl
Supernatant	15ml	4.5ml±?	15ml	3ml±?	15ml	2ml±?
Cold absolute ethanol		9ml±?		6ml±?		4ml±?
70% ethanol		1.0ml		1ml		1.0ml
TE buffer		500µl?		500µl?		200-500µl?

6.1.8 Protocol for processing plasma and serum samples

PROTOCOL FOR PROCESSING BLOODS FOR CHARLES AMD PROJECT

Separation of plasma (purple top vacutainer EDTA tube) /serum (red top vacutainer tube) from whole blood

1. Ensure **serum left standing** at room temperature for at least 2**0 mins until visible retraction of clot from vacutainer.**
2. **Centrifuge** 10 ml blood tube at room temp.

- Serum 3897 rpm for 5 minutes

- Plasma 2600 rpm for 10 minutes

3. **Pipette separated serum into eppendorf tubes and perform high speed (14 000 rpm) separation in microcentrifuge for 2 minutes**
4. Pipette **5 x 200ul aliquots** of supernatant into 1.5ml screw top tubes. Pipette the remaining volume into **1ml aliquots**. Be careful not to disturb the red blood cells.

- Serum □ Yellow Topped

- Plasma □ Green Topped

5. **Label each tube** with:
    i. Patient study code
    ii. Constituent (plasma / serum)
    iii. Volume (ul)
    iv. Visit number
6. Replace lids on 10ml blood tubes and dispose of in the **blue autoclave box**, clean work area with **Virkon.**
7. Place in **-80 freezer** in LD81

Storage of EDTA (purple top) collection tubes for DNA

1. Remove pt ID and label each tube with patient study code
2. Place plastic collection tubes in **-20 freezer** in bag marked “Charles”

Extra precautions to be taken for all blood samples (due to potential HIV / HBV / HCV infection)

1. No sharps (inc no glass tubes).
2. Prepare 1% Virkon beforehand for cleaning spills and disposing of tips.
3. Ensure the lids are used when spinning in the centrifuge.

6.1.9 Two stage protocol for processing serum samples

PROTOCOL FOR PROCESSING BLOODS FOR CHARLES AMD PROJECT

Separation of plasma (purple top vacutainer EDTA tube) /serum (red top vacutainer tube) from whole blood

8. Ensure **serum left standing** at room temperature for at least 2**0 mins until visible retraction of clot from vacutainer.**
9. **Centrifuge** 10 ml blood tube at room temp.

- Serum 3897 rpm for 5 minutes

- Plasma 2600 rpm for 10 minutes

10. **Pipette separated serum into eppendorf tubes and perform high speed (14 000 rpm) separation in microcentrifuge for 2 minutes**
11. Pipette **5 x 200ul aliquots** of supernatant into 1.5ml screw top tubes. Pipette the remaining volume into **1ml aliquots**. Be careful not to disturb the red blood cells.

- Serum □ Yellow Topped

- Plasma □ Green Topped

12. **Label each tube** with:
    i. Patient study code
    ii. Constituent (plasma / serum)
    iii. Volume (ul)
    iv. Visit number
13. Replace lids on 10ml blood tubes and dispose of in the **blue autoclave box**, clean work area with **Virkon.**
14. Place in **-80 freezer** in LD81

Storage of EDTA (purple top) collection tubes for DNA

3. Remove pt ID and label each tube with patient study code
4. Place plastic collection tubes in **-20 freezer** in bag marked “Charles”

Extra precautions to be taken for all blood samples (due to potential HIV / HBV / HCV infection)

4. No sharps (inc no glass tubes).
5. Prepare 1% Virkon beforehand for cleaning spills and disposing of tips.
6. Ensure the lids are used when spinning in the centrifuge

7 Reference List

1. Resnikoff S, Pascolini D, Etya'ale D et al. Global data on visual impairment in the year 2002. Bull World Health Organ 2004;82(11):844-851.

2. Klein R, Cruickshanks KJ, Nash SD et al. The prevalence of age-related macular degeneration and associated risk factors. Arch Ophthalmol 2010;128(6):750-758.

3. Seland JH, Vingerling JR, Augood CA et al. Visual impairment and quality of life in the older European population, the EUREYE study. Acta Ophthalmol 2011;89(7):608-613.

4. Bunce C, Wormald R. Leading causes of certification for blindness and partial sight in England & Wales. BMC Public Health 2006;6:58.

5. Ferris FL, III, Wilkinson CP, Bird A et al. Clinical classification of age-related macular degeneration. Ophthalmology 2013;120(4):844-851.

6. Owen CG, Fletcher AE, Donoghue M, Rudnicka AR. How big is the burden of visual loss caused by age related macular degeneration in the United Kingdom? Br J Ophthalmol 2003;87(3):312-317.

7. Gehrs KM, Anderson DH, Johnson LV, Hageman GS. Age-related macular degeneration--emerging pathogenetic and therapeutic concepts. Ann Med 2006;38(7):450-471.

8. Chakravarthy U, Harding SP, Rogers CA et al. Ranibizumab versus bevacizumab to treat neovascular age-related macular degeneration: one-year findings from the IVAN randomized trial. Ophthalmology 2012;119(7):1399-1411.

9. Masland RH. The fundamental plan of the retina. Nat Neurosci 2001;4(9):877-886.

10. Neubauer AS, Priglinger S, Ullrich S et al. Comparison of foveal thickness measured with the retinal thickness analyzer and optical coherence tomography. Retina 2001;21(6):596-601.

11. Yamada E. Some structural features of the fovea centralis in the human retina. Arch Ophthalmol 1969;82(2):151-159.

12. Berson DM, Dunn FA, Takao M. Phototransduction by retinal ganglion cells that set the circadian clock. Science 2002;295(5557):1070-1073.

13. Boycott BB, Wassle H. Morphological Classification of Bipolar Cells of the Primate Retina. Eur J Neurosci 1991;3(11):1069-1088.

14. Strauss O. The retinal pigment epithelium in visual function. Physiol Rev 2005;85(3):845-881.

15. Jonas JB, Schneider U, Naumann GO. Count and density of human retinal photoreceptors. Graefes Arch Clin Exp Ophthalmol 1992;230(6):505-510.

16. HOGAN MJ. Ultrastructure of the choroid. Its role in the pathogenesis of chorioretinal disease. Trans Pac Coast Otoophthalmol Soc Annu Meet 1961;42:61-87.

17. Wolf G. The visual cycle of the cone photoreceptors of the retina. Nutr Rev 2004;62(7 Pt 1):283-286.

18. Gass JD. Drusen and disciform macular detachment and degeneration. 1972. Retina 2003;23(6 Suppl):409-436.

19. Sarks S, Cherepanoff S, Killingsworth M, Sarks J. Relationship of Basal laminar deposit and membranous debris to the clinical presentation of early age-related macular degeneration. Invest Ophthalmol Vis Sci 2007;48(3):968-977.

20. Rudolf M, Clark ME, Chimento MF, Li CM, Medeiros NE, Curcio CA. Prevalence and morphology of druse types in the macula and periphery of eyes with age-related maculopathy. Invest Ophthalmol Vis Sci 2008;49(3):1200-1209.

21. Anderson DH, Talaga KC, Rivest AJ, Barron E, Hageman GS, Johnson LV. Characterization of beta amyloid assemblies in drusen: the deposits associated with aging and age-related macular degeneration. Exp Eye Res 2004;78(2):243-256.

22. Hageman GS, Mullins RF, Russell SR, Johnson LV, Anderson DH. Vitronectin is a constituent of ocular drusen and the vitronectin gene is expressed in human retinal pigmented epithelial cells. FASEB J 1999;13(3):477-484.

23. Curcio CA, Johnson M, Rudolf M, Huang JD. The oil spill in ageing Bruch membrane. Br J Ophthalmol 2011;95(12):1638-1645.

24. Risk factors for choroidal neovascularization in the second eye of patients with juxtafoveal or subfoveal choroidal neovascularization secondary to age-related macular degeneration. Macular Photocoagulation Study Group. Arch Ophthalmol 1997;115(6):741-747.

25. Klein R, Klein BE, Knudtson MD, Meuer SM, Swift M, Gangnon RE. Fifteen-year cumulative incidence of age-related macular degeneration: the Beaver Dam Eye Study. Ophthalmology 2007;114(2):253-262.

26. Green WR, Key SN, III. Senile macular degeneration: a histopathologic study. Trans Am Ophthalmol Soc 1977;75:180-254.

27. Sunness JS, Bressler NM, Maguire MG. Scanning laser ophthalmoscopic analysis of the pattern of visual loss in age-related geographic atrophy of the macula. Am J Ophthalmol 1995;119(2):143-151.

28. Joachim N, Mitchell P, Kifley A, Rochtchina E, Hong T, Wang JJ. Incidence and progression of geographic atrophy: observations from a population-based cohort. Ophthalmology 2013;120(10):2042-2050.

29. Maguire P, Vine AK. Geographic atrophy of the retinal pigment epithelium. Am J Ophthalmol 1986;102(5):621-625.

30. Sarks JP, Sarks SH, Killingsworth MC. Evolution of geographic atrophy of the retinal pigment epithelium. Eye (Lond) 1988;2 (Pt 5):552-577.

31. Green WR, Enger C. Age-related macular degeneration histopathologic studies: the 1992 Lorenz E. Zimmerman Lecture. 1992. Retina 2005;25(5 Suppl):1519-1535.

32. Hartnett ME, Weiter JJ, Garsd A, Jalkh AE. Classification of retinal pigment epithelial detachments associated with drusen. Graefes Arch Clin Exp Ophthalmol 1992;230(1):11-19.

33. Kuhn D, Meunier I, Soubrane G, Coscas G. Imaging of chorioretinal anastomoses in vascularized retinal pigment epithelium detachments. Arch Ophthalmol 1995;113(11):1392-1398.

34. Hartnett ME, Weiter JJ, Staurenghi G, Elsner AE. Deep retinal vascular anomalous complexes in advanced age-related macular degeneration. Ophthalmology 1996;103(12):2042-2053.

35. Slakter JS, Yannuzzi LA, Schneider U et al. Retinal choroidal anastomoses and occult choroidal neovascularization in age-related macular degeneration. Ophthalmology 2000;107(4):742-753.

36. Casswell AG, Kohen D, Bird AC. Retinal pigment epithelial detachments in the elderly: classification and outcome. Br J Ophthalmol 1985;69(6):397-403.

37. Elman MJ, Fine SL, Murphy RP, Patz A, Auer C. The natural history of serous retinal pigment epithelium detachment in patients with age-related macular degeneration. Ophthalmology 1986;93(2):224-230.

38. Klein R, Klein BE, Tomany SC, Meuer SM, Huang GH. Ten-year incidence and progression of age-related maculopathy: The Beaver Dam eye study. Ophthalmology 2002;109(10):1767-1779.

39. Wang JJ, Rochtchina E, Lee AJ et al. Ten-year incidence and progression of age-related maculopathy: the blue Mountains Eye Study. Ophthalmology 2007;114(1):92-98.

40. Jonasson F, Fisher DE, Eiriksdottir G et al. Five-year incidence, progression, and risk factors for age-related macular degeneration: the age, gene/environment susceptibility study. Ophthalmology 2014;121(9):1766-1772.

41. Tomany SC, Wang JJ, Van LR et al. Risk factors for incident age-related macular degeneration: pooled findings from 3 continents. Ophthalmology 2004;111(7):1280-1287.

42. Tan JS, Mitchell P, Kifley A, Flood V, Smith W, Wang JJ. Smoking and the long-term incidence of age-related macular degeneration: the Blue Mountains Eye Study. Arch Ophthalmol 2007;125(8):1089-1095.

43. Smith W, Mitchell P, Leeder SR. Smoking and age-related maculopathy. The Blue Mountains Eye Study. Arch Ophthalmol 1996;114(12):1518-1523.

44. Risk factors associated with age-related macular degeneration. A case-control study in the age-related eye disease study: Age-Related Eye Disease Study Report Number 3. Ophthalmology 2000;107(12):2224-2232.

45. Klein R, Klein BE, Linton KL, DeMets DL. The Beaver Dam Eye Study: the relation of age-related maculopathy to smoking. Am J Epidemiol 1993;137(2):190-200.

46. Cho E, Stampfer MJ, Seddon JM et al. Prospective study of zinc intake and the risk of age-related macular degeneration. Ann Epidemiol 2001;11(5):328-336.

47. Querques G, Souied EH. The role of omega-3 and micronutrients in age-related macular degeneration. Surv Ophthalmol 2014;59(5):532-539.

48. Lutein + zeaxanthin and omega-3 fatty acids for age-related macular degeneration: the Age-Related Eye Disease Study 2 (AREDS2) randomized clinical trial. JAMA 2013;309(19):2005-2015.

49. Smith W, Mitchell P, Leeder SR. Dietary fat and fish intake and age-related maculopathy. Arch Ophthalmol 2000;118(3):401-404.

50. Smith W, Mitchell P, Leeder SR, Wang JJ. Plasma fibrinogen levels, other cardiovascular risk factors, and age-related maculopathy: the Blue Mountains Eye Study. Arch Ophthalmol 1998;116(5):583-587.

51. Gehlbach P, Li T, Hatef E. Statins for age-related macular degeneration. Cochrane Database Syst Rev 2015;2:CD006927.

52. Ersoy L, Ristau T, Lechanteur YT et al. Nutritional risk factors for age-related macular degeneration. Biomed Res Int 2014;2014:413150.

53. Machalinska A, Kawa MP, Marlicz W, Machalinski B. Complement system activation and endothelial dysfunction in patients with age-related macular degeneration (AMD): possible relationship between AMD and atherosclerosis. Acta Ophthalmol 2012;90(8):695-703.

54. Mullins RF, Russell SR, Anderson DH, Hageman GS. Drusen associated with aging and age-related macular degeneration contain proteins common to extracellular deposits associated with atherosclerosis, elastosis, amyloidosis, and dense deposit disease. FASEB J 2000;14(7):835-846.

55. Mullins RF, Aptsiauri N, Hageman GS. Structure and composition of drusen associated with glomerulonephritis: implications for the role of complement activation in drusen biogenesis. Eye (Lond) 2001;15(Pt 3):390-395.

56. Anderson DH, Radeke MJ, Gallo NB et al. The pivotal role of the complement system in aging and age-related macular degeneration: hypothesis re-visited. Prog Retin Eye Res 2010;29(2):95-112.

57. Dunkelberger JR, Song WC. Complement and its role in innate and adaptive immune responses. Cell Res 2010;20(1):34-50.

58. Klein R, Cruickshanks KJ, Myers CE et al. The relationship of atherosclerosis to the 10-year cumulative incidence of age-related macular degeneration: the Beaver Dam studies. Ophthalmology 2013;120(5):1012-1019.

59. Grunin M, Hagbi-Levi S, Chowers I. The role of monocytes and macrophages in age-related macular degeneration. Adv Exp Med Biol 2014;801:199-205.

60. Chakravarthy U, Wong TY, Fletcher A et al. Clinical risk factors for age-related macular degeneration: a systematic review and meta-analysis. BMC Ophthalmol 2010;10:31.

61. Metelitsina TI, Grunwald JE, DuPont JC, Ying GS. Effect of systemic hypertension on foveolar choroidal blood flow in age related macular degeneration. Br J Ophthalmol 2006;90(3):342-346.

62. Hyman L, Schachat AP, He Q, Leske MC. Hypertension, cardiovascular disease, and age-related macular degeneration. Age-Related Macular Degeneration Risk Factors Study Group. Arch Ophthalmol 2000;118(3):351-358.

63. Ennis S, Jomary C, Mullins R et al. Association between the SERPING1 gene and age-related macular degeneration: a two-stage case-control study. Lancet 2008;372(9652):1828-1834.

64. Lotery A, Trump D. Progress in defining the molecular biology of age related macular degeneration. Hum Genet 2007;122(3-4):219-236.

65. Walport MJ. Complement. First of two parts. N Engl J Med 2001;344(14):1058-1066.

66. Gelfand JA, Sherins RJ, Alling DW, Frank MM. Treatment of hereditary angioedema with danazol. Reversal of clinical and biochemical abnormalities. N Engl J Med 1976;295(26):1444-1448.

67. Park KH, Ryu E, Tosakulwong N, Wu Y, Edwards AO. Common variation in the SERPING1 gene is not associated with age-related macular degeneration in two independent groups of subjects. Mol Vis 2009;15:200-207.

68. Allikmets R, Dean M, Hageman GS et al. The SERPING1 gene and age-related macular degeneration. Lancet 2009;374(9693):875-876.

69. McGwin G, Jr. Incorrect study design and analysis: the effect of genetic variants in SERPING1 on the risk of neovascular age-related macular degeneration. Br J Ophthalmol 2011;95(11):1616-1617.

70. Gibson J, Hakobyan S, Cree AJ et al. Variation in complement component C1 inhibitor in age-related macular degeneration. Immunobiology 2012;217(2):251-255.

71. Nozaki M, Raisler BJ, Sakurai E et al. Drusen complement components C3a and C5a promote choroidal neovascularization. Proc Natl Acad Sci U S A 2006;103(7):2328-2333.

72. Hageman GS, Luthert PJ, Victor Chong NH, Johnson LV, Anderson DH, Mullins RF. An integrated hypothesis that considers drusen as biomarkers of immune-mediated processes at the RPE-Bruch's membrane interface in aging and age-related macular degeneration. Prog Retin Eye Res 2001;20(6):705-732.

73. Klein RJ, Zeiss C, Chew EY et al. Complement factor H polymorphism in age-related macular degeneration. Science 2005;308(5720):385-389.

74. Clark SJ, Bishop PN. Role of Factor H and Related Proteins in Regulating Complement Activation in the Macula, and Relevance to Age-Related Macular Degeneration. J Clin Med 2015;4(1):18-31.

75. Edwards AO, Ritter R, III, Abel KJ, Manning A, Panhuysen C, Farrer LA. Complement factor H polymorphism and age-related macular degeneration. Science 2005;308(5720):421-424.

76. Klein ML, Francis PJ, Rosner B et al. CFH and LOC387715/ARMS2 genotypes and treatment with antioxidants and zinc for age-related macular degeneration. Ophthalmology 2008;115(6):1019-1025.

77. Donoso LA, Vrabec T, Kuivaniemi H. The role of complement Factor H in age-related macular degeneration: a review. Surv Ophthalmol 2010;55(3):227-246.

78. Leveziel N, Zerbib J, Richard F et al. Genotype-phenotype correlations for exudative age-related macular degeneration associated with homozygous HTRA1 and CFH genotypes. Invest Ophthalmol Vis Sci 2008;49(7):3090-3094.

79. Seitsonen S, Jarvela I, Meri S, Tommila P, Ranta P, Immonen I. Complement factor H Y402H polymorphism and characteristics of exudative age-related macular degeneration lesions. Acta Ophthalmol 2008;86(4):390-394.

80. Wegscheider BJ, Weger M, Renner W et al. Association of complement factor H Y402H gene polymorphism with different subtypes of exudative age-related macular degeneration. Ophthalmology 2007;114(4):738-742.

81. Magnusson KP, Duan S, Sigurdsson H et al. CFH Y402H confers similar risk of soft drusen and both forms of advanced AMD. PLoS Med 2006;3(1):e5.

82. Smailhodzic D, Muether PS, Chen J et al. Cumulative effect of risk alleles in CFH, ARMS2, and VEGFA on the response to ranibizumab treatment in age-related macular degeneration. Ophthalmology 2012;119(11):2304-2311.

83. Brantley MA, Jr., Fang AM, King JM, Tewari A, Kymes SM, Shiels A. Association of complement factor H and LOC387715 genotypes with response of exudative age-related macular degeneration to intravitreal bevacizumab. Ophthalmology 2007;114(12):2168-2173.

84. Khandhadia S, Foster S, Cree A et al. Chlamydia infection status, genotype, and age-related macular degeneration. Mol Vis 2012;18:29-37.

85. Robman L, Mahdi O, McCarty C et al. Exposure to Chlamydia pneumoniae infection and progression of age-related macular degeneration. Am J Epidemiol 2005;161(11):1013-1019.

86. Kalayoglu MV, Bula D, Arroyo J, Gragoudas ES, D'Amico D, Miller JW. Identification of Chlamydia pneumoniae within human choroidal neovascular membranes secondary to age-related macular degeneration. Graefes Arch Clin Exp Ophthalmol 2005;243(11):1080-1090.

87. Lechanteur YT, van de Camp PL, Smailhodzic D et al. Association of Smoking and CFH and ARMS2 Risk Variants With Younger Age at Onset of Neovascular Age-Related Macular Degeneration. JAMA Ophthalmol 2015.

88. Smith W, Assink J, Klein R et al. Risk factors for age-related macular degeneration: Pooled findings from three continents. Ophthalmology 2001;108(4):697-704.

89. Vingerling JR, Hofman A, Grobbee DE, De Jong PT. Age-related macular degeneration and smoking. The Rotterdam Study. Arch Ophthalmol 1996;114(10):1193-1196.

90. Kavanagh D, Yu Y, Schramm EC et al. Rare Genetic Variants in the CFI Gene are Associated with Advanced Age-Related Macular Degeneration and Commonly Result in Reduced Serum Factor I Levels. Hum Mol Genet 2015.

91. Alexander P, Gibson J, Cree AJ, Ennis S, Lotery AJ. Complement factor I and age-related macular degeneration. Mol Vis 2014;20:1253-1257.

92. Gold B, Merriam JE, Zernant J et al. Variation in factor B (BF) and complement component 2 (C2) genes is associated with age-related macular degeneration. Nat Genet 2006;38(4):458-462.

93. Yates JR, Sepp T, Matharu BK et al. Complement C3 variant and the risk of age-related macular degeneration. N Engl J Med 2007;357(6):553-561.

94. Baggiolini M, Clark-Lewis I. Interleukin-8, a chemotactic and inflammatory cytokine. FEBS Lett 1992;307(1):97-101.

95. Goverdhan SV, Ennis S, Hannan SR et al. Interleukin-8 promoter polymorphism -251A/T is a risk factor for age-related macular degeneration. Br J Ophthalmol 2008;92(4):537-540.

96. Falk MK, Singh A, Faber C, Nissen MH, Hviid T, Sorensen TL. CX3CL1/CX3CR1 and CCL2/CCR2 Chemokine/Chemokine Receptor Complex in Patients with AMD. PLoS One 2014;9(12):e112473.

97. Gupta D, Gupta V, Singh V et al. Study of Polymorphisms in CX3CR1, PLEKHA1 and VEGF genes as risk factors for age-related macular degeneration in Indian patients. Arch Med Res 2014;45(6):489-494.

98. Chan CC, Tuo J, Bojanowski CM, Csaky KG, Green WR. Detection of CX3CR1 single nucleotide polymorphism and expression on archived eyes with age-related macular degeneration. Histol Histopathol 2005;20(3):857-863.

99. Tuo J, Smith BC, Bojanowski CM et al. The involvement of sequence variation and expression of CX3CR1 in the pathogenesis of age-related macular degeneration. FASEB J 2004;18(11):1297-1299.

100. Combadiere C, Feumi C, Raoul W et al. CX3CR1-dependent subretinal microglia cell accumulation is associated with cardinal features of age-related macular degeneration. J Clin Invest 2007;117(10):2920-2928.

101. Iejima D, Itabashi T, Kawamura Y et al. HTRA1 (High Temperature Requirement A Serine Peptidase 1) Gene Is Transcriptionally Regulated by Insertion/Deletion Nucleotides Located at the 3' End of the ARMS2 (Age-related Maculopathy Susceptibility 2) Gene in Patients with Age-related Macular Degeneration. J Biol Chem 2015;290(5):2784-2797.

102. Kanda A, Chen W, Othman M et al. A variant of mitochondrial protein LOC387715/ARMS2, not HTRA1, is strongly associated with age-related macular degeneration. Proc Natl Acad Sci U S A 2007;104(41):16227-16232.

103. Cascella R, Ragazzo M, Strafella C et al. Age-related macular degeneration: insights into inflammatory genes. J Ophthalmol 2014;2014:582842.

104. Levy O, Calippe B, Lavalette S et al. Apolipoprotein E promotes subretinal mononuclear phagocyte survival and chronic inflammation in age-related macular degeneration. EMBO Mol Med 2015;7(2):211-226.

105. Klaver CC, Kliffen M, van Duijn CM et al. Genetic association of apolipoprotein E with age-related macular degeneration. Am J Hum Genet 1998;63(1):200-206.

106. Baird PN, Richardson AJ, Robman LD et al. Apolipoprotein (APOE) gene is associated with progression of age-related macular degeneration (AMD). Hum Mutat 2006;27(4):337-342.

107. Schmidt S, Klaver C, Saunders A et al. A pooled case-control study of the apolipoprotein E (APOE) gene in age-related maculopathy. Ophthalmic Genet 2002;23(4):209-223.

108. Allikmets R, Shroyer NF, Singh N et al. Mutation of the Stargardt disease gene (ABCR) in age-related macular degeneration. Science 1997;277(5333):1805-1807.

109. Senger DR, Galli SJ, Dvorak AM, Perruzzi CA, Harvey VS, Dvorak HF. Tumor cells secrete a vascular permeability factor that promotes accumulation of ascites fluid. Science 1983;219(4587):983-985.

110. Connolly DT, Olander JV, Heuvelman D et al. Human vascular permeability factor. Isolation from U937 cells. J Biol Chem 1989;264(33):20017-20024.

111. Dehghanian F, Hojati Z, Kay M. New Insights into VEGF-A Alternative Splicing: Key Regulatory Switching in the Pathological Process. Avicenna J Med Biotechnol 2014;6(4):192-199.

112. Houck KA, Ferrara N, Winer J, Cachianes G, Li B, Leung DW. The vascular endothelial growth factor family: identification of a fourth molecular species and characterization of alternative splicing of RNA. Mol Endocrinol 1991;5(12):1806-1814.

113. Ferrara N. Vascular endothelial growth factor and age-related macular degeneration: from basic science to therapy. Nat Med 2010;16(10):1107-1111.

114. Presta LG, Chen H, O'Connor SJ et al. Humanization of an anti-vascular endothelial growth factor monoclonal antibody for the therapy of solid tumors and other disorders. Cancer Res 1997;57(20):4593-4599.

115. Yuan X, Gu X, Crabb JS et al. Quantitative proteomics: comparison of the macular Bruch membrane/choroid complex from age-related macular degeneration and normal eyes. Mol Cell Proteomics 2010;9(6):1031-1046.

116. Reynolds R, Hartnett ME, Atkinson JP, Giclas PC, Rosner B, Seddon JM. Plasma complement components and activation fragments: associations with age-related macular degeneration genotypes and phenotypes. Invest Ophthalmol Vis Sci 2009;50(12):5818-5827.

117. Bhutto IA, Baba T, Merges C, Juriasinghani V, McLeod DS, Lutty GA. C-reactive protein and complement factor H in aged human eyes and eyes with age-related macular degeneration. Br J Ophthalmol 2011;95(9):1323-1330.

118. Johnson PT, Betts KE, Radeke MJ, Hageman GS, Anderson DH, Johnson LV. Individuals homozygous for the age-related macular degeneration risk-conferring variant of complement factor H have elevated levels of CRP in the choroid. Proc Natl Acad Sci U S A 2006;103(46):17456-17461.

119. Karlstetter M, Langmann T. Microglia in the aging retina. Adv Exp Med Biol 2014;801:207-212.

120. Xu H, Chen M, Forrester JV. Para-inflammation in the aging retina. Prog Retin Eye Res 2009;28(5):348-368.

121. Ardeljan CP, Ardeljan D, Abu-Asab M, Chan CC. Inflammation and Cell Death in Age-Related Macular Degeneration: An Immunopathological and Ultrastructural Model. J Clin Med 2014;3(4):1542-1560.

122. Gupta N, Brown KE, Milam AH. Activated microglia in human retinitis pigmentosa, late-onset retinal degeneration, and age-related macular degeneration. Exp Eye Res 2003;76(4):463-471.

123. Plafker SM, O'Mealey GB, Szweda LI. Mechanisms for countering oxidative stress and damage in retinal pigment epithelium. Int Rev Cell Mol Biol 2012;298:135-177.

124. Kinnunen K, Petrovski G, Moe MC, Berta A, Kaarniranta K. Molecular mechanisms of retinal pigment epithelium damage and development of age-related macular degeneration. Acta Ophthalmol 2012;90(4):299-309.

125. Combadiere C, Feumi C, Raoul W et al. CX3CR1-dependent subretinal microglia cell accumulation is associated with cardinal features of age-related macular degeneration. J Clin Invest 2007;117(10):2920-2928.

126. Chan CC, Ross RJ, Shen D et al. Ccl2/Cx3cr1-deficient mice: an animal model for age-related macular degeneration. Ophthalmic Res 2008;40(3-4):124-128.

127. Tuo J, Smith BC, Bojanowski CM et al. The involvement of sequence variation and expression of CX3CR1 in the pathogenesis of age-related macular degeneration. FASEB J 2004;18(11):1297-1299.

128. Chan CC, Ross RJ, Shen D et al. Ccl2/Cx3cr1-deficient mice: an animal model for age-related macular degeneration. Ophthalmic Res 2008;40(3-4):124-128.

129. Ross RJ, Zhou M, Shen D et al. Immunological protein expression profile in Ccl2/Cx3cr1 deficient mice with lesions similar to age-related macular degeneration. Exp Eye Res 2008;86(4):675-683.

130. Raoul W, Auvynet C, Camelo S et al. CCL2/CCR2 and CX3CL1/CX3CR1 chemokine axes and their possible involvement in age-related macular degeneration. J Neuroinflammation 2010;7:87.

131. Mattapallil MJ, Wawrousek EF, Chan CC et al. The Rd8 mutation of the Crb1 gene is present in vendor lines of C57BL/6N mice and embryonic stem cells, and confounds ocular induced mutant phenotypes. Invest Ophthalmol Vis Sci 2012;53(6):2921-2927.

132. Malek G, Johnson LV, Mace BE et al. Apolipoprotein E allele-dependent pathogenesis: a model for age-related retinal degeneration. Proc Natl Acad Sci U S A 2005;102(33):11900-11905.

133. Imamura Y, Noda S, Hashizume K et al. Drusen, choroidal neovascularization, and retinal pigment epithelium dysfunction in SOD1-deficient mice: a model of age-related macular degeneration. Proc Natl Acad Sci U S A 2006;103(30):11282-11287.

134. Coffey PJ, Gias C, McDermott CJ et al. Complement factor H deficiency in aged mice causes retinal abnormalities and visual dysfunction. Proc Natl Acad Sci U S A 2007;104(42):16651-16656.

135. Weng J, Mata NL, Azarian SM, Tzekov RT, Birch DG, Travis GH. Insights into the function of Rim protein in photoreceptors and etiology of Stargardt's disease from the phenotype in abcr knockout mice. Cell 1999;98(1):13-23.

136. Dobi ET, Puliafito CA, Destro M. A new model of experimental choroidal neovascularization in the rat. Arch Ophthalmol 1989;107(2):264-269.

137. Ufret-Vincenty RL, Aredo B, Liu X et al. Transgenic mice expressing variants of complement factor H develop AMD-like retinal findings. Invest Ophthalmol Vis Sci 2010;51(11):5878-5887.

138. Hoh KJ, Lenassi E, Malik TH, Pickering MC, Jeffery G. Complement component C3 plays a critical role in protecting the aging retina in a murine model of age-related macular degeneration. Am J Pathol 2013;183(2):480-492.

139. Ambati J, Anand A, Fernandez S et al. An animal model of age-related macular degeneration in senescent Ccl-2- or Ccr-2-deficient mice. Nat Med 2003;9(11):1390-1397.

140. Hollyfield JG, Bonilha VL, Rayborn ME et al. Oxidative damage-induced inflammation initiates age-related macular degeneration. Nat Med 2008;14(2):194-198.

141. Laser photocoagulation of subfoveal neovascular lesions of age-related macular degeneration. Updated findings from two clinical trials. Macular Photocoagulation Study Group. Arch Ophthalmol 1993;111(9):1200-1209.

142. Photodynamic therapy of subfoveal choroidal neovascularization in age-related macular degeneration with verteporfin: one-year results of 2 randomized clinical trials--TAP report. Treatment of age-related macular degeneration with photodynamic therapy (TAP) Study Group. Arch Ophthalmol 1999;117(10):1329-1345.

143. Ng EW, Shima DT, Calias P, Cunningham ET, Jr., Guyer DR, Adamis AP. Pegaptanib, a targeted anti-VEGF aptamer for ocular vascular disease. Nat Rev Drug Discov 2006;5(2):123-132.

144. Gragoudas ES, Adamis AP, Cunningham ET, Jr., Feinsod M, Guyer DR. Pegaptanib for neovascular age-related macular degeneration. N Engl J Med 2004;351(27):2805-2816.

145. Adamis AP, Shima DT, Tolentino MJ et al. Inhibition of vascular endothelial growth factor prevents retinal ischemia-associated iris neovascularization in a nonhuman primate. Arch Ophthalmol 1996;114(1):66-71.

146. Gordon MS, Margolin K, Talpaz M et al. Phase I safety and pharmacokinetic study of recombinant human anti-vascular endothelial growth factor in patients with advanced cancer. J Clin Oncol 2001;19(3):843-850.

147. Mordenti J, Cuthbertson RA, Ferrara N et al. Comparisons of the intraocular tissue distribution, pharmacokinetics, and safety of 125I-labeled full-length and Fab antibodies in rhesus monkeys following intravitreal administration. Toxicol Pathol 1999;27(5):536-544.

148. Holash J, Davis S, Papadopoulos N et al. VEGF-Trap: a VEGF blocker with potent antitumor effects. Proc Natl Acad Sci U S A 2002;99(17):11393-11398.

149. Stewart MW, Rosenfeld PJ. Predicted biological activity of intravitreal VEGF Trap. Br J Ophthalmol 2008;92(5):667-668.

150. Brown DM, Kaiser PK, Michels M et al. Ranibizumab versus verteporfin for neovascular age-related macular degeneration. N Engl J Med 2006;355(14):1432-1444.

151. Rosenfeld PJ, Brown DM, Heier JS et al. Ranibizumab for neovascular age-related macular degeneration. N Engl J Med 2006;355(14):1419-1431.

152. Abraham P, Yue H, Wilson L. Randomized, double-masked, sham-controlled trial of ranibizumab for neovascular age-related macular degeneration: PIER study year 2. Am J Ophthalmol 2010;150(3):315-324.

153. Lalwani GA, Rosenfeld PJ, Fung AE et al. A variable-dosing regimen with intravitreal ranibizumab for neovascular age-related macular degeneration: year 2 of the PrONTO Study. Am J Ophthalmol 2009;148(1):43-58.

154. Martin DF, Maguire MG, Fine SL et al. Ranibizumab and bevacizumab for treatment of neovascular age-related macular degeneration: two-year results. Ophthalmology 2012;119(7):1388-1398.

155. Chakravarthy U, Harding SP, Rogers CA et al. Ranibizumab versus bevacizumab to treat neovascular age-related macular degeneration: one-year findings from the IVAN randomized trial. Ophthalmology 2012;119(7):1399-1411.

156. Heier JS, Brown DM, Chong V et al. Intravitreal aflibercept (VEGF trap-eye) in wet age-related macular degeneration. Ophthalmology 2012;119(12):2537-2548.

157. Orzalesi N, Pierrottet CO, Zenoni S, Savaresi C. The IOL-Vip System: a double intraocular lens implant for visual rehabilitation of patients with macular disease. Ophthalmology 2007;114(5):860-865.

158. Takeuchi K, Kachi S, Iwata E, Ishikawa K, Terasaki H. Visual function 5 years or more after macular translocation surgery for myopic choroidal neovascularisation and age-related macular degeneration. Eye (Lond) 2012;26(1):51-60.

159. Zrenner E, Bartz-Schmidt KU, Benav H et al. Subretinal electronic chips allow blind patients to read letters and combine them to words. Proc Biol Sci 2011;278(1711):1489-1497.

160. Consensus recommendations for the postmortem diagnosis of Alzheimer's disease. The National Institute on Aging, and Reagan Institute Working Group on Diagnostic Criteria for the Neuropathological Assessment of Alzheimer's Disease. Neurobiol Aging 1997;18(4 Suppl):S1-S2.

161. Querfurth HW, LaFerla FM. Alzheimer's disease. N Engl J Med 2010;362(4):329-344.

162. Beatty S, Koh H, Phil M, Henson D, Boulton M. The role of oxidative stress in the pathogenesis of age-related macular degeneration. Surv Ophthalmol 2000;45(2):115-134.

163. Grimm S, Hohn A, Grune T. Oxidative protein damage and the proteasome. Amino Acids 2012;42(1):23-38.

164. Holz FG, Schutt F, Kopitz J et al. Inhibition of lysosomal degradative functions in RPE cells by a retinoid component of lipofuscin. Invest Ophthalmol Vis Sci 1999;40(3):737-743.

165. He X, Hahn P, Iacovelli J et al. Iron homeostasis and toxicity in retinal degeneration. Prog Retin Eye Res 2007;26(6):649-673.

166. Kurz T, Terman A, Gustafsson B, Brunk UT. Lysosomes and oxidative stress in aging and apoptosis. Biochim Biophys Acta 2008;1780(11):1291-1303.

167. Holmes C, Cunningham C, Zotova E et al. Systemic inflammation and disease progression in Alzheimer disease. Neurology 2009;73(10):768-774.

168. Ponath PD, Qin S, Ringler DJ et al. Cloning of the human eosinophil chemoattractant, eotaxin. Expression, receptor binding, and functional properties suggest a mechanism for the selective recruitment of eosinophils. J Clin Invest 1996;97(3):604-612.

169. Takeda A, Baffi JZ, Kleinman ME et al. CCR3 is a target for age-related macular degeneration diagnosis and therapy. Nature 2009;460(7252):225-230.

170. Sharma NK, Prabhakar S, Gupta A et al. New biomarker for neovascular age-related macular degeneration: eotaxin-2. DNA Cell Biol 2012;31(11):1618-1627.

171. Ingram G, Hakobyan S, Hirst CL et al. Complement regulator factor H as a serum biomarker of multiple sclerosis disease state. Brain 2010;133(Pt 6):1602-1611.

172. Popp N, Chu XK, Shen D, Tuo J, Chan CC. Evaluating Potential Therapies in a Mouse Model of Focal Retinal Degeneration with Age-related Macular Degeneration (AMD)-Like Lesions. J Clin Exp Ophthalmol 2013;4(5):1000296.

173. Luhmann UF, Carvalho LS, Robbie SJ et al. Ccl2, Cx3cr1 and Ccl2/Cx3cr1 chemokine deficiencies are not sufficient to cause age-related retinal degeneration. Exp Eye Res 2013;107:80-87.

174. Vessey KA, Greferath U, Jobling AI et al. Ccl2/Cx3cr1 knockout mice have inner retinal dysfunction but are not an accelerated model of AMD. Invest Ophthalmol Vis Sci 2012;53(12):7833-7846.

175. Nita M, Grzybowski A, Ascaso FJ, Huerva V. Age-related macular degeneration in the aspect of chronic low-grade inflammation (pathophysiological parainflammation). Mediators Inflamm 2014;2014:930671.

176. Grossniklaus HE, Martinez JA, Brown VB et al. Immunohistochemical and histochemical properties of surgically excised subretinal neovascular membranes in age-related macular degeneration. Am J Ophthalmol 1992;114(4):464-472.

177. Curcio CA, Medeiros NE, Millican CL. Photoreceptor loss in age-related macular degeneration. Invest Ophthalmol Vis Sci 1996;37(7):1236-1249.

178. Mullins RF, Schoo DP, Sohn EH et al. The membrane attack complex in aging human choriocapillaris: relationship to macular degeneration and choroidal thinning. Am J Pathol 2014;184(11):3142-3153.

179. Whitmore SS, Sohn EH, Chirco KR et al. Complement activation and choriocapillaris loss in early AMD: implications for pathophysiology and therapy. Prog Retin Eye Res 2015;45:1-29.

180. Kanan Y, Siefert JC, Kinter M, Al-Ubaidi MR. Complement factor H, vitronectin, and opticin are tyrosine-sulfated proteins of the retinal pigment epithelium. PLoS One 2014;9(8):e105409.

181. Dunaief JL, Dentchev T, Ying GS, Milam AH. The role of apoptosis in age-related macular degeneration. Arch Ophthalmol 2002;120(11):1435-1442.

182. Fine SL, Berger JW, Maguire MG, Ho AC. Age-related macular degeneration. N Engl J Med 2000;342(7):483-492.

183. Sharma K, Sharma NK, Anand A. Why AMD is a disease of ageing and not of development: mechanisms and insights. Front Aging Neurosci 2014;6:151.

184. Boyer DS, Antoszyk AN, Awh CC, Bhisitkul RB, Shapiro H, Acharya NR. Subgroup analysis of the MARINA study of ranibizumab in neovascular age-related macular degeneration. Ophthalmology 2007;114(2):246-252.

185. Kaiser PK, Brown DM, Zhang K et al. Ranibizumab for predominantly classic neovascular age-related macular degeneration: subgroup analysis of first-year ANCHOR results. Am J Ophthalmol 2007;144(6):850-857.

186. Maralani HG, Tai BC, Wong TY et al. Metabolic syndrome and risk of age-related macular degeneration. Retina 2015;35(3):459-466.

187. Klein R, Knudtson MD, Cruickshanks KJ, Klein BE. Further observations on the association between smoking and the long-term incidence and progression of age-related macular degeneration: the Beaver Dam Eye Study. Arch Ophthalmol 2008;126(1):115-121.

188. Piermarocchi S, Miotto S, Colavito D, Leon A, Segato T. Combined effects of genetic and non-genetic risk factors affect response to ranibizumab in exudative age-related macular degeneration. Acta Ophthalmol 2014.

189. Tan JS, Mitchell P, Smith W, Wang JJ. Cardiovascular risk factors and the long-term incidence of age-related macular degeneration: the Blue Mountains Eye Study. Ophthalmology 2007;114(6):1143-1150.

190. Hagstrom SA, Ying GS, Pauer GJ et al. Pharmacogenetics for genes associated with age-related macular degeneration in the Comparison of AMD Treatments Trials (CATT). Ophthalmology 2013;120(3):593-599.

191. Amoaku WM, Chakravarthy U, Gale R et al. Defining response to anti-VEGF therapies in neovascular AMD. Eye (Lond) 2015.

192. Van de Ven JP, Nilsson SC, Tan PL et al. A functional variant in the CFI gene confers a high risk of age-related macular degeneration. Nat Genet 2013;45(7):813-817.

193. Kloeckener-Gruissem B, Barthelmes D, Labs S et al. Genetic association with response to intravitreal ranibizumab in patients with neovascular AMD. Invest Ophthalmol Vis Sci 2011;52(7):4694-4702.

194. Lee AY, Raya AK, Kymes SM, Shiels A, Brantley MA, Jr. Pharmacogenetics of complement factor H (Y402H) and treatment of exudative age-related macular degeneration with ranibizumab. Br J Ophthalmol 2009;93(5):610-613.

195. McKibbin M, Ali M, Bansal S et al. CFH, VEGF and HTRA1 promoter genotype may influence the response to intravitreal ranibizumab therapy for neovascular age-related macular degeneration. Br J Ophthalmol 2012;96(2):208-212.

196. Orlin A, Hadley D, Chang W et al. Association between high-risk disease loci and response to anti-vascular endothelial growth factor treatment for wet age-related macular degeneration. Retina 2012;32(1):4-9.

197. Teper SJ, Nowinska A, Pilat J, Palucha A, Wylegala E. Involvement of genetic factors in the response to a variable-dosing ranibizumab treatment regimen for age-related macular degeneration. Mol Vis 2010;16:2598-2604.

198. Yamashiro K, Tomita K, Tsujikawa A et al. Factors associated with the response of age-related macular degeneration to intravitreal ranibizumab treatment. Am J Ophthalmol 2012;154(1):125-136.

199. Francis PJ. The influence of genetics on response to treatment with ranibizumab (Lucentis) for age-related macular degeneration: the Lucentis Genotype Study (an American Ophthalmological Society thesis). Trans Am Ophthalmol Soc 2011;109:115-156.

200. Tian J, Qin X, Fang K et al. Association of genetic polymorphisms with response to bevacizumab for neovascular age-related macular degeneration in the Chinese population. Pharmacogenomics 2012;13(7):779-787.

201. Luhmann UF, Robbie SJ, Bainbridge JW, Ali RR. The relevance of chemokine signalling in modulating inherited and age-related retinal degenerations. Adv Exp Med Biol 2014;801:427-433.

202. Wickremasinghe SS, Xie J, Lim J et al. Variants in the APOE gene are associated with improved outcome after anti-VEGF treatment for neovascular AMD. Invest Ophthalmol Vis Sci 2011;52(7):4072-4079.

203. Abedi F, Wickremasinghe S, Richardson AJ, Islam AF, Guymer RH, Baird PN. Genetic influences on the outcome of anti-vascular endothelial growth factor treatment in neovascular age-related macular degeneration. Ophthalmology 2013;120(8):1641-1648.

204. McHarg S, Clark SJ, Day AJ, Bishop PN. Age-related macular degeneration and the role of the complement system. Mol Immunol 2015.

205. Scholl HP, Charbel IP, Walier M et al. Systemic complement activation in age-related macular degeneration. PLoS One 2008;3(7):e2593.

206. Forssmann U, Uguccioni M, Loetscher P et al. Eotaxin-2, a novel CC chemokine that is selective for the chemokine receptor CCR3, and acts like eotaxin on human eosinophil and basophil leukocytes. J Exp Med 1997;185(12):2171-2176.

207. Sharma NK, Prabhakar S, Gupta A et al. New biomarker for neovascular age-related macular degeneration: eotaxin-2. DNA Cell Biol 2012;31(11):1618-1627.

208. Tseng WA, Thein T, Kinnunen K et al. NLRP3 inflammasome activation in retinal pigment epithelial cells by lysosomal destabilization: implications for age-related macular degeneration. Invest Ophthalmol Vis Sci 2013;54(1):110-120.

209. Anderson OA, Finkelstein A, Shima DT. A2E induces IL-1ss production in retinal pigment epithelial cells via the NLRP3 inflammasome. PLoS One 2013;8(6):e67263.

210. Seddon JM, George S, Rosner B, Rifai N. Progression of age-related macular degeneration: prospective assessment of C-reactive protein, interleukin 6, and other cardiovascular biomarkers. Arch Ophthalmol 2005;123(6):774-782.

211. Klein R, Myers CE, Cruickshanks KJ et al. Markers of inflammation, oxidative stress, and endothelial dysfunction and the 20-year cumulative incidence of early age-related macular degeneration: the Beaver Dam Eye Study. JAMA Ophthalmol 2014;132(4):446-455.

212. Holmes C, Cunningham C, Zotova E et al. Systemic inflammation and disease progression in Alzheimer disease. Neurology 2009;73(10):768-774.

213. Holmes C, Butchart J. Systemic inflammation and Alzheimer's disease. Biochem Soc Trans 2011;39(4):898-901.